Energy

FOSSIL

FWC/FWDC/TR-84/17
(DE84013997)

# INVESTIGATION OF PYRITE AS A CONTRIBUTOR TO SLAGGING IN EASTERN BITUMINOUS COALS

Quarterly Progress Report for the Period October 1—December 31, 1983

June 1984

Work Performed Under Contract No. AC22-81PC40268

Foster Wheeler Development Corporation
Livingston, New Jersey

Technical Information Center
Office of Scientific and Technical Information
United States Department of Energy

## DISCLAIMER

## DISCLAIMER



This report has been reproduced directly from the best available copy.

Available from the National Technical Information Service, U. S. Department of Commerce, Springfield, Virginia 22161.

Price: Printed Copy A08
Microfiche A01

Codes are used for pricing all publications. The code is determined by the number of pages in the publication. Information pertaining to the pricing codes can be found in the current issues of the following publications, which are generally available in most libraries: *Energy Research Abstracts (ERA); Government Reports Announcements* and Index (*GRA* and I); *Scientific and Technical Abstract Reports (STAR);* and publication NTIS-PR-360 available from NTIS at the above address.

FWC/FWDC/TR-84/17
(DE84013997)
Distribution Category UC-90b

# Investigation of Pyrite as a Contributor To Slagging in Eastern Bituminous Coals

Quarterly Progress Report 9

October 1 through December 31, 1983

Prepared for

Pittsburgh Energy Technology Center
U.S. Department of Energy
Pittsburgh, Pennsylvania

By

Richard W. Bryers
Program Manager

June 1984

Contract DE-AC22-81PC40268
FWDC No. 9-41-3210

FOSTER WHEELER DEVELOPMENT CORPORATION
12 Peach Tree Hill Road, Livingston, New Jersey 07039

CONTENTS


| Section | | Page |
|---|---|---|
| 1 | INTRODUCTION | 1-1 |
| 2 | SELECTION OF COALS | 2-1 |
| 3 | CHARACTERIZATION OF COAL SAMPLES AND WASHED COAL PRODUCT | 3-1 |
| | Introduction | 3-1 |
| | Kentucky No. 9, Henderson County, Kentucky | 3-3 |
| 4 | COMBUSTION TESTS AND ANALYSIS OF SLAG DEPOSITS AND FLY ASH | 4-1 |
| | Introduction | 4-1 |
| | Experimental Set-Up | 4-1 |
| | Furnace | 4-3 |
| | Flue Pass | 4-3 |
| | Ash Deposit Sampling Probes | 4-3 |
| | Experimental Test Procedures | 4-9 |
| | Analysis of Deposits and Fly Ash | 4-10 |
| 5 | IMPACT OF COAL WASHING IN FIRESIDE DEPOSITS | 5-1 |
| | Introduction | 5-1 |
| | Washability Tests | 5-1 |
| | Coal Washing | 5-15 |
| | Coal Variability | 5-28 |
| | Combustion Tests of Washed Coal | 5-45 |

# ILLUSTRATIONS


| Number | | Page |
|---|---|---|
| 1.1 | Milestone Schedule and Status Report | 1-3 |
| 3.1 | Size Distribution of Pulverized Coal Used in Fractionation Analysis | 3-8 |
| 3.2 | Relationship Between Ash Softening Temperature and Percentage of Basic Constituents in Ash for All Size and Gravity Fractionated Coals Examined | 3-12 |
| 3.3 | Fusibility Diagram--Kentucky No. 9 Coal, Henderson County | 3-14 |
| 3.4 | Distribution of Iron by Size and Gravity in Fractionated Kentucky No. 9 Coal, Henderson County | 3-15 |
| 3.5 | Distribution of Iron by Size and Gravity in Fractionated Kentucky No. 11 Coal | 3-16 |
| 3.6 | Distribution of Iron by Size and Gravity in Fractionated Illinois No. 6 Coal | 3-17 |
| 3.7 | Distribution of Iron by Size and Gravity in Fractionated Kentucky No. 9 Coal, Union County | 3-18 |
| 3.8 | Distribution of Iron by Size and Gravity in Fractionated Lower Freeport Coal | 3-19 |
| 3.9 | Distribution of Iron by Size and Gravity in Fractionated Upper Freeport Coal | 3-20 |
| 3.10 | Combustion Profile of Pure Pyrite Compared with Profiles of Composite Samples of Various Coals | 3-24 |
| 3.11 | Combustion Profiles of Pure Pyrite and Composite Coal Sample Compared with Sink 2.85 Gravity Fraction (+140 mesh) of Kentucky No. 9 Coal, Henderson County | 3-25 |
| 3.12 | Combustion Profiles of Pure Pyrite and Composite Coal Sample Compared with Various Gravity Fractions (-140/+200 mesh) of Kentucky No. 9 Coal, Henderson County | 3-26 |
| 3.13 | Combustion Profiles of Pure Pyrite and Composite Coal Sample Compared with Various Gravity Fractions (-200/+325 mesh) of Kentucky No. 9 Coal, Henderson County | 3-27 |

ILLUSTRATIONS (Cont'd)


| Number | | Page |
|---|---|---|
| 3.14 | Combustion Profiles of Pure Pyrite and Composite Coal Sample Compared with Various Gravity Fractions (-325 mesh) of Kentucky No. 9 Coal, Henderson County | 3-28 |
| 3.15 | Comparison of Combustion Profiles of Pure Pyrite with Those of Heavy Gravity Fractions (-1.80/+2.85) of Various Eastern Bituminous Coals | 3-30 |
| 3.16 | Combustion Profile of Pure Pyrite Compared with Profiles of Sink 2.85 Gravity Fractions of Various Coals Characterized | 3-31 |
| 4.1 | System Schematic | 4-4 |
| 4.2 | Furnace Cross Section | 4-5 |
| 4.3 | Schematic of Air-Cooled Furnace Probe | 4-7 |
| 4.4 | Slagging Probe | 4-8 |
| 4.5 | Deposit Accumulation in Vena Contracta at Entrance to Convection Pass After Firing Kentucky No. 9 Coal | 4-12 |
| 4.6 | Accumulation of Deposits in First Fouling Probe as a Result of Attempt to Clear Vena Contracta While On Line | 4-13 |
| 4.7 | Comparison of First Convective Fouling Probe After Firing Kentucky No. 11 and Kentucky No. 9 | 4-14 |
| 4.8 | Vertical Convective Fouling Probe After Firing Kentucky No. 9, Henderson County, for 2-1/2 Hours | 4-15 |
| 4.9a | Center and Lower Furnace Wall Slagging Probes After Firing Kentucky No. 9, Henderson County, for Only 2-1/2 Hours (Trial 1) | 4-16 |
| 4.9b | Center and Lower Furnace Wall Slagging Probes After Firing Kentucky No. 9, Henderson County, Coal for Only 3 Hours (Trial 2) | 4-17 |
| 4.10 | Deposits Formed on Lower Side of Slagging Probe Perpendicular to Flue Gas Flow After Firing Kentucky No. 9, Henderson County, for 2-1/2 Hours | 4-18 |

ILLUSTRATIONS (Cont'd)


| Number | | Page |
|---|---|---|
| 4.11 | Ash Softening Temperature vs. Percentage Basic Constituents for Fractionated Kentucky No. 9, Henderson County | 4-21 |
| 4.12 | Influence of Percentage of Basic Constituents in Ash on Ash Softening Temperatures Under Reducing Conditions for Different Ranks of Coal | 4-22 |
| 4.13 | SEM Photomicrograph and EDX Scan--Surface Morphology and Elemental Composition of Composite Powder Comprising First Layer on Lower Slag Probe | 4-24 |
| 4.14 | SEM Photomicrographs and EDX Scans--Surface Morphology and Elemental Composition of Individual Species Comprising Powdery Layer on First Slagging Probe | 4-25 |
| 4.15 | SEM Photomicrographs and EDX Scans--Surface Morphology and Elemental Analysis of Fused Outer Surface of Slag on Lower Probe | 4-27 |
| 4.16 | SEM Photomicrograph and EDX Scan--Surface Morphology and Elemental Composition of Fly Ash Species Initiating Slag on Center Slagging Probe | 4-28 |
| 4.17 | SEM Photomicrographs and EDX Scans--Surface Morphology and Elemental Composition of Cross Section and Surface of Outside Molten Layer | 4-30 |
| 4.18 | SEM Photomicrographs and EDX Scans--Surface Morphology and Elemental Composition of Molten Surface of Deposited Formed on Center Slagging Probe | 4-31 |
| 4.19 | SEM Photomicrographs and EDX Scans--Surface Morphology and Elemental Composition of Perpendicular Probe Tube Scale Bonded to Ash Deposit | 4-32 |
| 4.20 | SEM Photomicrographs and EDX Scans--Surface Morphology and Elemental Analysis of Molten Nodules Formed on Lower Surface of Perpendicular Probe | 4-33 |
| 4.21 | SEM Photomicrographs and EDX Scans--Surface Morphology and Elemental Analysis of Inside Powdery Layer and Cross Section of Deposit on Top Side of Probe Perpendicular to Gas Stream | 4-34 |

ILLUSTRATIONS (Cont'd)


| Number | | Page |
|---|---|---|
| 4.22 | SEM Photomicrographs and EDX Scans--Surface Morphology and Elemental Composition of Spent Pyrite Particles and Molten Potassium Silicate Matrix Responsible for Deposition on Slag Probe | 4-36 |
| 4.23 | SEM Photomicrographs and EDX Scans--Surface Morphology and Elemental Composition of Surface and Cross Section of Wall Slag | 4-37 |
| 4.24 | Comparison of Sintered Deposit Formed on Furnace Wall with Sintered Deposit Formed in Entrance to Convection Pass | 4-38 |
| 4.25 | Typical Fly Ash Captured in Air Heater Cyclone and Baghouse While Firing Kentucky No. 9 Coal | 4-40 |
| 5.1 | Process Flow Diagram for Washing 300-lb Sample of Upper Freeport Coal, Indiana County, Pennsylvania | 5-3 |
| 5.2 | Cumulative Float (% Yield) vs. Specific Gravity for Various Size Fractions | 5-11 |
| 5.3 | Impact of Beneficiation on Coal Ash Quality of Individual Size and Gravity Fractions as Defined by Physicochemical Properties of Ash, Percentage Basicity, and Ash Softening Temperature | 5-13 |
| 5.4 | Fusibility Diagrams for Various Size Fractions | 5-14 |
| 5.5 | Percentage Reduction in Individual Elements vs. Percentage Yield of Washed Product | 5-15 |
| 5.6 | Washed Coal Process Flow Diagram | 5-17 |
| 5.7 | Softening Temperature of Washed Coal Ash Compared with Unwashed Coal Ash Fractionated by Size and Gravity | 5-21 |
| 5.8 | Comparison of Softening Temperatures of Fractionated Washed and Unwashed Pulverized Coal | 5-26 |
| 5.9 | Fusibility Diagrams of Fractionated Coal Ash for Washed and Unwashed Upper Freeport Coal | 5-27 |
| 5.10 | Distribution of Iron Among Gravity Fractions in Washed and Unwashed Upper Freeport Coal | 5-28 |

ILLUSTRATIONS (Cont'd)


| Number | | Page |
|---|---|---|
| 5.11 | Comparison of TGA Thermograms for Washed and Unwashed Upper Freeport Coal | 5-30 |
| 5.12 | Comparison of TGA Thermograms for Various Gravity Fractions of Washed Upper Freeport Coal With Composite Coal Sample and Pure Pyrite | 5-31 |
| 5.13 | Comparison of Combustion Profile of Sink 2.85 Fraction From Washed Upper Freeport Coal with Sink 2.85 Fraction From Unwashed Upper Freeport Coal, Pure Pyrite, and Heavy Fractions From Other Coals | 5-32 |
| 5.14 | Generalized Stratigraphy of Upper Freeport Coal Bed/Lucern No. 6-Homer City No. 1 Mines (from Cecil, Stanton, and Dulong) | 5-34 |
| 5.15 | Fence Diagram of Upper Freeport Coal Facies/Lucense No. 6-Homer City No. 1 Mintes (from Cecil, Stanton, and Dulong) | 5-35 |
| 5.16 | Sample Numbers and Map of Complete and Bench-Channel Samples From Lucerne No. 6 and Homer City No. 1 Mines (from Cecil, Stanton, and Dulong) | 5-37 |
| 5.17 | Generalized Major Oxide and Corresponding Mineral Data by Coal Facies (from Cecil, Stanton, and Dulong) | 5-39 |
| 5.18 | Iron Disulfide Forms, Associations, and Grain Sizes in Samples From HEL-2R and H2-42P, Upper Freeport Coal, Homer City, Pennsylvania (from Cecil, Stanton, and Dulong) | 5-41 |
| 5.19 | Iron Disulfide Forms, Associations, and Grain Sizes in Samples From LUC-NM and H2-5/3L, Upper Freeport Coal, Homer City, Pennsylvania (from Cecil, Stanton, and Dulong) | 5-42 |
| 5.20 | Concentration of Pyritic Sulfurs in Complete- and Bench-Channel Samples From Lucerne No. 6 and Homer City No. 1 Mines (from Cecil, Stanton, and Dulong) | 5-44 |
| 5.21 | Concentration of Iron (Fe) in Complete- and Bench-Channel Samples From Lucerne No. 6 and Homer City No. 1 Mines (from Cecil, Stanton, and Dulong) | 5-45 |
| 5.22 | Viscosities of Coals and Their Deposits | 5-48 |

ILLUSTRATIONS (Cont'd)


| Number | | Page |
|---|---|---|
| 5.23 | Ash Viscosities of Various Coals | 5-49 |
| 5.24 | Comparison of Lower Slagging Probe After Firing Unwashed (top) and Washed (bottom) Upper Freeport Coal | 5-50 |
| 5.25 | Comparison of Center Slagging Probe After Firing Unwashed (top) and Washed (bottom) Upper Freeport Coal | 5-51 |
| 5.26 | Flame (top) and Furnace Exit (bottom) Sides of Probe Immersed Perpendicular to Gas Flow in Furnace--After Firing Washed Coal | 5-52 |
| 5.27 | Direct Comparison of Fouling Probes After Firing Raw Coal (top) and Coal in which Liberated Pyrite Was Removed by Washing (bottom) | 5-53 |
| 5.28 | Comparison of Inner and Outer Layers of Ash Formed on Lower Slagging Probe While Firing Unwashed and Washed Upper Freeport Coal, Indiana County | 5-57 |
| 5.29 | SEM Photomicrograph and EDX Scan Comparing Change in Surface Morphology and Elemental Comparison of Deposit on Center Slagging Probe | 5-59 |
| 5.30 | SEM Photomicrographs and EDX Scans of Cross Section of Wall Slag, Representing Advanced Stages of Slagging | 5-61 |
| 5.31 | SEM Photomicrographs and EDX Analyses of Top Surface and Cross Section of Fused Burner Deposit Fromed While Firing Air-Micronized Coal | 5-62 |
| 5.32 | SEM Photomicrographs and EDX Analyses of Gas-Side Surface of Fly Ash Deposited on Furnace Boiler Tube Surface While Firing Steam-Micronized Coal | 5-63 |
| 5.33 | SEM Photomicrographs and EDX Scans Showing Surface Morphology of Deposits Accumulated on Frame Side of the Slagging Probe Perpendicular to the Flue Gas Stream | 5-64 |
| 5.34 | SEM Photomicrographs and EDX Scans Showing Surface Morphology and Elemental Composition of Deposit Forming on Top Side of Probe Perpendicular to Flow of Flue Gas in Furnace | 5-66 |

ILLUSTRATIONS (Cont'd)


| Number | | Page |
|---|---|---|
| 5.35 | SEM Photomicrographs and EDAX Scans of Deposit Removed from Refractory in Segment 8 at the Furnace Exit | 5-67 |
| 5.36 | Surface Morphology and Elemental Composition of Dust Removed From Fouling Probes After Firing Washed Upper Freeport Coal | 5-68 |
| 5.37 | Comparison of Surface Morphology and Elemental Composition of Sintered Deposits Removed From Refractory Surface After Firing Washed and Unwashed Upper Freeport Coal | 5-69 |

TABLES


| Number | | Page |
|---|---|---|
| 1.1 | Milestone Schedule and Status Report | 1-3 |
| 2.1 | Desirable Characteristics of Sample Coals | 2-1 |
| 2.2 | Composite Fueld Analysis--Illinois No. 5 and Lower Kittaning (Dry) | 2-3 |
| 3.1 | Fuel Analyses--Kentucky No. 11; Illinois No. 6; Upper Freeport, Indiana County, Pennsylvania; Lower Freeport, Cambria County, Pennsylvania; Kentucky No. 9, Union County; and Kentucky No. 9, Henderson County | 3-4 |
| 3.2 | Composite Coal Analyses--Kentucky No. 11; Illinois No. 6; Upper Freeport, Indiana County, Pennsylvania; Lower Freeport, Cambria County, Pennsylvania; Kentucky No. 9, Union County; and Kentucky No. 9, Henderson County | 3-5 |
| 3.3 | Summary of Mineral Analysis Determined From Low-Temperature Ash for Five Eastern Bituminous Coals | 3-6 |
| 3.4 | Ash Chemistry for Size and Gravity Fractionated Pulverized Kentucky No. 9 Coal, Henderson County, Kentucky | 3-9 |
| 3.5 | Ash Chemistry--Size and Gravity Fractionated Pulverized Kentucky No. 9 Coal, Henderson County | 3-10 |
| 3.6 | Ash Fusion Temperatures--Size and Gravity Fractionated Pulverized Kentucky No. 9 Coal, Henderson County | 3-11 |
| 4.1 | Time-Averaged Operating Conditions | 4-2 |
| 4.2 | Summary of Ash Chemistry and Ash Fusion Data--Combustion Trial 1, Kentucky No. 9 Coal, Henderson County, Kentucky | 4-19 |
| 4.3 | Summary of Ash Chemistry and Ash Fusion Data--Combustion Trial 2, Kentucky No. 9 Coal, Henderson County, Kentucky | 4-20 |
| 5.1 | Weight Distribution of Screened Coal Samples | 5-4 |
| 5.2 | Summary of Washability Data for Upper Freeport Coal, Indiana County, Pennsylvania--Size 3/4 in. x 14 mesh (3/8 in. x 0 stream) | 5-5 |
| 5.3 | Summary of Washability Data for Upper Freeport Coal, Indiana County, Pennsylvania--Size 14 x 100 mesh (3/8 in. x 0 stream) | 5-6 |

TABLES (Cont'd)


| Number | | Page |
|---|---|---|
| 5.4 | Summary of Washability Data for Upper Freeport Coal, Indiana County, Pennsylvania--Size 14 x 100 mesh (14 mesh x 0 stream) | 5-7 |
| 5.5 | Summary of Washability Data for Upper Freeport, Indiana County, Pennsylvania--Size 200 Mesh x 0 Stream | 5-8 |
| 5.6 | Ash Chemistry and Ash Fusion Data for Washed, Upper Freeport Coal, Indiana County, Pennsylvania | 5-9 |
| 5.7 | Liberation of Elemental Constituents in Ash from Pulverized Coal | 5-10 |
| 5.8 | Comparison of Ash Chemistry of Washed Coal (14 x 100 Mesh, +1.80 Sp Gr) With Float 1.80 and 1.30 Gravity Fractions of Various Coal Sizes Examined in Washability Study | 5-19 |
| 5.9 | Comparison of Ash Chemistry of Unwashed 200 Mesh x 0 Coal with 200 Mesh x 0 Coal Washed at 14 Mesh x 0 | 5-20 |
| 5.10 | Comparison of Mineral Analysis of Reject Material from Coal Washery with Run of Mine Coal | 5-22 |
| 5.11 | Comparison of Ash Chemistry and Ash Fusion Temperatures for Unwashed and Washed 200 Mesh x 0 Samples | 5-25 |
| 5.12 | Comparison of Total Iron in 14 x 100 Mesh and 200 Mesh x 0 Unwashed Coal With Pulverized Coal Washed at 14 Mesh x 0 | 5-36 |
| 5.13 | Minerals in Upper Freeport Coal as Interpreted from SEM Data | 5-38 |
| 5.14 | Summary of Ash Chemistry and Ash Fusion Data--Combustion Tests of Washed Upper Freeport Coal | 5-54 |
| 5.15 | Comparison of Ash Chemistry of Slag Formed by Washed and Unwashed Coal | 5-56 |

# Section 1

# INTRODUCTION

Slagging of utility steam generator furnaces while firing eastern bituminous coals has been attributed to the pyritic iron in the coal ash. Investigators have also learned that coals with similar pyritic levels fired in furnaces of similar design do not always produce the same degree of slagging. Since separation of pyrite from other mineral matter does occur in some coals and since the physicochemical behavior upon heating the pyrite and pyrite mixed with other mineral matter or coal may be quite different, the degree of furnace slagging may possibly be attributed to the size and orientation of the pyrite in coal in addition to its concentration level.

The objective of this program is to examine slags formed as a result of firing coals with varying concentration levels, size distribution, and orientation of pyrite with regard to mineral matter in the coal in a laboratory furnace.

The program tasks are:

Task 1--Selection of eight candidate coals

Task 2--Chemical characterization of the coal samples and identification of the pyrite size, distribution, and orientation with respect to other mineral matter and concentration levels

Task 3--Testing of the candidate coals in a laboratory furnace

Task 4--Chemical and physical characterization of the slag and fly ash samples created by the impurities in the coal sample

Task 5--Influence of coal beneficiation on furnace slagging

Task 6--Analysis of data and identification of parameters influencing the contribution of pyrite to slagging problems.

Washing of the Upper Freeport coal from Indiana County, Pennsylvania, was completed by the last quarter of 1983. The washed product was characterized for mineral content, and a combustion test was performed. Kentucky No. 9 from Henderson County, Kentucky, selected as the sixth coal to be investigated, was characterized using size and gravity fractionation techniques and was combusted in the laboratory furnace to evaluate its slagging and fouling potential. The remaining two coals to be characterized and combusted were identified as Illinois No. 5 and Lower Kittanning from Clarion County, Pennsylvania.

Figure 1.1 is the revised milestone schedule and status report.

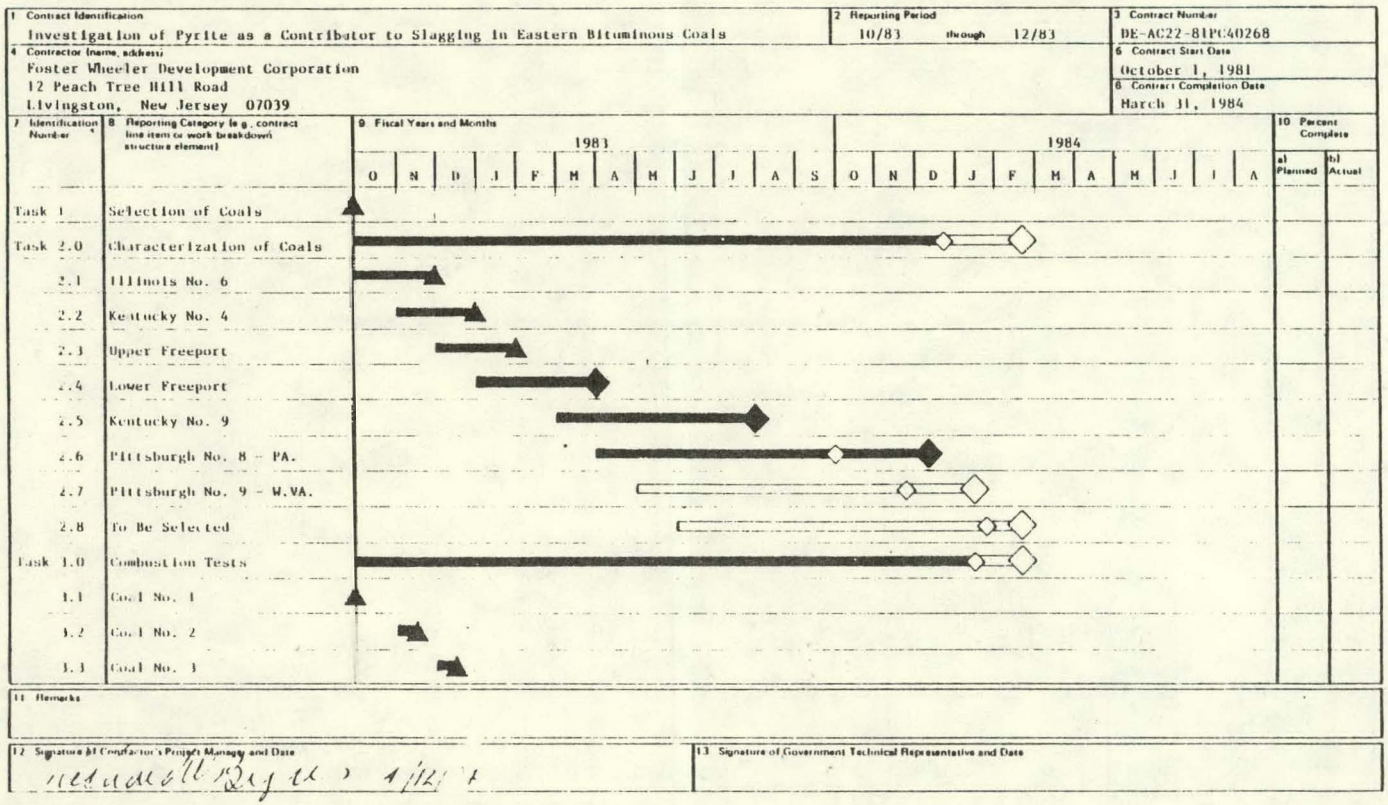


Figure 1.1 Milestone Schedule and Status Report

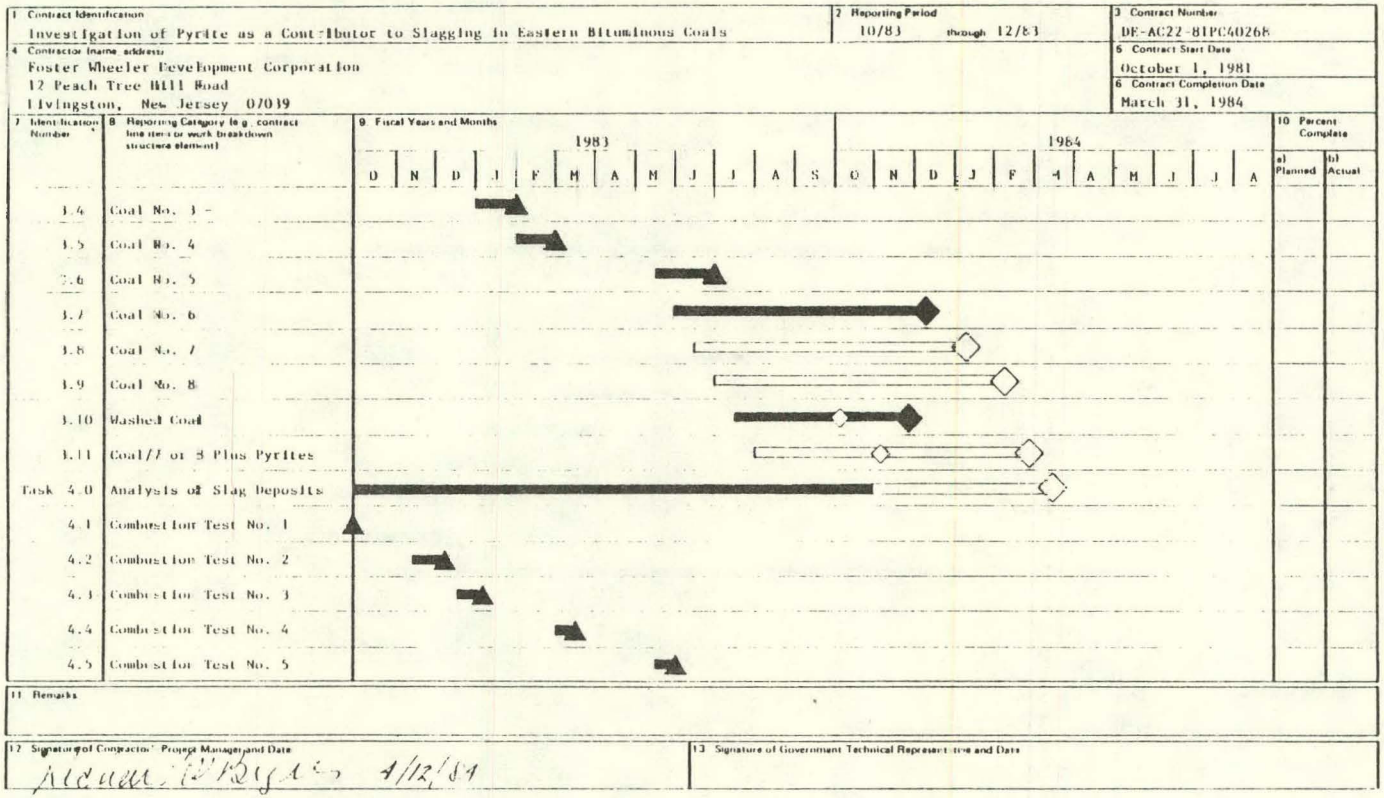


Figure 1.1 Milestone Schedule and Status Report (Cont)

1 Contract Identification: Investigation of Pyrite as a Contributor to Slagging In Eastern Bituminous Coals

2 Reporting Period: 10/83 through 12/83

3 Contract Number: DE-AC22-81PC40268

4 Contractor (name, address): Foster Wheeler Development Corporation, 12 Peach Tree Hill Road, Livingston, New Jersey 07039

5 Contract Start Date: October 1, 1981

6 Contract Completion Date: March 31, 1984

| 7 Identification Number | 8 Reporting Category (e.g. contract line item or work breakdown structure element) | 10 Percent Complete a) Planned | 10 Percent Complete b) Actual |
|---|---|---|---|
| 4.6 | Combustion Test No. 6 | | |
| 4.7 | Combustion Test No. 7 | | |
| 4.8 | Combustion Test No. 8 | | |
| 4.9 | Combustion Test No. 9 | | |
| 4.10 | Combustion Test No. 10 | | |
| 4.11 | Combustion Test No. 11 | | |
| Task 5 | Washability Study | | |
| Task 6 | Evaluation of Data | | |
| Task 7.0 | Program Management | | |
| 7.1 | Monthly Reports | | |
| 7.2 | Quarterly Reports | | |
| 7.3 | Final Report | | |

9 Fiscal Years and Months: 1983 (O N D J F M A M J J A S) 1984 (O N D J F M A M J J A)

11 Remarks

12 Signature of Contractor's Project Manager and Date: Edward W Bigus 4/12/84

13 Signature of Government Technical Representative and Date

Figure 1.1 Milestone Schedule and Status Report (Cont)

Section 2

TASK 1--SELECTION OF COALS

Originally eight candidate coals were selected based on variation in pyrite size, concentration, and distribution according to the specifications of the test matrix described in Table 2.1. The objectives of selecting coals containing minerals of variable size and distribution with regard to coal and other mineral matter were to identify the species responsible for slagging and the options available for modification of fuel preparation procedures, steam generator design, or steam generator operation necessary to inhibit slag formation. This would be accomplished by characterizing the pyrite present in a given coal, test firing the coal, and analyzing the resultant fireside deposits. Variation in fireside deposit chemistry and total accumulation with changes in mineral size and association should reveal the species responsible for slagging. The original selections were made on the basis of the best data available in the literature.

Table 2.1 Desirable Characteristics of Sample Coals

- 3 to 6% Sulfur, Moderate Ash Level, Coarse and Isolated Pyrite
- 3 to 4% Sulfur, High Ash Level, Coarse and Isolated Pyrite
- 3 to 4% Sulfur, Moderate Ash Level, Isolated and Finely Divided Pyrite
- 3 to 4% Sulfur, Moderate Ash Level, Pyrite and Ash Mixed
- 2% Sulfur, Coarse and Isolated Pyrite
- 1% Sulfur, Coarse and Isolated Pyrite

Since characterizing and combustion testing six of the eight coals proposed in the original scope of the program, we have learned that the purity and total concentration of the iron reporting to the heaviest gravity fraction have a substantial impact on slagging. Since we know that a reduction in sulfur and hence a reduction in iron in proportion to the non-iron-bearing minerals in the coal will reduce slagging, there is more to be gained by examining the impact of liberated pyrite on slagging them on total sulfur. Therefore, alternative fuels with high sulfur levels, high iron concentrations in the ash, and easily liberated pyrite and ash were selected to replace the 1- and 2-percent sulfur coals originally proposed. After considering availability and other logistics problems, Illinois No. 5 from Gallatin County, Illinois, and Upper Kittanning from Clarion County, Pennsylvania, were the coals selected. The composite fuel analyses are described in Table 2.2.

Table 2.2 Composite Fuel Analysis--Illinois No. 5 and Lower Kittanning (Dry)

| Description | Illinois No. 5* Gallatin County | Lower Kittanning† Clarion County, Pennsylvania |
|---|---|---|
| **Proximate Analysis (Wt%)** | | |
| Fixed Carbon | 42.64 | 49.62 |
| Volatile Matter | 30.51 | 42.46 |
| Ash | 26.85 | 7.92 |
| **Ultimate Analysis (Wt%)** | | |
| Carbon | 57.86 | 78.48 |
| Hydrogen | 4.41 | 4.95 |
| Oxygen | 5.62 | 5.24 |
| Nitrogen | 1.02 | 1.04 |
| Sulfur | 4.24 | 2.37 |
| Ash | 26.85 | 7.92 |
| HHV (Btu/lb) | 10,836 | 13,463 |
| **Forms of Sulfur (%)** | | |
| Sulfatic | 0.03 | 0.4 |
| Pyritic | 2.04 | 0.33 |
| Organic | 1.90 | 1.42 |
| **Ash Chemistry (%)** | | |
| $SiO_2$ | 52.0 | 52.1 |
| $Al_2O_3$ | 20.1 | 21.5 |
| $TiO_2$ | 1.0 | Nil |
| $Fe_2O_3$ | 14.7 | 24.4 |
| CaO | 4.3 | 11.2 |
| MgO | 0.8 | 0.5 |
| $Na_2O$ | 0.8 | 0.3 |
| $K_2O$ | 3.1 | 0.9 |
| $SO_3$ | 4.3 | 11.1 |
| $P_2O_5$ | 0.2 | 0.1 |
| **Ash Fusion (°F)** | | |
| Reducing: | | |
| Initial Deformation | 2050 | 2040 |
| Softening (Sph.) | 2080 | 2100 |
| Softening (Hem.) | 2120 | 2180 |
| Fluid | 2150 | 2540 |
| Oxidizing: | | |
| Initial Deformation | 2290 | 2400 |
| Softening (Sph.) | 2320 | 2600 |
| Softening (Hem.) | 2340 | 2640 |
| Fluid | 2380 | 2680 |

*Actual sample analysis.
†Analysis upon which sample was selected.

Section 3

# TASK 2--CHARACTERIZATION OF COAL SAMPLES AND WASHED COAL PRODUCT

## INTRODUCTION

Slagging of utility steam generator furnaces by ash in eastern bituminous coals is generally attributed to the fluxing action of the iron found in pyrite on the acidic constituents comprising the major portion of the remaining coal impurities (e.g., $Al_2O_3$, $SiO_2$). On occasion, coals with identical ash composition have been known to produce decidedly different slagging conditions in identically designed boilers operated in the same mode. Variations in composition of the slag when compared with the coal ash have led some investigators to believe fly ash is being selectively deposited on the furnace wall according to its gravity, composition, and physicochemical properties upon being heated. The implications are that coal ash is heterogeneous in nature and that each particle behaves independently as it is introduced into the furnace.

As the coal and ash are being pulverized, they are reduced in size and subdivided into many size and gravity fractions with differing coal compositions and ash chemistries. The final composition of the individual species will depend to a large extent on the original distribution and orientation of mineral matter in the coal. Slagging may be caused by the individual species with the lowest melting temperature and greatest potential for attaching itself to the furnace wall. If the composition of an individual ash species is altered while it is being pulverized, so that a portion of the ash has a higher melting temperature than the composite ash sample and the melting temperature of the remaining portion of the particulate has a melting temperature lower than that of the

composite ash sample, furnace slagging may occur unexpectedly with coals identified as nonslagging on the basis of a composite analysis.

In Step 1 coals are characterized by analyzing a composite sample for:

- Proximate Analysis
- Ultimate Analysis
- Forms of Sulfur
  - Pyritic
  - Organic
  - Sulfatic
- Ash Fusion Temperatures
- Ash Chemistry
- Hardgrove Grindability
- Thermal Analysis
  - Thermogravimetric Analysis
  - Differential Scanning Calorimetry
- Low-Temperature Ashing
  - Mineral Analysis
  - Thermogravimetric Analysis
  - Differential Thermal Analysis

At the present time, most investigators base their predictions on the quantitative elemental analysis of the composite coal sample determined during the first step of characterizing coal. If the analyses are inadequate and individual low-melting species are indeed the source of slagging and fouling, the coal must be further characterized by analyzing the size- and gravity-fractionated coal.

In Step 2 pyrite size and distribution in the coal are further characterized by pulverizing a 200-lb sample to 70 percent through 50 mesh and analyzing it for equally weighted size fractions, gravimetrically separated into +1.30, -1.30/+1.80, -1.80/+2.85, and -2.85 gravity fractions for ash chemistry, ash fusion temperatures, percentage of ash, and percentage of pyrite. We selected 70 percent through 50 mesh, rather than through 200 mesh, to provide sufficient samples for analysis in the coarse size range of the pulverized coal. The number of gravity separations was restricted to four for economic reasons. A

portion of the four gravity fractions with a +50 mesh size was retained for low-temperature ashing and mineral and thermal analyses.

Six coals have been characterized according to the analyses just described in Steps 1 and 2. The results of the analyses of five of these coals have been reported in previous progress reports. During the period covered by this quarterly report, a sixth coal, identified as Kentucky No. 9 from Henderson County, Kentucky, was characterized in depth.

KENTUCKY NO. 9, HENDERSON COUNTY, KENTUCKY

Tables 3.1 and 3.2, fuel analyses and composite coal analyses, directly compare Kentucky No. 9 coal, Henderson County, with previously analyzed coals. Mineral analyses of the various fuels is compared in Table 3.3. The composite analysis of the coal reveals an increase in pyritic sulfur and percentage of iron with little change in ash level, as compared with the previously analyzed Kentucky No. 9 coal from Union County. There was also a slight increase in calcium. The slight changes in mineral composition, as reflected in the ash analysis, increased the slagging potential from medium to high. The fouling potential increased from low to medium as a result of a change in base-to-acid ratio. There is a substantial increase in the differential between the ash fusion temperature under oxidizing and reducing temperatures when compared with previously characterized fuels. Fusion temperatures under reducing conditions are lower than for most of the coals previously analyzed. Conversely, they are considerably higher under oxidizing conditions than for any of the coals previously analyzed. There is no obvious explanation for the large difference.

Table 3.1 Fuel Analyses--Kentucky No. 11; Illinois No. 6; Upper Freeport, Indiana County, Pennsylvania; Lower Freeport, Cambria County, Pennsylvania; Kentucky No. 9, Union County; and Kentucky No. 9, Henderson County

| Description | Kentucky No. 11 | Illinois No. 6 Gallatin County | Upper Freeport Indiana County | Lower Freeport Cambria County | Kentucky No. 9 Union County | Kentucky No. 9 Henderson County |
|---|---|---|---|---|---|---|
| **Proximate Analysis (Wt%)** | | | | | | |
| Fixed Carbon | 40.71 | 41.54 | 52.58 | 56.87 | 41.17 | 38.99 |
| Volatile Matter | 39.16 | 36.93 | 20.64 | 22.00 | 36.49 | 29.93 |
| Ash | 14.90 | 9.36 | 23.58 | 16.43 | 18.01 | 18.41 |
| Moisture | 5.23 | 12.17 | 3.20 | 4.70 | 4.33 | 12.67 |
| Total | 100.00 | 100.00 | 100.00 | 100.00 | 100.00 | 100.00 |
| **Ultimate Analysis (Wt%)** | | | | | | |
| Carbon | 62.45 | 61.36 | 62.54 | 69.09 | 60.17 | 58.21 |
| Hydrogen | 4.78 | 4.32 | 4.22 | 4.42 | 4.43 | 3.83 |
| Oxygen | 7.94 | 7.83 | 2.80 | 2.70 | 8.24 | 1.55 |
| Nitrogen | 1.24 | 1.17 | 0.70 | 1.20 | 1.14 | 1.04 |
| Sulfur | 3.46 | 3.79 | 2.96 | 3.46 | 3.68 | 4.24 |
| Ash | 14.90 | 9.36 | 23.58 | 16.43 | 18.01 | 18.41 |
| Moisture | 5.23 | 12.17 | 3.20 | 4.70 | 4.33 | 12.67 |
| Total | 100.00 | 100.00 | 100.00 | 100.00 | 100.00 | 100.00 |
| Higher Heating Value (Btu/lb) | 11,529 | 10,927 | 11,080 | 12,113 | 10,774 | 9,883 |
| **Forms of Sulfur (%)** | | | | | | |
| Sulfatic | 0.24 | 0.00 | 0.00 | 0.01 | 0.00 | 0.00 |
| Pyritic | 2.15 | 1.15 | 1.97 | 0.63 | 1.43 | 2.28 |
| Organic | 1.07 | 2.64 | 0.55 | 0.82 | 2.25 | 2.64 |

Table 3.2 Composite Coal Analyses--Kentucky No. 11; Illinois No. 6; Upper Freeport, Indiana County, Pennsylvania; Lower Freeport, Cambria County, Pennsylvania; Kentucky No. 9, Union County; and Kentucky No. 9, Henderson County

| Description | Kentucky No. 11 | Illinois No. 6 Gallatin County | Upper Freeport Indiana County | Lower Freeport Cambria County | Kentucky No. 9 Union County | Kentucky No. 9 Henderson County |
|---|---|---|---|---|---|---|
| Ash Chemistry (%): | | | | | | |
| $SiO_2$ | 46.3 | 50.9 | 48.6 | 51.3 | 45.3 | 40.0 |
| $Al_2O_3$ | 20.4 | 18.3 | 25.5 | 26.3 | 18.2 | 16.4 |
| $TiO_2$ | 1.1 | 0.9 | 1.1 | 1.4 | 0.9 | 0.8 |
| $Fe_2O_3$ | 21.5 | 18.5 | 16.6 | 10.3 | 17.2 | 20.5 |
| CaO | 4.3 | 4.0 | 2.9 | 3.9 | 5.7 | 7.8 |
| MgO | 0.7 | 1.2 | 0.9 | 0.7 | 0.7 | 1.1 |
| $Na_2O$ | 0.4 | 1.4 | 0.3 | 0.3 | 0.9 | 0.8 |
| $K_2O$ | 2.6 | 2.3 | 2.9 | 2.5 | 2.8 | 2.3 |
| $SO_3$ | 3.6 | 3.3 | 2.8 | 3.4 | 6.7 | 9.4 |
| $P_2O_5$ | 0.3 | 0.3 | 0.4 | 0.3 | 0.4 | 0.1 |
| Ash Fusion (°F) | | | | | | |
| Reducing: | | | | | | |
| Initial Deformation | 2070 | 1980 | 2063 | 2355 | 2061 | 2016 |
| Softening (Sph.) | 2100 | 2030 | 2134 | 2397 | 2170 | 2042 |
| Softening (Hem.) | 2130 | 2080 | 2245 | 2443 | 2368 | 2100 |
| Fluid | 2160 | 2160 | 2460 | 2575 | 2400 | 2111 |
| Oxidizing: | | | | | | |
| Initial Deformation | 2370 | 2280 | 2473 | 2531 | 2115 | 2360 |
| Softening (Sph.) | 2390 | 2320 | 2487 | 2596 | 2420 | 2490 |
| Softening (Hem.) | 2410 | 2350 | 2540 | 2643 | 2420 | 2700 |
| Fluid | 2430 | 2480 | 2585 | 2712 | 2574 | 2700 |
| Percentage Basic | 31.0 | 28.5 | 24.3 | 18.6 | 29.7 | 35.9 |
| Base/Acid Ratio | 0.44 | 0.38 | 0.32 | 0.22 | 0.43 | 0.56 |
| Slagging Index (B/A x %S) | 1.44 (Med.) | 1.29 (Med.) | 0.92 (Med.) | 0.31 (Low) | 1.63 (Med.) | 2.40 (High) |
| Fouling Factor (B/A x %$Na_2O$) | 0.18 (Low) | 0.54 (Med.) | 0.10 (Med.) | 0.06 (Low) | 0.18 (Low) | 0.448 (Med.) |

## Table 3.3 Summary of Mineral Analysis Determined From Low-Temperature Ash for Five Eastern Bituminous Coals

| Raw Coal and Gravity Fractionation | Kentucky No. 11 | | Illinois No. 6 | | Kentucky No. 9 Union County | | Upper Freeport Indiana County | | Lower Freeport Cambria County | | Kentucky No. 9 Henderson County | |
|---|---|---|---|---|---|---|---|---|---|---|---|---|
| | Major | Minor | Major | Minor | Major | Minor | Major | Minor | Major | Minor | Major | Minor |
| Raw Coal | Quartz Kaolinite Pyrite | Illite Muscovite | Quartz Kaolinite Pyrite | Illite Feldspar | Quartz Kaolinite Pyrite Calcite | Illite | Quartz Kaolinite Pyrite Illite | | Quartz Pyrite Kaolinite Calcite | Muscovite | Quartz Pyrite Kaolinite Calcite | Illite Feldspar H-C* |
| Gravity Fraction | | | | | | | | | | | | |
| +1.30 | Quartz Kaolinite | Muscovite | Quartz Kaolinite Pyrite | Illite | Quartz Kaolinite Pyrite | Illite | Quartz Kaolinite Pyrite | Illite | Quartz Kaolinite | Muscovite | Quartz Kaolinite | Pyrite Calcite Apatite H-C |
| -1.30/+1.85 | Quartz Kaolinite | Muscovite | Quartz Kaolinite Pyrite | Illite | Quartz Kaolinite Pyrite | Illite | Quartz Kaolinite Pyrite Illite | Calcite | Quartz Kaolinite | Muscovite | Quartz Pyrite H-C Kaolinite | Illite Apatite Calcite |
| -1.80/+2.85 | Quartz Kaolinite Pyrite | Illite Muscovite | Quartz Kaolinite Pyrite | Calcite Illite | Insufficient Data | | Quartz Kaolinite Pyrite Illite | Calcite | Quartz Kaolinite Pyrite | Muscovite | Quartz Pyrite H-C Kaolinite | Illite Apatite Calcite |
| -2.85 | Insufficient Sample | | Insufficient Sample | | Quartz Kaolinite Pyrite | Illite | | | Quartz Kaolinite Pyrite Calcite | Muscovite | Pyrite Calcite | Marcasite |

*Alleghanite-Clinoptilolite.

Based on an assumption that the ash would behave in a homogeneous fashion, deposits formed while firing this coal should be quite voluminous because of the large temperature range over which the ash is plastic and apparently quite viscous.

The coal was fractionated into four size fractions (+105, -105/+74, -74/+44, and -44 μm) as shown in Figure 3.1, and each size fraction was further divided into four gravity fractions (+1.30, +1.80/-1.30, +2.85/-1.80, and -2.85). Each size and gravity fraction was weighed, ashed, and analyzed for pyritic sulfur, ash chemistry, and ash fusion temperatures. Thermogravimetric analysis (TGA) was performed on each sample to be certain that no individual species had unusual combustion characteristics as a result of partitioning of maceral groups and to determine the contribution of pyrite to the combustion profile. The coarse size fraction was low-temperature ashed for mineral and thermal analyses. This work is not yet complete.

The weight, ash concentration, and pyrite concentration are summarized in Table 3.4. The ash chemistry of the individual size and gravity fractions is summarized in Table 3.5. The ASTM ash fusion temperatures of the fractionated coal appear in Table 3.6. For interpretation, the data have been plotted in Figure 3.2 on a curve illustrating the relationship between ash softening temperature under reducing conditions and ash chemistry expressed in terms of the percentage of basic constituents [i.e., $\Sigma$ $Fe_2O_3$ + CaO + MgO + $Na_2O$ + $K_2O$)]. In

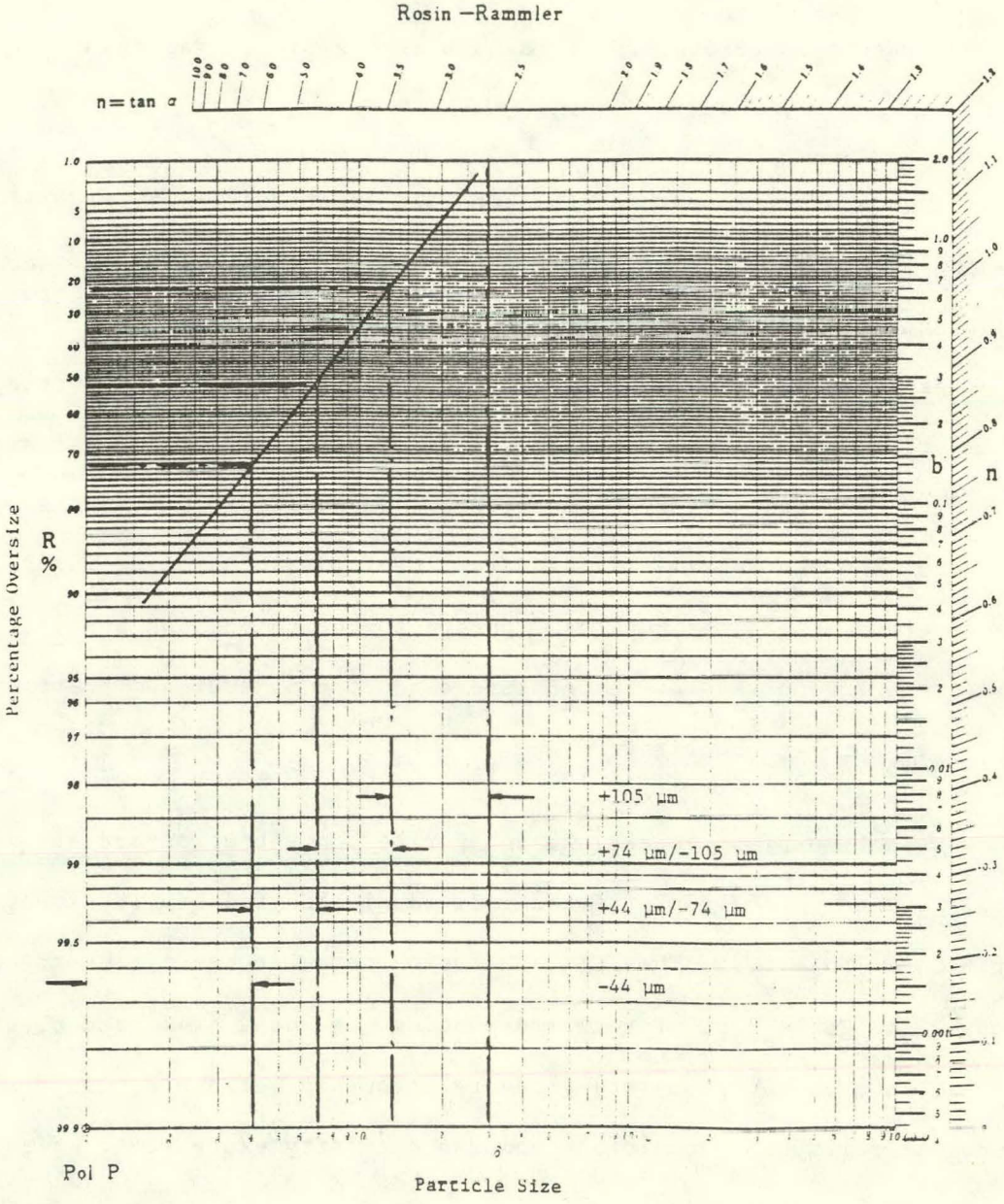


Figure 3.1 Size Distribution of Pulverized Coal Used in Fractionation Analysis

Table 3.4 Ash Chemistry for Size and Gravity Fractionated Pulverized Kentucky No. 9 Coal, Henderson County, Kentucky

| Density Fraction | Wt% | Ash (%) | Total Ash (%) | Cumulative Ash (%) | Pyritic Sulfur(%) | Total Pyritic Sulfur (%) | Cumulative Pyritic Sulfur (%) |
|---|---|---|---|---|---|---|---|
| Size: -105 μm Wt%: 21.3 | | | | | | | |
| Float-Sink | | | | | | | |
| +1.30 | 55.6 | 10.20 | 5.67 | 5.67 | 0.18 | 0.10 | 0.10 |
| +1.80/-1.30 | 37.2 | 9.28 | 3.45 | 9.12 | 0.14 | 0.05 | 0.15 |
| +2.85/-1.80 | 4.0 | 64.06 | 2.56 | 11.68 | 1.45 | 0.06 | 0.21 |
| -2.85 Sink | 3.2 | 69.54 | 2.23 | 13.91 | 38.53 | 0.16 | 0.37 |
| Size: -105/+74 μm Wt%: 30.2 | | | | | | | |
| Float-Sink | | | | | | | |
| +1.30 | Insufficient Sample | | | | | | |
| +1.80/-1.30 | 86.0 | 9.67 | 8.32 | 8.32 | 0.17 | 0.15 | 0.15 |
| +2.85/-1.80 | 12.0 | 67.71 | 8.13 | 16.45 | 5.11 | 0.61 | 0.76 |
| -2.85 Sink | 2.0 | 62.67 | 1.25 | 17.70 | 48.65 | 0.26 | 1.02 |
| Size: -74/+44 μm Wt%: 20.8 | | | | | | | |
| Float-Sink | | | | | | | |
| +1.30 | Insufficient Sample | | | | | | |
| +1.80/-1.30 | 90.5 | 12.48 | 11.29 | 11.29 | 0.35 | 0.32 | 0.32 |
| +2.85/-1.80 | 6.9 | 72.64 | 5.01 | 16.31 | 2.79 | 0.19 | 0.51 |
| -2.85 Sink | 2.6 | 63.09 | 1.64 | 17.95 | 46.92 | 0.13 | 0.64 |
| Size: -44 μm Wt%: 27.7 | | | | | | | |
| Float-Sink | | | | | | | |
| +1.30 | Insufficient Sample | | | | | | |
| +1.80/-1.30 | 88.1 | 17.97 | 15.83 | 15.83 | 0.33 | 0.29 | 0.29 |
| +2.85/-1.80 | 11.2 | 70.96 | 7.95 | 23.78 | 1.64 | 0.18 | 0.47 |
| -2.85 Sink | 0.7 | 64.34 | 0.45 | 24.23 | 43.17 | 0.03 | 0.50 |

*These values were estimated based on the percentage of iron in the pyrite and the percentage of iron in the ash. All iron in the coal was assumed to be concentrated in the pyrite.

Table 3.5 Ash Chemistry--Size and Gravity Fractionated Pulverized Kentucky No. 9 Coal, Henderson County

| Density Fraction | Ash (%) | Pyritic Sulfur (%) | Ash Chemistry (% of Total) | | | | | | | | | |
|---|---|---|---|---|---|---|---|---|---|---|---|---|
| | | | $SiO_2$ | $Al_2O_3$ | $TiO_2$ | $Fe_2O_3$ | CaO | MgO | $Na_2O$ | $K_2O$ | $SO_3$ | $P_2O_5$ |
| Size: +105 µm<br>Wt% : 21.3 | | | | | | | | | | | | |
| +1.30 | 10.20 | 0.18 | 55.2 | 21.0 | 1.2 | 8.7 | 4.8 | 0.8 | 6.0 | 2.5 | 1.4 | 0.1 |
| +1.80/-1.30 | 9.28 | 0.14 | 53.4 | 22.1 | 1.2 | 13.8 | 3.6 | 0.7 | 2.2 | 2.5 | 1.8 | 0.1 |
| +2.85/-1.80 | 64.06 | 1.45 | 53.1 | 18.0 | 0.6 | 18.0 | 4.1 | 0.7 | 1.6 | 2.8 | 0.7 | 0.1 |
| -2.85 Sink | 69.54 | 4.93 | 8.7 | 2.9 | 0 | 69.4 | 10.5 | 0.2 | 0.2 | 0.4 | 8.6 | 0.3 |
| Size: -105/+74 µm<br>Wt%: 30.2 | | | | | | | | | | | | |
| Float-Sink<br>+1.30 | Insufficient Sample | | | | | | | | | | | |
| +1.80/-1.30 | 9.67 | 0.17 | 55.8 | 22.3 | 1.4 | 8.9 | 5.4 | 0.9 | 3.4 | 2.4 | 1.1 | 0.1 |
| +2.85/-1.80 | 67.71 | 5.11 | 55.1 | 18.2 | 0.6 | 11.6 | 6.0 | 0.6 | 2.0 | 2.5 | 4.7 | 0.1 |
| -2.85 Sink | 62.67 | 13.10 | 3.8 | 3.5 | 0 | 92.2 | 0.6 | 0.1 | 0.1 | 0.3 | 0.2 | 0.2 |
| Size: -74/+44 µm<br>Wt%: 20.8 | | | | | | | | | | | | |
| Float-Sink<br>+1.30 | Insufficient Sample | | | | | | | | | | | |
| +1.80/-1.30 | 12.48 | 0.35 | 56.7 | 21.1 | 1.0 | 8.5 | 5.0 | 0.8 | 3.2 | 2.4 | 1.0 | 0.1 |
| +2.85/-1.80 | 72.64 | 2.79 | 52.0 | 18.0 | 0.6 | 14.5 | 6.3 | 0.7 | 1.7 | 2.6 | 3.7 | 0.1 |
| -2.85 Sink | 63.09 | 4.81 | 6.2 | 2.7 | 0 | 88.5 | 0.9 | 0.1 | 0.3 | 0.3 | 1.1 | 0.2 |
| Size: -44 µm<br>Wt%: 27.7 | | | | | | | | | | | | |
| Float-Sink<br>+1.30 | Insufficient Sample | | | | | | | | | | | |
| +1.80/-1.30 | 17.97 | 0.33 | 59.3 | 22.1 | 1.0 | 6.5 | 4.9 | 0.8 | 3.1 | 2.4 | 0.7 | 0.1 |
| +2.85/-1.80 | 70.96 | 1.64 | 54.0 | 17.2 | 0.6 | 17.3 | 4.5 | 0.5 | 1.8 | 2.4 | 2.8 | 0.1 |
| -2.85 Sink | 64.36 | 4.92 | 6.2 | 2.5 | 0.2 | 86.3 | 2.8 | 0.1 | 0.3 | 0.3 | 1.8 | 0.3 |

Table 3.6 Ash Fusion Temperatures--Size and Gravity Fractionated Pulverized Kentucky No. 9 Coal, Henderson County

| Density Fraction | Reducing (°F) | | | | Oxidizing (°F) | | | |
|---|---|---|---|---|---|---|---|---|
| | I.D. | Softening (Sph.) | Softening (Hem.) | F.T. | I.D. | Softening (Sph.) | Softening (Hem.) | F.T. |
| **Size: +105 μm Wt%: 21.3** | | | | | | | | |
| Float-Sink | | | | | | | | |
| +1.30 | 2030 | 2050 | 2130 | 2220 | 2300 | 2340 | 2370 | 2420 |
| +1.80/-1.30 | 2040 | 2100 | 2140 | 2210 | 2310 | 2420 | 2480 | 2510 |
| +2.85/-1.80 | 2030 | 2060 | 2100 | 2150 | 2310 | 2360 | 2370 | 2420 |
| -2.85 Sink | 2070 | 2130 | 2260 | 2300 | 2320 | 2440 | 2520 | 2550 |
| **Size: -105/+74 μm Wt%: 30.2** | | | | | | | | |
| Float-Sink | | | | | | | | |
| +1.30 | Insufficient Sample | | | | | | | |
| +1.80/-1.30 | 2150 | 2190 | 2300 | 2390 | 2380 | 2420 | 2540 | 2600 |
| +2.85/-1.80 | 2130 | 2170 | 2270 | 2350 | 2370 | 2410 | 2510 | 2590 |
| -2.85 Sink | 2440 | 2460 | 2510 | 2540 | 2580 | 2600+ | 2600+ | 2600+ |
| **Size: -74/+44 μm Wt%: 20.8** | | | | | | | | |
| Float-Sink | | | | | | | | |
| +1.30 | Insufficient Sample | | | | | | | |
| +1.80/-1.30 | 2160 | 2250 | 2280 | 2300 | 2270 | 2320 | 2400 | 2480 |
| +2.85/-1.80 | 2080 | 2170 | 2200 | 2360 | 2190 | 2290 | 2411 | 2500 |
| -2.85 Sink | 2280 | 2330 | 2390 | 2430 | 2390 | 2460 | 2500 | 2550 |
| **Size: -44 μm Wt%: 27.7** | | | | | | | | |
| Float-Sink | | | | | | | | |
| +1.30 | Insufficient Sample | | | | | | | |
| +1.80/-1.30 | 2060 | 2140 | 2200 | 2210 | 2240 | 2300 | 2360 | 2440 |
| +2.85/-1.80 | 2200 | 2230 | 2300 | 2310 | 2310 | 2360 | 2440 | 2500 |
| -2.85 Sink | 2250 | 2180 | 2420 | 2540 | 2310 | 2420 | 2550 | 2575 |

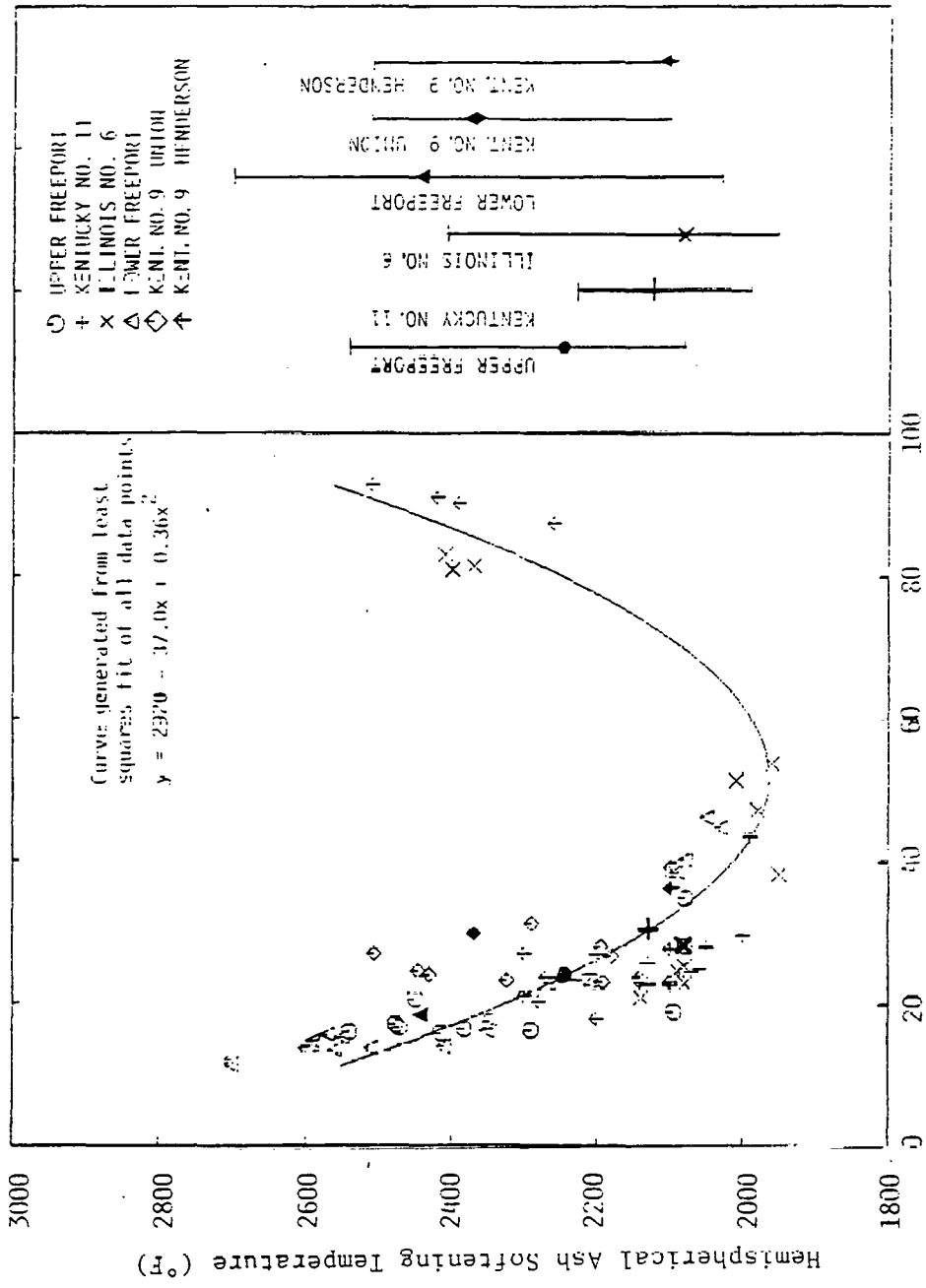


Figure 3.2 Relationship Between Ash Softening Temperature and Percentage of Basic Constituents in Ash for All Size and Gravity Fractionated Coals Examined

Figure 3.3 these data are quantified with regard to the weight of ash in the individual size and gravity fractions. Figure 3.4 illustrates the distribution of iron between the liberated ash and the lighter coal fractions.

The variability of the ash softening temperature in the fractionated coal species of Kentucky No. 9 from Henderson County is less than either of the Freeport coals from Pennsylvania, greater than either Illinois No. 6 or Kentucky No. 11, and identical to Kentucky No. 9, Union County, mined only a few miles away. The distribution of mineral matter within the two Kentucky No. 9 coals is decidedly different. Kentucky No. 9 from Henderson County is the only coal in which the softening temperatures of the fractionated coal ash species are all greater than the composite coal ash, illustrating good partitioning of the pyrite from other mineral matter. The heaviest gravity fractions are highly basic and are composed of the highest purity pyritic iron (see Figure 3.2 and Table 3.5). The fusibility diagram in Figure 3.3 suggests the liberated pyrite is concentrated in the coarse size fractions. In all the previous coals analyzed, the liberated pyrite was concentrated in the fines. At least two coals revealed very little liberation of pyrite. The distribution of pyrite among the weighted coal fractions, appearing in Figure 3.4, suggests the pyrite size in the raw coal is bimodal, accounting for the decrease in liberated pyrite with a reduction in particle size and an increase in nonliberated pyrites--also with a reduction in size. Figures 3.5 through 3.9 illustrate the distribution of pyritic iron in the other coals analyzed by size and gravity, permitting a direct comparison of liberated pyrite by size with that of Kentucky No. 9, Henderson County.

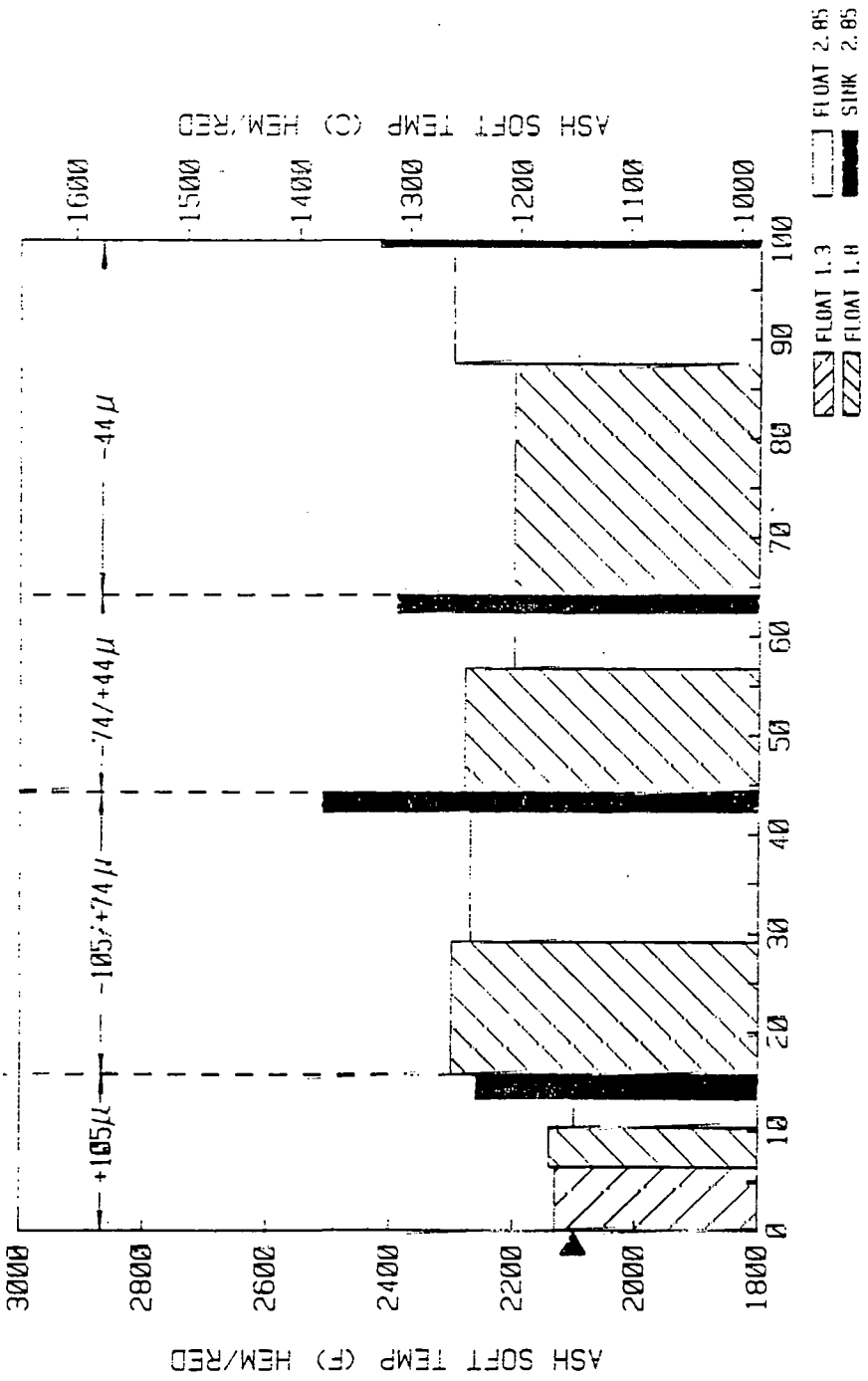


Figure 3.3 Fusibility Diagram--Kentucky No. 9 Coal, Henderson County

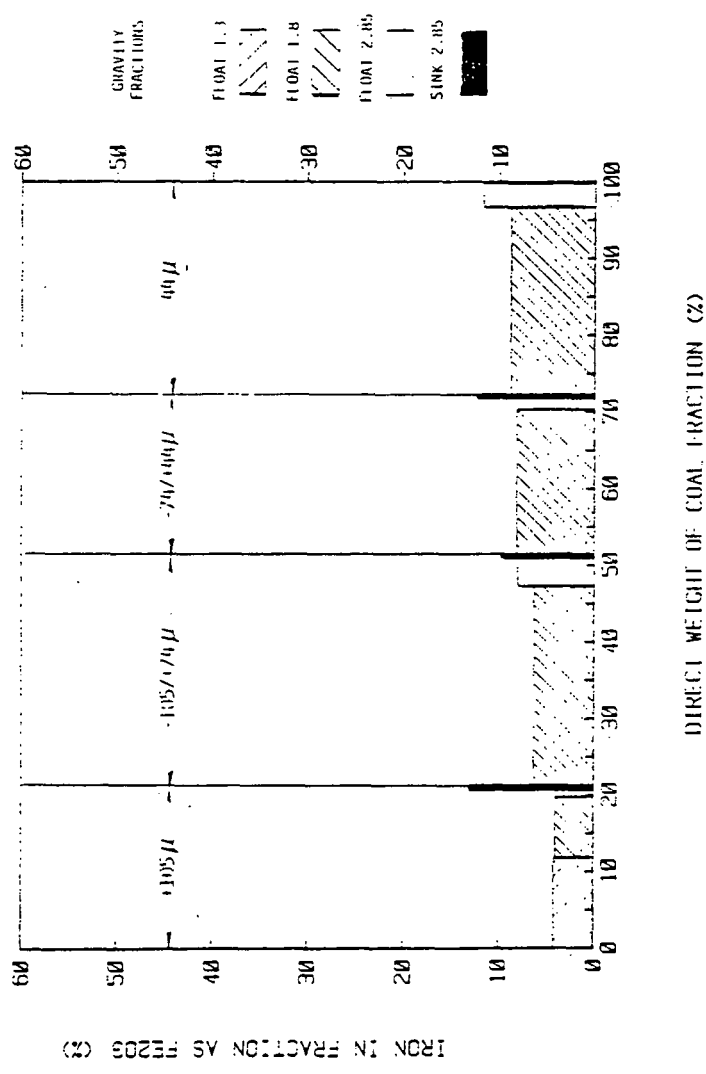


Figure 3.4 Distribution of Iron by Size and Gravity in Fractionated Kentucky No. 9 Coal, Henderson County

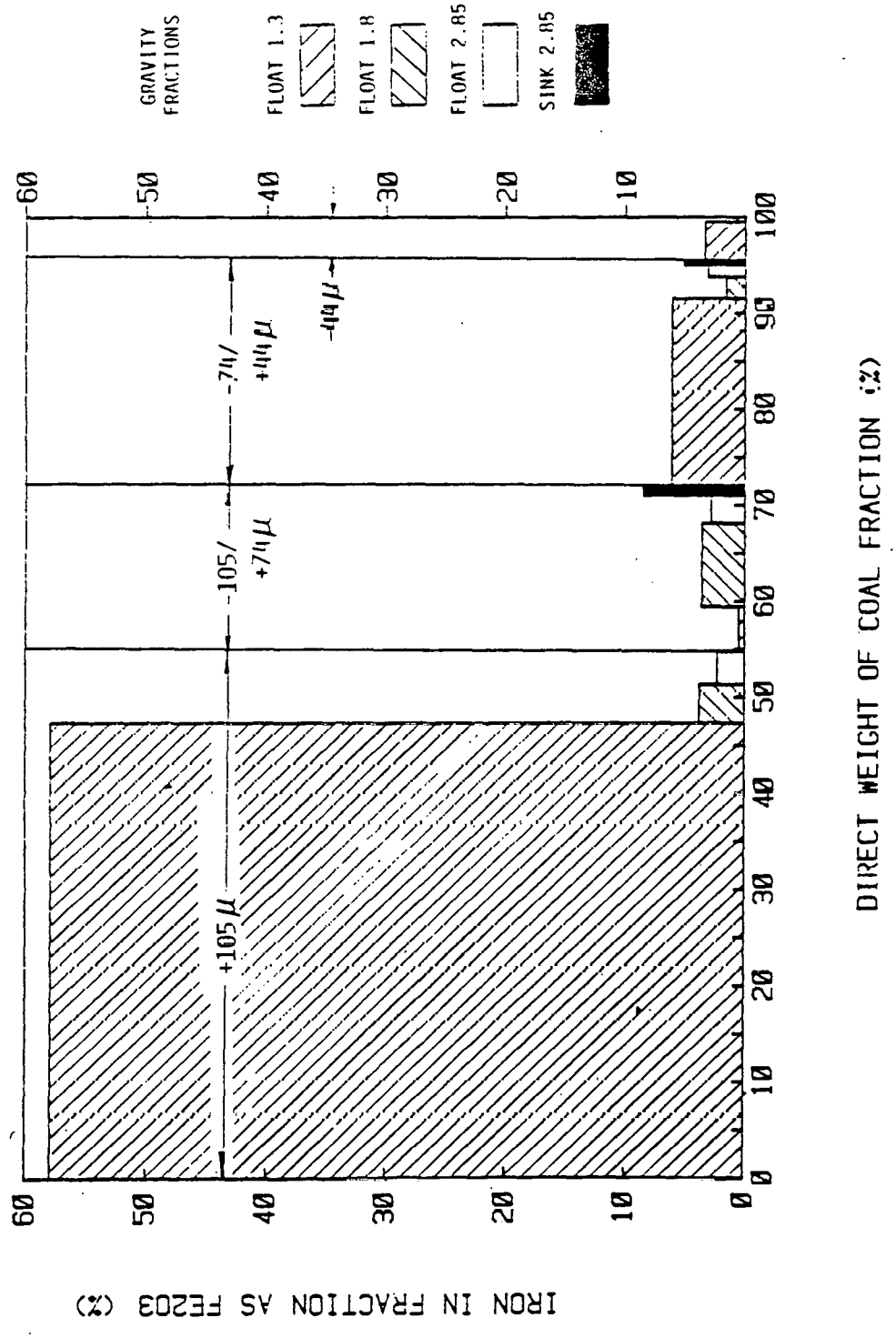


Figure 3.5 Distribution of Iron by Size and Gravity in Fractionated Kentucky No. 11 Coal

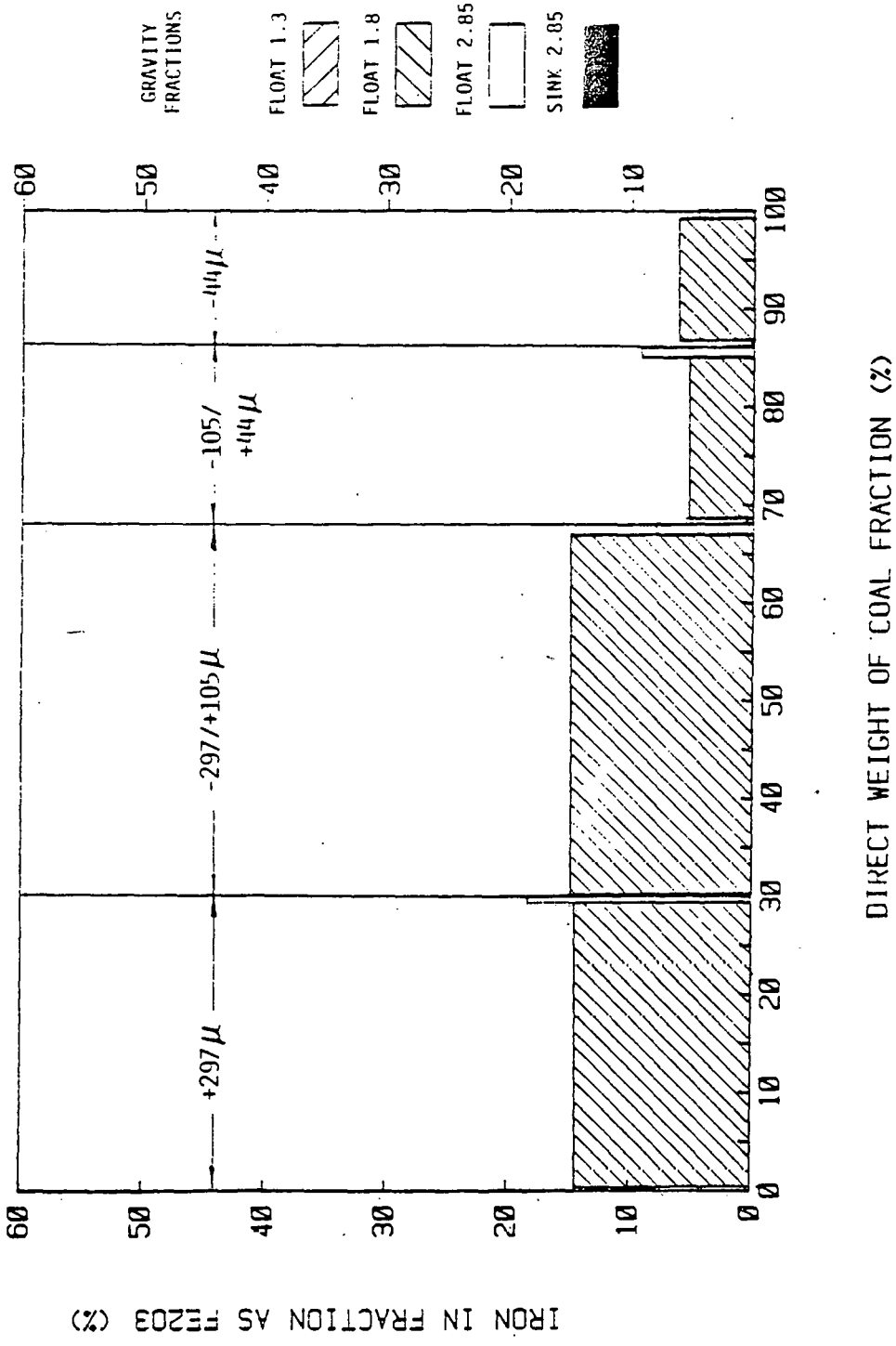


Figure 3.6 Distribution of Iron by Size and Gravity in Fractionated Illinois No. 6 Coal

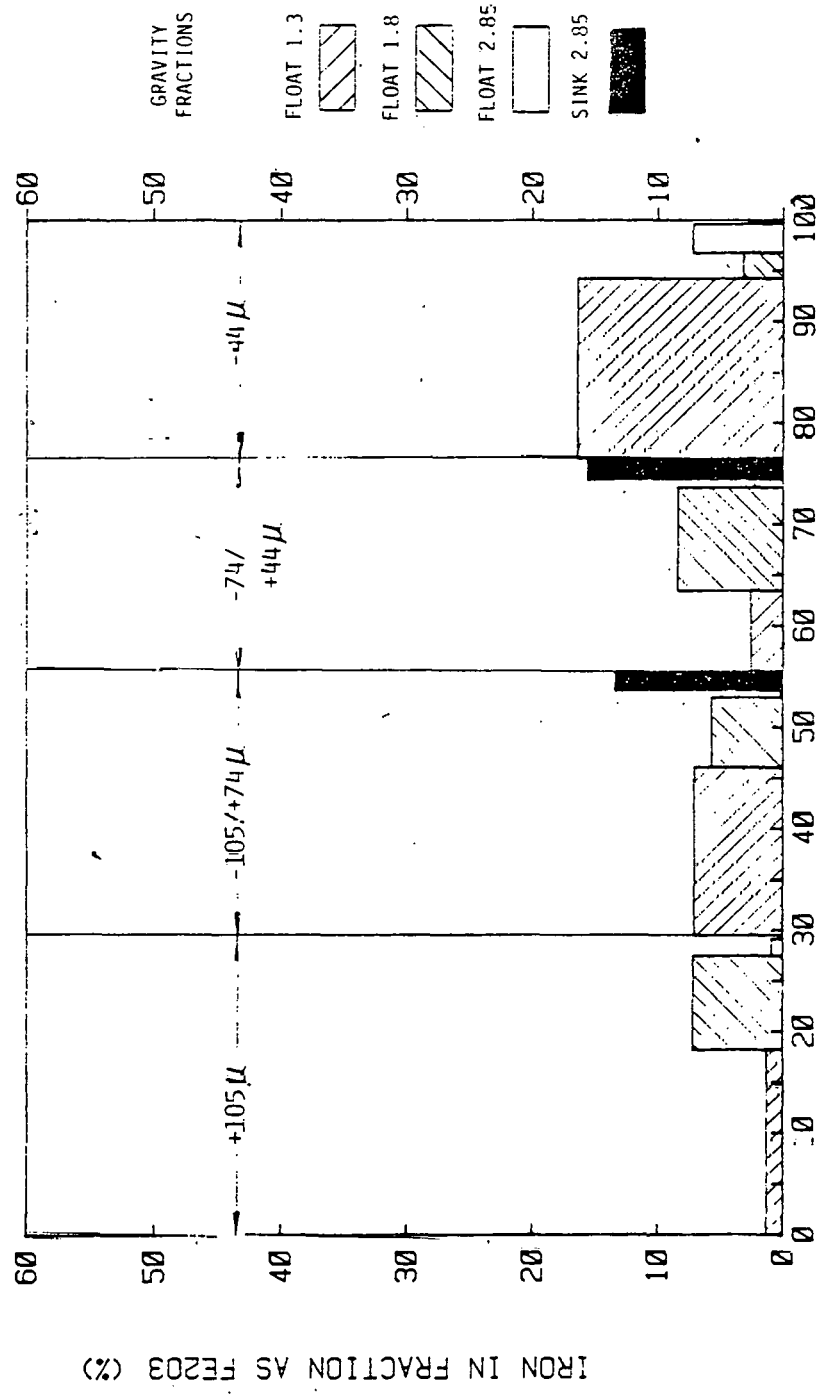


Figure 3.7 Distribution of Iron by Size and Gravity in Fractionated Kentucky No. 9 Coal, Union County

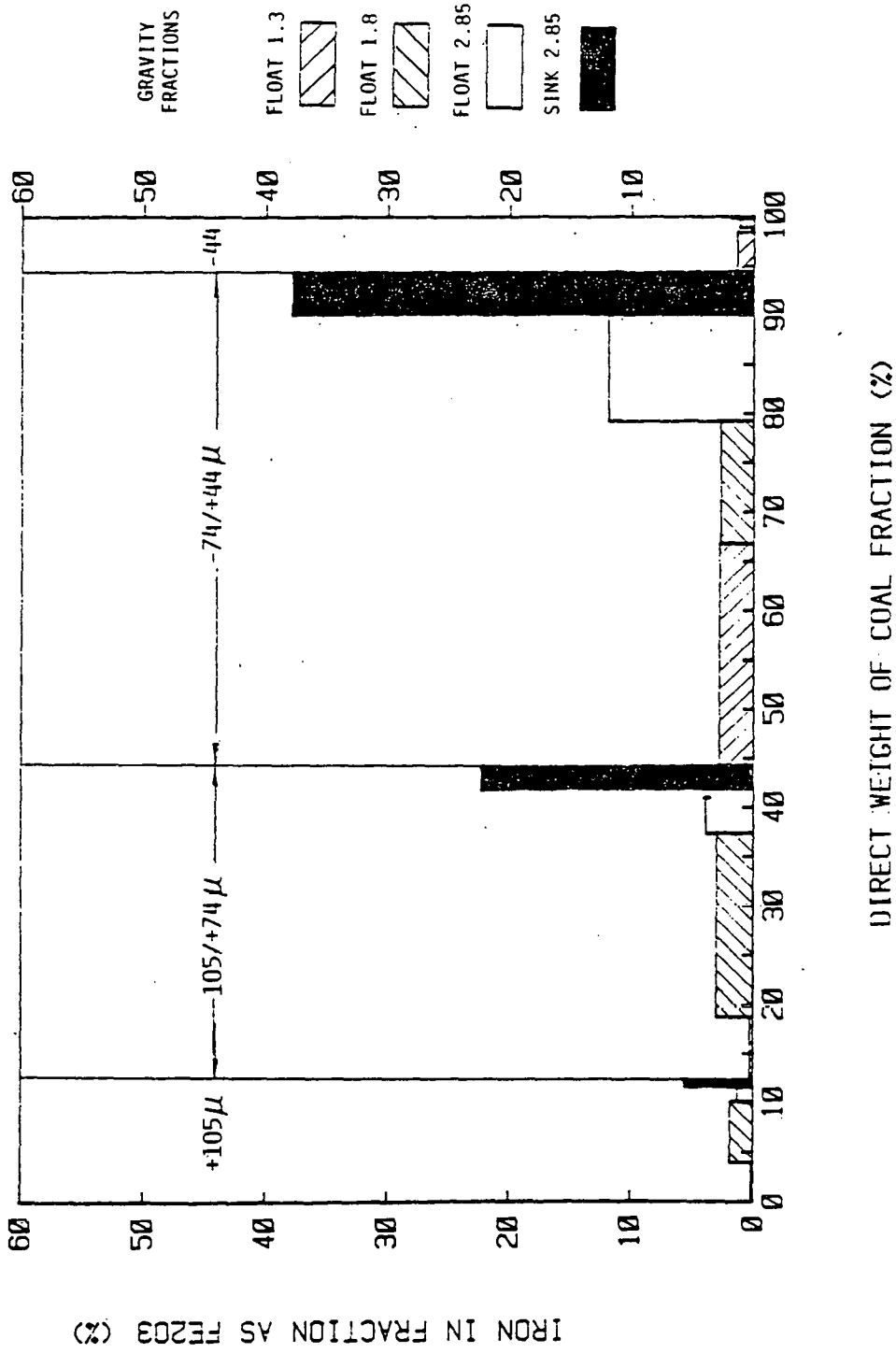


Figure 3.8 Distribution of Iron by Size and Gravity in Fractionated Lower Freeport Coal

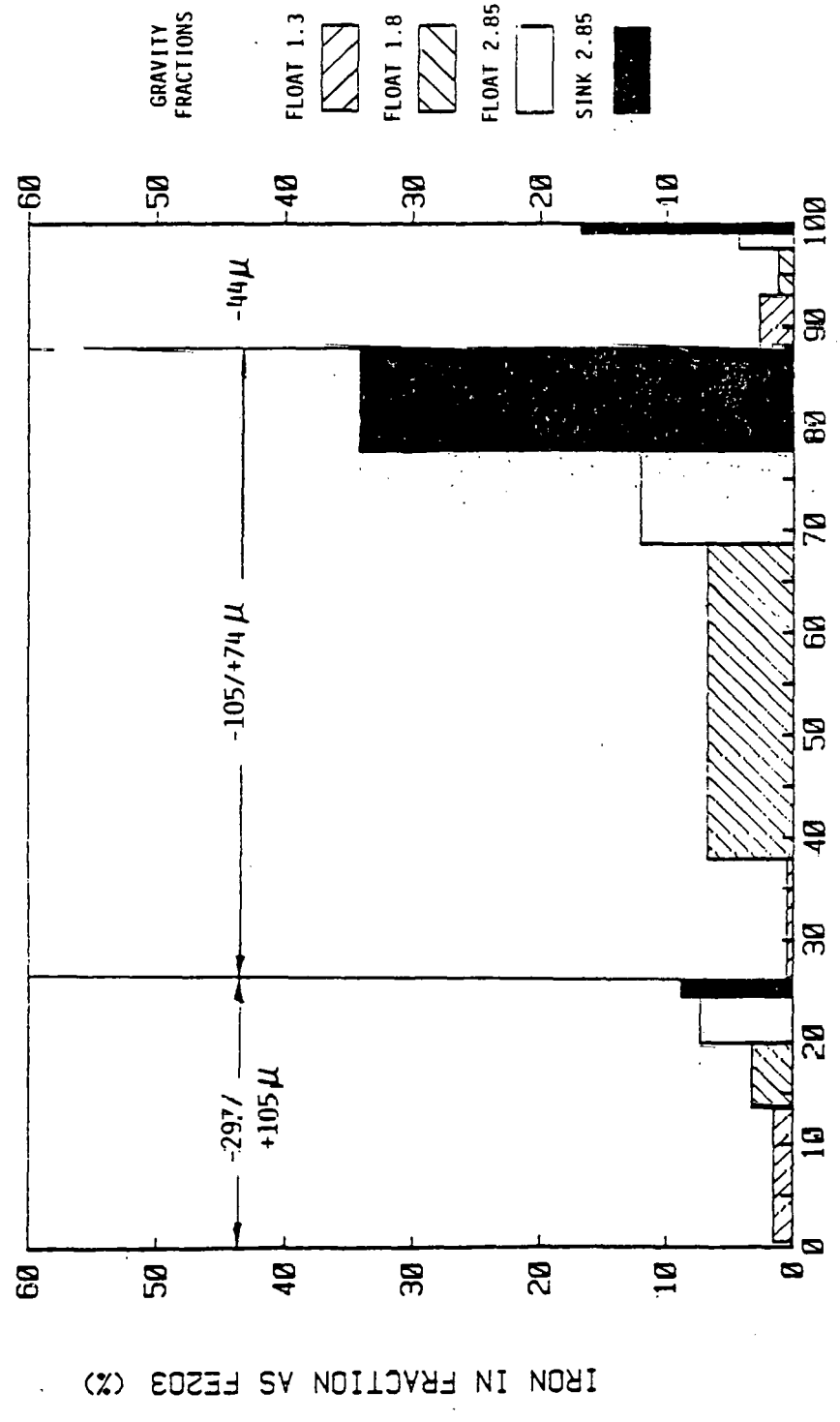


Figure 3.9 Distribution of Iron by Size and Gravity in Fractionated Upper Freeport Coal

The analysis of the size and gravity fractionated coal indicates Kentucky No. 9, Henderson County, has the greatest potential for producing iron-segregated deposits at the furnace exit, based on the quantity of iron liberated in the coarse size fraction. Since deposition is believed to be dependent upon the combustibility of pyrite and burnout time required, in addition to the total quantity of coarse pyrite liberated, further assessment of the formation of iron-enriched deposit formation must be made by examining TGA combustion profiles. TGA thermograms will be reviewed in the following section.

During earlier combustion tests, we learned that furnace wall slagging of surfaces subjected to axially symmetric flow at low velocities was initiated by ash with high levels of potassium. Subsequent deposit growth and advanced stages of slagging were dependent upon the physicochemical properties of the sink 1.80 gravity fractions and their concentration levels in the coal. Table 3.7 summarizes the initial deformation temperatures, fluid temperatures, and the ash/lb coal fired for the -1.80/+2.85 gravity fraction. The coals are listed according to the degree of slagging. The coals causing the least slagging are tabulated on the far left; those causing the most severe slagging, on the far right. Except for the ash from the Lower Freeport -1.80/+2.85 coal gravity fraction, the initial deformation temperatures of all ashed species are 2050°F ± 150°F. Variations in the fluid temperature are somewhat greater. Kentucky No. 11 and Illinois No. 6 caused the least slagging, even though the initial deformation temperatures were 50 to 145°F below the mean value for all heavy gravity fractions. The percentage of ash/lb coal having these low initial deformation temperatures is very low. In fact, the -1.80/+2.85 gravity fraction

of the coals responsible for the least slagging contains approximately one-tenth of the ash/lb coal of the comparable gravity fraction of the most severely slagging coals. Quite apparently, the advanced stage of slagging is more sensitive to ash loading than to the precise ash softening temperature. Under the circumstances, Kentucky No. 9, Henderson County, should cause more severe furnace slagging than Kentucky No. 9, Union County, but less than Lower Freeport, Cambria County.

Unlike any of the preceding coals analyzed, the size and gravity fractionation analysis of Kentucky No. 9, Henderson County, revealed a concentration of sodium as high as 6 percent in the float 1.30 fraction. The form in which it occurs is uncertain. Since carbon is the only other element in the various gravity fractions in a concentration paralleling sodium, there is a good possibility the sodium exists as organically bound mineral matter. However, since chlorine was not determined, there still remains the possibility of sodium occurring as sodium chloride. The presence of sodium silicates as feldspars cannot be discounted, even though there is no obvious correlation between silica and sodium and there is little evidence of liberation of sodium upon pulverizing. The elemental analysis tells us very little about the mineral forms present and thus reveals no information on the change in distribution of silica between the various mineral forms (i.e., kaolinite, quartz, illite, and feldspars). Any correlation of sodium and silica may be masked by variations in distribution among these other mineral forms.

The high sodium level in the float fraction may cause troublesome sintering if, indeed, it is retained on only a portion of the silicates producing fly ash

wetted by a sticky, low-temperature melt. If, on the other hand, sodium vaporizes and recondenses indiscriminately on all fly ash and slag deposit surfaces, the effect of the high concentration of sodium in the float 1.30 fraction should be no different from that of a composite coal ash containing 1.1-percent sodium. An attempt will have to be made to determine the exact form of sodium. There is a potential for unusually high sintered deposit formation at the furnace exit.

TGA was performed on the composite raw coal sample and the individual size and gravity fractions of Kentucky No. 9 coal, Henderson County, to identify any deviations in combustion profile of individual gravity fractions from the composite coal sample that might be the the result of enrichment of pyrite or inertinites. The combustion profiles of samples known to be enriched with pyrite or pure pyrite were compared directly with the composite coal sample and laboratory-grade pyrite to give a qualitative assessment of burnout.

The combustion profile of the composite coal sample is identical to those of Illinois No. 6, Kentucky No. 11, and Kentucky No. 9, Union County, indicating this sample is a very reactive, bituminous coal (see Figure 3.10). The combustion profiles of individual gravity fractions for a given size fraction are compared in Figures 3.11 through 3.14. This bituminous is believed to be quite porous, as were Kentucky No. 11 and Illinois No. 6, permitting the absorption of some of the organics used during the partitioning process. These organics alter the combustion profiles of the lighter fractions during the initial stages of combustion. As indicated by the thermograms, the heaviest gravity fractions are virtually pure pyrite, free of ash.

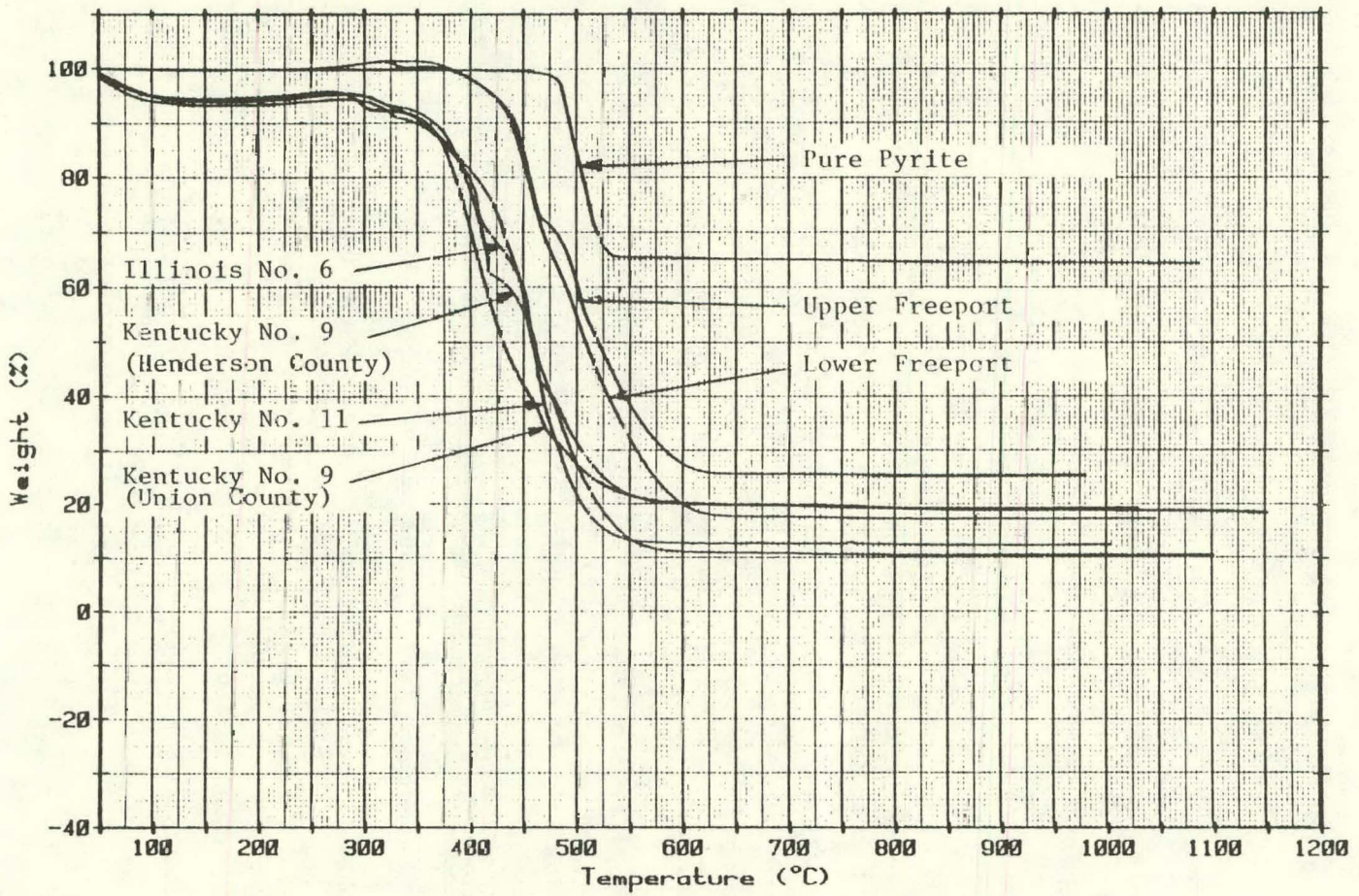


Figure 3.10 Combustion Profile of Pure Pyrite Compared With Profiles of Composite Samples of Various Coals

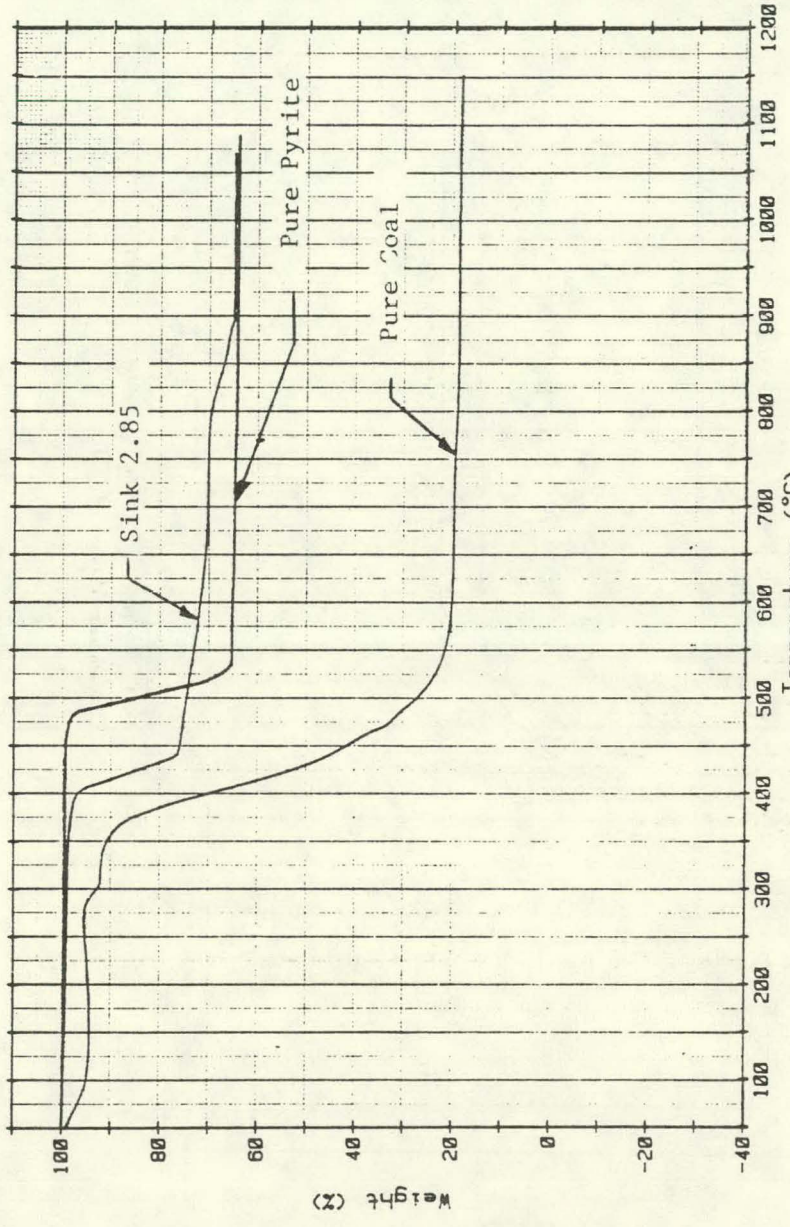


Figure 3.11 Combustion Profiles of Pure Pyrite and Composite Coal Sample Compared With Sink 2.85 Gravity Fraction (+140 mesh) of Kentucky No. 9 Coal, Henderson County

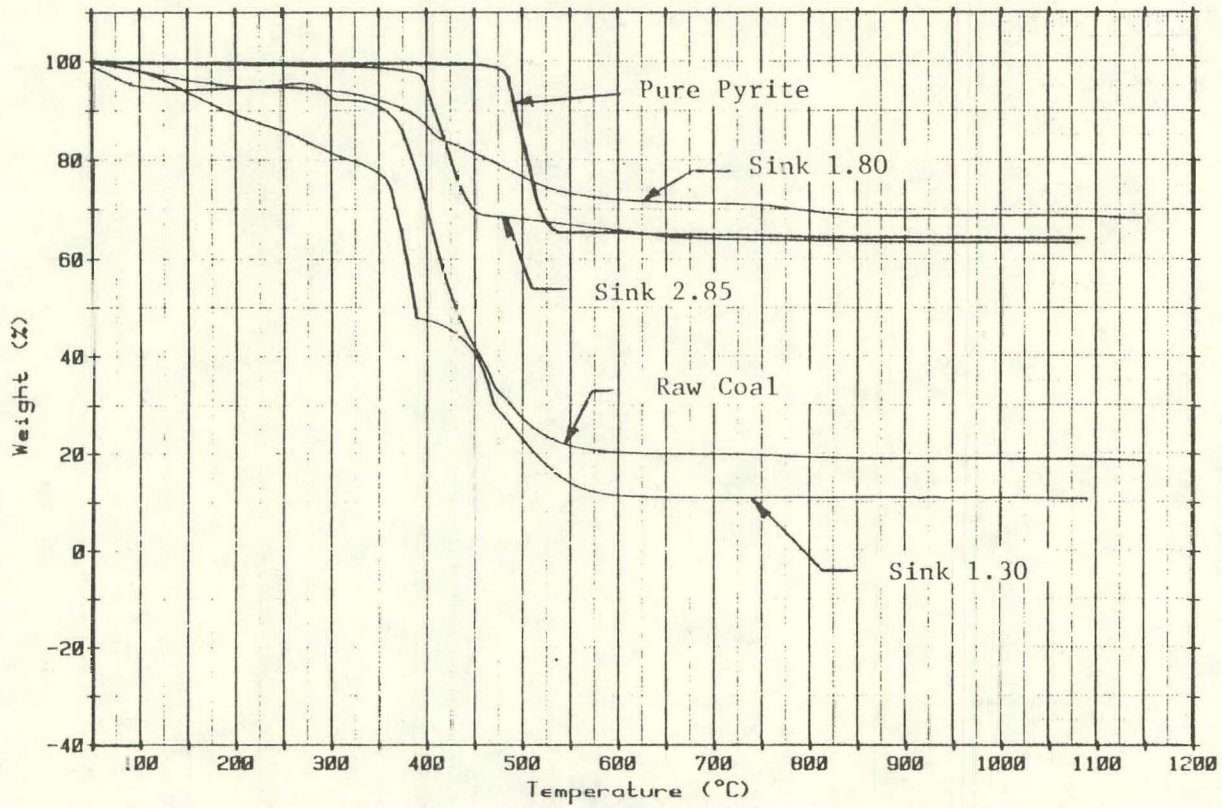


Figure 3.12 Combustion Profiles of Pure Pyrite and Composite Coal Sample Compared With Various Gravity Fractions (-140/+200 mesh) of Kentucky No. 9 Coal, Henderson County

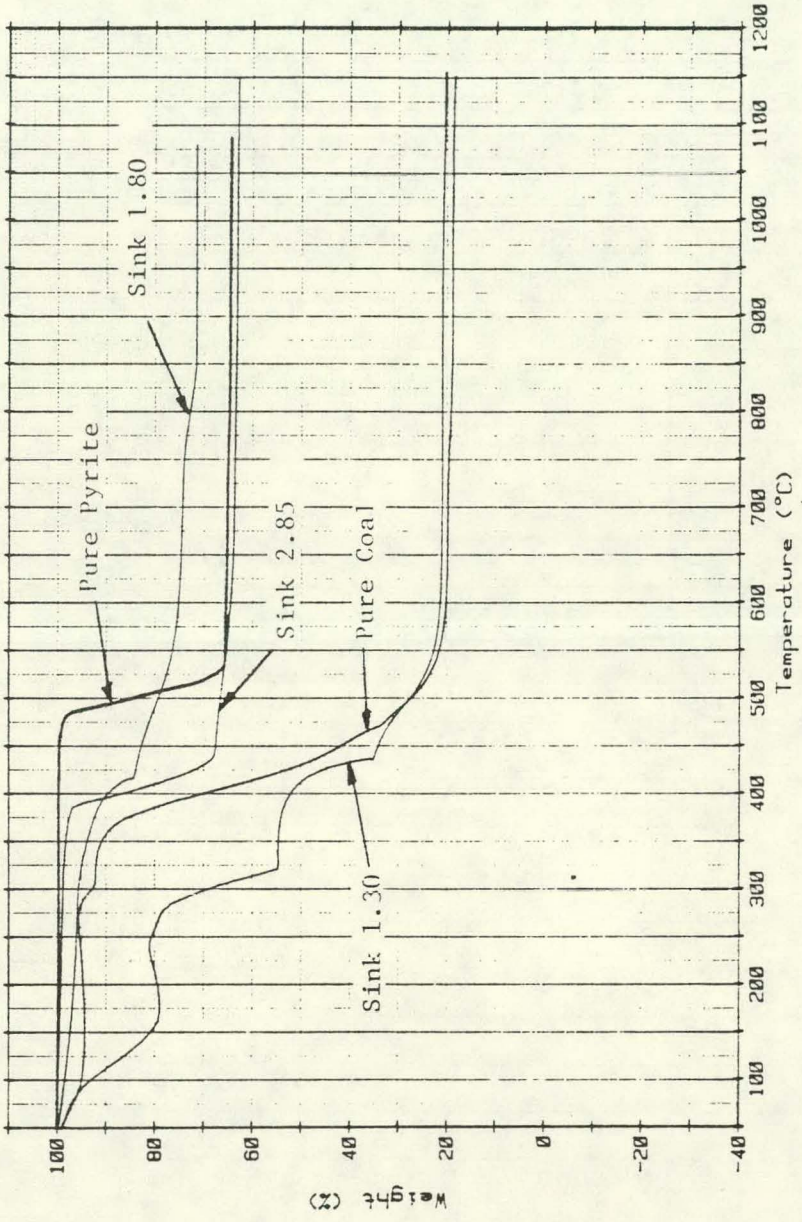


Figure 3.13 Combustion Profiles of Pure Pyrite and Composite Coal Sample Compared With Various Gravity Fractions (-200/+325 mesh) of Kentucky No. 9 Coal, Henderson County

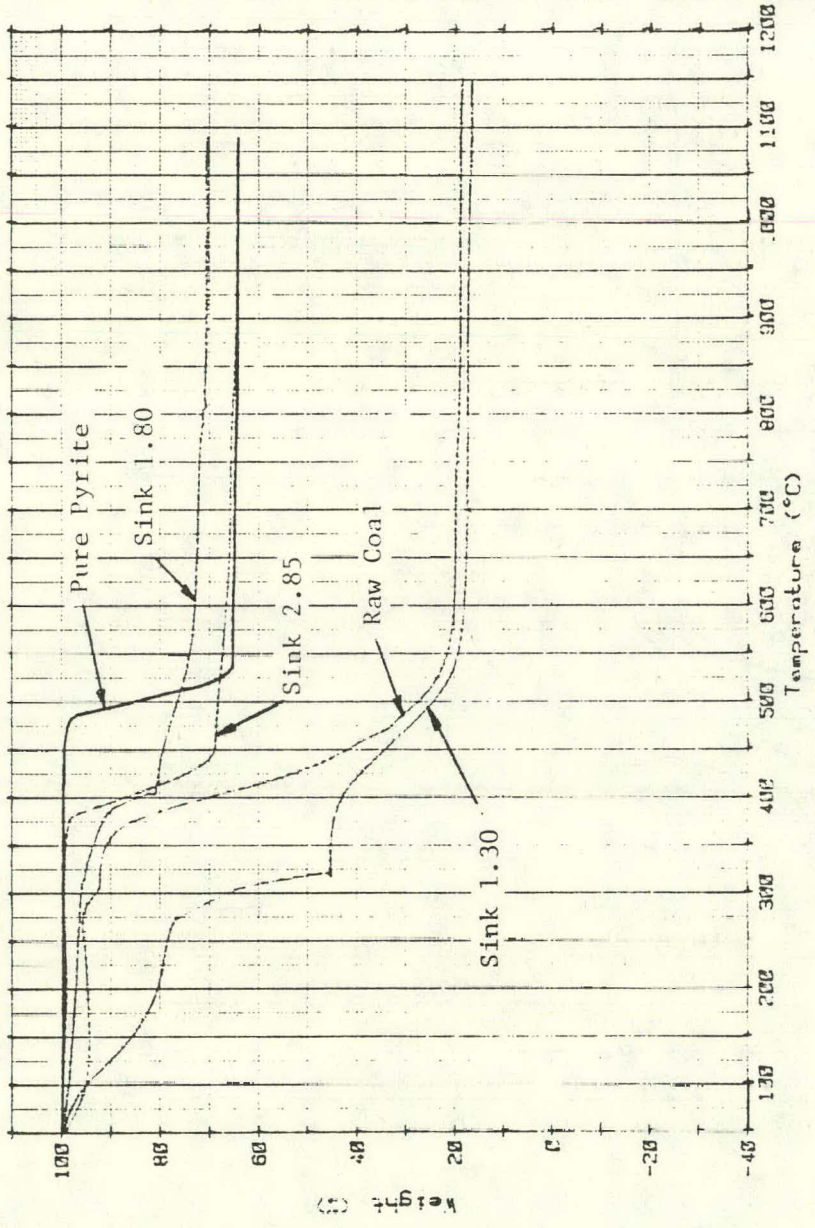


Figure 3.14 Combustion Profiles of Pure Pyrite and Composite Coal Sample Compared With Various Gravity Fractions (-325 mesh) of Kentucky No. 9 Coal, Henderson County

Figure 3.15 compares all the heavy gravity fractions with pure laboratory-grade pyrite. Ignition is improved by almost 100°C, and the weight loss appears to occur at the same rate in a single-step process for about 85 percent of the weight loss. The remaining loss in weight proceeds at a much slower rate and extends burnout by about 150°C. The improvement in ignition may be from trace quantities of carbon or reduced pyrite grain size. The extension of burnout probably results from the formation and ultimate decomposition of FeS in the presence of small quantities of carbon. The burnout time of the slightly lighter of the two heaviest gravity fractions (i.e., -1.80/+2.85) is greatly extended by the presence of small quantities of carbon in the presence of moderate quantities of pyrite.

Figure 3.16 compares the sink 2.85 gravity fraction of Kentucky No. 9, Henderson County, with the sink 2.85 gravity fractions of other coals tested and laboratory-grade pyrite. The combustion profile of pyrite in Kentucky No. 9 from Henderson County compares quite favorably with the combustion profile of pyrite in Kentucky No. 9, Union County, but it differs substantially from the combustion profiles of pyrite from the other coals tested. The difference is probably the result of grain size, adventitious carbon, and chemical composition.

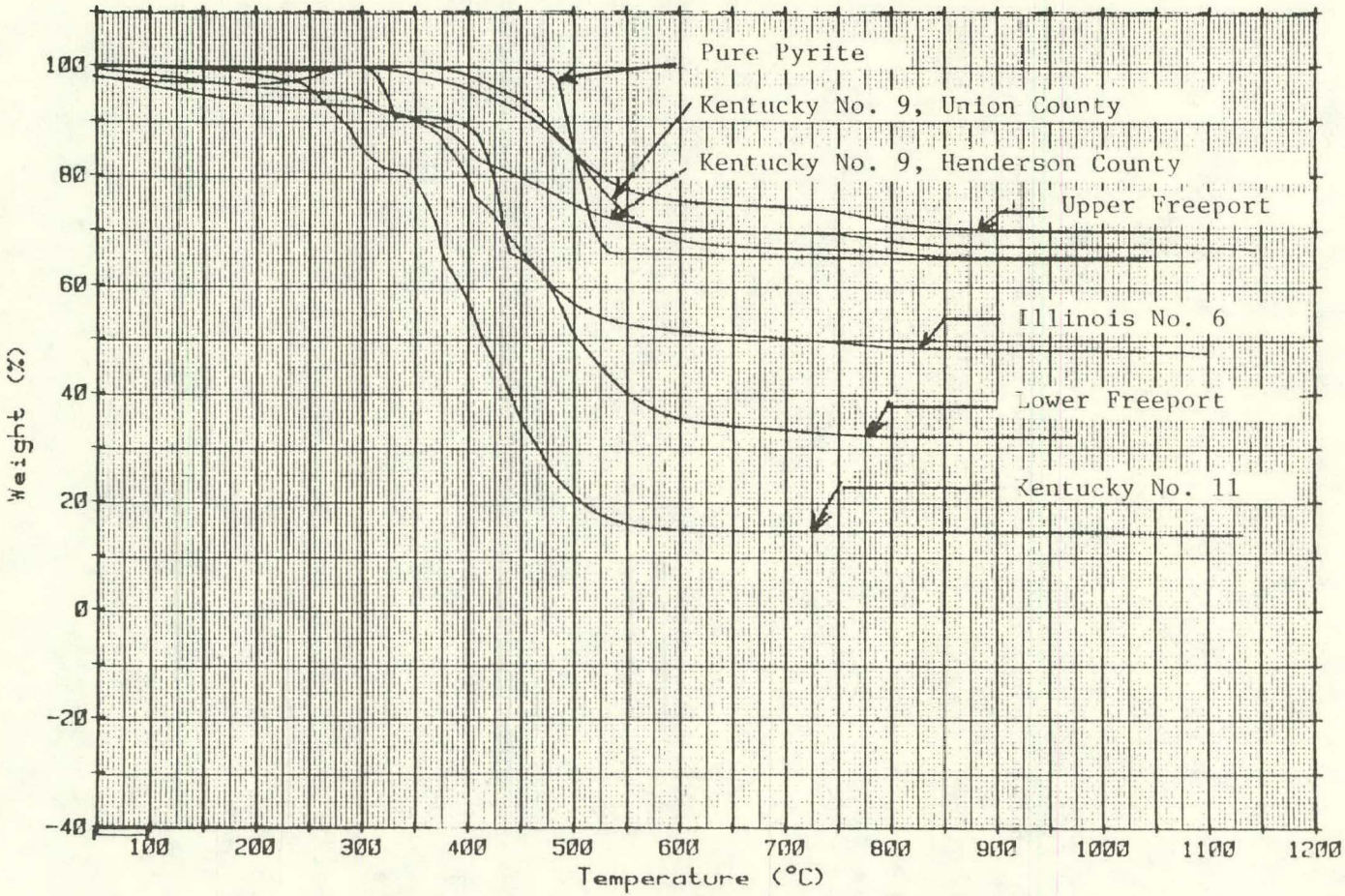


Figure 3.15 Comparison of Combustion Profiles of Pure Pyrite With Those of Heavy Gravity Fractions (-1.80/+2.85) of Various Eastern Bituminous Coals

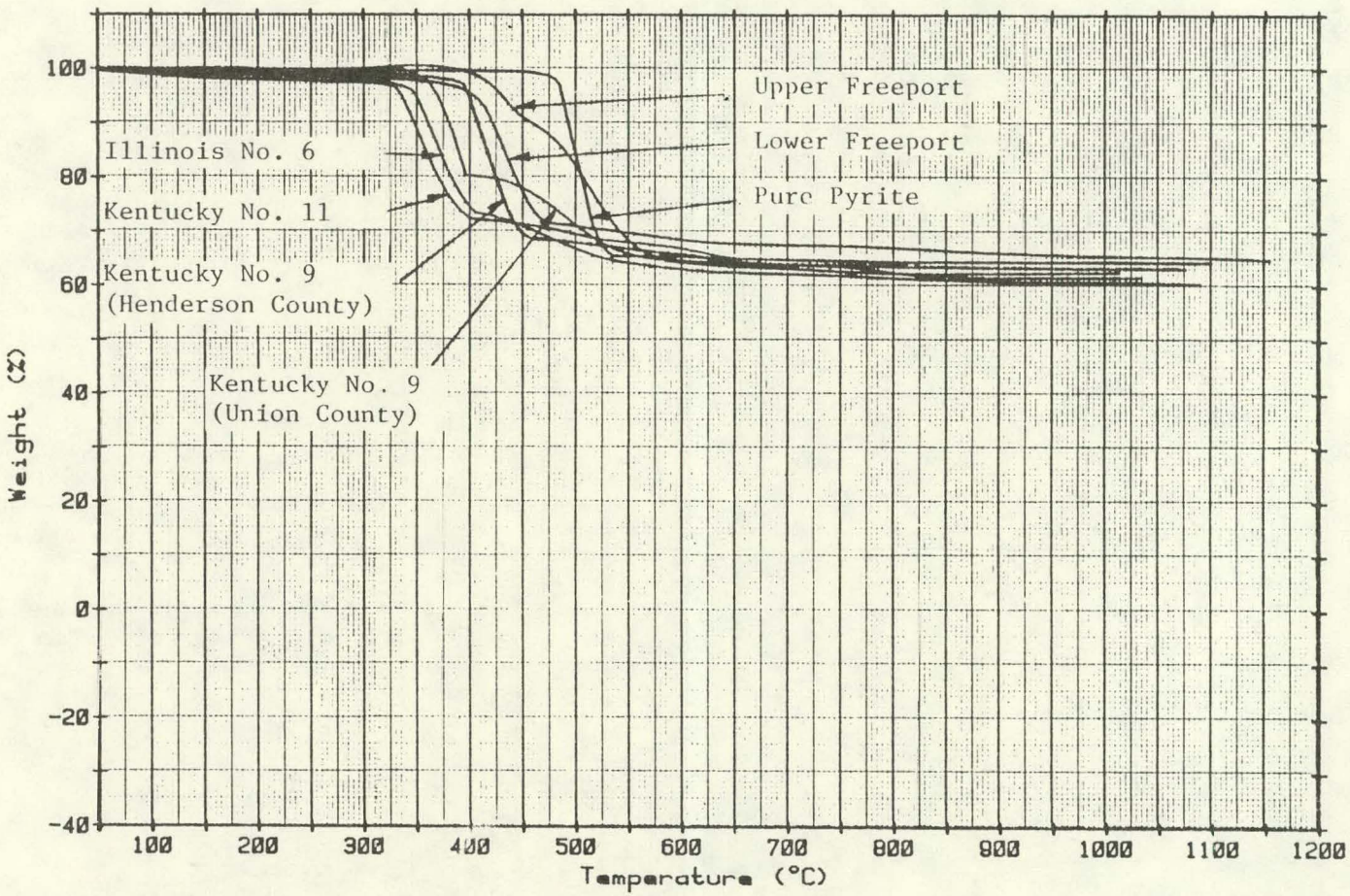


Figure 3.16 Combustion Profile of Pure Pyrite Compared With Profiles of Sink 2.85 Gravity Fractions of Various Coals Characterized

Section 4

# TASKS 3 AND 4--COMBUSTION TESTS AND ANALYSIS OF SLAG DEPOSITS AND FLY ASH

## INTRODUCTION

A combustion test was performed during the fourth quarter of 1983 on Kentucky No. 9 from Henderson County, Kentucky. The pulverized coal was fired at a rate of 100 lb/h for only 3 hours, after which the furnace exit became severely plugged with sintered deposits and the combustor had to be shut down. A second test was performed on the coal for approximately the same length of time, after which the furnace exit once again became severely plugged. During this test the coal was pulverized to 70 percent through 200 mesh. The excess air was set at 19 percent. The furnace exit temperature was maintained at ≈2000°F. Slagging probe surfaces operated at ≈800 to 1000°F, and fouling probe surfaces operated at ≈1000°F. Table 4.1 compares the time-averaged operating conditions of this test with tests of other coals.

A second combustion test was performed using washed Upper Freeport coal from Indiana County, Pennsylvania. The results of these tests will be discussed in Section 5.

## EXPERIMENTAL TEST SET-UP

The experimental test set-up has been described in each of the preceding quarterly reports. For convenience, an abbreviated description is included here.

The combustor is a vertically upward-fired furnace with a horizontal and vertical downward flue gas pass. In addition to the furnace and convective

## Table 4.1 Time-Averaged Operating Conditions

| Measurement Location | Kentucky No. 11 | Illinois No. 6 Gallatin County | Upper Freeport Indiana County | Lower Freeport Cambria County | Kentucky No. 9 Union County | Kentucky No. 9 Henderson County |
|---|---|---|---|---|---|---|
| Furnace Centerline: Segment 3, °F | 2327 | 2401 | 2467 | 2501 | 2409 | 2420 |
| Furnace Exit, °F | 1956 | 1940 | 2002 | 2108 | 1956 | 2010 |
| Flue Duct Upstream of: | | | | | | |
| 1st Fouling Bank, °F | 1678 | 1683 | --- | --- | --- | 1830 |
| 3rd Fouling Bank, °F | 1594 | 1593 | 1574 | 1590 | 1597 | 1623 |
| 4th Fouling Bank, °F | 1372 | 1411 | 1421 | 1561 | 1453 | 1477 |
| Secondary Air Preheat, °F | 281 | 309 | 301 | 312 | 292 | 306 |
| Slagging Probe Tubes, °F | | | | | | |
| Lower Probe | --- | --- | 973 | 955 | 991 | 730 |
| Center Probe | 1052 | 788 | 859 | 912 | 836 | 889 |
| Upper Probe | 877 | 775 | 854 | 848 | 812 | 1093 |
| Fouling Probe Tubes, °F | | | | | | |
| 1st Bank: | | | | | | |
| 1st Tube | 1034 | 979 | 1036 | 1151 | 1022 | 1171 |
| 2nd Tube | 986 | 971 | 993 | 975 | 1019 | 1058 |
| 3rd Tube | 988 | 977 | 1030 | 995 | 957 | 1070 |
| 3rd Bank: 2nd Tube | 729 | 904 | 1003 | 975 | 920 | 1096 |
| 4th Bank: 2nd Tube | 900 | 969 | 995 | 976 | --- | 954 |
| Coal Feed Rate, lb/h | ≈100 | 95 | 102 | 101 | 125 | 129 |
| Combustion Air Flow Rate, lb/h | 1014 | 1010 | 1030 | 1111 | 1110 | 1206 |
| Excess Air, % | --- | 25 | 17 | 15 | 19 | 15 |
| Duration of Run, h | 9.3 | 14 | 14 | 16.2 | 12 | 3 |

pass, the combustion system includes a heat-recovery system, a particulate-emission control system, fans, and associated monitoring and control equipment. Figure 4.1 is a system schematic.

Furnace

The furnace is a cylindrical chamber, 18 ft long x 28 in. in diameter (internal dimensions), designed to simulate the radiant section of a utility steam generator. Nominal, bulk fluid velocity is ≈6.5 ft/s in the furnace zone when firing a typical eastern bituminous coal at 100 lb/h and 15 percent excess air, resulting in a furnace residence time of ≈2.8 seconds (see Figure 4.2).

Flue Pass

Upon leaving the furnace section, flue gases pass into a horizontal duct and over a bank of heat exchange tubes that simulate the convective section of a utility steam generator. The rectangular duct is 7-1/4 in. high x 11-1/4 in. wide. Nominal, bulk fluid velocities of 50 ft/s exist in this section when firing a typical eastern bituminous coal at 100 lb/h and 15 percent excess air.

Ash Deposit Sampling Probes

Fouling Probes. Three fouling probe assemblies collect deposits for examination and analyses. One assembly is in the high-temperature, horizontal gas pass. Two are in the cooler, vertical gas pass. All assemblies can be removed at the end of a test for deposit examination. In addition, the last two probe banks along the flow path are equipped with refractory access plugs for quick service.

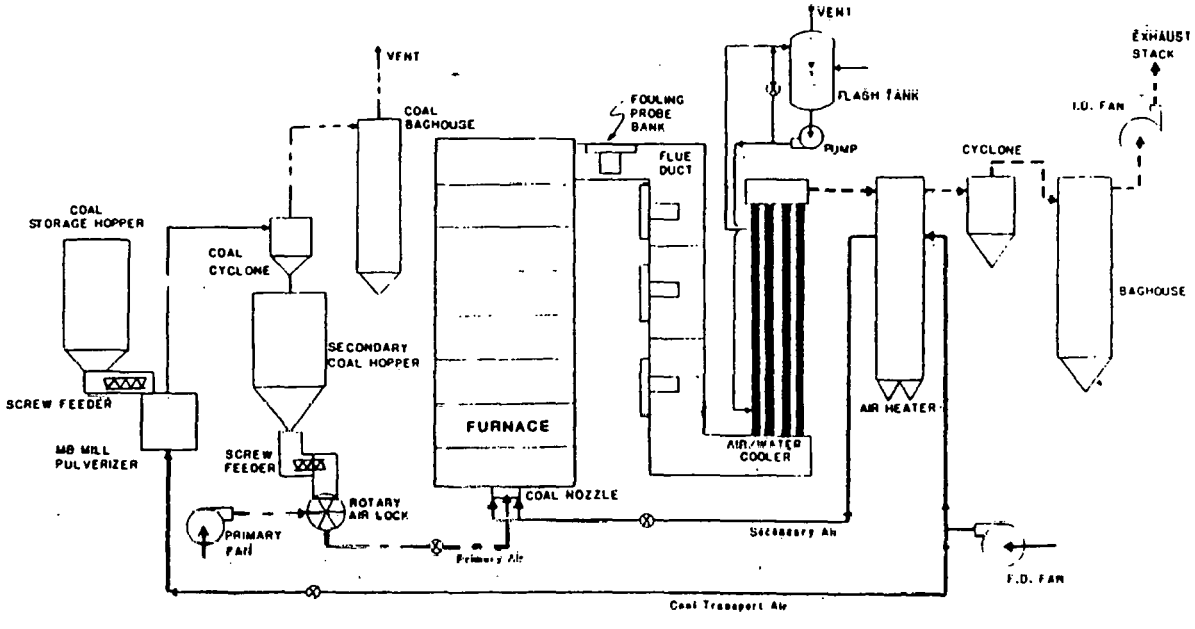


Figure 4.1 System Schematic

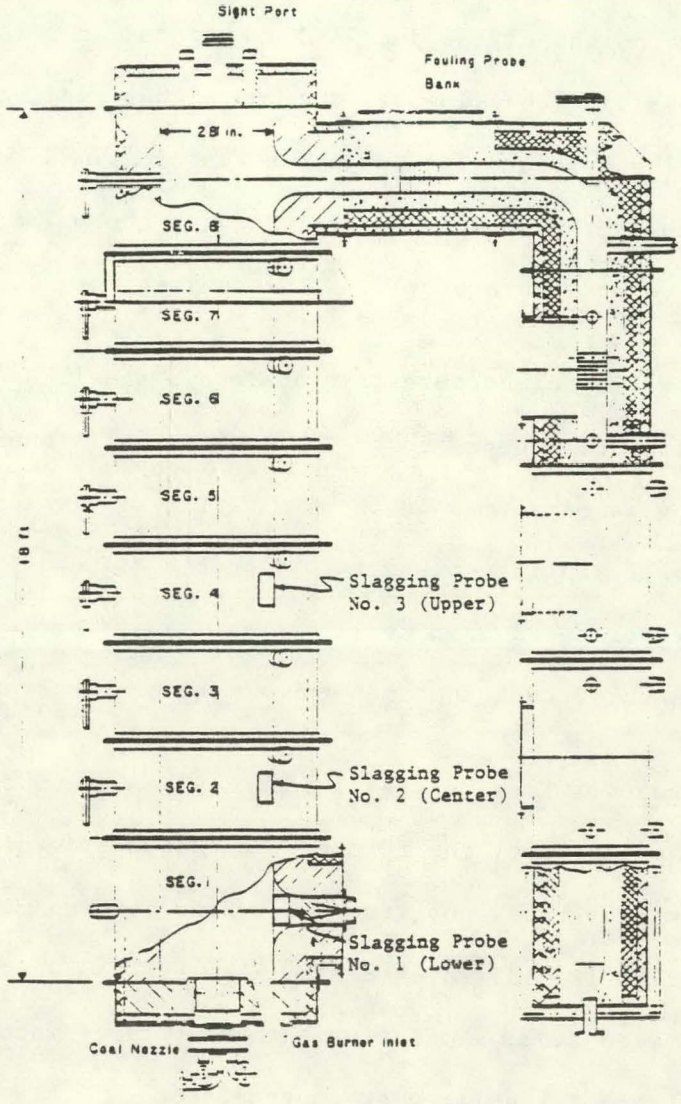


Figure 4.2 Furnace Cross Section

Each probe bank contains three in-line, 2-in.-dia test specimen tubes situated along the centerline of flow, as shown in Figure 4.3. The test tubes extend across the height of the duct and are spaced on 3-1/2 in. centers. Monofin wall tubes line the flue gas duct on either side of the test specimen tubes to shield the deposits formed on the test specimen from the effects of radiation imposed by the hot refractory, to give thermal similitude in the flue gas stream, and to provide a heat sink for cooling the flue gas.

The three test specimen tubes are stainless steel, as are superheater tubes in a utility steam generator. The monofin wall tubes are carbon steel; since no sampling is performed on them, material simulation is irrelevant. Each tube is air cooled in a bayonet fashion to maintain outer surface temperatures at those experienced in a utility steam generator. Thermocouple probes implanted in the three test specimen tubes monitor temperature.

Slagging Probes. Three slagging probes were inserted into Segments 1, 2, and 4 through the inside of the furnace. Each slagging probe (Figure 4.4) consists of a pair of tubes cut from 2-in. Sch. 40 pipe mounted in parallel on a rectangular, flat 1/4-in. thick plate. The tubes are welded to the plate, with spacing between them, simulating the geometry of waterwall tube array in the radiant section of a utility steam generator.

The surface temperatures along the probes are controlled by a compressed air cooling system. Each probe has one thermocouple mounted on the outermost tube surface, one mounted at the web between the tubes, and one mounted at the air exhaust. A low conductivity, castable refractory is used as a backing to

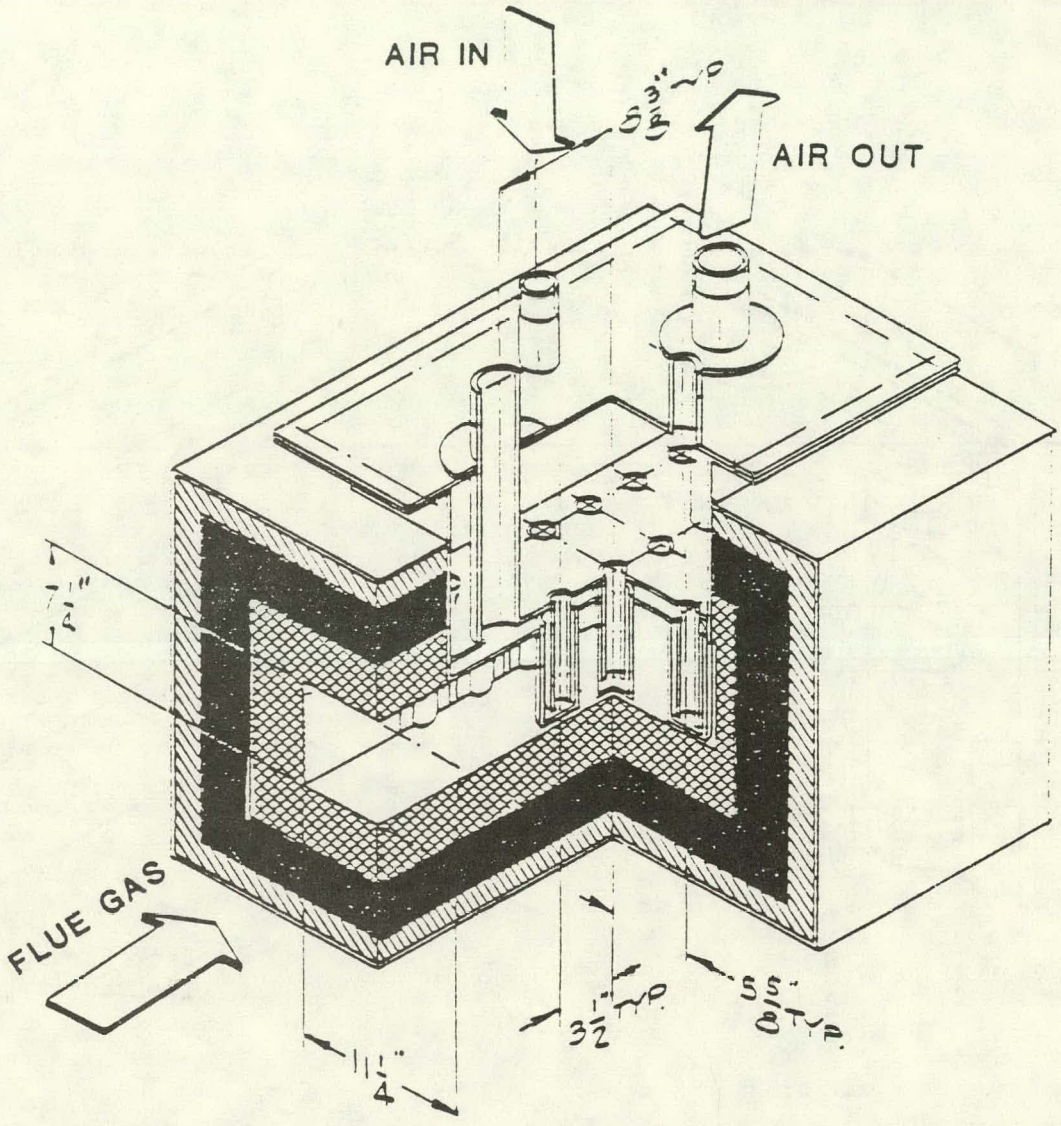


Figure 4.3 Schematic of Air-Cooled Furnace Probe

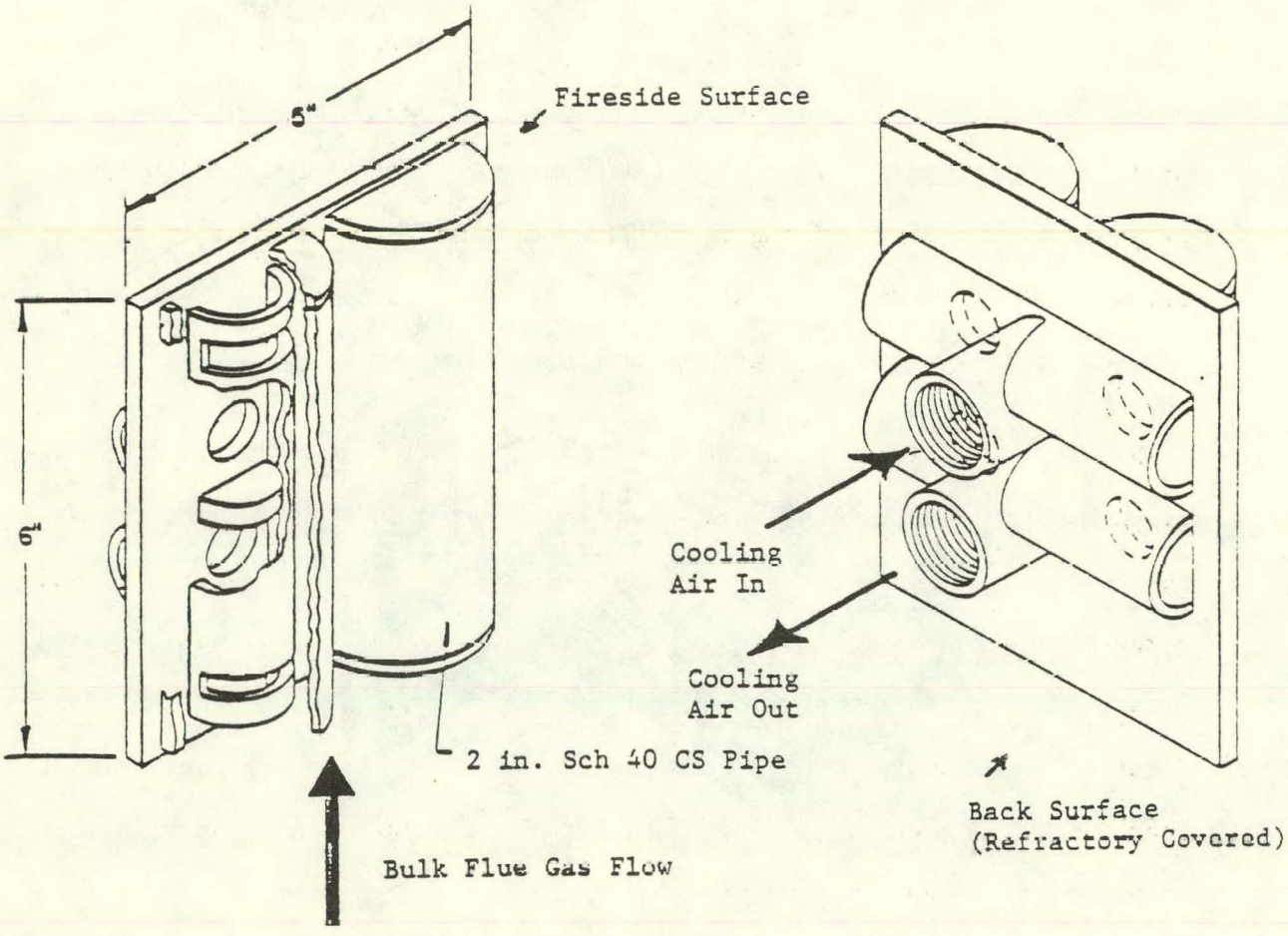


Figure 4.4 Slagging Probe

minimize heat conduction from the not refractory walls. The slagging surfaces are entirely carbon steel, as are those surfaces found in the waterwall section of a utility steam generator.

EXPERIMENTAL TEST PROCEDURES

A preheat period of about 24 hours at $10^6$ Btu/h was allowed to attain near steady-state temperatures throughout the unit. Preheating was done with the natural gas burner and its associated equipment. During this time compressed air was supplied to the fouling probe banks to maintain surface temperatures at or below 1000°F, and the three slagging probes were cooled by compressed air. The oxygen meter was given a calibration check before start-up on coal.

When all preliminary procedures for start-up had been performed, the natural gas burner output was downrated to about 500 x $10^3$ Btu/h. The actual output could not be determined since the gas flow metering system is not suitable for measurements in this low range. The secondary airflow was adjusted to that required for coal combustion at 15-percent excess air and 100 lb/h fuel feed rate. The primary air system was switched on to introduce the fuel into the combustion chamber and thus begin firing. At start-up the fuel feed indicator was set for 100 lb/h delivery.

Pressure, temperature, flow rate, and flue gas analysis date were recorded at periodic intervals from start-up to termination of running. Fouling probe cooling air was adjusted throughout the test to attempt to maintain the probe surface temperatures at about 1000°F. Similarly, slagging probe cooling air was adjusted to keep these surface temperatures in the desired operating range.

Visual inspections of the various probe surfaces were made periodically throughout the runs, as were inspections of furnace and flue duct, flame, and gas stream conditions.

The natural gas burner was shut off when it was certain that the coal flame was stable. At this time supplemental heat was not supplied to the combustion chamber, and the coal flame was allowed to sustain itself.

At the termination of each test, the coal feed was shut off; however, probe cooling air remained on to prevent overheating. The unit was allowed to cool down before any samples were extracted. At this time fly ash that had accumulated in the air heater, cyclone, and baghouse was removed and put in drums. Total material weights were recorded for each, and samples were taken for laboratory analyses.

Several days after each test, the coal burner and lower cap assembly were removed for inspection of the deposits. The top fouling probe bank was lifted out of the flue duct, and the refractory access plugs were removed from the third and fourth probe banks. Photographs were taken of each of these, including the inside furnace area.

During the following week, all deposit samples were removed from fouling tubes, slagging probes, and furnace and flue-pass surfaces. Weights of the various accumulations and their locations were recorded.

## ANALYSIS OF DEPOSITS AND FLY ASH

Both combustion tests of Kentucky No. 9 coal from Henderson County were terminated after 2-1/2 to 3 hours because of excessive deposit accumulation in

the vena contracta. Figure 4.5 shows the sintered accumulation at the entrance and exit of the throat. Figure 4.6 shows the accumulation plugging the first fouling probe bank as a result of attempts to remove the deposit on-line. Very little, if any, fouling occurred on the tube surfaces during the short duration of tne test program, as illustrated in Figures 4.7 and 4.8. The test was not a fair trial of selective deposition of free pyrites because it was so short. Very little ash accumulated on the first slagging probe, illustrated in Figures 4.9a and 4.9b. Deposits were powdery in texture and represent the very initial stages of slag formation. Beads of molten slag were just beginning to form on the higher temperature refractory immediately adjacent to the probe. The center slagging probe, located in a hotter portion of the furnace, showed signs of molten beads forming on the powdery base shortly after 2-1/2 nours of operation. No doubt these probes would have contained large accumulations of molten slag had the tests been allowed to continue for 14 to 16 nours. Molten beads were also forming on a sintered base layer of the probe immersed in the furnace perpendicular to the direction of gas flow (see Figure 4.10).

The chemical analysis of the deposits and fly ash are compared directly with the coal ash in Tables 4.2 and 4.3, representing Trials 1 and 2. In Figure 4.11 the data have been plotted on a softening-temperature curve vs. percentage basic curve and compared directly with the fractionated coal analysis. In Figure 4.12 a comparison is made with other bituminous coals whose silica/alumina ratio generally runs 2:1. With exception for the cyclone deposits, tne ash-softening temperatures of furnace slag deposits under reducing conditions are about 100°F below the fouling probe deposits, the fly ash, and the coal ash.

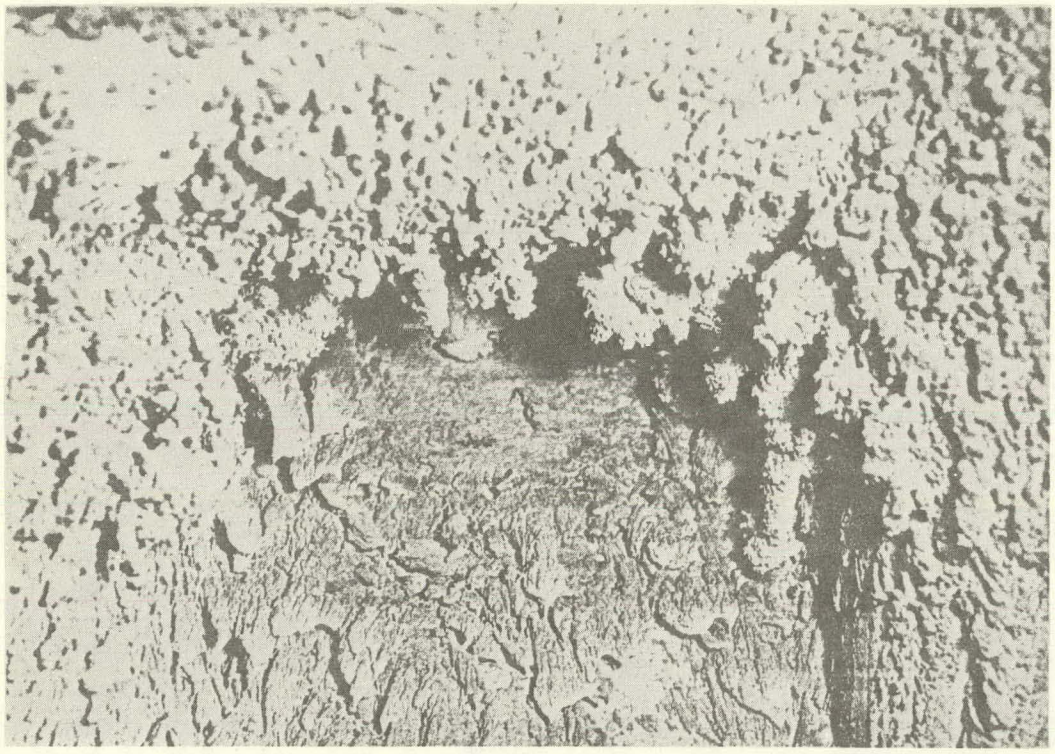

Gas Flow →

Furnace View

Gas Flow →

Convection Pass View

Figure 4.5 Deposit Accumulation in Vena Contracta at Entrance to Convection Pass After Firing Kentucky No. 9 Coal

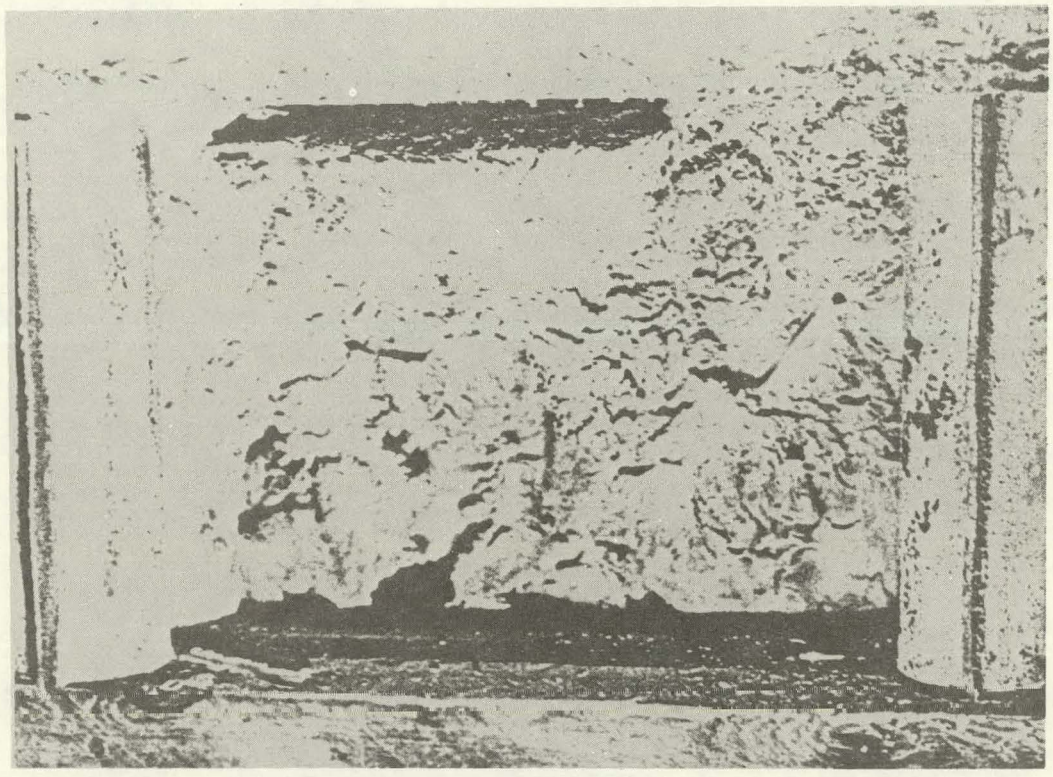

Figure 4.6 Accumulation of Deposits in First Fouling Probe as a Result of Attempt to Clear Vena Contracta While On Line

Kentucky No. 11 (9 hours)

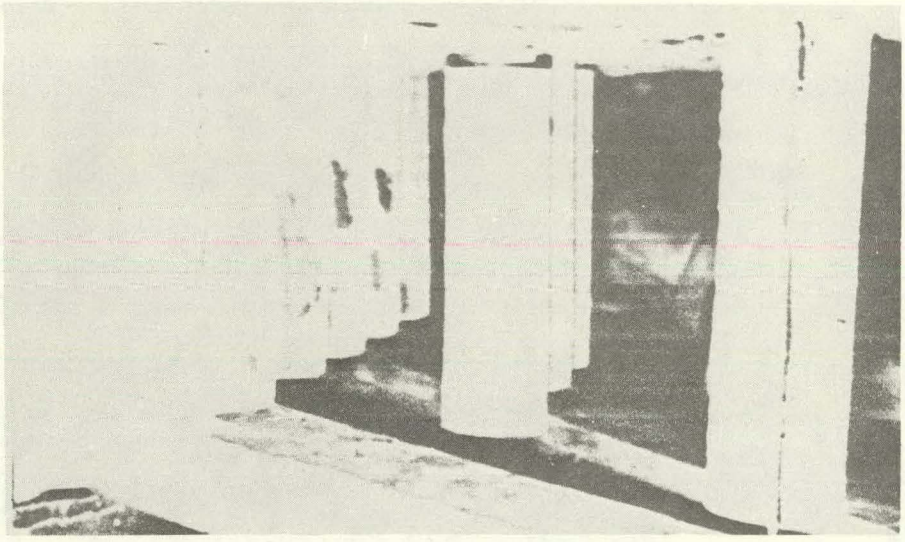

Kentucky No. 9, Henderson County (2-1/2 hours)

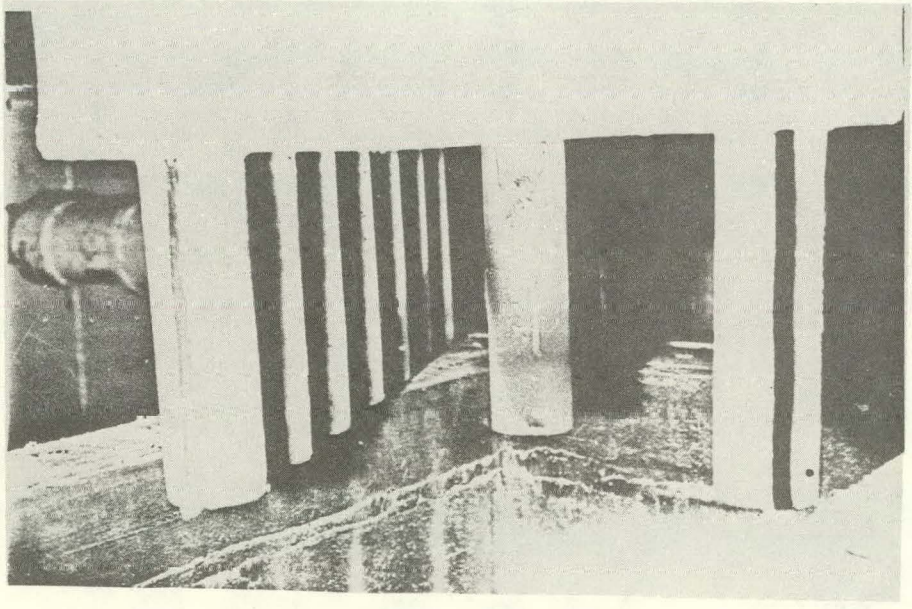

Figure 4.7 Comparison of First Convective Fouling Probe After Firing Kentucky No. 11 and Kentucky No. 9

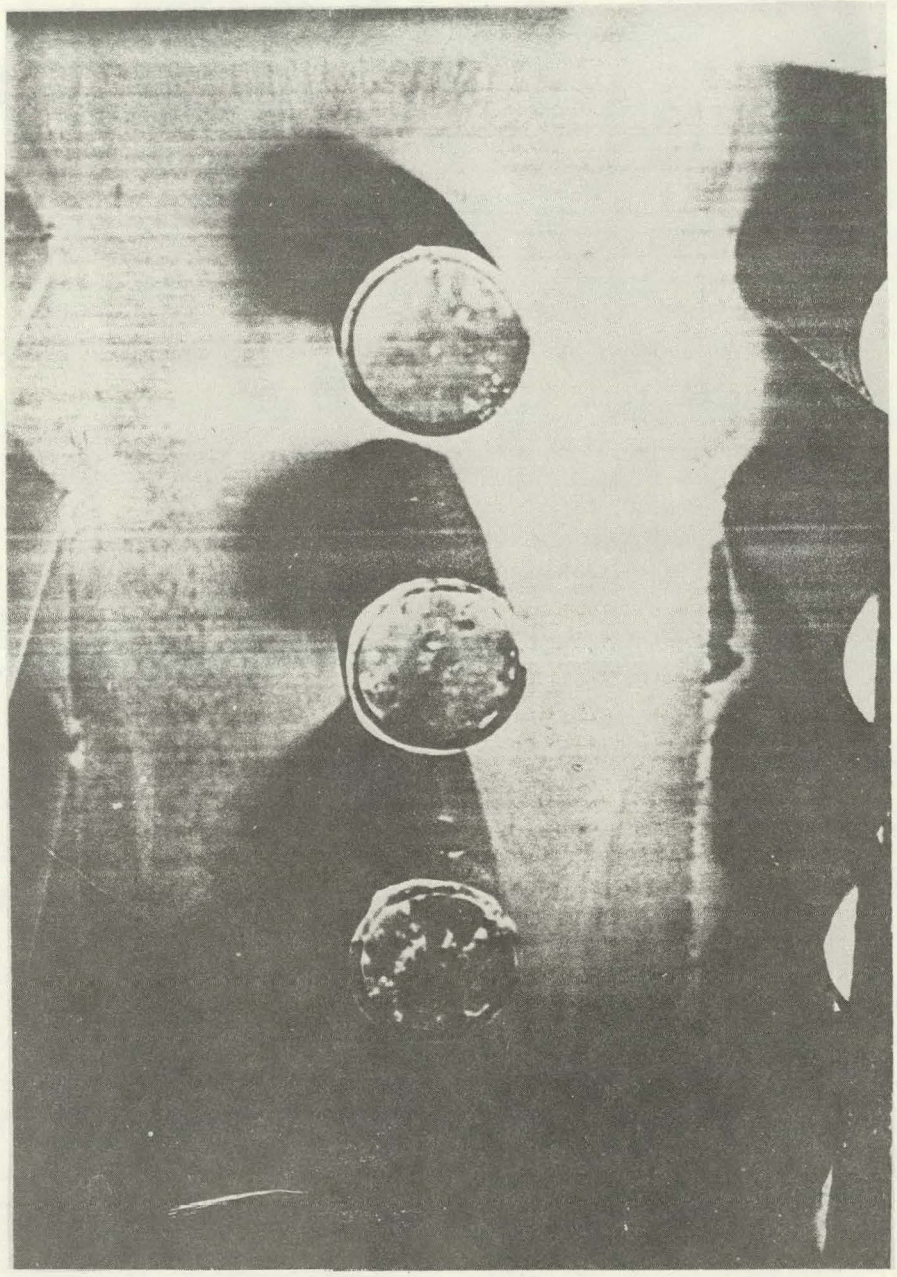

Figure 4.8 Vertical Convective Fouling Probe After Firing Kentucky No. 9, Henderson County, for 2-1/2 Hours

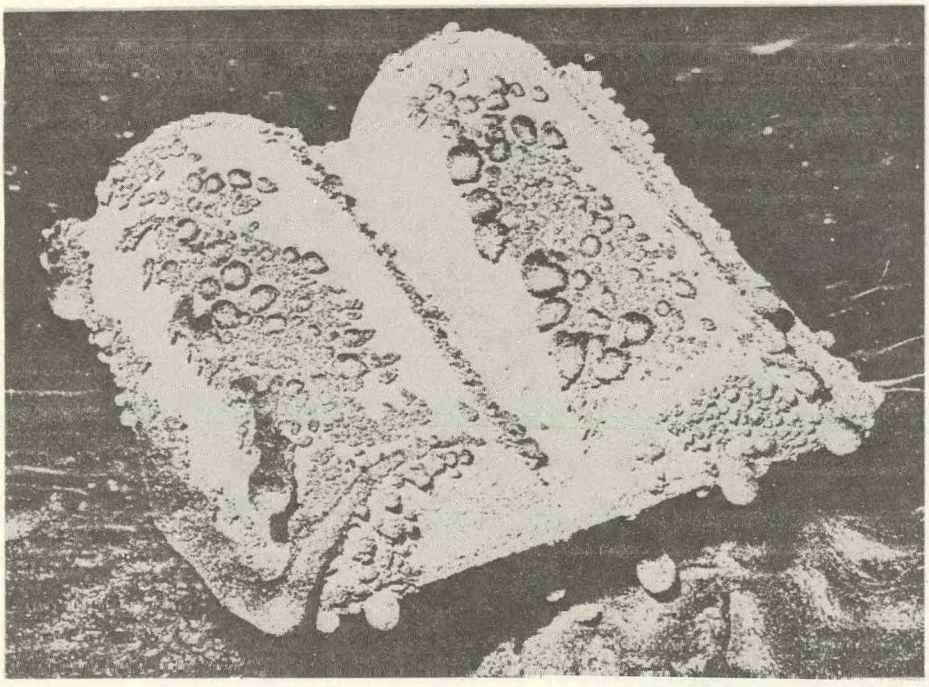

Center Slagging Probe

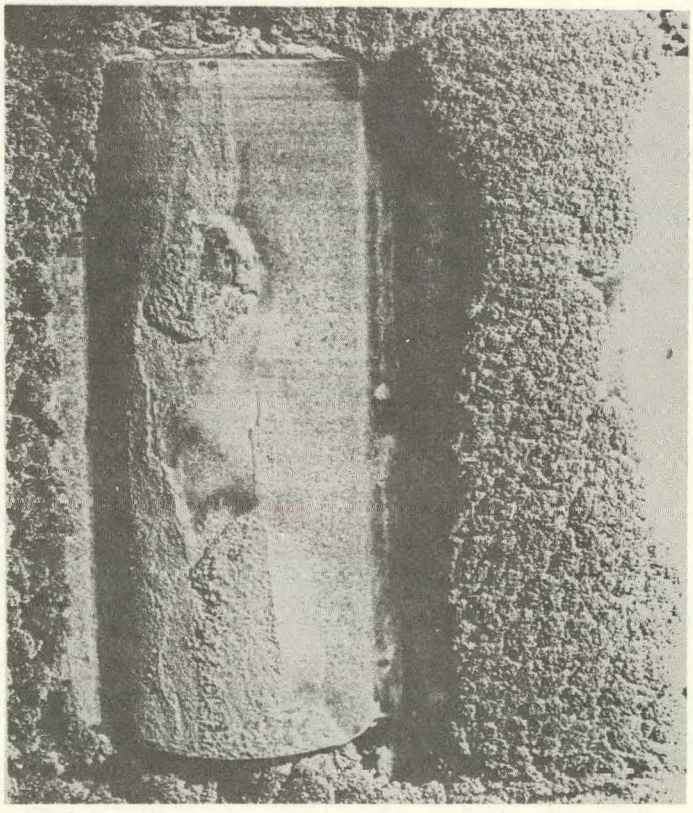

Lower Slagging Probe

Figure 4.9a Center and Lower Furnace Wall Slagging Probes After Firing Kentucky No. 9, Henderson County, for Only 2-1/2 Hours (Trial 1)

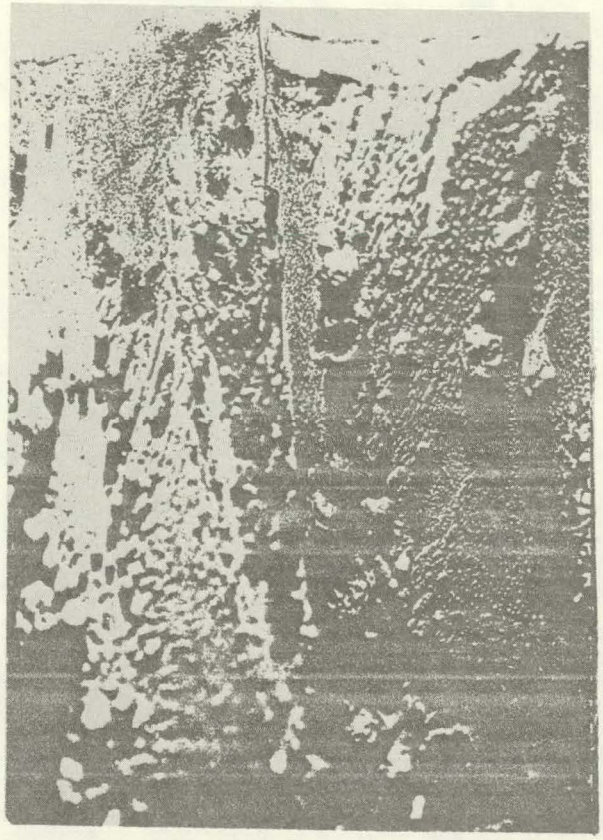

Center Slagging Probe

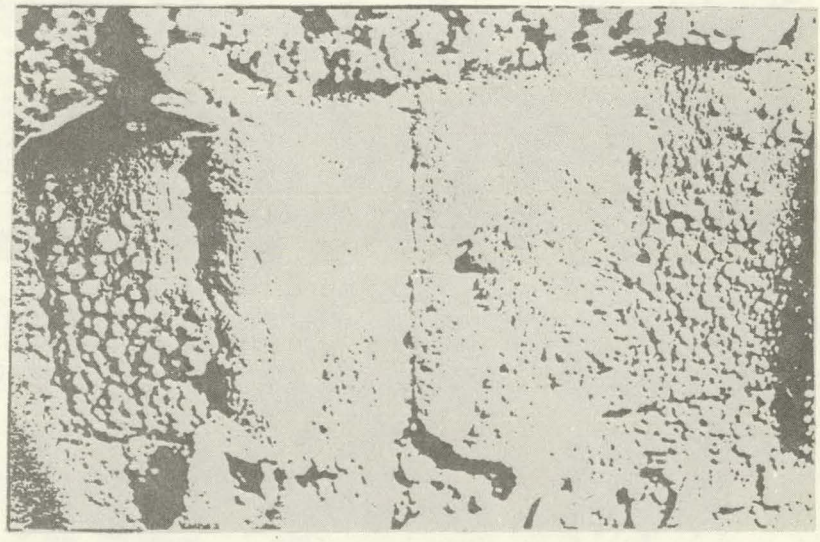

Lower Slagging Probe

Figure 4.9b Center and Lower Furnace Wall Slagging Probes After Firing Kentucky No. 9, Henderson County, Coal for Only 3 Hours (Trial 2)

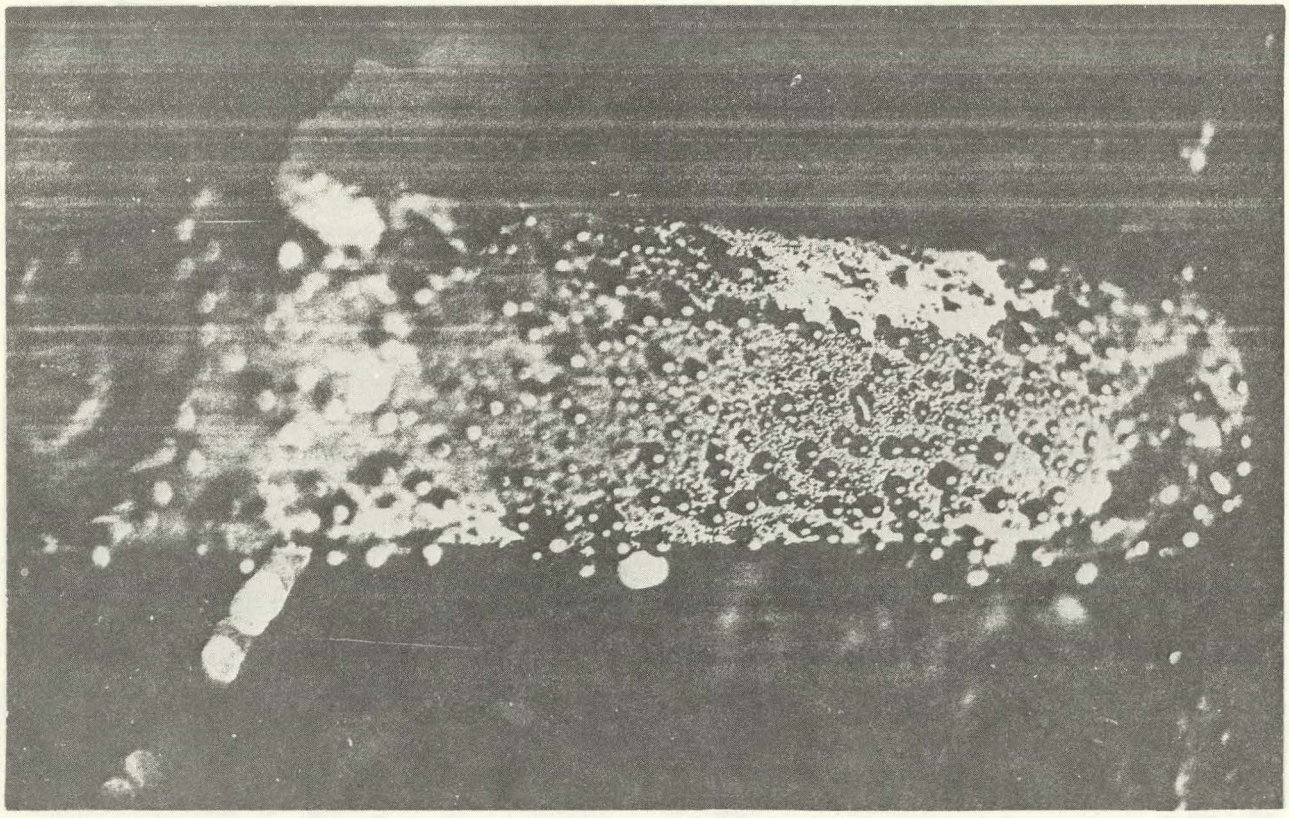

Figure 4.10 Deposits Formed on Lower Side of Slagging Probe Perpendicular to Flue Gas Flow After Firing Kentucky No. 9, Henderson County, for 2-1/2 Hours

Table 4.2 Summary of Ash Chemistry and Ash Fusion Data--Combustion Trial 1, Kentucky No. 9 Coal, Henderson County, Kentucky*

| Description | Coal Ash | Air Heater | Cyclone | Baghouse | Wall Slag | Slagging Probes | | | Fouling Probe 1 | Furnace Exit |
|---|---|---|---|---|---|---|---|---|---|---|
| | | | | | | Upper | Center | Lower | | |
| **Ash Chemistry (%)** | | | | | | | | | | |
| $SiO_2$ | 40.0 | 52.6 | 40.0 | 55.2 | 51.2 | 34.0 | 41.7 | 46.4 | 53.2 | 53.4 |
| $Al_2O_3$ | 16.4 | 21.8 | 19.1 | 22.3 | 17.6 | 13.3 | 15.7 | 16.6 | 20.4 | 20.0 |
| $TiO_2$ | 0.8 | 1.0 | 1.1 | 1.1 | 0.7 | 0.6 | 0.7 | 0.7 | 1.1 | 0.9 |
| $Fe_2O_3$ | 20.5 | 11.1 | 20.5 | 9.2 | 19.6 | 41.3 | 32.0 | 27.3 | 10.8 | 14.6 |
| CaO | 7.8 | 5.7 | 6.9 | 5.5 | 4.8 | 5.2 | 4.9 | 4.3 | 7.0 | 5.1 |
| MgO | 1.1 | 0.7 | 1.3 | 0.7 | 0.8 | 0.6 | 0.6 | 0.5 | 0.8 | 0.8 |
| $Na_2O$ | 0.8 | 2.8 | 1.9 | 2.6 | 2.6 | 1.4 | 1.8 | 2.3 | 4.8 | 3.4 |
| $K_2O$ | 2.3 | 2.1 | 1.4 | 2.3 | 2.2 | 1.6 | 2.0 | 2.0 | 2.2 | 2.4 |
| $SO_3$ | 9.4 | 2.6 | 5.2 | 2.5 | 0.1 | 1.0 | 0.8 | 0.8 | 1.3 | 0.3 |
| $P_2O_5$ | 0.1 | 0.1 | 0.4 | 0.1 | 0.1 | 0.1 | 0.1 | 0.1 | 0.1 | 0.1 |
| **Ash Fusion (°F)** | | | | | | | | | | |
| Reducing: | | | | | | | | | | |
| Initial Deformation | 2016 | 2020 | 2180 | 1940 | 1987 | 1940 | 1940 | 1960 | 2057 | 2000 |
| Softening (Sph.) | 2042 | 2060 | 2200 | 1950 | 2000 | 1980 | 1950 | 1980 | 2083 | 2049 |
| Softening (Hem.) | 2100 | 2090 | 2270 | 1960 | 2042 | 2000 | 1960 | 1990 | 2106 | 2091 |
| Fluid | 2111 | 2160 | 2390 | 1980 | 2138 | 2020 | 1980 | 2060 | 2223 | 2173 |
| Oxidizing: | | | | | | | | | | |
| Initial Deformation | 2169 | 2260 | 2300 | 2220 | 2280 | 2240 | 2220 | 2240 | 2257 | 2263 |
| Softening (Sph.) | 2490 | 2300 | 2330 | 2240 | 2292 | 2340 | 2240 | 2250 | 2292 | 2292 |
| Softening (Hem.) | 2700 | 2330 | 2390 | 2280 | 2350 | 2360 | 2280 | 2320 | 2350 | 2350 |
| Fluid | 2700 | 2400 | 2470 | 2460 | 2378 | 2480 | 2460 | 2420 | 2378 | 2378 |

*Legend for symbols in Figures 4.11 and 4.12.

Table 4.3 Summary of Ash Chemistry and Ash Fusion Data--Combustion Trial 2, Kentucky No. 9 Coal, Henderson County, Kentucky*

| Description | Coal Ash | Wall Slag | | Upper Slagging Probe | | Center Slagging Probe | Lower Slagging Probe | Furnace Exit |
|---|---|---|---|---|---|---|---|---|
| | | Location 1 | Location 2 | Upper Side | Lower Side | | | |
| | ✚ | ■ | ● | ◥ | ◥ | ▼ | ◆ | ● |
| **Ash Chemistry (%)** | | | | | | | | |
| $SiO_2$ | 40.0 | 39.2 | 41.7 | 43.1 | 37.6 | 38.5 | 45.1 | 51.7 |
| $Al_2O_3$ | 16.4 | 13.8 | 15.8 | 16.5 | 13.9 | 15.0 | 17.1 | 19.7 |
| $TiO_2$ | 0.8 | 0.7 | 0.7 | 0.7 | 0.6 | 0.6 | 0.7 | 1.0 |
| $Fe_2O_3$ | 20.5 | 25.5 | 26.4 | 29.6 | 37.3 | 33.8 | 24.9 | 17.1 |
| CaO | 7.8 | 8.9 | 7.8 | 6.0 | 5.2 | 6.3 | 5.9 | 6.0 |
| MgO | 1.1 | 0.6 | 0.7 | 0.6 | 0.6 | 0.6 | 0.6 | 0.7 |
| $Na_2O$ | 0.8 | 0.6 | 1.4 | 1.0 | 0.8 | 1.0 | 1.3 | 1.7 |
| $K_2O$ | 2.3 | 1.7 | 1.9 | 2.0 | 1.8 | 1.8 | 2.1 | 2.4 |
| $SO_3$ | 9.4 | 0.1 | 1.6 | 0.5 | 0.7 | 1.9 | 2.2 | 0.3 |
| $P_2O_5$ | 0.1 | 0.3 | 0.1 | 0.1 | 0.1 | 0.1 | 0.2 | 0.1 |
| **Ash Fusion (°F)** | | | | | | | | |
| Reducing: | | | | | | | | |
| Initial Deformation | 2016 | 1990 | 1940 | --- | | 1900 | 1970 | 2080 |
| Softening (Sph.) | 2042 | 2000 | 1960 | --- | | 1920 | 2000 | 2100 |
| Softening (Hem.) | 2100 | 2020 | 1980 | --- | | 1950 | 2100 | 2140 |
| Fluid | 2111 | 2190 | 2000 | --- | | 1990 | 2200 | 2180 |
| Oxidizing: | | | | | | | | |
| Initial Deformation | 2360 | 2310 | 2290 | --- | | 2260 | 2320 | 2310 |
| Softening (Sph.) | 2490 | 2340 | 2340 | --- | | 2300 | 2350 | 2350 |
| Softening (Hem.) | 2700 | 2360 | 2360 | --- | | 2340 | 2390 | 2390 |
| Fluid | 2700 | 2410 | 2400 | --- | | 2380 | 2510 | 2500 |

*Legend for symbols in Figures 4.11 and 4.12.

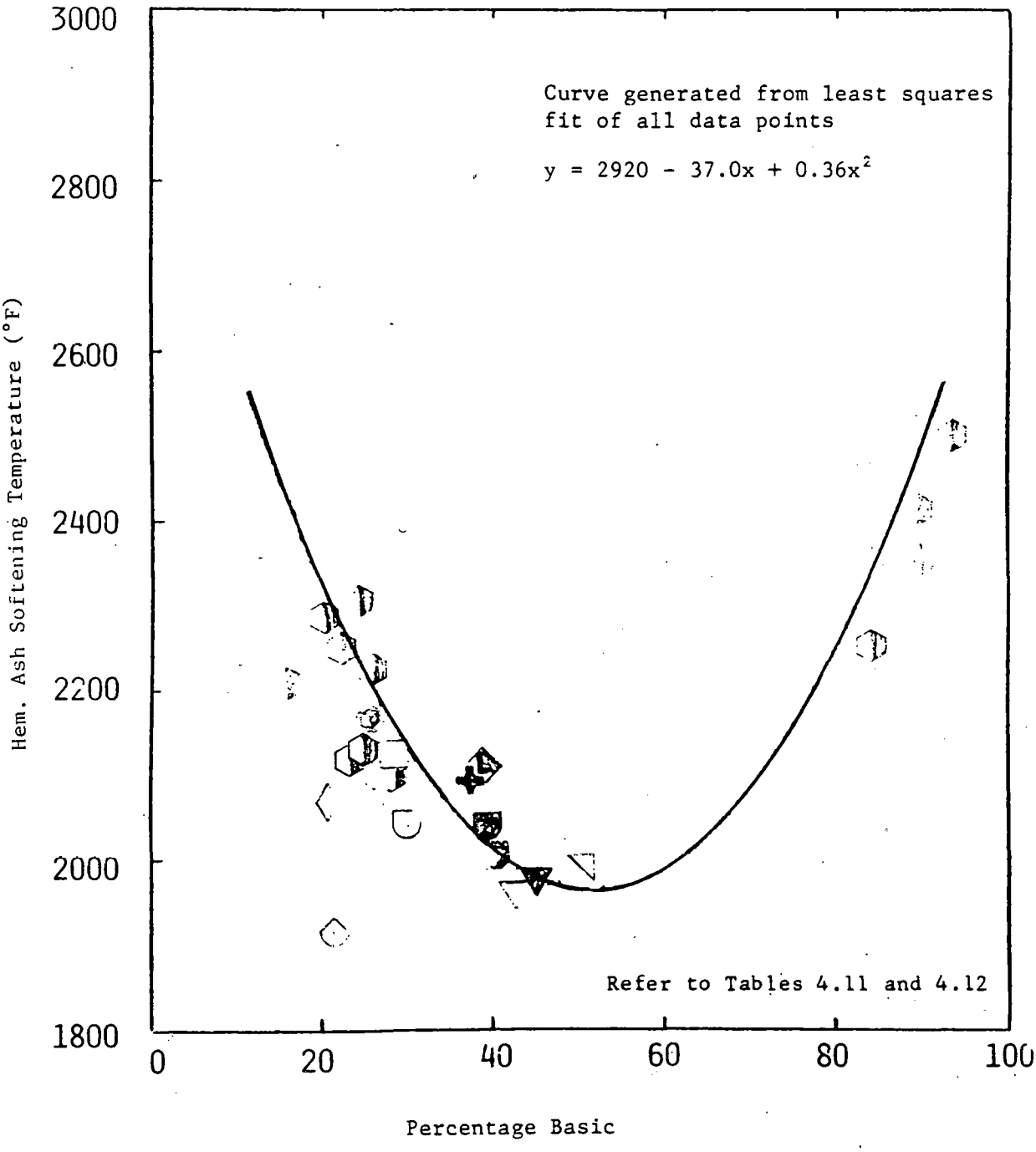


Figure 4.11 Ash Softening Temperature vs. Percentage Basic Constituents for Fractionated Kentucky No. 9, Henderson County

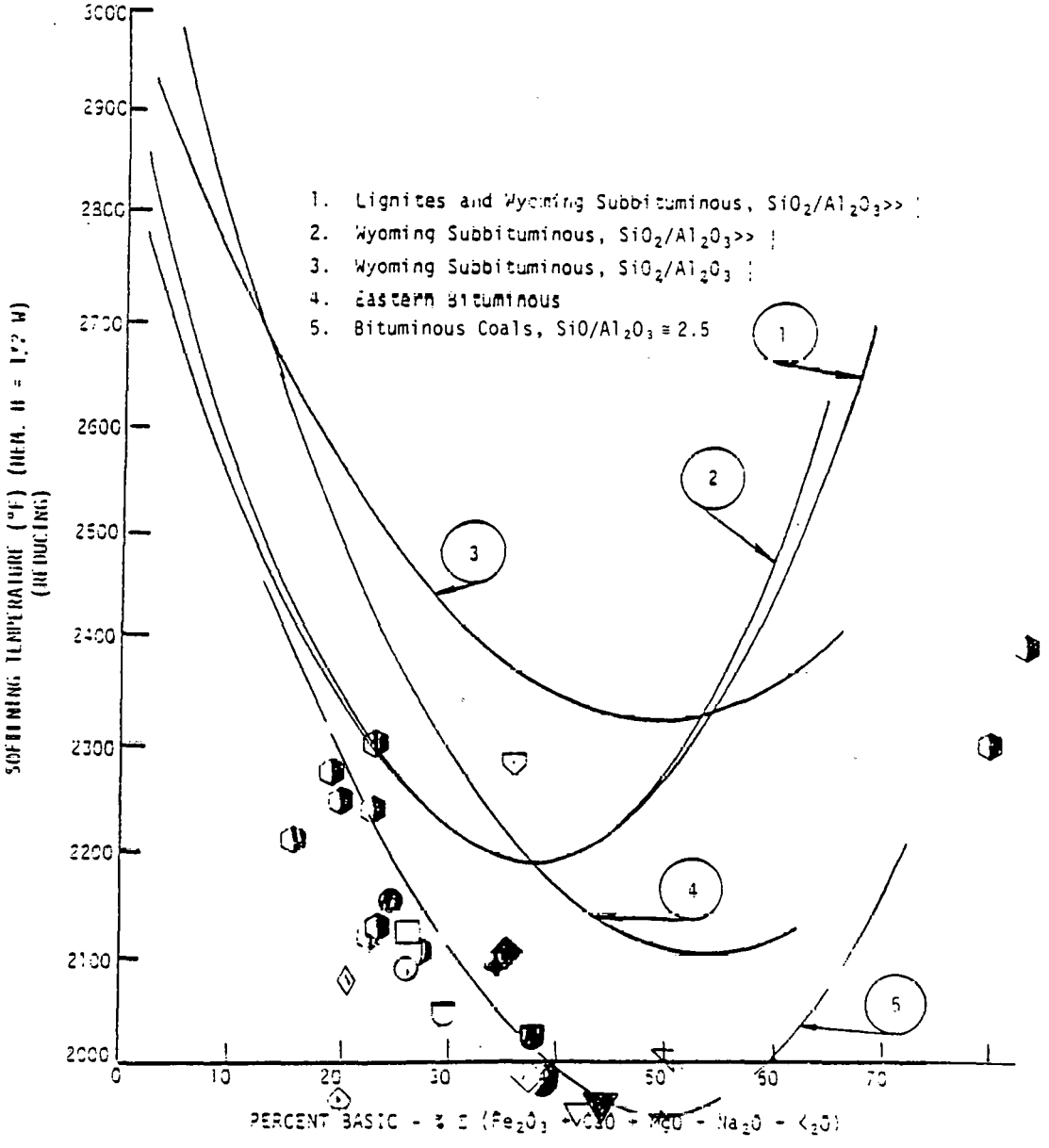


Refer to Tables 4.11 and 4.12

Figure 4.12 Influence of Percentage of Basic Constituents in Ash on Ash Softening Temperatures Under Reducing Conditions for Different Ranks of Coal

There is very little difference between the initial deformation temperatures and the softening temperature. Fusion temperatures under oxidizing conditions are 300 to 400°F higher. The extremely low fusion temperature probably accounts for the furnace exit fouling, as the flue gas temperatures in this zone are between the initial deformation temperature and the fluid temperature under reducing conditions. It is interesting to note the fluid temperatures under reducing conditions for all slag species are almost 200°F below the fractionated coal ash. The initial deformation temperatures are also 100°F lower under reducing conditions. The differences under oxidizing conditions are not as severe. The implication is that pure species may be selectively interacting at the furnace wall and on the heat-transfer surface to form eutectics with considerably lower fluid temperatures.

Only the deposits accumulated during Trial 2 were subjected to microscopic examination by scanning electron microscope (SEM) and x-ray diffraction (EDX). The results are summarized in Figures 4.13 through 4.25.

The overall surface morphology of powdery ash formed on the lower slagging probe is illustrated in Figure 4.13. The EDX scan indicates an overall chemistry, similar to that for the coal ash, depleted of iron. The individual species are illustrated in Figure 4.14, along with their chemistry. The semimolten sphere, appearing to be an agglomerate of smaller particles formed by a molten material wetting their surfaces, is rich in silica and potassium, with small quantities of iron. The iron is believed to be contributed by the small, submicron particles attached. This conclusion should become more obvious as further species are analyzed. The smooth spheres are predominantly silica and

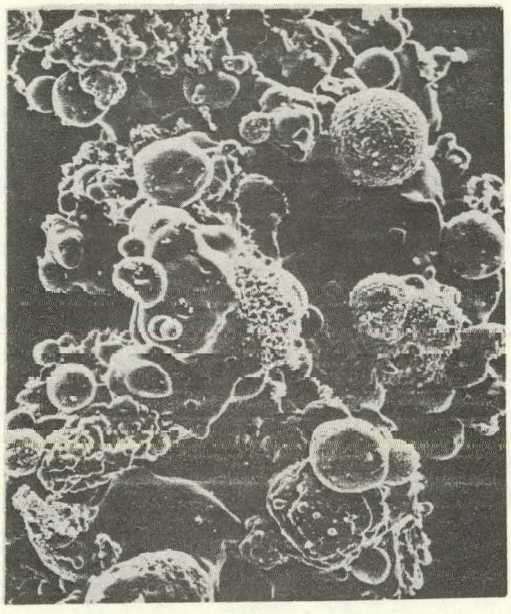

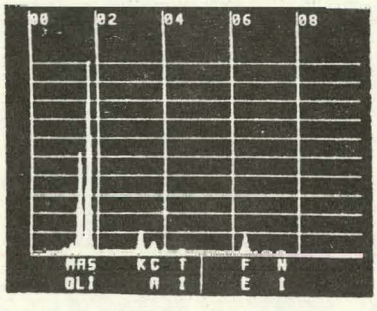


Figure 4.13 SEM Photomicrograph and EDX Scan--Surface Morphology and Elemental Composition of Composite Powder Comprising First Layer on Lower Slag Probe

600X

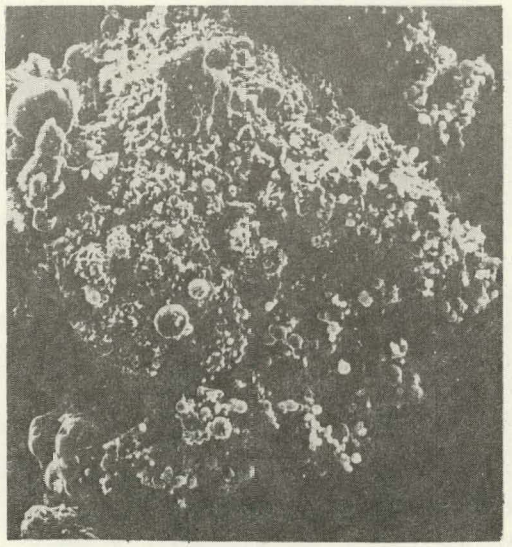

Submicron Agglomerates

1200X

Potassium-Rich Silicate

900X

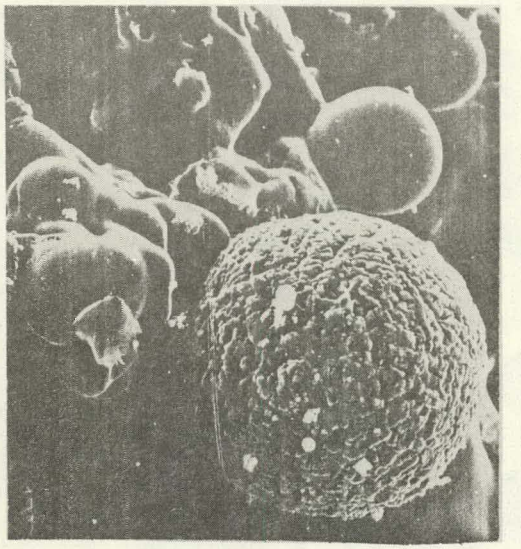

Iron-Enriched Spheroid

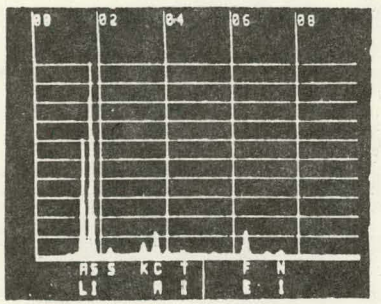


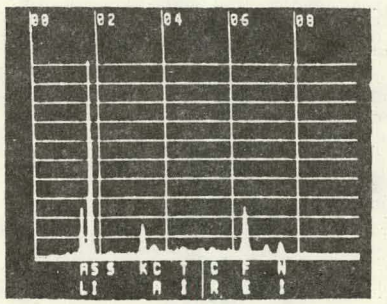


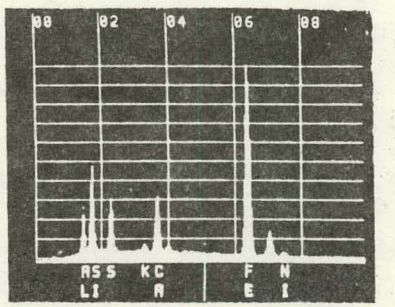


Figure 4.14 SEM Photomicrographs and EDX Scans--Surface Morphology and Elemental Composition of Individual Species Comprising Powdery Layer on First Slagging Probe

alumina, with small quantities of iron and sulfur. The same spheroids, incapsulated within small crystals, are enriched with calcium, iron, and sulfur. Clays such as kaolinite and possibly illite are the source of the small, fused spheroids. The incapsulated, submicron particulates originated as calcite and pyrite in the coal. The molten surface of the globules, shown in Figure 4.15 is predominantly quartz, to which extraneous pyritic spheres and inherent submicron particles of pyrite have attached themselves. The microphotographs clearly show that some of the particles are mechanically trapped while others are sintered by a molten bond of $SiO_2$ and $K_2O$, sulfidation of calcite, or bonded by FeO or FeS going into solution with $SiO_2$.

The inner layer of powdery ash formed on the center slagging probe is illustrated in Figure 4.16. The large, skeleton-like spheroids, composed of agglomerates of submicron particles, are remnants of spent char with a composition similar to the coal ash slightly enriched with quartz. The chemistry resembles that of the lighter coal ash fractions. The semimolten spheres containing blow holes are rich in silica and potassium and completely void of iron. There are also traces of sodium, which may be quite high because the EDX will not identify sodium below 5 percent. No doubt these particles originated as illite. The spheroids, containing small submicron attachments, are clay particles with iron going into solution at the surface. Within the cross section there is a molten phase rich in silica and iron, with trace amounts of calcium. This molten phase is formed by small quantities of calcium sulfate crystals, the illite spheroids, and submicron crystals of pyrite going into solution with the quartz as the surface temperature of the deposit increases with continued

300X

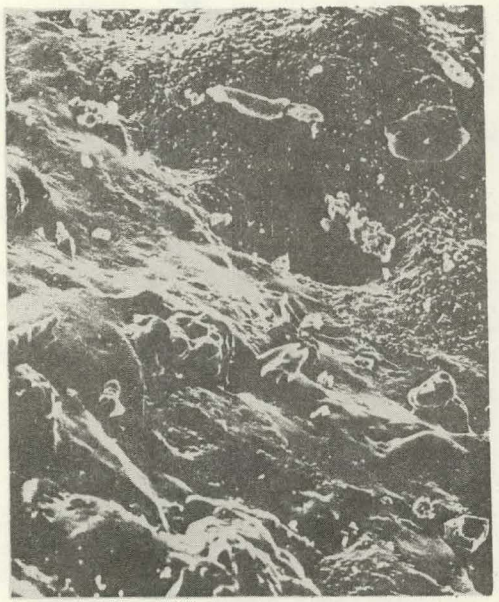

Smooth Fused Silica Matrix

1500X

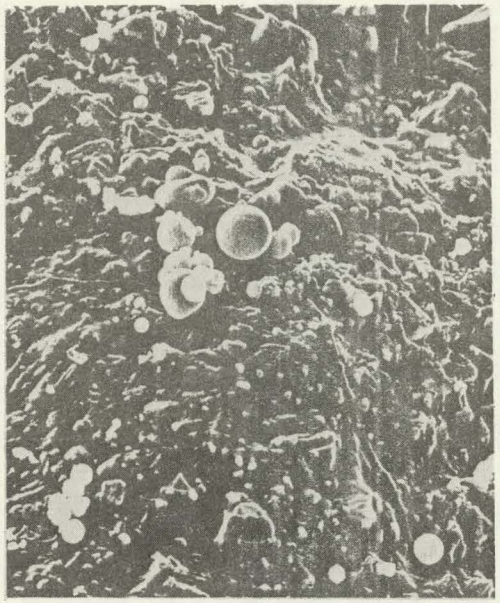

Small Crystals Going Into Solution

900X

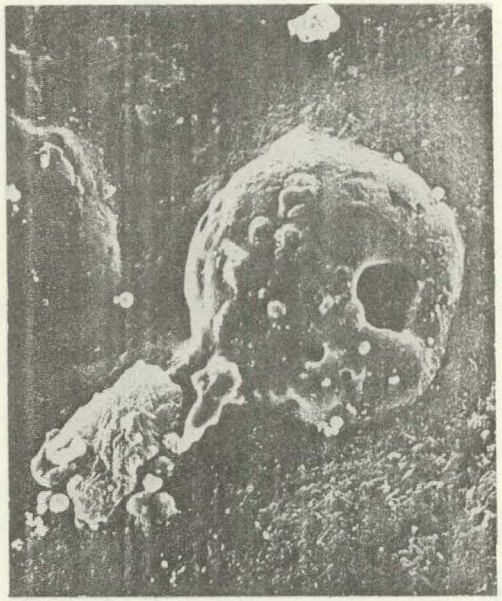

Large Iron Particles Going Into Solution

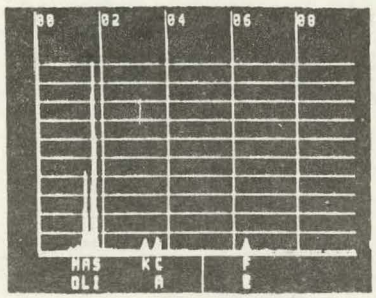


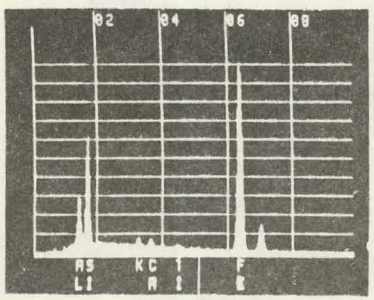


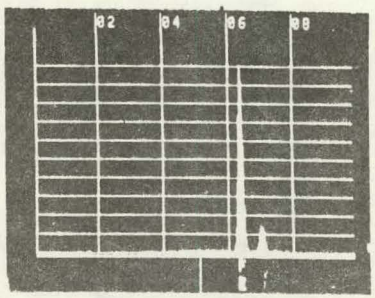


Figure 4.15 SEM Photomicrographs and EDX Scans--Surface Morphology and Elemental Analysis of Fused Outer Surface of Slag on Lower Probe

1500X

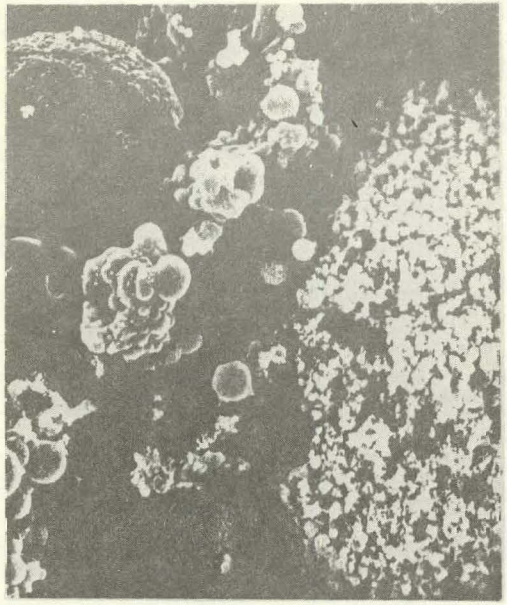

Large Iron Particle Encapsulated With Submicron Particles

1500X

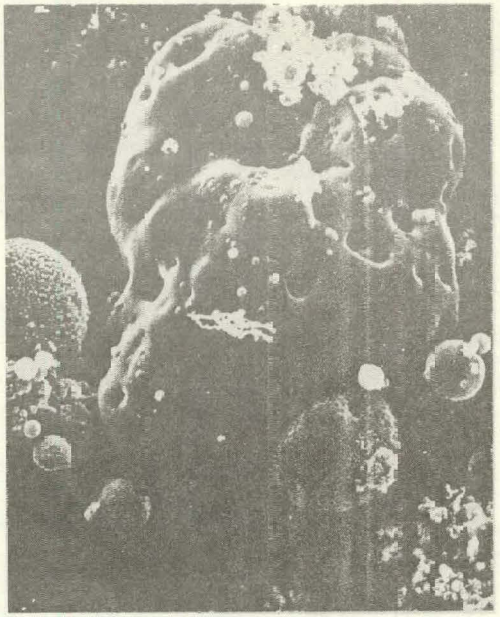

Large Semimolten Potassium Silicate Particle

1200X

Burned Out Remnant of Char

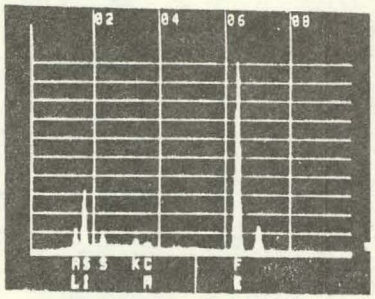

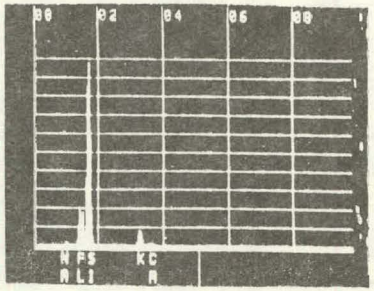

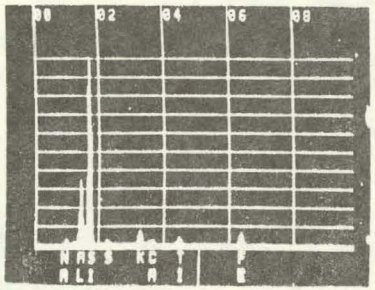

Figure 4.16 SEM Photomicrograph and EDX Scan--Surface Morphology and Elemental Composition of Fly Ash Species Initiating Slag On Center Slagging Probe

growth (see Figure 4.17). The outer layer of the deposit (Figure 4.18) is a dense, molten matrix composed primarily of iron, calcium, and silica. The concentration of calcium sulfate appears to have increased with temperature. There is evidence of desulfurized iron going into solution.

Figure 4.19 shows the cross section of deposit removed from the flame side of the slag probe immersed in the furnace perpendicular to the flow of the flue gas. The cross section represents the area between molten nodules, illustrated in Figure 4.10. A photomicrograph of the molten nodule appears in Figure 4.20, along with its EDX scan. The nodule is a molten solution of calcium, iron, alumina, and silica. The silica probably originated as illite and thus may include some potassium which has been depleted by dilution. The cross section shows an iron oxide substrate scale about 1/64 in. thick, to which the deposit is bonded. The solidified molten matrix forming the bond is rich in silica and contains small amounts of alumina potassium, and calcium. The smooth spheroids, to which rough appendages comprising submicron iron crystals are attached, are composed of silica, alumina, and calcium with trace quantities of potassium.

The iron appearing in the EDX scan may have the same origin as the other elements; however, it seems more likely its source is the pyrite crystals going into solution.

Except for the large molten nodules, which represent an advanced stage in the growth of the layer initiating the deposit, the ash on the top side of the tube resembles that on the bottom. The cross section appears in Figure 4.21. The inner layer consists of molten and semimolten particles rich in silica and

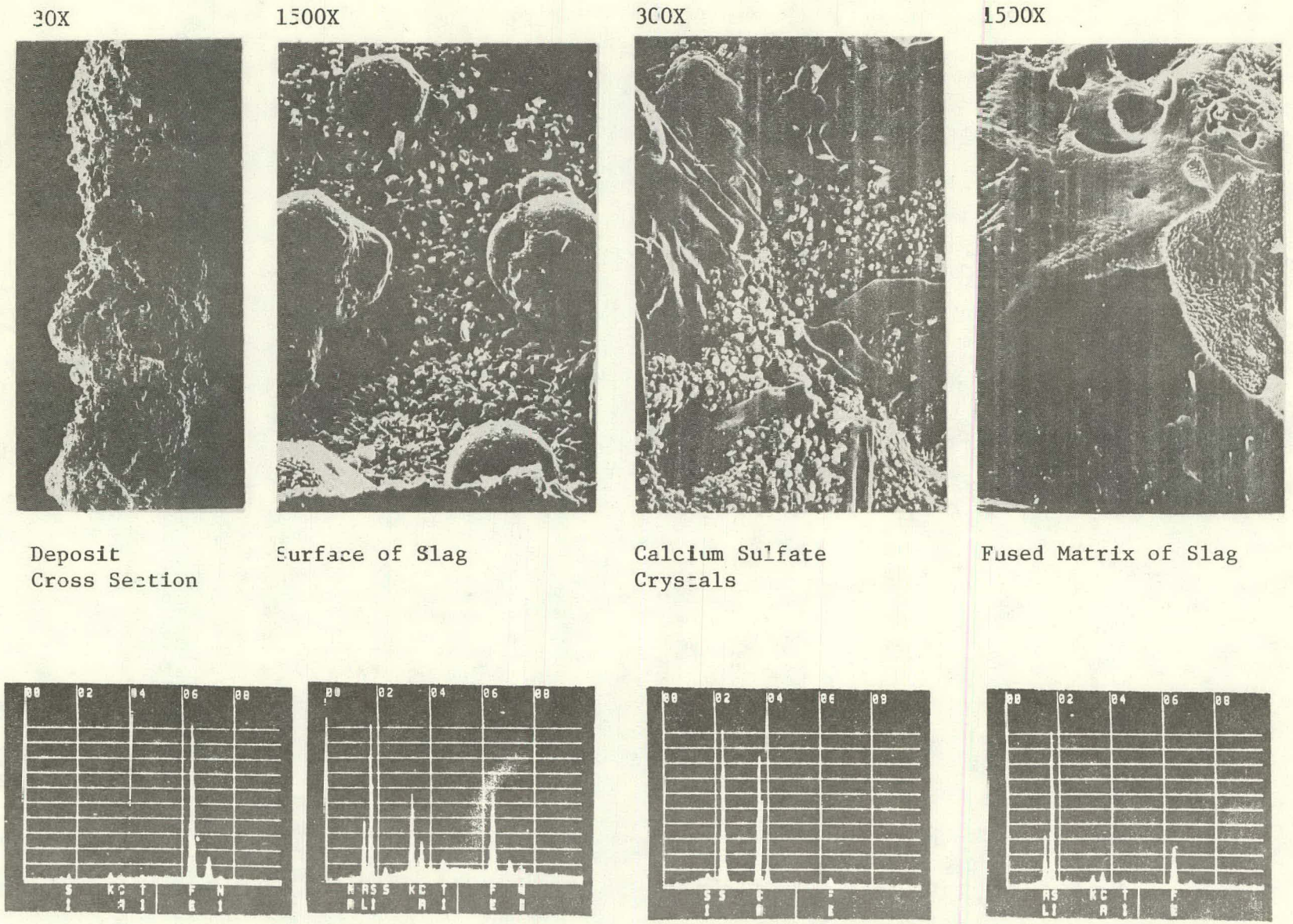


Figure 4.17 SEM Photomicrographs and EDX Scans--Surface Morphology and Elemental Composition of Cross Section and Surface of Outside Molten Layer

Molten Matrix

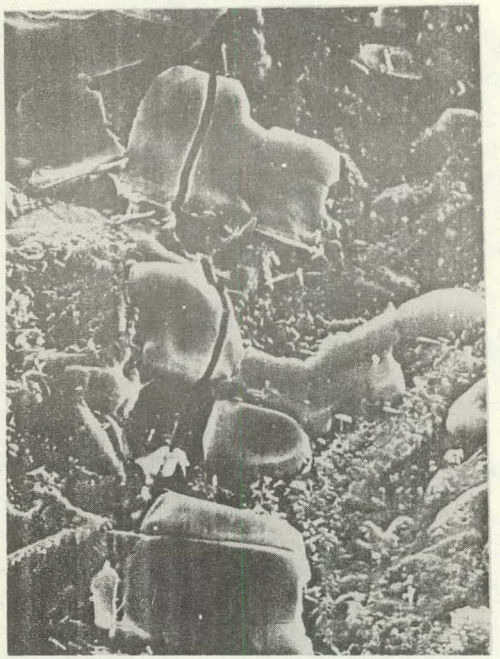

Calcium Sulfate Crystals

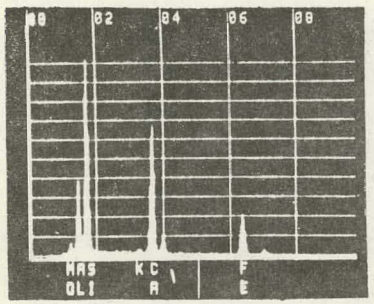


Matrix

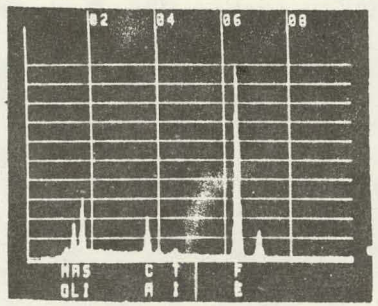


Crystals

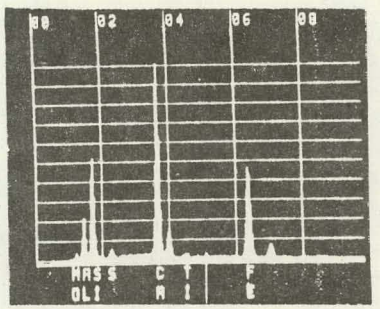


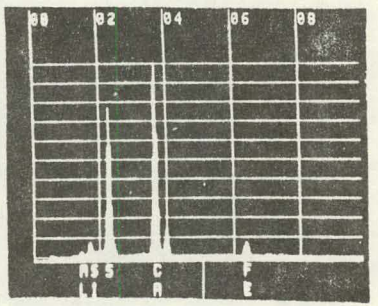


Figure 4.18 SEM Photomicrographs and EDX Scans--Surface Morphology and Elemental Composition of Molten Surface of Deposits Formed on Center Slagging Probe

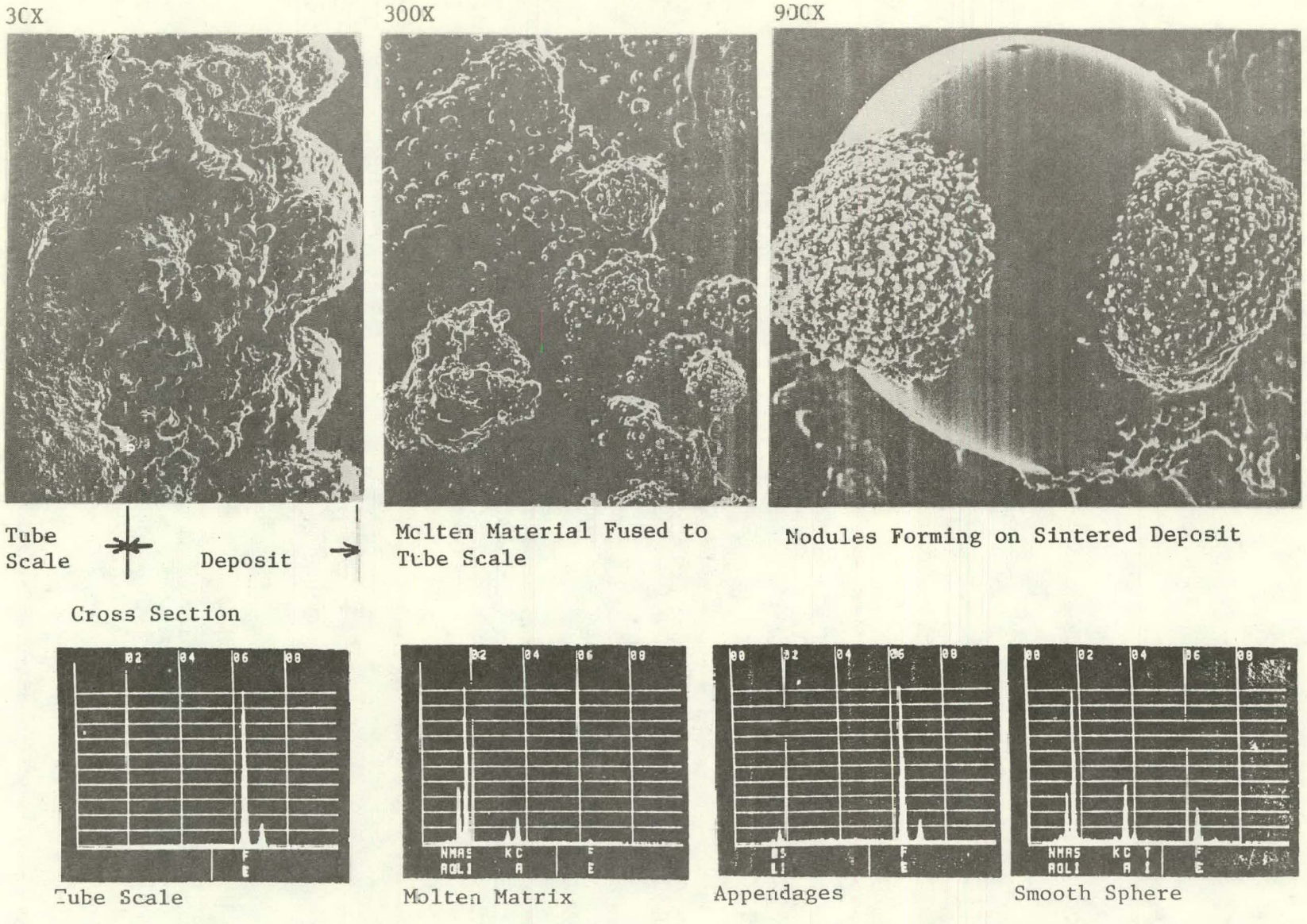


Figure 4.19 SEM Photomicrographs and EDX Scans--Surface Morphology and Elemental Composition of Perpendicular Probe Tube Scale Bonded to Ash Deposit

15X

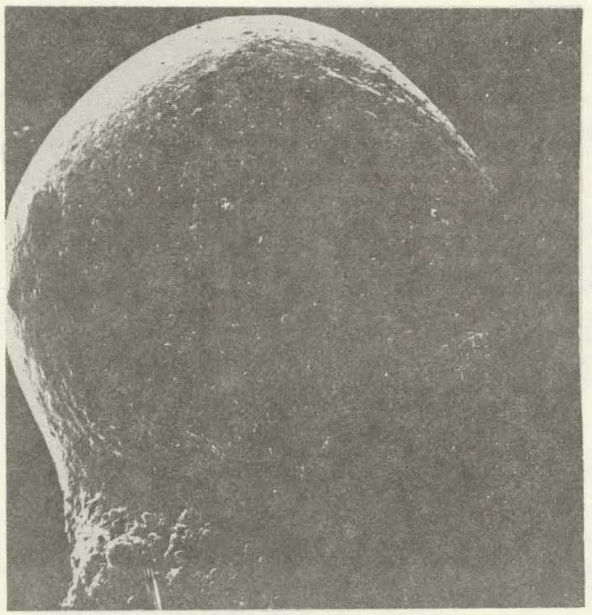

Molten Nodule

1200X

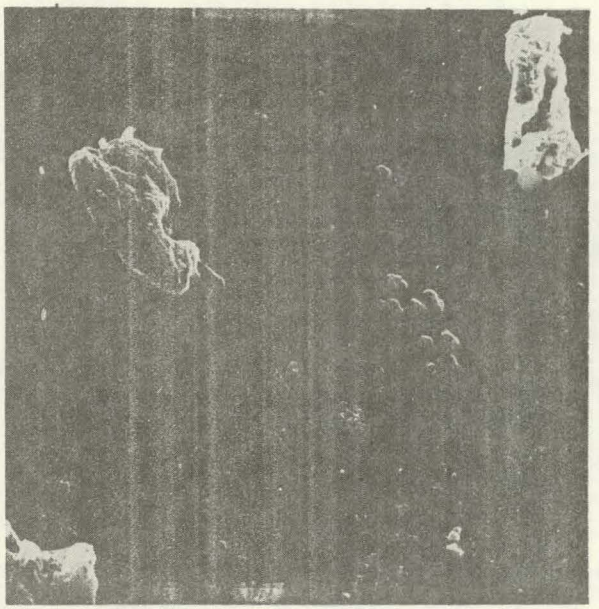

Silica Crystals

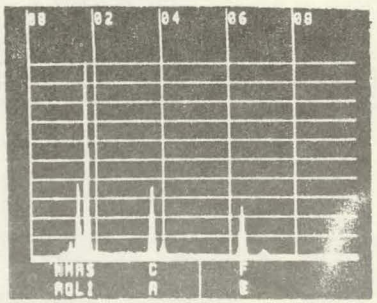


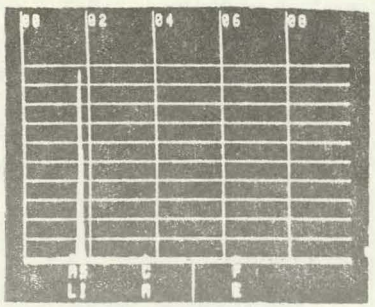


Figure 4.20 SEM Photomicrographs and EDX Scans--Surface Morphology and Elemental Analysis of Molten Nodules Formed on Lower Surface of Perpendicular Probe

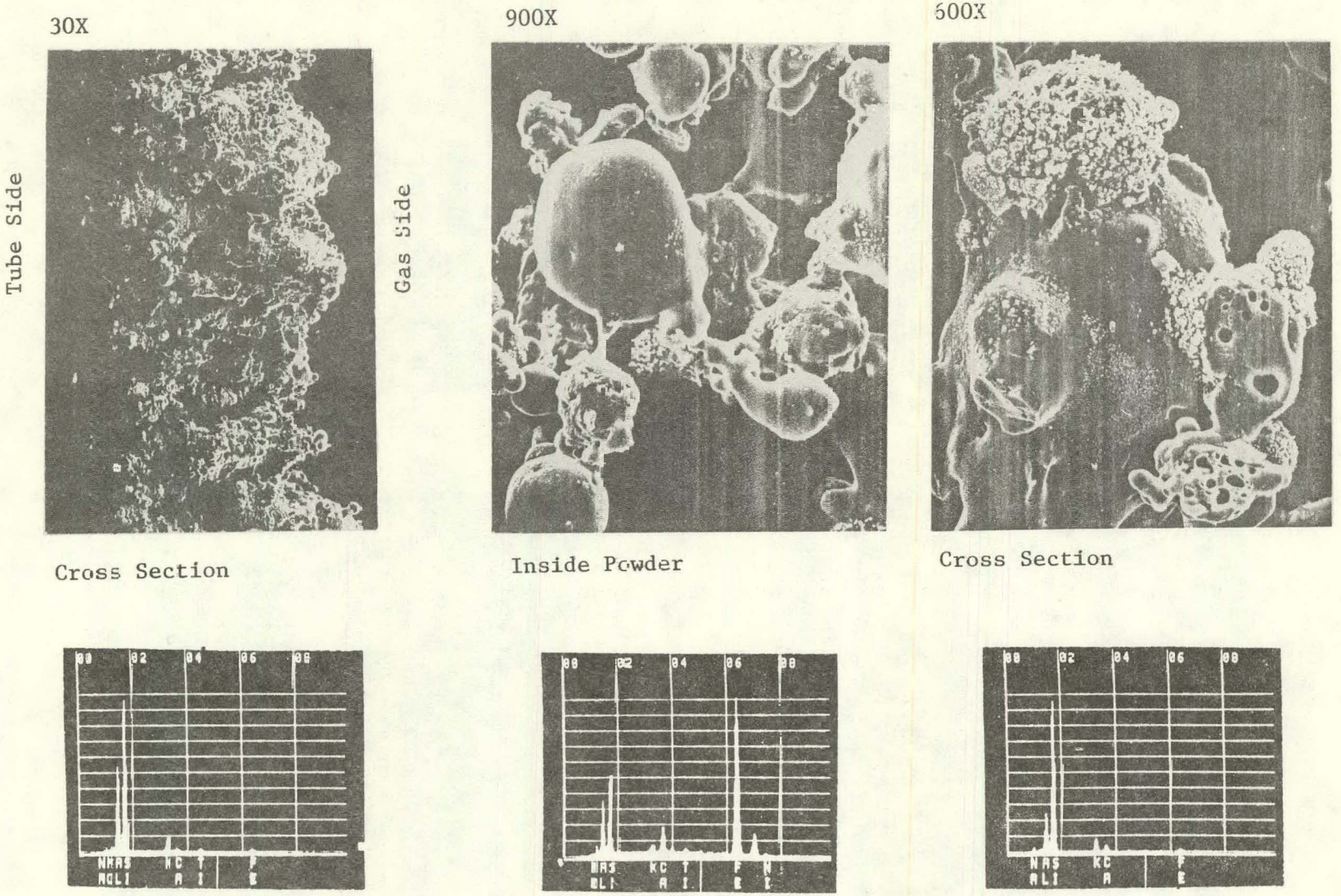


Figure 4.21 SEM Photomicrographs and EDX Scans--Surface Morphology and Elemental Analysis of Inside Powdery Layer and Cross Section of Deposit on Top Side of Probe Perpendicular to Gas Stream

alumina with trace quantities of sodium, potassium, iron, and calcium. The alkalies may be instrumental in forming the surface bonds. The cross section consists of a molten matrix of ash whose composition is primarily silica with traces of sodium and potassium (Figure 4.21) impregnated with submicron particulates rich in iron and containing minor concentrations of alumina, silica, and calcium. The outside layer is dominated by a silica-rich molten phase and small iron crystals. In some cases the spheroids, believed to be derivatives of frambodial pyrite, have attached themselves (Figure 4.22).

The furnace wall slag consists of a molten matrix of a silica-enriched substance containing crystals composed of iron, calcium, and silicon (see Figure 4.23). Unlike the advanced stage of slagging associated with other coals, there was no outer layer of nearly pure iron oxide. There is no explanation for this difference.

The sintered material formed on the upper furnace wall was similar to the material responsible for plugging the convection pass inlet (see Figure 4.24). The particles consist of two types of spheroids about 40 to 50 μm or smaller. One spheroid is smooth and appears to be slightly wetted by a thin film. Previous EDX scans have identified these spheres to be rich in silica with minor concentrations of potassium, calcium, and alumina. The second type of spheroid is completely incapsulated with submicron particles of iron whose origin is believed to be pyrite.

The composition of the bulk of the second type of spheroid is uncertain, but it is believed to be rich in quartz, as shown earlier in Figure 4.22.

1500X

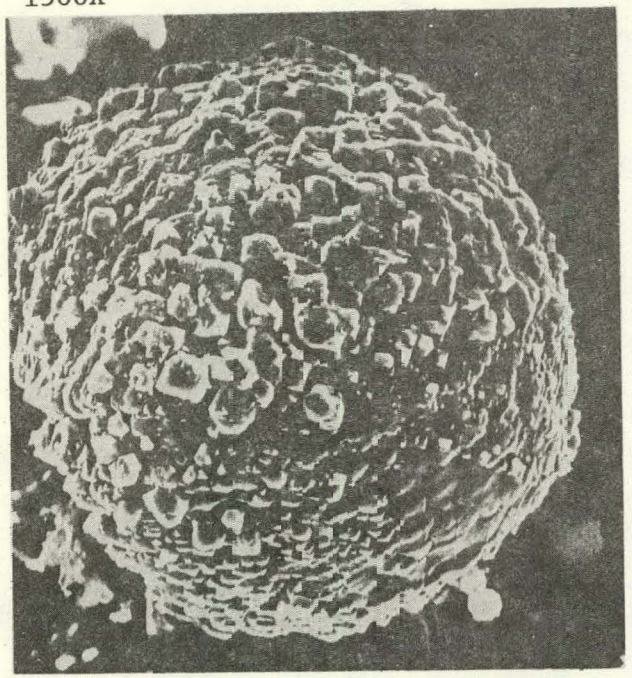

Derivative of Framboidal Pyrite

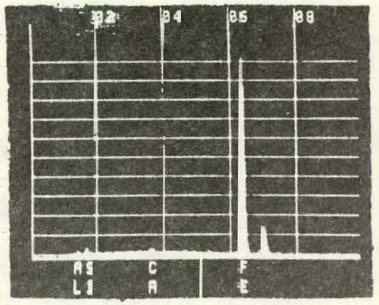


600X

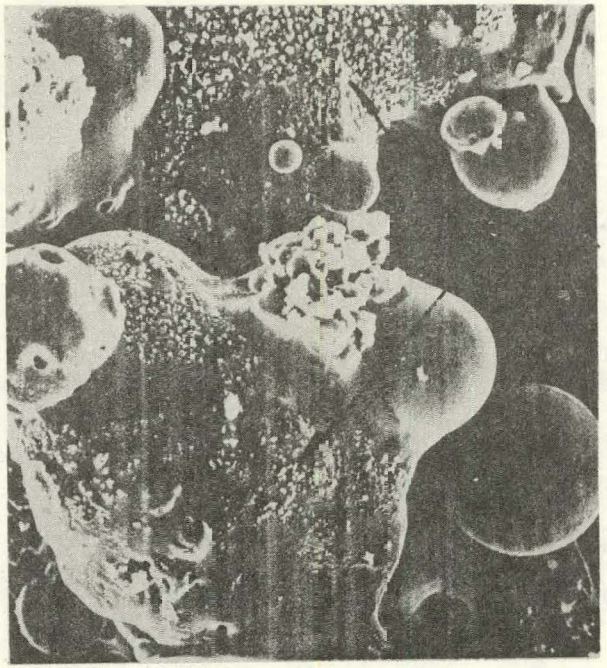

Submicron Iron Particles

Potassium Silicate Matrix

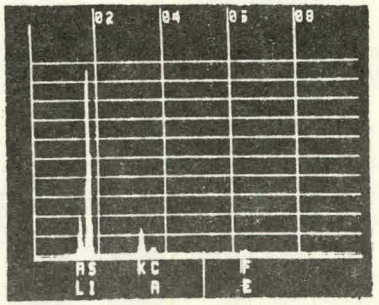


Figure 4.22 SEM Photomicrographs and EDX Scans--Surface Morpholcgy and Elemental Composition of Spent Pyrite Particles and Molten Potassium Silicate Matrix Responsible for Deposition on Slag Probe

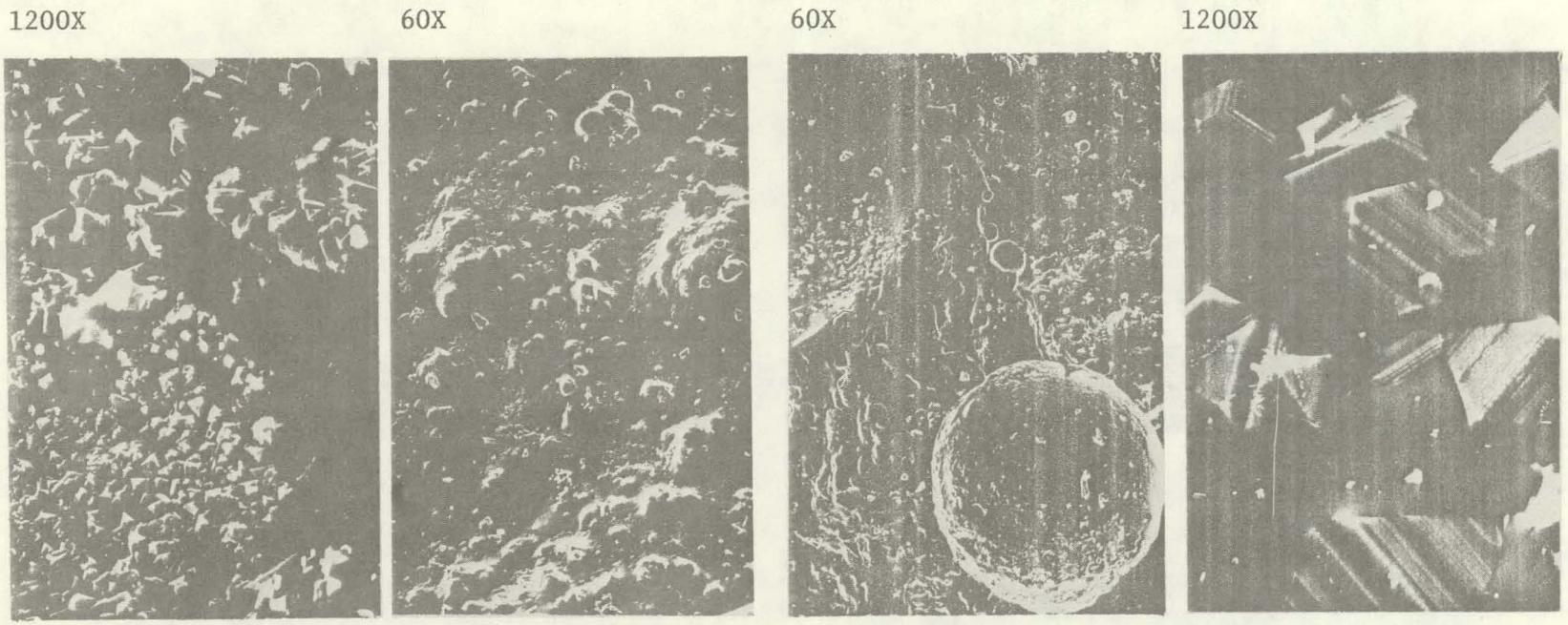


Figure 4.23 SEM Photomicrographs and EDX Scans--Surface Morphology and Elemental Composition of Surface and Cross Section of Wall Slag

600X

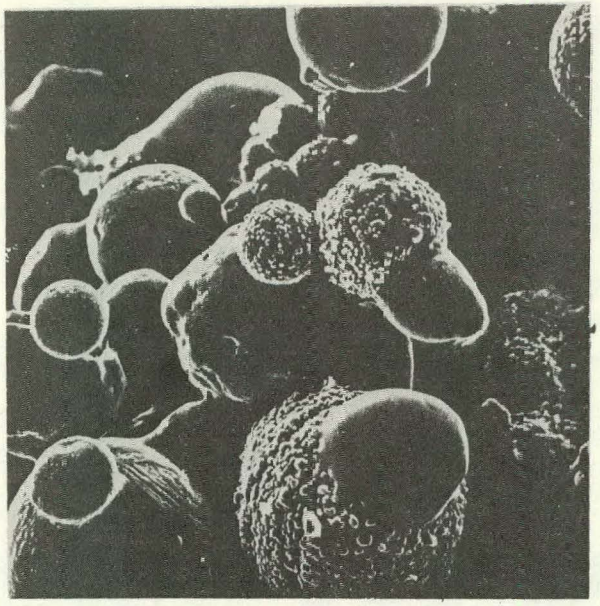

Segment 8 Furnace

600X

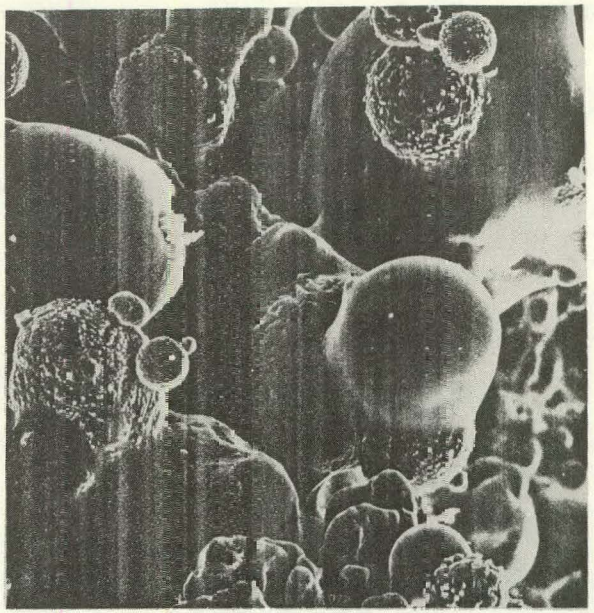

Entrance to Convection Pass

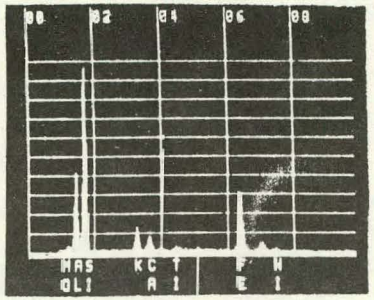

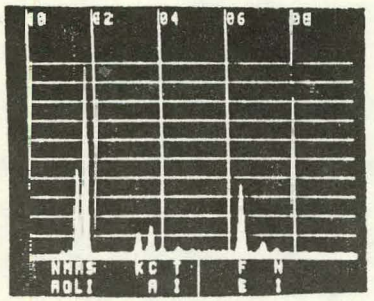

Figure 4.24 Comparison of Sintered Deposit Formed on Furnace Wall With Sintered Deposit Formed in Entrance to Convection Pass

There appears to be a subtle difference in the morphology of the smooth particles. The wetted film appears to be more dominant. This could be from the presence of sodium, detected only at the lower gas temperatures.

The fly ash resembled a collection of spheres already identified in previously discussed deposits. Figure 4.25 is a typical example.

600X

Air Heater

1500X

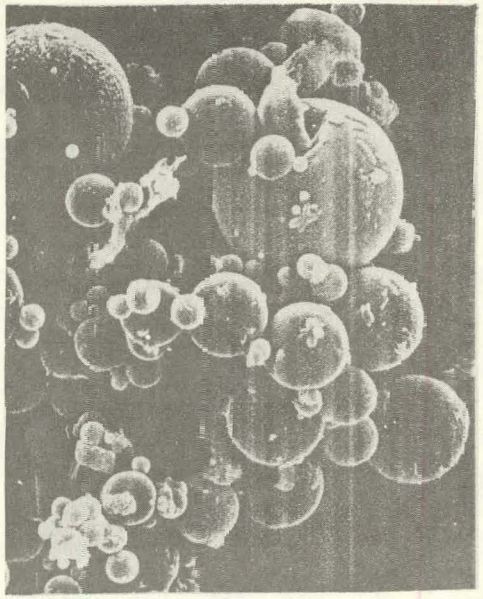

Cyclone

3000X

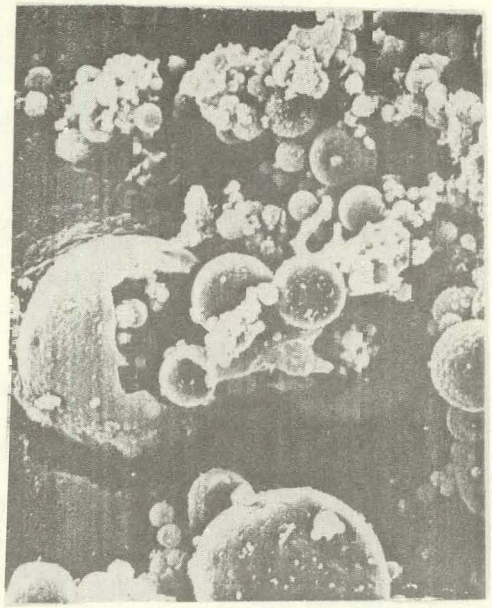

Baghouse

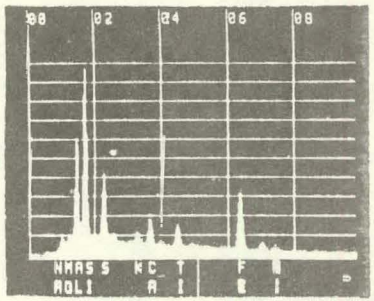

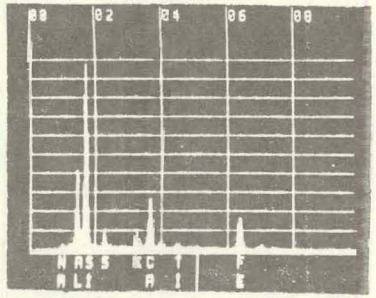

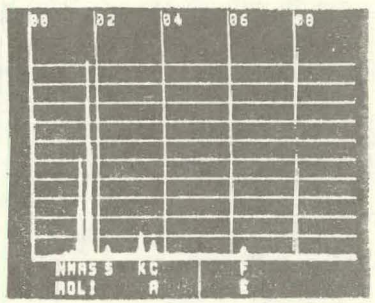

Figure 4.25 Typical Fly Ash Captured in Air Heater Cyclone and Baghouse While Firing Kentucky No. 9 Coal

Section 5

# IMPACT OF COAL WASHING ON FIRESIDE DEPOSITS

## INTRODUCTION

The most seriously slagging coal (i.e., Upper Freeport, Indiana County) was subjected to washability tests. The individual size and gravity fractions of the coal, crushed to 3/8 in. x 0, 14 mesh x 0, and 200 mesh x 0, were analyzed in detail for percentage ash and pyrite, ash chemistry, and ash fusion temperatures. By examining the elemental analysis and corresponding ash fusion temperatures of the raw coal and its mineral matter partitioned by size and gravity, the species of coal or mineral matter that should be removed by washing could be determined. The analysis also helped in selecting the particle size at which the washing should be performed. The coal was then crushed and washed. The washed product and residue were subjected to further analysis to determine the effectiveness of the cleaning operation on a large sample and to characterize the coal before combustion. The washed product was then fired in a 100 lb/h combustor for 10 hours to assess the fireside behavior of the mineral matter modified by beneficiation.

## WASHABILITY TESTS

The washability tests were reported earlier in Quarterly Progress Report 6. To maintain continuity in reporting the results, the procedure and data are briefly reviewed here.

A 300-lb sample was coned, long piled, shoveled into four piles according to ASTM specifications, and divided into two parts by combining opposite piles.

The coal was then screen-crushed and pulverized, according to the process flow diagram in Figure 5.1, into three streams--3/8 in. x 0, 14 mesh x 0, and 200 mesh x 0. The individual streams were further divided by size into increments of 3/8 in. x 14 mesh, 14 x 100 mesh, and 200 mesh x 0, as shown in Figure 5.??. Each size was sink floated at gravities of 1.26, 1.28, 1.30, 1.32, 1.34, 1.36, 1.38, 1.40, 1.50, 1.80, and 2.85 to develop washability data for ash partitioning and to estimate the liberation of ash with size. Each gravity fraction was analyzed for percentage ash, pyritic sulfur, and total sulfur. New gravity fractions were formed at +1.30, -1.30/+1.80, -1.80/+2.85, and 2.85 by combining portions of each gravity fraction proportion according to the original partitioned wt% distribution. Each of the newly formed weight fractions was analyzed for ash chemistry and ash fusion temperatures.

The weight distribution of the ash is summarized in Table 5.1; the washability data appear in Tables 5.2 through 5.5; the ash chemistry data appear in Table 5.6. The elemental analysis of the data is summarized in Table 5.7 in terms of the percentage of each element found in each gravity fraction. This table provides an insight into the degree of liberation of undesirable impurities.

The washability data are summarized in Figure 5.2. The data indicate there is only a slight improvement in liberation as the coal is crushed from 3/8 in. x 14 mesh to 14 x 100 mesh. At a 1.8 sp gr, the yield increases from 70 to 85 percent. When the coal is further pulverized to 200 mesh x 0, the yield goes down and appears to be almost identical to that of the coarse size fraction of coal crushed to 3/8 in. x 0. Whether this reduction in yield reflects the

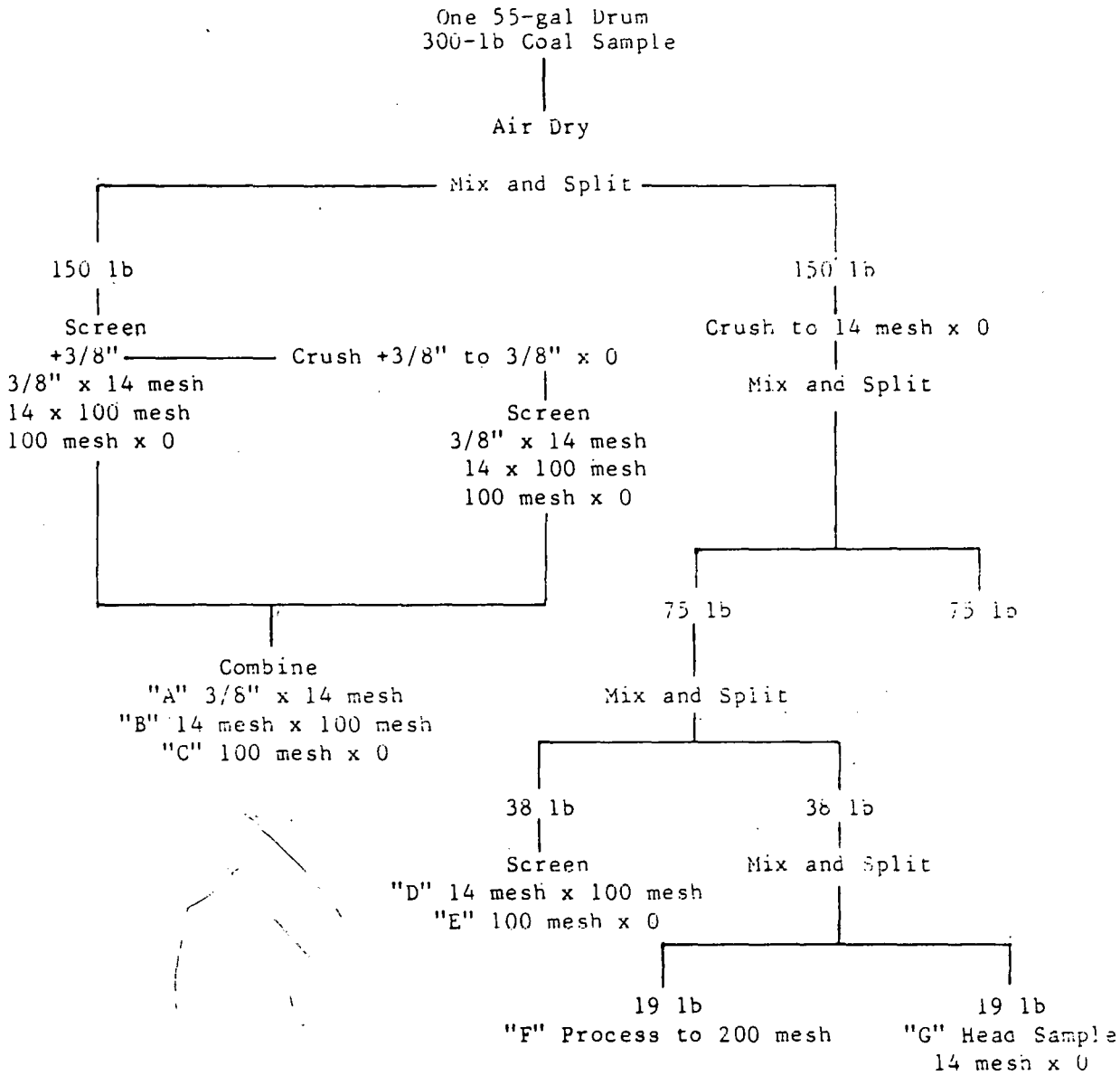


Fractions: "A", "B", "D", and "F" were sink-floated at 1.26, 1.28, 1.30, 1.32, 1.34, 1.36, 1.38, 1.40, 1.50, 1.80, and 2.85.

Figure 5.1 Process Flow Diagram for Washing 300-lb Sample of Upper Freeport Coal, Indiana County, Pennsylvania

Table 5.1 Weight Distribution of Screened Coal Samples

Air Dry Loss: 2.49 wt%

| Size | Weight (lb) | Direct Wt% | Cumulative Wt% |
|---|---|---|---|
| Screen Analysis, Portion 1 (half of representative sample): | | | |
| +3/8 in. | 21.12 | 14.5 | 14.5 |
| 3/8 in. x 14 mesh | 78.50 | 54.0 | 68.5 |
| 14 x 100 mesh | 35.54 | 24.4 | 92.9 |
| 100 mesh x 0 | 10.28 | 7.1 | 100.0 |
| Total | 145.44 | 100.00 | |
| The +3/8 in. was crushed to pass 3/8 in. and screened again: | | | |
| 3/8 in. x 14 mesh | 17.48 | 83.0 | 83.0 |
| 14 x 100 mesh | 2.84 | 13.5 | 96.5 |
| 100 mesh x 0 | 0.74 | 3.5 | 100.0 |
| Total | 21.06 | 100.0 | |
| Combined Screened Analysis (3/8 in. x 0): | | | |
| "A"--3/8 in. x 14 mesh | 95.98 | 66.0 | 66.0 |
| "B"--14 x 100 mesh | 38.38 | 26.4 | 92.4 |
| "C"--100 mesh x 0 | 11.02 | 7.6 | 100.0 |
| Total | 145.38 | 100.0 | |
| Screen Analysis, Portion 2--Crushed to 14 mesh x 0 (other half of representative sample): | | | |
| "D"--14 x 100 mesh | 27.68 | 74.7 | 74.7 |
| "E"--100 mesh x 0 | 9.38 | 25.3 | 100.0 |
| Total | 37.06 | 100.0 | |

Table 5.2 Summary of Washability Data for Upper Freeport Coal, Indiana County, Pennsylvania--Size 3/4 in. x 14 mesh (3/8 in. x 0 stream)

| Density Fraction Float/Sink | Wt% | Cumulative Weight (%) | Ash (%) | Total Ash (%) | Cumulative Ash (%) | Sulfur (%) | Total Sulfur (%) | Cumulative Sulfur (%) | Pyrite (%) | Total Pyrite (%) | Cumulative Pyrite (%) |
|---|---|---|---|---|---|---|---|---|---|---|---|
| +1.26 | 2.9 | 2.9 | 1.31 | 0.04 | 0.04 | 0.71 | 0.022 | 0.02 | 0.18 | 0.01 | 0.01 |
| +1.28/-1.26 | 11.9 | 14.8 | 2.09 | 0.24 | 0.28 | 0.75 | 0.089 | 0.11 | 0.22 | 0.03 | 0.04 |
| +1.30/-1.28 | 9.5 | 24.3 | 4.66 | 0.44 | 0.72 | 0.94 | 0.089 | 0.20 | 0.69 | 0.06 | 0.10 |
| +1.32/-1.30 | 7.4 | 31.7 | 7.03 | 0.52 | 1.24 | 1.23 | 0.091 | 0.29 | 0.89 | 0.06 | 0.16 |
| +1.34/-1.32 | 7.3 | 29.0 | 9.18 | 0.67 | 1.91 | 1.35 | 0.098 | 0.39 | 0.87 | 0.06 | 0.22 |
| +1.36/-1.34 | 5.1 | 44.1 | 11.76 | 0.59 | 2.50 | 1.33 | 0.067 | 0.42 | 0.97 | 0.05 | 0.27 |
| +1.38/-1.36 | 3.9 | 48.0 | 13.14 | 0.51 | 3.01 | 1.43 | 0.055 | 0.48 | 1.09 | 0.04 | 0.31 |
| +1.40/-1.38 | 3.1 | 51.1 | 14.83 | 0.45 | 3.46 | 1.67 | 0.051 | 0.53 | 1.25 | 0.04 | 0.35 |
| +1.50/-1.40 | 10.3 | 61.4 | 16.97 | 1.73 | 5.19 | 2.52 | 0.252 | 0.78 | 2.39 | 0.24 | 0.59 |
| +1.80/-1.50 | 11.4 | 72.8 | 31.14 | 3.54 | 8.73 | 4.60 | 0.53 | 1.31 | 3.98 | 0.45 | 1.04 |
| +2.85/-1.80 | 25.9 | 98.7 | 75.93 | 19.6 | 28.33 | 3.95 | 1.03 | 2.34 | 3.24 | 0.96 | 2.00 |
| -2.85 | 1.3 | 100.0 | 68.80 | 0.89 | 29.22 | 30.15 | 0.34 | 2.68 | 22.23 | 0.28 | 2.28 |

Table 5.3 (bottom section) Summary of Washability Data for Upper Freeport Coal, Indiana County, Pennsylvania--Size 14 x 100 mesh (3/8 in. x 0 stream)

| Density Fraction Float/Sink | Wt% | Cumulative Weight (%) | Ash (%) | Total Ash (%) | Cumulative Ash (%) | Sulfur (%) | Total Sulfur (%) | Cumulative Sulfur (%) | Pyrite (%) | Total Pyrite (%) | Cumulative Pyrite (%) |
|---|---|---|---|---|---|---|---|---|---|---|---|
| +1.26 | 5.2 | 5.2 | 1.20 | 0.06 | 0.06 | 0.61 | 0.03 | 0.03 | 0.10 | 0.005 | 0.005 |
| +1.28/-1.26 | 23.6 | 28.8 | 1.96 | 0.45 | 0.51 | 0.75 | 0.177 | 0.20 | 0.15 | 0.035 | 0.04 |
| +1.30/-1.28 | 10.9 | 39.7 | 7.22 | 0.78 | 1.29 | 1.04 | 0.113 | 0.32 | 0.30 | 0.032 | 0.07 |
| +1.32/-1.30 | 8.3 | 48.0 | 11.53 | 0.95 | 2.24 | 1.63 | 0.13 | 0.45 | 0.71 | 0.058 | 0.13 |
| +1.34/-1.32 | 6.8 | 54.8 | 11.16 | 0.75 | 2.99 | 1.51 | 0.10 | 0.55 | 0.60 | 0.04 | 0.16 |
| +1.36/-1.34 | 3.0 | 57.8 | 11.10 | 0.33 | 3.32 | 1.50 | 0.045 | 0.59 | 0.59 | 0.04 | 0.20 |
| +1.38/-1.36 | 2.9 | 60.1 | 13.50 | 0.39 | 3.71 | 1.63 | 0.047 | 0.64 | 0.68 | 0.02 | 0.22 |
| +1.40/-1.38 | 2.9 | 63.6 | 14.79 | 0.42 | 4.13 | 1.73 | 0.05 | 0.69 | 0.76 | 0.02 | 0.24 |
| +1.50/-1.40 | 7.2 | 70.8 | 18.86 | 1.35 | 5.48 | 2.29 | 0.16 | 0.85 | 0.98 | 0.28 | 0.52 |
| +1.80/-1.50 | 10.0 | 80.8 | 30.13 | 3.01 | 8.49 | 3.44 | 0.34 | 1.19 | 2.50 | 0.25 | 0.77 |
| +2.85/-1.80 | 17.2 | 98.0 | 71.93 | 12.3 | 20.79 | 5.86 | 1.01 | 2.20 | 4.30 | 0.73 | 1.50 |
| -2.85 | 2.0 | 100.0 | 55.68 | 1.11 | 21.90 | 6.30 | 0.12 | 2.21 | 15.07 | 0.30 | 1.80 |
| Size 100 mesh x 0 (3/8 in. x 0 stream) | --- | --- | 20.06 | --- | --- | 3.07 | --- | --- | 2.44 | --- | --- |

Table 5.4 Summary of Washability Data for Upper Freeport Coal, Indiana County, Pennsylvania--Size 14 x 100 mesh (14 mesh x 0 stream)

| Density Fraction Float/Sink | Wt% | Cumulative Weight (%) | Ash (%) | Total Ash (%) | Cumulative Ash (%) | Sulfur (%) | Total Sulfur (%) | Cumulative Sulfur (%) | Pyrite (%) | Total Pyrite (%) | Cumulative Pyrite (%) |
|---|---|---|---|---|---|---|---|---|---|---|---|
| +1.26 | 2.9 | 2.9 | 2.95 | 0.08 | 0.8 | 1.07 | 0.03 | 0.03 | 0.42 | 0.012 | 0.012 |
| +1.28/-1.26 | 28.7 | 31.6 | 3.80 | 1.09 | 1.17 | 0.96 | 0.27 | 0.30 | 0.45 | 0.12 | 0.132 |
| +1.30/-1.28 | 17.6 | 49.2 | 5.93 | 1.04 | 2.28 | 1.16 | 0.20 | 0.50 | 0.57 | 0.100 | 0.232 |
| +1.32/-1.30 | 7.4 | 56.6 | 7.77 | 0.57 | 2.78 | 1.59 | 0.11 | 0.61 | 0.92 | 0.06 | 0.292 |
| +1.34/-1.32 | 5.1 | 61.7 | 8.50 | 0.43 | 3.21 | 1.61 | 0.08 | 0.69 | 0.92 | 0.04 | 0.33 |
| +1.36/-1.34 | 2.6 | 64.3 | 14.70 | 0.38 | 3.59 | 1.69 | 0.04 | 0.73 | 1.43 | 0.03 | 0.36 |
| +1.38/-1.36 | 3.4 | 67.7 | 17.94 | 0.60 | 4.19 | 3.55 | 0.12 | 0.85 | 3.15 | 0.10 | 0.37 |
| +1.40/-1.38 | 2.8 | 70.5 | 13.32 | 0.37 | 4.56 | 1.98 | 0.05 | 0.90 | 1.43 | 0.40 | 0.77 |
| +1.50/-1.40 | 6.9 | 77.4 | 17.14 | 1.48 | 5.74 | 2.71 | 0.18 | 1.08 | 2.15 | 0.14 | 0.91 |
| +1.80/-1.50 | 8.0 | 85.4 | 27.35 | 2.18 | 7.92 | 3.57 | 0.28 | 1.36 | 2.82 | 0.22 | 1.13 |
| +2.85/-1.80 | 11.0 | 96.4 | 69.93 | 7.69 | 15.6 | 4.36 | 0.47 | 1.83 | 4.73 | 0.52 | 1.65 |
| -2.85 | 3.6 | 100.0 | 73.90 | 2.66 | 18.2 | 18.21 | 0.65 | 2.48 | 15.50 | 0.55 | 2.20 |
| Size 100 mesh x 0 (14 mesh x 0 stream) | --- | --- | 25.40 | --- | --- | 3.06 | --- | --- | 1.21 | --- | --- |





REF.: DE-AC22-81PC40268
DATE: June 1984

Table 5.5 Summary of Washability Data for Upper Freeport, Indiana County, Pennsylvania--Size 200 Mesh x 0 Stream

| Density Fraction Float/Sink | Wt% | Cumulative Weight (%) | Ash (%) | Total Ash (%) | Cumulative Ash (%) | Sulfur (%) | Total Sulfur (%) | Cumulative Sulfur (%) | Pyrite (%) | Total Pyrite (%) | Cumulative Pyrite (%) |
|---|---|---|---|---|---|---|---|---|---|---|---|
| +1.26 | 1.0 | 1.0 | 1.50 | 0.015 | 0.015 | 0.71 | 0.007 | 0.007 | 0.06 | 0.0006 | 0.001 |
| +1.28/-1.26 | 7.2 | 8.2 | 1.86 | 0.13 | 0.145 | 0.69 | 0.049 | 0.056 | 0.08 | 0.005 | 0.005 |
| +1.30/-1.28 | 8.8 | 17.0 | 3.07 | 0.27 | 0.415 | 0.69 | 0.061 | 0.117 | 0.15 | 0.132 | 0.137 |
| +1.32/-1.30 | 8.1 | 25.1 | 3.89 | 0.31 | 0.725 | 0.71 | 0.057 | 0.17 | 0.23 | 0.018 | 0.155 |
| +1.34/-1.32 | 6.6 | 31.7 | 5.81 | 0.38 | 1.105 | 0.74 | 0.048 | 0.22 | 0.37 | 0.24 | 0.39 |
| +1.36/-1.34 | 4.0 | 35.7 | 6.53 | 0.26 | 1.36 | 0.68 | 0.027 | 0.24 | 0.37 | 0.014 | 0.409 |
| +1.38/-1.36 | 4.0 | 39.7 | 7.17 | 0.28 | 1.64 | 0.69 | 0.027 | 0.27 | 0.41 | 0.016 | 0.425 |
| +1.40/-1.38 | 5.2 | 44.9 | 8.73 | 0.45 | 2.09 | 0.66 | 0.034 | 0.31 | 0.49 | 0.025 | 0.451 |
| +1.50/-1.40 | 12.1 | 57.0 | 12.39 | 1.48 | 3.57 | 0.93 | 0.112 | 0.42 | 0.80 | 0.096 | 0.546 |
| -1.80/-1.50 | 18.4 | 75.4 | 21.63 | 3.97 | 7.54 | 1.59 | 0.29 | 0.71 | 1.58 | 0.29 | 0.836 |
| +2.85/-1.80 | 20.5 | 95.9 | 63.15 | 12.92 | 20.46 | 2.66 | 0.54 | 1.25 | 2.27 | 0.46 | 1.29 |
| -2.85 | 4.1 | 100.0 | 64.40 | 2.62 | 23.1 | 36.47 | 1.49 | 2.74 | 35.08 | 1.43 | 2.72 |

Table 5.6 Ash Chemistry and Ash Fusion Data for Washed, Upper Freeport Coal, Indiana County, Pennsylvania*

| Density Fraction | Wt% | Ash (%) | Ash Chemistry (%) | | | | | | | | | | Ash Fusion (°F) | | | | | | | |
|---|---|---|---|---|---|---|---|---|---|---|---|---|---|---|---|---|---|---|---|---|
| | | | | | | | | | | | | | Reducing | | | | Oxidizing | | | |
| | | | $SiO_2$ | $Al_2O_3$ | $TiO_2$ | $Fe_2O_3$ | CaO | MgO | $Na_2O$ | $K_2O$ | $SO_3$ | $P_2O_5$ | I.D. | S.T. (Sph.) | S.T. (Hem.) | F.T. | I.D. | S.T. (Sph.) | S.T. (Hem.) | F.T. |
| 3/8 x 0 Stream: | | | | | | | | | | | | | | | | | | | | |
| Size: 3.8 x 14-Mesh | | | | | | | | | | | | | | | | | | | | |
| Wt%: 66.0 | | | | | | | | | | | | | | | | | | | | |
| Float-Sink | | | | | | | | | | | | | | | | | | | | |
| +1.30 | 24.3 | 2.9 | 42.0 | 30.8 | 1.5 | 16.3 | 4.8 | 0.6 | 0.7 | 2.1 | 0.4 | 1.1 | 2190 | 2240 | 2270 | 2300 | 2530 | 2560 | 2590 | 2610 |
| +1.80/-1.30 | 48.5 | 16.5 | 45.9 | 28.3 | 1.2 | 17.8 | 2.5 | 0.6 | 0.4 | 2.8 | 1.7 | 0.5 | 2220 | 2260 | 2300 | 2340 | 2560 | 2550 | 2570 | 2590 |
| +2.85/-1.80 | 25.9 | 75.93 | 54.6 | 25.8 | 1.1 | 11.6 | 1.0 | 7.0 | 0.4 | 3.4 | 0.7 | 0.3 | 2240 | 2280 | 2330 | 2370 | 2390 | 2420 | 2460 | 2490 |
| Sink | 1.3 | 68.80 | 21.3 | 20.5 | 0.4 | 54.9 | 1.2 | 0.4 | 0.1 | 1.1 | 0.8 | 0.3 | 1980 | 2020 | 2060 | 2100 | 2600 | 2620 | 2630 | 2660 |
| Size: 14 x 100 Mesh | | | | | | | | | | | | | | | | | | | | |
| Wt%: 26.4 | | | | | | | | | | | | | | | | | | | | |
| Float-Sink | | | | | | | | | | | | | | | | | | | | |
| +1.30 | 39.7 | 7.1 | 42.4 | 28.8 | 2.2 | 13.5 | 5.9 | 0.9 | 0.6 | 2.5 | 4.6 | 1.1 | 2220 | 2230 | 2280 | 2320 | 2440 | 2470 | 2490 | 2560 |
| +1.80/-1.30 | 41.1 | 17.5 | 46.3 | 29.7 | 1.3 | 16.1 | 1.8 | 0.7 | 0.4 | 2.8 | 1.5 | 0.6 | 2470 | 2500 | 2510 | 2530 | 2650 | 2670 | 2090 | 2780 |
| +2.85/-1.80 | 17.2 | 71.93 | 47.9 | 26.7 | 1.0 | 13.8 | 2.5 | 0.9 | 0.4 | 3.1 | 0.7 | 0.3 | 2090 | 2140 | 2190 | 2230 | 2300 | 2340 | 2370 | 2390 |
| Sink | 2.0 | 55.68 | 15.2 | 16.3 | 0.3 | 65.0 | 1.2 | 0.3 | 0.1 | 0.8 | 0.6 | 0.3 | 1960 | 2000 | 2040 | 2070 | 2630 | 2640 | 2360 | 2670 |
| Size: 100 Mesh x 0<br>Wt%: 7.6 | 7.6 | 20.06 | 38.6 | 18.5 | 0.9 | 17.7 | 9.5 | 0.8 | 0.4 | 2.3 | 10.9 | 0.3 | 2220 | 2240 | 2260 | 2280 | 2350 | 2380 | 2390 | 2420 |
| 14 Mesh x 0 Stream: | | | | | | | | | | | | | | | | | | | | |
| Size: 14 x 100 Mesh | | | | | | | | | | | | | | | | | | | | |
| Wt%: 74.7 | | | | | | | | | | | | | | | | | | | | |
| Float-Sink | | | | | | | | | | | | | | | | | | | | |
| +1.30 | 49.2 | 4.9 | 40.3 | 27.1 | 2.0 | 15.5 | 5.5 | 0.9 | 0.6 | 2.3 | 4.2 | 1.9 | 2180 | 2210 | 2270 | 2290 | 2410 | 2430 | 2460 | 2500 |
| +1.80/-1.30 | 63.8 | 8.9 | 42.7 | 28.0 | 1.2 | 10.4 | 2.0 | 0.4 | 0.4 | 2.6 | 1.9 | 0.5 | 2400 | 2440 | 2470 | 2500 | 2560 | 2570 | 2590 | 2610 |
| +2.85/-1.80 | 11.0 | 69.93 | 51.3 | 25.7 | 1.0 | 11.9 | 3.3 | 1.0 | 0.4 | 3.2 | 0.9 | 0.3 | 2170 | 2250 | 2290 | 2320 | 2330 | 2370 | 2390 | 2410 |
| Sink | 3.6 | 73.90 | 25.9 | 11.6 | 0.4 | 33.9 | 13.1 | 0.6 | 0.2 | 1.5 | 10.3 | 0.2 | 1970 | 2010 | 2050 | 2080 | 2230 | 2310 | 2330 | 2350 |
| Size: 100M x 0<br>Wt%: 25.3 | 25.3 | 20.73 | 42.3 | 24.2 | 1.0 | 17.7 | 6.0 | 0.9 | 0.4 | 2.7 | 6.0 | 0.4 | 2160 | 2200 | 2220 | 2240 | 2380 | 2390 | 2410 | 2450 |
| 200M x 0 Stream: | | | | | | | | | | | | | | | | | | | | |
| Size: 200M x 0 | | | | | | | | | | | | | | | | | | | | |
| Wt% 100 | | | | | | | | | | | | | | | | | | | | |
| Float-Sink | | | | | | | | | | | | | | | | | | | | |
| +1.30 | 17.0 | 2.8 | 46.0 | 31.5 | 2.9 | 8.5 | 5.7 | 1.1 | 0.5 | 2.9 | 3.1 | 0.7 | 2360 | 2380 | 2400 | 2420 | 2420 | 2460 | 2500 | 2540 |
| +1.80/-1.30 | 58.6 | 12.1 | 48.0 | 31.0 | 1.4 | 9.3 | 1.7 | 0.9 | 0.4 | 3.3 | 1.1 | 0.5 | 2400 | 2430 | 2460 | 2490 | 2650 | 2680 | 2700 | 2700 |
| +2.85/-1.80 | 20.5 | 63.15 | 53.0 | 27.6 | 1.0 | 8.5 | 3.5 | 0.8 | 0.4 | 3.2 | 2.0 | 0.4 | 2120 | 2230 | 2260 | 2310 | 2330 | 2360 | 2410 | 2460 |
| Sink | 4.1 | 64.40 | 25.3 | 16.3 | 0.6 | 49.6 | 1.6 | 0.5 | 0.2 | 1.6 | 1.5 | 0.2 | 2020 | 2040 | 2070 | 2100 | 2590 | 2620 | 2640 | 2660 |

*Symbols plotted in Figure 5.3.



FOSTER WHEELER DEVELOPMENT CORPORATION
REF.: DE-AC22-81PC40263
DATE: June 1984

Table 5.7 Liberation of Elemental Constituents in Ash from Pulverized Coal

| Density Fraction | Ash Chemistry (% of Total) | | | | | | | | | |
|---|---|---|---|---|---|---|---|---|---|---|
| | $SiO_2$ | $Al_2O_3$ | $TiO_2$ | $Fe_2O_3$ | CaO | MgO | $Mn_3O$ | $K_2O$ | $SO_3$ | $P_2O_5$ |
| 3/8 x 0 Stream | | | | | | | | | | |
| Size 3/8 x 14M Wt% 66.9 | | | | | | | | | | |
| Float-Sink | | | | | | | | | | |
| +1.30 | 1.9 | 2.8 | 3.0 | 2.6 | 7.7 | 1.6 | 4.2 | 1.2 | 1.0 | 6.9 |
| +1.80/-1.30 | 24.7 | 29.3 | 29.5 | 33.1 | 45.4 | 19.2 | 27.6 | 26.2 | 48.9 | 39.8 |
| +2.85/-1.80 | 72.1 | 65.5 | 66.2 | 52.8 | 44.5 | 77.8 | 67.3 | 72.7 | 47.11 | 49.8 |
| Sink | 1.2 | 2.3 | 1.1 | 11.3 | 2.3 | 1.4 | 0.7 | 1.1 | 2.5 | 2.5 |
| Size 14M x 100M Wt% 26.4 | | | | | | | | | | |
| Float-Sink | | | | | | | | | | |
| +1.30 | 11.1 | 12.6 | 5.2 | 9.7 | 26.7 | 13.2 | 17.4 | 10.6 | 40.1 | 27.2 |
| +1.80/-1.30 | 31.4 | 33.1 | 81.5 | 29.8 | 20.9 | 26.5 | 28.7 | 30.3 | 31.1 | 37.7 |
| +2.85/-1.80 | 55.7 | 51.2 | 10.5 | 42.8 | 50.2 | 58.5 | 50.3 | 57.7 | 26.7 | 32.4 |
| Sink | 1.5 | 2.8 | 2.6 | 17.5 | 2.1 | 1.57 | 3.3 | 1.2 | 2.0 | 2.6 |
| 14M x 0 Stream | | | | | | | | | | |
| Size 14M x 300 Wt% 74.7 | | | | | | | | | | |
| Float-Sink | | | | | | | | | | |
| +1.30 | 12.2 | 14.5 | 24.0 | 11.6 | 15.8 | 15.9 | 19.7 | 12.0 | 18.5 | 21.9 |
| +1.80/-1.30 | 30.2 | 34.9 | 33.5 | 22.4 | 33.4 | 16.5 | 30.9 | 26.2 | 19.9 | 36.2 |
| +2.85/-1.80 | 49.1 | 43.7 | 38.0 | 20.3 | 29.4 | 56.1 | 42.1 | 53.8 | 12.8 | 24.2 |
| Sink | 8.4 | 6.7 | 5.0 | 27.6 | 40.7 | 11.5 | 7.3 | 8.7 | 48.8 | 6.7 |
| 200M x 0 Stream | | | | | | | | | | |
| Size 200M x 0 Wt% 100 | | | | | | | | | | |
| Float-Sink | | | | | | | | | | |
| +1.30 | 1.95 | 2.2 | 4.8 | 1.2 | 4.2 | 22.4 | 2.6 | 1.9 | 3.7 | 3.7 |
| +1.80/-1.30 | 30.6 | 34.7 | 36.6 | 21.2 | 38.6 | 27.2 | 32.4 | 33.2 | 19.8 | 43.2 |
| +2.85/-1.80 | 61.6 | 56.6 | 52.6 | 35.3 | 70.5 | 44.5 | 59.1 | 58.9 | 66.3 | 46.9 |
| Sink | 5.9 | 6.7 | 5.8 | 42.1 | 6.5 | 5.7 | 5.7 | 6.0 | 10.0 | 6.2 |

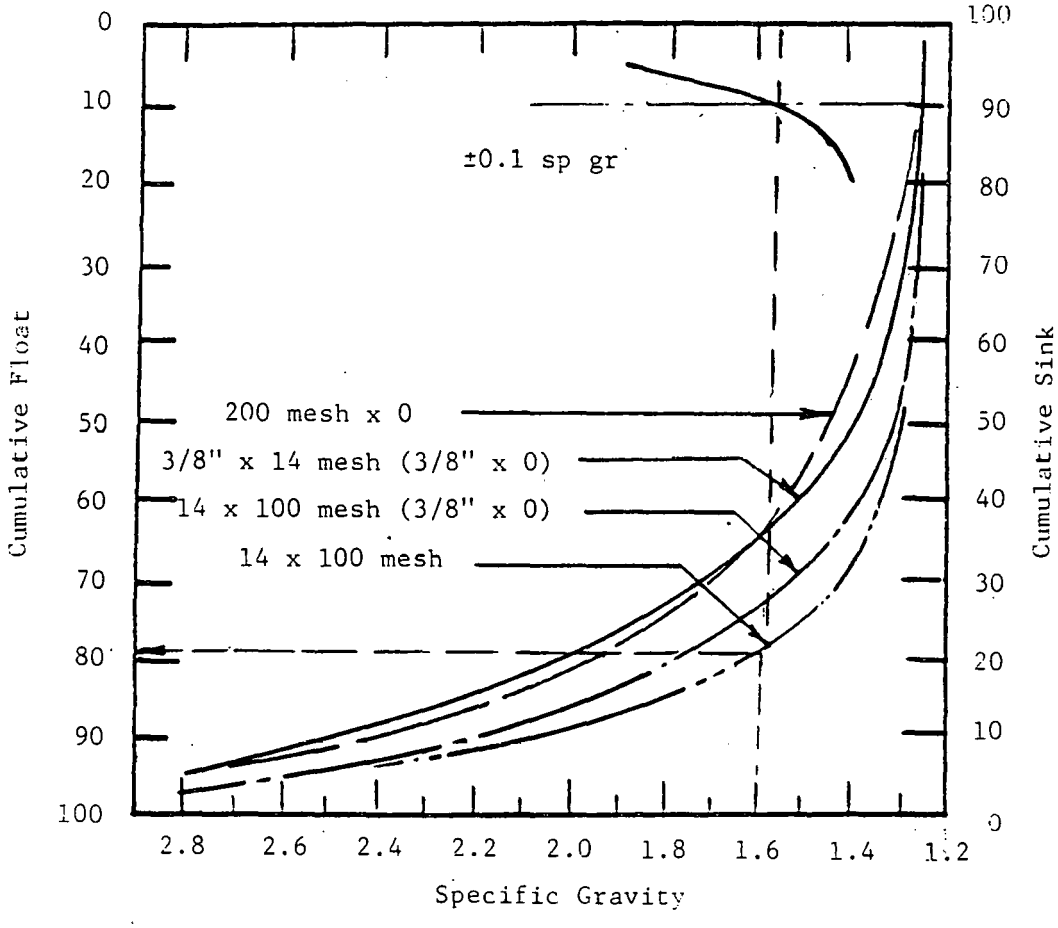


Scale of Values of Near-Gravity Material:

| Quantity Within ±0.10 sp gr range (%) | Separation Problem |
|---|---|
| 0 - 7 | Simple |
| 7 - 10 | Moderately Difficult |
| 10 - 15 | Difficult |
| 15 - 20 | Very Difficult |
| 20 - 25 | Exceedingly Difficult |
| Above 25 | Formidable |

J. W. Leonard and D. R. Mitchell, "Coal Preparation," The American Institute of Mining, Metallurgical, and Petroleum Engineers, New York, 1968.

Figure 5.2 Cumulative Float (% Yield) vs. Specific Gravity for Various Size Fractions

difficulty of separation at the smaller size fractions or variability in mineral size and association within the coal is not certain. The curve illustrating the quantity of near gravity material within the ±10 sp gr range indicates good separation can be achieved at gravities greater than 1.6 sp gr. The selection of the optimum gravity level for performing a separation is not explicit, as the percentage yield vs. gravity curve is exponential. A qualitative assessment of the curves suggests that the 1.80 gravity separation of coal crushed to 14 x 100 mesh gives a yield of about 82 percent while liberating about 60 percent of the ash and 51.3 percent of the pyrite. The product should contain about 7.92-percent ash and 1.13-percent pyrites. The ash chemistry and ash fusion data, summarized in Figures 5.3 and 5.4 on the ash softening temperature vs. percentage basic curve and the ash fusibility curve, indicate the lowest melting and most troublesome ash are contained in the gravity fractions heavier than 1.80, which will be removed during the beneficiation process. The fusibility curves indicate there is very little change in the physicochemical properties as the coal is pulverized to 200 mesh x 0. Therefore, although the coal is washed at the 14 mesh x 0 size, further pulverizing to 200 mesh x 0 before combustion should have little effect on the fireside characteristics of the ash. The fusibility curves also indicate the inherent ash contained in the float 1.30 coal has melting characteristics similar to the composite coal ash chemistry. The heavier fractions have been depleted of pyrite during crushing; consequently, they have a higher softening temperature than the raw coal, reflecting the reduction in iron concentration in the ash. The final composite softening temperature of the washed coal should be 100 to 200°F higher than the raw coal. The reduction in individual elements as a function of yield in the

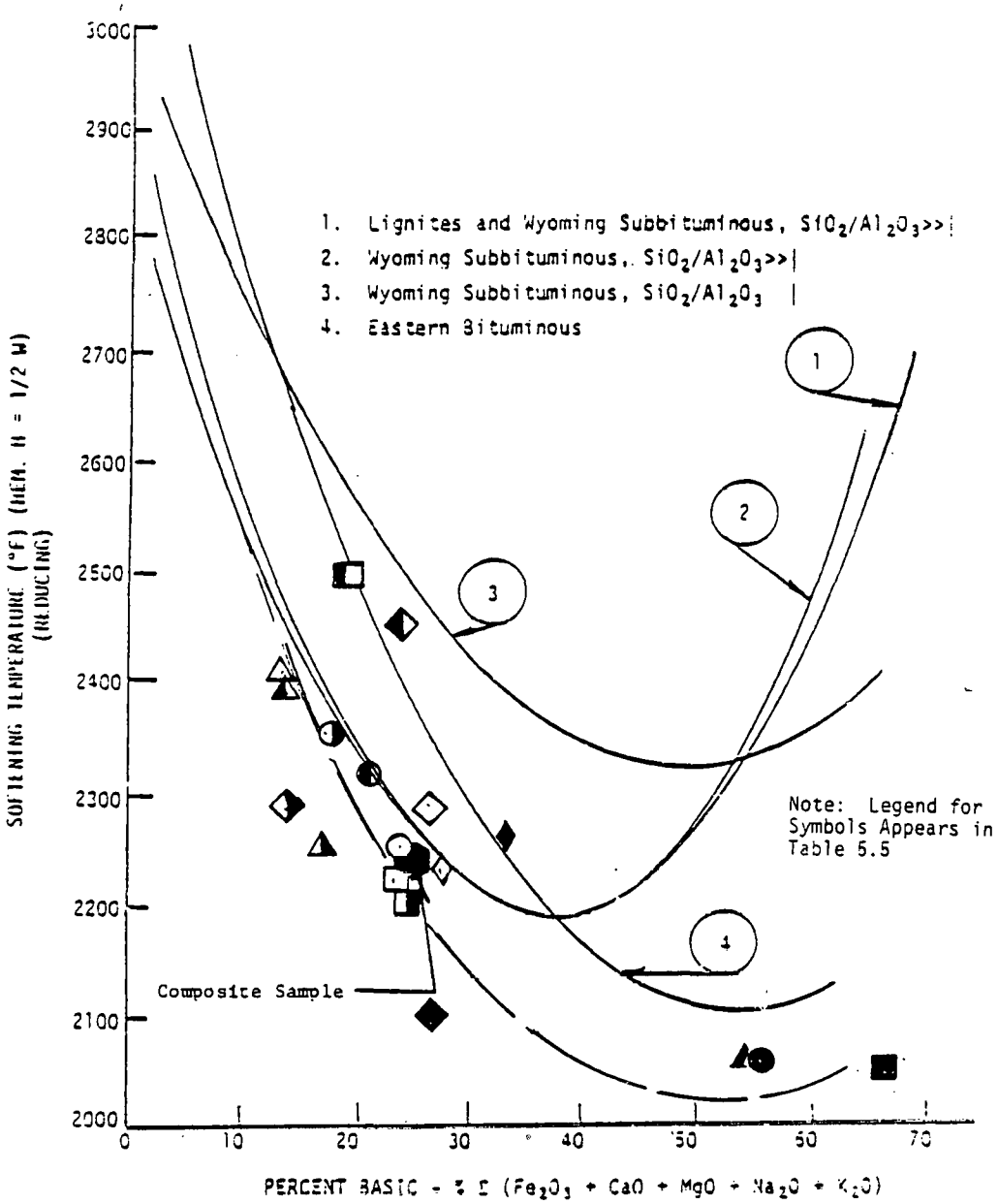


Figure 5.3 Impact of Beneficiation on Coal Ash Quality of Individual Size and Gravity Fractions as Defined by Physicochemical Properties of Ash, Percentage Basicity, and Ash Softening Temperature

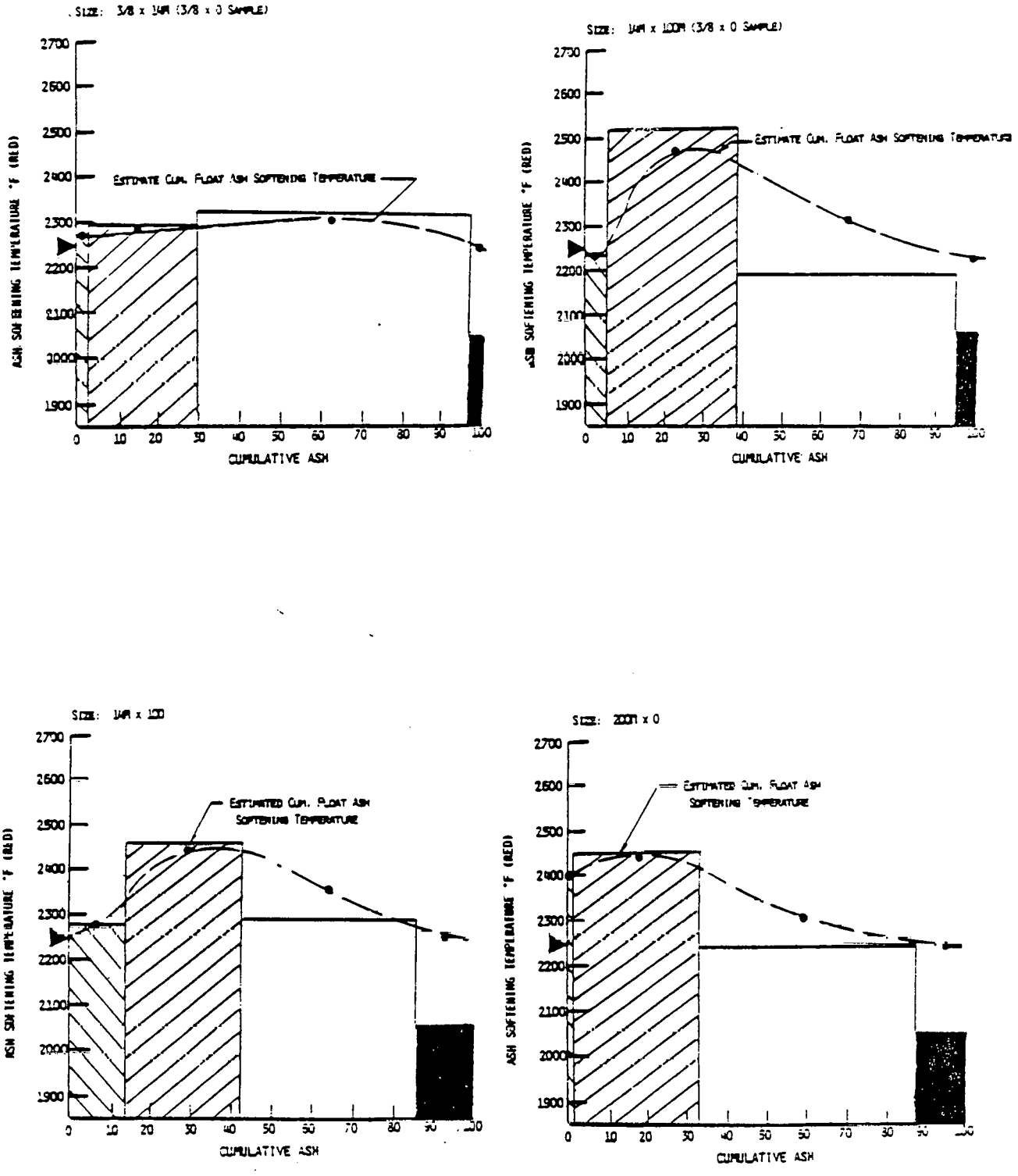


Figure 5.4 Fusibility Diagrams for Various Size Fractions

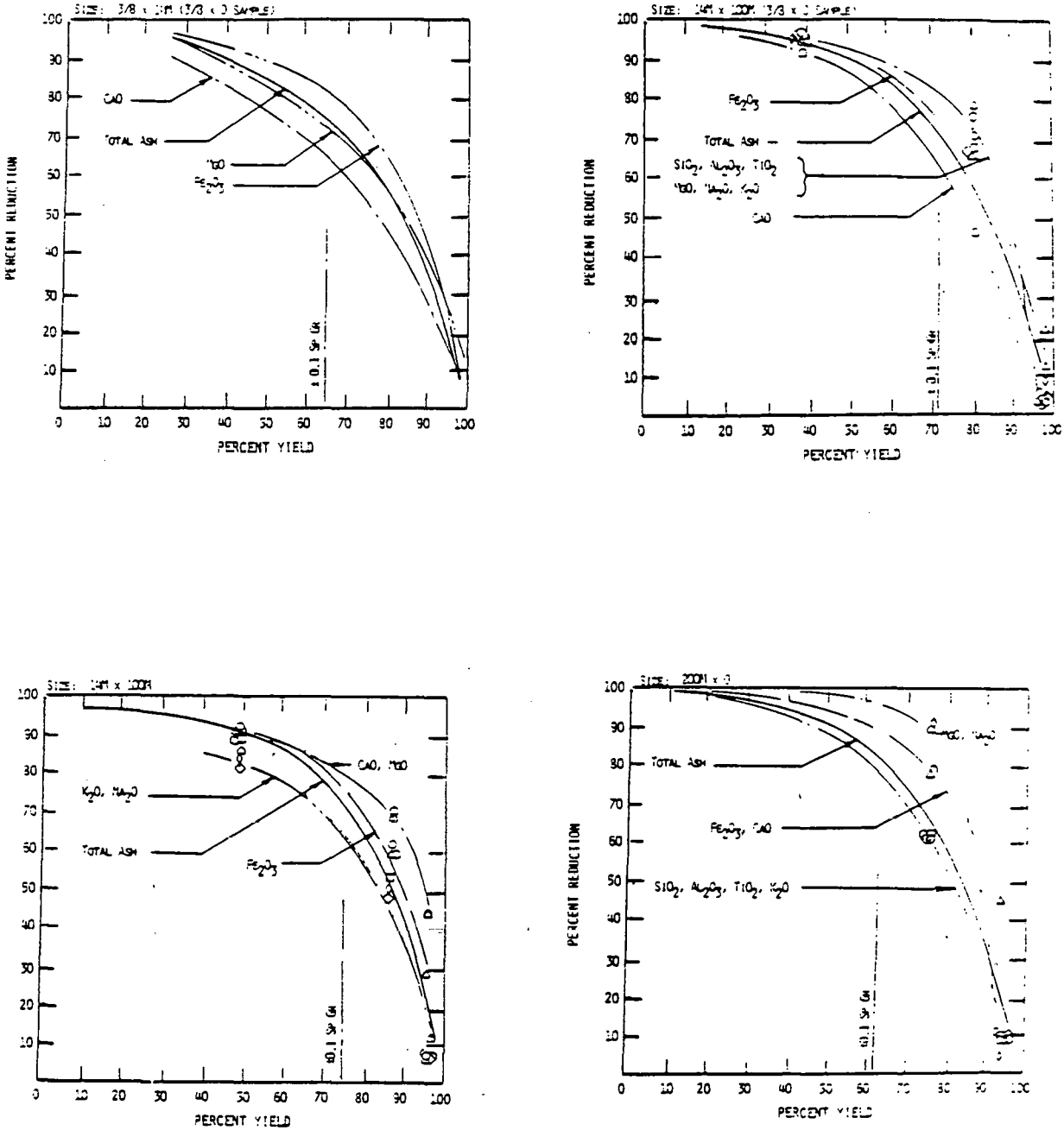


Figure 5.5 Percentage Reduction in Individual Elements vs. Percentage Yield of Washed Product

washing process indicates the most "effective" reduction in elemental impurity occurs at about 70 percent yield or 1.80 sp gr. $FeS_2$ is preferentially removed at the higher levels of yield, reflecting the partitioning of $FeS_2$ and other mineral matter in the heaviest gravity fractions (see Figure 5.5).

COAL WASHING

The washability data indicated the most beneficial improvement in fireside deposits should occur as a result of washing 14 x 100 mesh coal at 1.80 sp gr. Therefore, 2000 lb of coal was hand washed according to the process flow diagram in Figure 5.6. The 3/8 in. x 14 mesh material was sink floated at 1.80 sp gr to remove the oversized ash before crushing. All the 14 mesh x 0 streams were screened of 100 mesh x 0 material before washing at 1.80 sp gr. Product and refuse streams were saved for analysis. The chemical analysis of the washed coal was compared with the raw coal and the comparable gravity fractions (i.e., +1.30, -1.30/+2.80) in each size fraction of the washability study. The data indicate a 56-percent reduction in ash and a 46-percent reduction in pyritic sulfur. The yield is 68 percent, including 100 mesh x 0 fines of the clean coal that account for 15 percent of the yield. Screening of the fines would reduce the overall yield to 53 percent, which is not economical.

Very much to our surprise, the ash chemistry of the washed product does not resemble the float 1.80 gravity fractions generated during the washability studies, nor does the ash chemistry of the pulverized form of the washed product resemble the ash chemistry of the fractionated pulverized unwashed coal

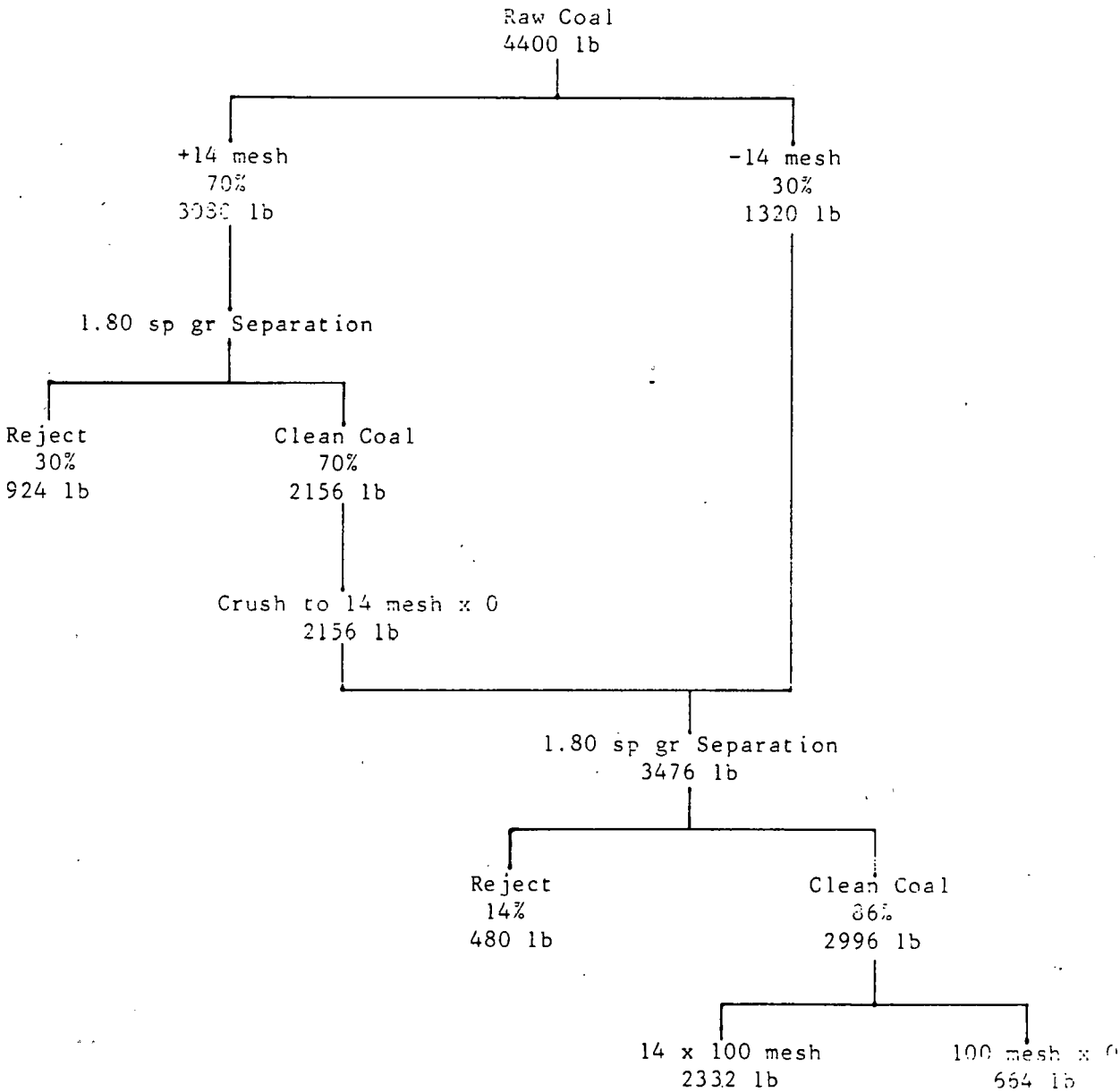


Figure 5.6 Washed Coal Process Flow Diagram

studies, as illustrated in Tables 5.8 and 5.9 and Figure 5.7. Instead, the ash chemistry and ash fusion temperatures resemble the head sample and the unwashed fines (i.e., <100 mesh). The ash fusion temperatures under oxidizing and reducing conditions are 100 to 200°F below those predicted from the washability study. The percentage of pyrite and ash, however, is considerably lower than predicted. X-ray analysis of low-temperature ash (Table 5.10) indicates that despite similarities in elemental composition of the washed coal and the head sample, the mineral composition of the washed product was altered. Illite was reported as a major constituent in the raw coal and a minor constituent in the washed product. Therefore, it appears that substantial quantities of illite were removed during washing. This could represent a significant improvement in the fireside behavior of the coal, as earlier combustion testing of bituminous coals has indicated that illite may be the mineral initiating the slag deposits.

Pyrite is generally considered to be the dominant mineral source of iron in coal ash. However, iron may also be found as pyrrhotite, hematite, siderite, or ankerite. As discussed in the previous progress report, their physicochemical behavior during combustion is quite different; therefore, as pure species their contribution to fireside deposits is quite different. An estimation of the distribution of iron between pyritic and nonpyritic iron-bearing minerals in the ash of the washed coal and the coal fractionated during the washability studies indicates a decided difference in mineral source of the iron in the washed coal compared with the equivalent gravity fractions generated during the washability study. Only 53 percent of the iron in the washed coal can be attributed directly to pyrite, based on the percentage of pyritic sulfur

Table 5.8 Comparison of Ash Chemistry of Washed Coal (14 x 100 Mesh, +1.80 Sp Gr) With Float 1.80 and 1.30 Gravity Fractions of Various Coal Sizes Examined in Washability Study

| | | | | Washability Study | | | | | | | | Rejects | |
|---|---|---|---|---|---|---|---|---|---|---|---|---|---|
| Description | Raw Coal* | Raw Coal† | Washed Coal 14 x 100 Mesh | 3/8 in. x 14 Mesh +1.30 | 3/8 in. x 14 Mesh -1.30/+1.80 | 14 x 100 Mesh +1.30 | 14 x 100 Mesh -1.30/+1.80 | 14 x 100 Mesh +1.30 | 14 x 100 Mesh -1.30/+1.80 | 200 x 0 Mesh +1.30 | 200 x 0 Mesh -1.30/+1.80 | 3/8 in. x 14 Mesh | 14 x 0 Mesh |
| Ash (%) | 24.36 | 25.55 | 10.75 | 2.9 | 16.5 | 4.6 | 17.5 | 4.2 | 22.6 | 2.8 | 12.1 | 76.87 | 60.89 |
| Pyritic Sulfur (%) | 1.44 | 1.22 | 0.79 | 0.4 | 2.1 | 0.17 | 1.70 | 0.5 | 2.48 | 0.11 | 1.19 | 5.21 | 8.41 |
| Fraction (wt%) | 100 | 100 | 53 | 24.3 | 48.5 | 39.7 | 41.2 | 49.2 | 36.1 | 17.0 | 58.6 | | |
| Ash Chemistry (%) | | | | | | | | | | | | | |
| $SiO_2$ | 48.6 | 48.5 | 41.3 | 42.0 | 45.9 | 42.4 | 46.3 | 40.3 | 42.7 | 46.0 | 48.0 | 54.1 | 42.6 |
| $Al_2O_3$ | 25.5 | 25.4 | 25.7 | 30.8 | 28.3 | 28.8 | 29.7 | 27.1 | 28.0 | 31.5 | 31.0 | 25.0 | 21.2 |
| $TiO_2$ | 1.1 | 1.1 | 1.1 | 1.5 | 1.2 | 2.2 | 1.3 | 2.0 | 1.2 | 2.4 | 1.4 | 1.2 | 0.8 |
| $Fe_2O_3$ | 16.6 | 15.8 | 17.1 | 16.3 | 17.8 | 13.5 | 16.1 | 15.5 | 10.4 | 8.5 | 9.3 | 13.9 | 23.1 |
| CaO | 2.9 | 2.4 | 6.4 | 4.8 | 2.5 | 5.9 | 1.8 | 5.5 | 2.0 | 5.7 | 1.7 | 0.9 | 4.4 |
| MgO | 0.9 | 0.9 | 0.4 | 0.6 | 0.6 | 0.9 | 0.7 | 0.9 | 0.4 | 1.1 | 0.9 | 1.2 | 0.8 |
| $Na_2O$ | 0.3 | 0.4 | 0.5 | 0.7 | 0.4 | 0.6 | 0.4 | 0.6 | 0.4 | 0.5 | 0.4 | 0.3 | 0.3 |
| $K_2O$ | 2.9 | 3.0 | 2.5 | 2.1 | 2.8 | 2.5 | 2.8 | 2.3 | 2.6 | 2.9 | 3.3 | 3.6 | 2.7 |
| $SO_3$ | 2.8 | 2.0 | 5.3 | 0.4 | 1.7 | 4.6 | 1.5 | 4.2 | 1.9 | 3.1 | 1.1 | 0.7 | 4.0 |
| $P_2O_5$ | 0.4 | 0.3 | 0.6 | 1.1 | 0.5 | 1.1 | 0.6 | 1.9 | 0.5 | 0.7 | 0.5 | 0.4 | 0.3 |
| Ash Fusion (°F) | | | | | | | | | | | | | |
| Reducing: | | | | | | | | | | | | | |
| Initial Deformation | 2063 | 2100 | 2190 | 2190 | 2220 | 2220 | 2470 | 2180 | 2400 | 2300 | 2400 | 2190 | |
| Softening (Sph.) | 2134 | 2140 | 2200 | 2240 | 2260 | 2210 | 2500 | 2210 | 2440 | 2380 | 2430 | 2200 | 2060 |
| Softening (Hem.) | 2245 | 2180 | 2240 | 2270 | 2300 | 2280 | 2510 | 2270 | 2470 | 2400 | 2460 | 2270 | 2080 |
| Fluid | 2460 | 2220 | 2270 | 2300 | 2140 | 2320 | 2530 | 2290 | 2500 | 2420 | 2400 | 2480 | 2100 |
| Oxidizing: | | | | | | | | | | | | | |
| Initial Deform. | 2473 | 2450 | 2440 | 2530 | 2540 | 2440 | 2650 | 2410 | 2560 | 2420 | 2650 | 2450 | 2150 |
| Softening (Sph.) | 2487 | 2460 | 2450 | 2560 | 2550 | 2470 | 2670 | 2430 | 2570 | 2460 | 2680 | 2500 | 2440 |
| Softening (Hem.) | 2540 | 2470 | 2460 | 2590 | 2570 | 2490 | 2690 | 2460 | 2590 | 2500 | 2700 | 2520 | 2450 |
| Fluid | 2585 | 2480 | 2470 | 2610 | 2590 | 2540 | 2780 | 2500 | 2610 | 2540 | 2700 | 2530 | 2560 |
| Total from in-Pyritic Form (%) | 43.7 | 36.8 | 52.8 | 100 | 85 | 92.1 | 76 | 80 | 100 | 55§ | 90 | 59.8 | 73.0 |

*Used during combustion test of unwashed coal.
†Head sample.
§Probably in error because of the very small concentration of pyrite (i.e., 0.11%)

TABLE 5.9 Comparison of Ash Chemistry of Unwashed 200 Mesh x 0 Coal with 200 Mesh x 0 Coal Washed at 14 Mesh x 0

| | Gravity Fraction | | | | | | | |
|---|---|---|---|---|---|---|---|---|
| | +1.30 | | -1.30/+1.80 | | -1.80/+2.85 | | -2.85 | |
| Description | Raw | Washed | Raw | Washed | Raw | Washed | Raw | Washed |
| **Ash Chemistry (%)** | | | | | | | | |
| $SiO_2$ | 46.0 | 39.9 | 48.0 | 47.5 | 53.0 | 38.6 | 25.3 | 3.9 |
| $Al_2O_3$ | 31.5 | 24.4 | 31.0 | 28.9 | 27.6 | 18.5 | 16.3 | 2.0 |
| $TiO_2$ | 2.9 | 1.3 | 1.4 | 1.5 | 1.0 | 0.5 | 0.6 | 0.1 |
| $Fe_2O_3$ | 8.5 | 17.4 | 9.3 | 12.5 | 8.5 | 14.0 | 49.6 | 87.7 |
| CaO | 5.7 | 7.0 | 1.7 | 3.3 | 3.5 | 13.8 | 1.6 | 2.1 |
| MgO | 1.1 | 1.0 | 0.9 | 0.8 | 0.8 | 0.8 | 0.5 | 0.2 |
| $Na_2O$ | 0.5 | 0.7 | 0.4 | 0.6 | 0.4 | 0.4 | 0.2 | 0.1 |
| $K_2O$ | 2.9 | 2.6 | 3.3 | 2.8 | 3.2 | 2.0 | 1.6 | 0.2 |
| $SO_3$ | 3.1 | 5.5 | 1.1 | 2.0 | 2.0 | 17.3 | 1.5 | 1.9 |
| **Ash Fusion (°F)** | | | | | | | | |
| Reducing: | | | | | | | | |
| Initial Deformation | 2360 | 2100 | 2400 | 2250 | 2120 | 2100 | 2020 | 2270 |
| Softening (Sph.) | 2380 | 2180 | 2410 | 2400 | 2230 | 2190 | 2040 | 2400 |
| Softening (Hem.) | 2400 | 2210 | 2460 | 2430 | 2260 | 2210 | 2070 | 2440 |
| Fluid | 2470 | 2270 | 2490 | 2480 | 2310 | 2290 | 2100 | 2470 |
| Oxidizing: | | | | | | | | |
| Initial Deformation | 2420 | 2280 | 2650 | 2550 | 2330 | 2270 | 2590 | 2700 |
| Softening (Sph.) | 2460 | 2310 | 2680 | 2590 | 2360 | 2280 | 2620 | 2700 |
| Softening (Hem.) | 2500 | 2330 | 2700 | 2600 | 2410 | 2290 | 2640 | 2700 |
| Fluid | 2540 | 2380 | 2700 | 2610 | 2440 | 2340 | 2690 | 2700 |



FOSTER WHEELER DEVELOPMENT CORPORATION
REF.: DE-AC22-81PC40268
DATE: June 1984

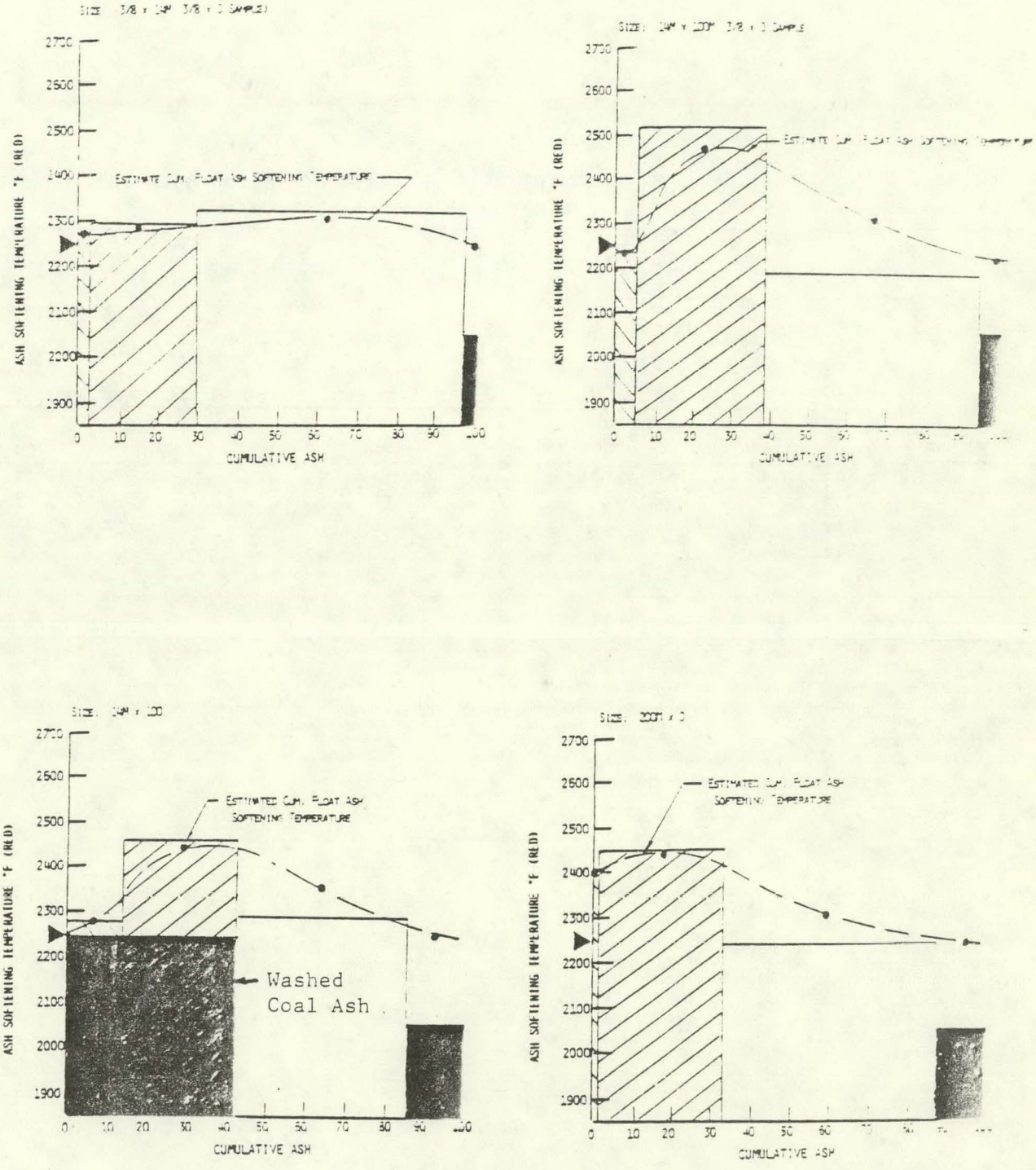


Figure 5.7 Softening Temperature of Washed Coal Ash Compared With Unwashed Coal Ash Fractionated by Size and Gravity

Table 5.10 Comparison of Mineral Analysis of Reject Material from Coal Washery with Run of Mine Coal

| | Run of Mine | Washed Coal | Washery 3/8" x 14 mesh, -1.80 | Rejects -14 mesh x 0, -1.80 |
|---|---|---|---|---|
| MAJOR | Kaolinite<br>Quartz<br>Pyrite<br>Illite | Kaolinite<br>Quartz<br>Pyrite | Kaolinite<br>Quartz<br>Pyrite | Kaolinite<br>Quartz<br>Pyrite |
| MINOR | --- | Illite | Illite | Muscovite<br>Illite |

reported. The remaining iron must come from one of the other iron-bearing minerals previously mentioned. However, between 80 and 100 percent of the iron in the ash of the light gravity fractions, generated in the washability study, originates as pyrites in the coal. A further examination of the fines and heavier gravity fractions indicates that 100 percent of the iron in the ash of the fines originates in pyrite, whereas 40 to 50 percent of the iron in the heavier gravity fractions occurs as nonpyritic mineral-bearing iron. Thermogravimetric analysis of the heavier gravity fractions, reported in Progress Report 7, revealed a substantial reduction in reactivity of the heaviest gravity fraction compared with other coal-derived pyrite, confirming the presence of nonpyritic impurities which could be either pyrrhotite or siderite. Since the head sample contained only 36 percent of the iron as pyrite, the washability study indicates nonpyritic iron-bearing mineral matter would be selectively removed during beneficiation. The analysis of the washed coals indicates pyrite was selectively removed. Despite the fact that the coal samples were taken from the same seam at the same time, the mineral forms, size, and distribution are quite different.

One sample of pulverized coal was set aside for gravimetric partitioning and analysis to determine the impact that pulverizing 14 mesh x 0 coal to 70 percent <200 mesh might have on further liberation of mineral matter. The analysis of the partitioned sample also permits a direct comparison with the 200 mesh x 0 stream generated during the washability study.

The chemical analyses of the ash and ash fusion temperatures of the minerals in the individual gravity fractions of the washed and unwashed coal appear in

Table 5.11. The quantitative data indicate about 57 percent reduction in total ash. The iron and calcium concentrations in all the fractionated samples are high, accounting for the lower fusion temperatures of all the fractionated ash, excepting the sink 2.85 fraction, when compared with their counterparts in the unwashed coal (Figure 5.8). The heaviest fraction is rich in pure pyrite, which is responsible for the higher fusion temperatures in reducing and oxidizing environments. The sink 1.80/float 2.85 and the sink 2.85 represent mineral species released as a result of pulverizing from 14 mesh x 0 to 200 mesh x 0. The fusibility diagram in Figure 5.9 and the percentage distribution of iron diagram appearing in Figure 5.10 indicate these two fractions represent less than 6 percent of the total coal but contain about 30 percent of the total ash and 45 percent of the pyritic iron. Liberation of pyrite during the final step of comminution from 14 mesh x 0 to 200 mesh x 0 is slightly greater than liberation of either quartz or calcite. A comparison of the percentage of iron determined by the pyritic sulfur in the individual gravity fractions with the iron reported in the ash indicates virtually all the iron in the washed coal originated from pyrite. The nonpyritic iron species appears to have been washed from the coal.

The high concentration of ash in the float 1.30 fraction and the high concentration of iron and calcite in all species compared with the washed coal suggest slight differences in mineral composition, size, and association with coal and other mineral matter exist between the raw coal samples used for the washability test and the washing operation, despite the fact that they were sampled at the same time. The differences must be because of the variability within the mine, accounting for substantial variations in composition over a short interval in time. Coal variability is discussed in the next section.

Table 5.11 Comparison of Ash Chemistry and Ash Fusion Temperatures for Unwashed and Washed 200 Mesh x 0 Samples

| | Head Sample | | Float 1.30 | | Float 1.8/Sink 1.80 | | Float 2.85/Sink 1.80 | | Sink 2.85 | |
|---|---|---|---|---|---|---|---|---|---|---|
| Coal | Unwashed | Washed | Unwashed | Washed | Unwashed | Washed | Unwashed | Washed | Unwashed | Washed |
| **Ash Chemistry (%)** | | | | | | | | | | |
| $SiO_2$ | 48.5 | 41.1 | 46.0 | 39.9 | 48.0 | 41.5 | 51.0 | 38.6 | 25.3 | 3.9 |
| $Al_2O_3$ | 25.4 | 25.7 | 31.5 | 24.4 | 31.0 | 28.9 | 27.6 | 18.5 | 16.3 | 2.0 |
| $TiO_2$ | 1.1 | 1.1 | 2.9 | 1.3 | 1.4 | 1.5 | 1.0 | 0.5 | 0.6 | 0.1 |
| $Fe_2O_3$ | 15.8 | 17.1 | 8.5 | 17.4 | 9.1 | 12.5 | 8.5 | 14.0 | 49.6 | 87.7 |
| CaO | 2.7 | 6.4 | 5.7 | 7.0 | 1.7 | 3.3 | 1.5 | 13.8 | 1.6 | 2.1 |
| MgO | 0.9 | 0.4 | 1.1 | 1.0 | 0.9 | 0.8 | 0.8 | 0.8 | 0.5 | 0.2 |
| $Na_2O$ | 0.4 | 0.5 | 0.5 | 0.7 | 0.4 | 0.6 | 0.4 | 0.4 | 0.2 | 0.1 |
| $K_2O$ | 3.0 | 2.5 | 2.9 | 2.6 | 3.3 | 2.8 | 3.2 | 2.0 | 1.6 | 0.2 |
| $SO_3$ | 2.8 | 5.1 | 1.1 | 5.5 | 1.1 | 2.0 | 2.0 | 12.3 | 1.5 | 1.9 |
| $P_2O_5$ | 0.3 | 0.6 | 0.7 | 0.5 | 0.5 | 0.3 | 0.3 | 0.4 | 0.2 | 0.2 |
| **Ash Fusion (°F)** | | | | | | | | | | |
| Reducing: | | | | | | | | | | |
| Initial Deformation | 2100 | 2190 | 2360 | 2100 | 2400 | 2250 | 2120 | 2100 | 2020 | 2270 |
| Softening (Sph.) | 2140 | 2220 | 2480 | 2180 | 2430 | 2400 | 2230 | 2190 | 2060 | 2400 |
| Softening (Hem.) | 2180 | 2270 | 2600 | 2210 | 2460 | 2430 | 2260 | 2210 | 2070 | 2660 |
| Fluid | 2220 | 2480 | 2620 | 2270 | 2480 | 2480 | 2310 | 2290 | 2100 | 2670 |
| Oxidizing: | | | | | | | | | | |
| Initial Deformation | 2450 | 2450 | 2620 | 2280 | 2650 | 2550 | 2330 | 2270 | 2590 | 2760 |
| Softening (Sph.) | 2460 | 2500 | 2660 | 2340 | 2680 | 2590 | 2360 | 2280 | 2620 | 2780 |
| Softening (Hem.) | 2470 | 2520 | 2680 | 2360 | 2700 | 2600 | 2410 | 2290 | 2640 | 2780 |
| Fluid | 2480 | 2530 | 2640 | 2380 | 2700 | 2610 | 2460 | 2360 | 2660 | 2780 |
| Ash (%) | 25.55 | 10.75 | 7.8 | 10.84 | 12.1 | 8.07 | 63.15 | 61.80 | 65.40 | 65.57 |

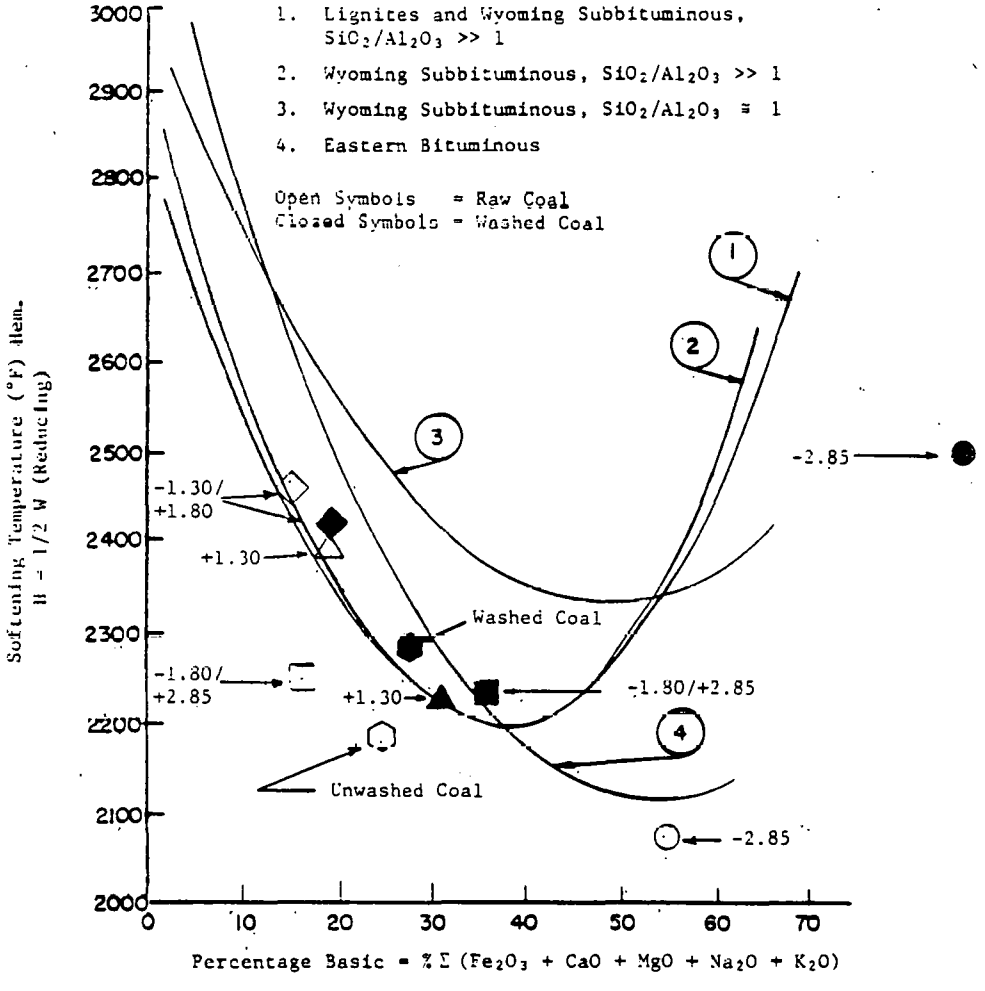


Figure 5.8 Comparison of Softening Temperatures of Fractionated Washed and Unwashed Pulverized Coal

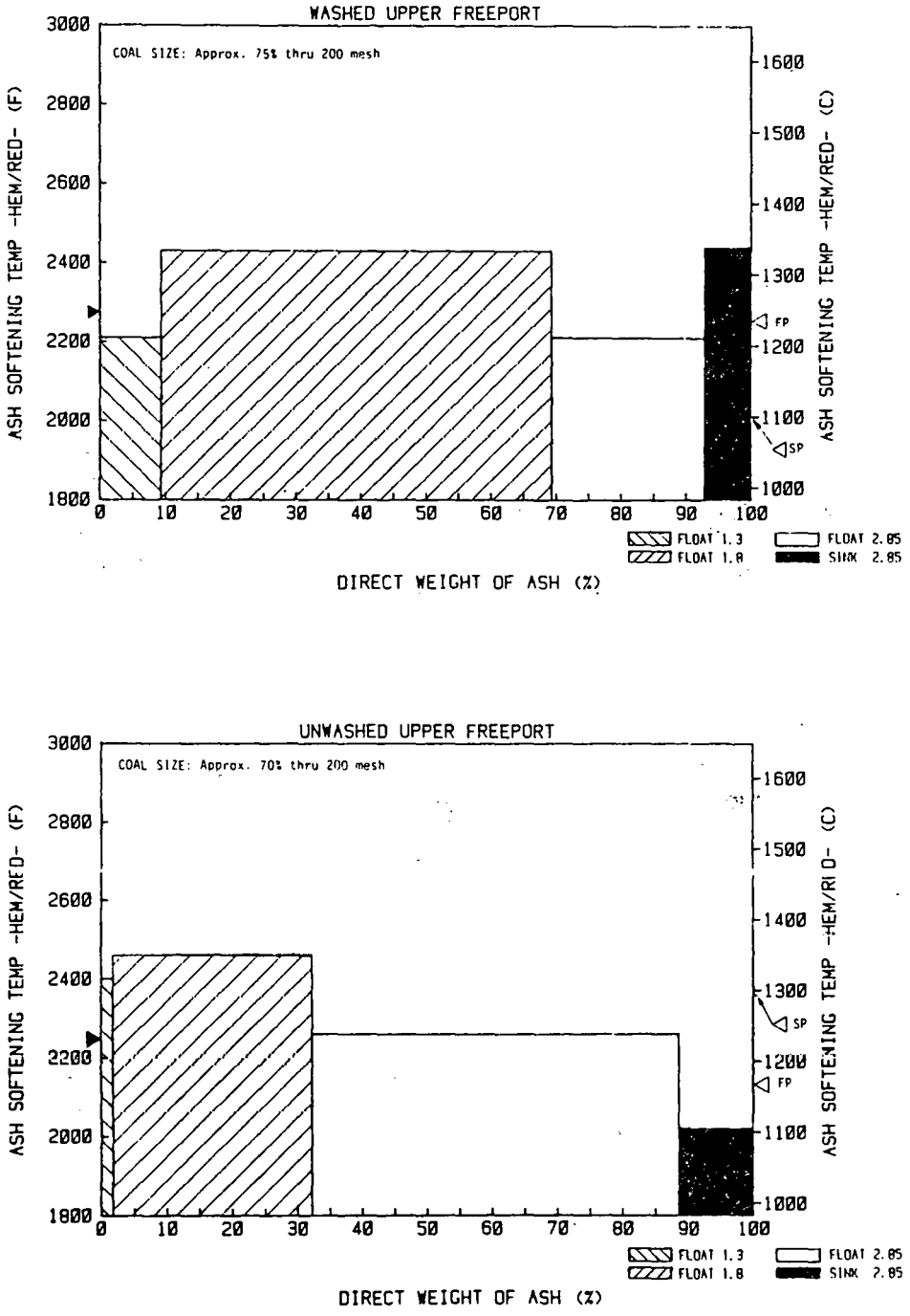


Figure 5.9 Fusibility Diagrams of Fractionated Coal Ash for Washed and Unwashed Upper Freeport Coal

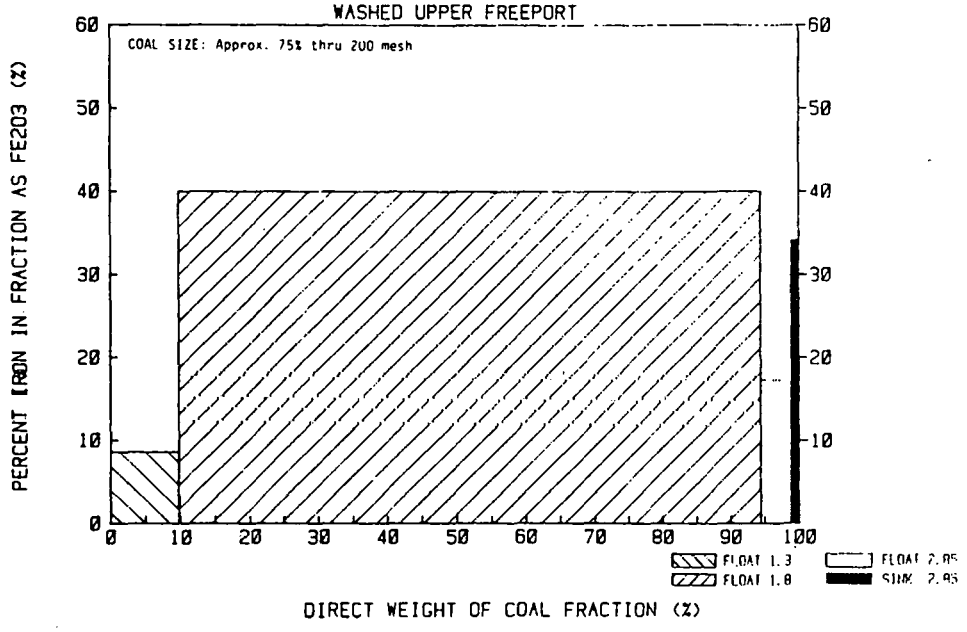


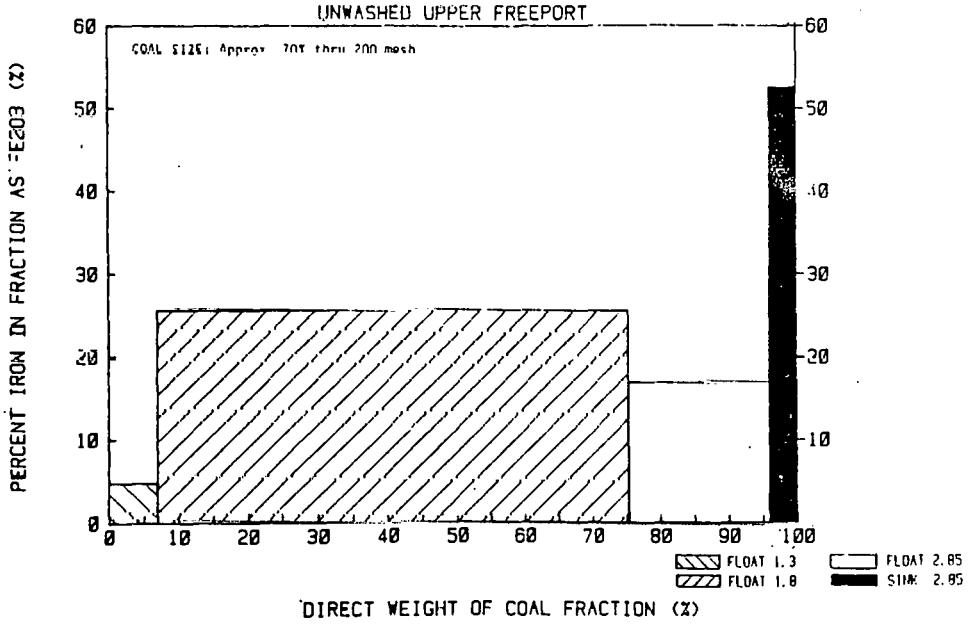


Figure 5.10 Distribution of Iron Among Gravity Fractions in Washed and Unwashed Upper Freeport Coal

Thermograms performed on the washed coal and compared with the raw coal in Figure 5.11 indicate there was no change in the combustion profile as a result of washing. TGA thermograms performed on each gravity fraction and compared with the raw coal and the pure pyrite in Figure 5.12 show that the pure pyrite was as reactive as the coal and burnout was achieved in the same amount of time as was coal burnout. The pyrite retained in the sink 1.80/float 2.85 gravity fraction goes through a two-stage combustion process, and burnout is not achieved until 800°C, about 200°C higher than the clean coal. Apparently, pyrrhotite is formed at an intermediate stage. This species is potentially the most troublesome with regard to fireside deposition.

In Figure 5.13 the combustion profile of the 2.85 gravity fraction is compared with the combustion profiles of pure pyrite, the 2.85 gravity fraction of the unwashed Upper Freeport coal, and the 2.85 gravity fraction of other coals. There is little difference between the combustion profiles of coal-derived pyrite liberated from bituminous other than Upper Freeport and the pyrite reporting to the 2.85 gravity fraction of the washed coal. However, a significant difference exists between the 2.85 gravity fractions of the washed and unwashed coal. The slower reacting pyrite derived from the raw coal is contaminated by other mineral matter, and there is a strong suspicion that a substantial portion of the iron exists as hematite, siderite, or some other iron-enriched mineral.

## COAL VARIABILITY

Drs. Cecil, Stanton, and Dulong of the United States Geological Survey have made an extensive study of maceral and mineral composition and distribution in

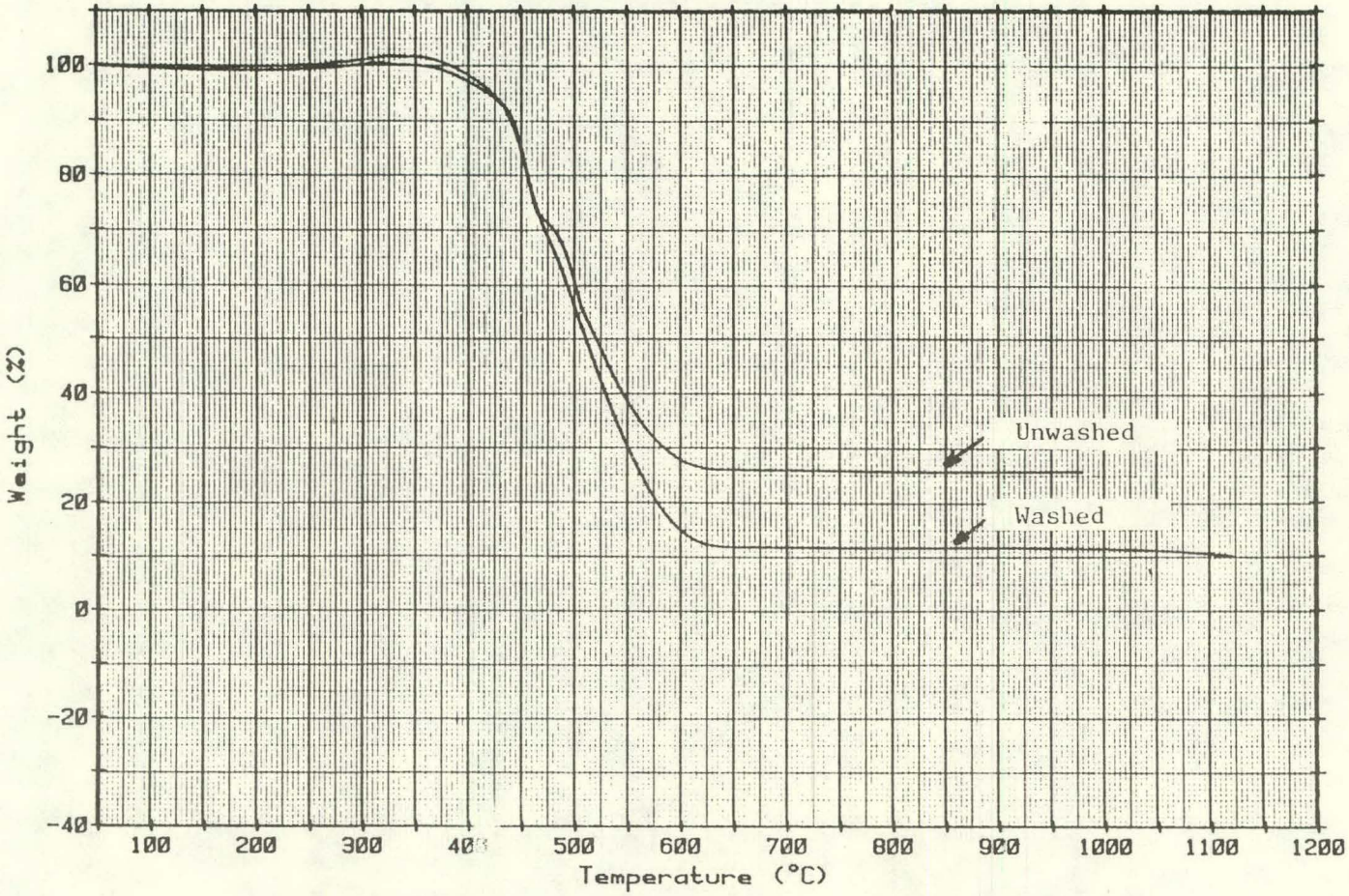


Figure 5.11 Comparison of TGA Thermograms for Washed and Unwashed Upper Freeport Coal

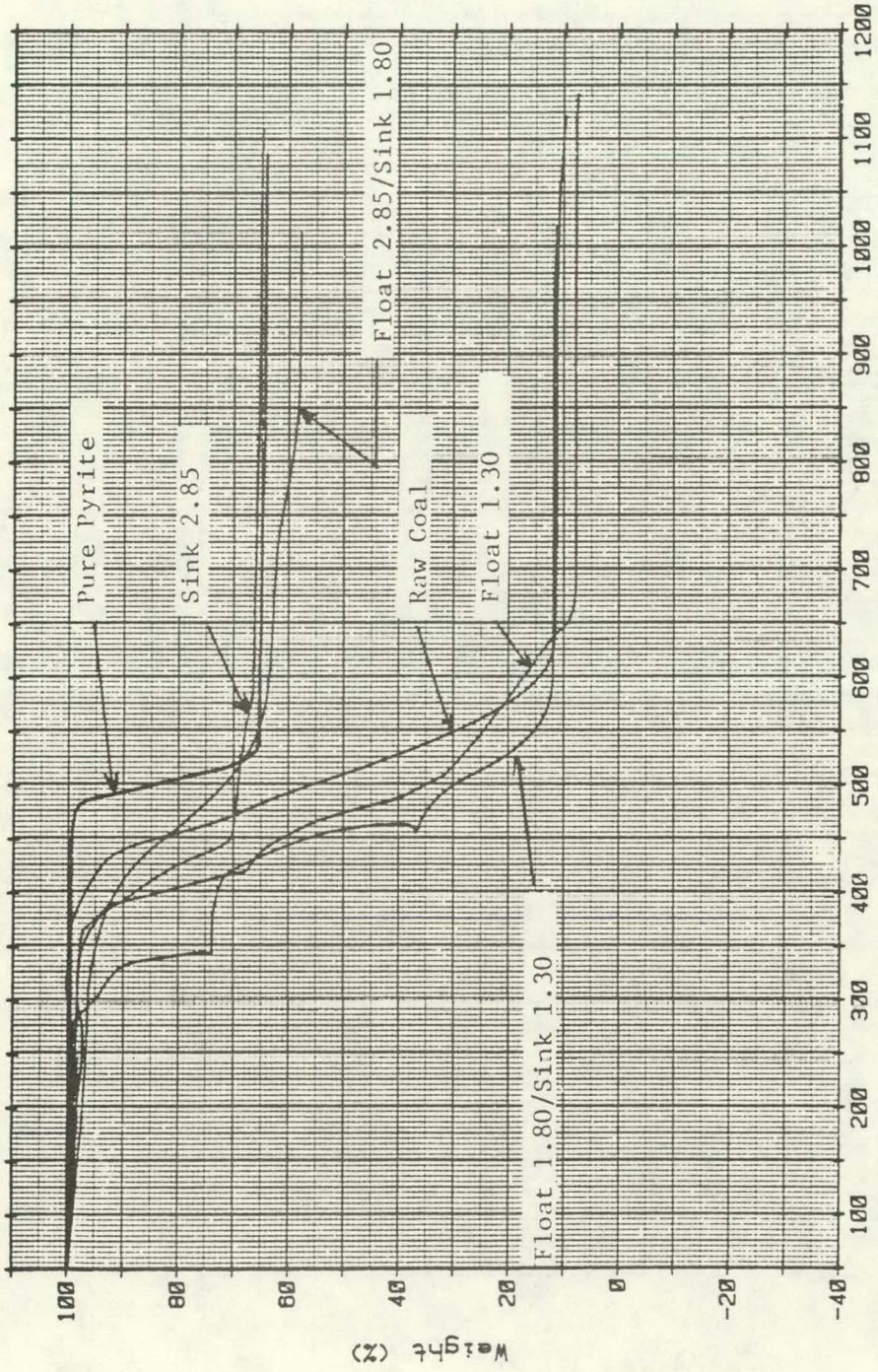


Figure 5.12 Comparison of TGA Thermograms for Various Gravity Fractions of Washed Upper Freeport Coal With Composite Coal Sample and Pure Pyrite

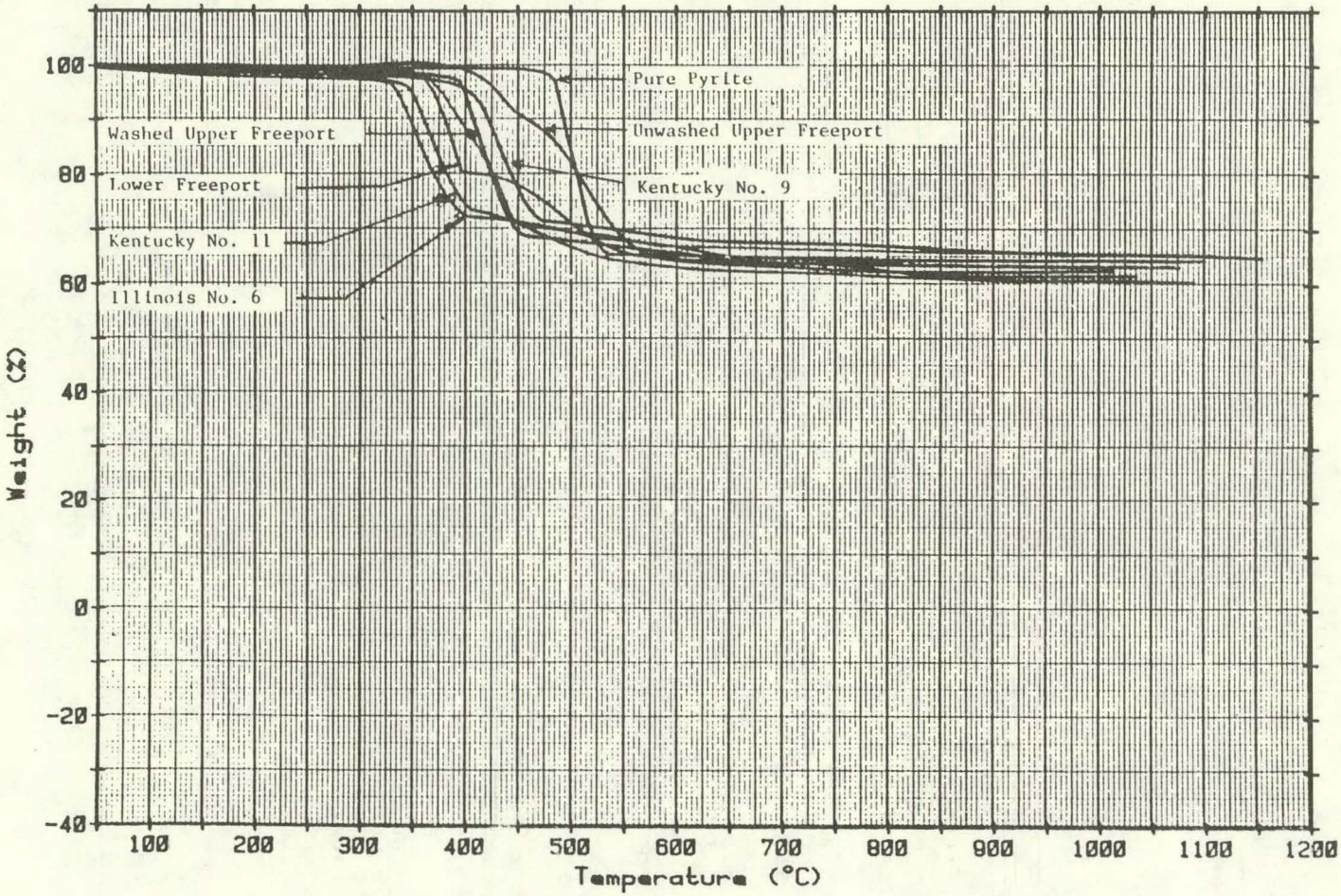


Figure 5.13 Comparison of Combustion Profile of Sink 2.85 Fraction From Washed Upper Freeport Coal With Sink 2.85 Fraction From Unwashed Upper Freeport Coal, Pure Pyrite, and Heavy Fractions From Other Coals

the Upper Freeport coal, Indiana County.* At the Homer City No. 1 Mine and the Lucerne No. 6 Mine, field investigations included detailed descriptions and sampling of the coal and associated rocks (21 complete-channel and 75 bench-channel samples). Laboratory analyses included determination of the concentrations of 70 elements; ultimate, proximate, and sulfur forms; maceral analysis; pyrite morphological analysis; low-temperature x-ray mineralogy; and scanning electron microscope and electron probe analyses on selected samples.

The Upper Freeport coal bed in the study area can be divided in the field into eight facies--two nonbanded coal facies, four banded coal facies, and two shale partings. Figure 5.14 illustrates the generalized stratigraphy of the Upper Freeport coal, identifying and briefly describing these eight facies. Figure 5.15 is a fence diagram illustrating some of the changes in the stratigraphy of the Upper Freeport coal with geographic location. In particular, the diagram illustrates changes that might be expected in pyrite morphology with location.

The coal bed averages 83 in. thick in the northern part of the area where all eight facies are present. Only the four lower facies are present in the southern part, where the average thickness is 40 in.

Microscopic analysis of pyrite and marcasite forms and their petrographic associations shows definite differences among the coal facies. Specifically, the bottom facies has framboidal pyrite, whereas the other facies tend to

*C. B. Cecil, R. W. Stanton, and F. T. Dulong, "Geology of Contaminants in Coal: Phase I Report of Investigations," U.S. Department of the Interior Geological Survey Preliminary Report 81-953-A.

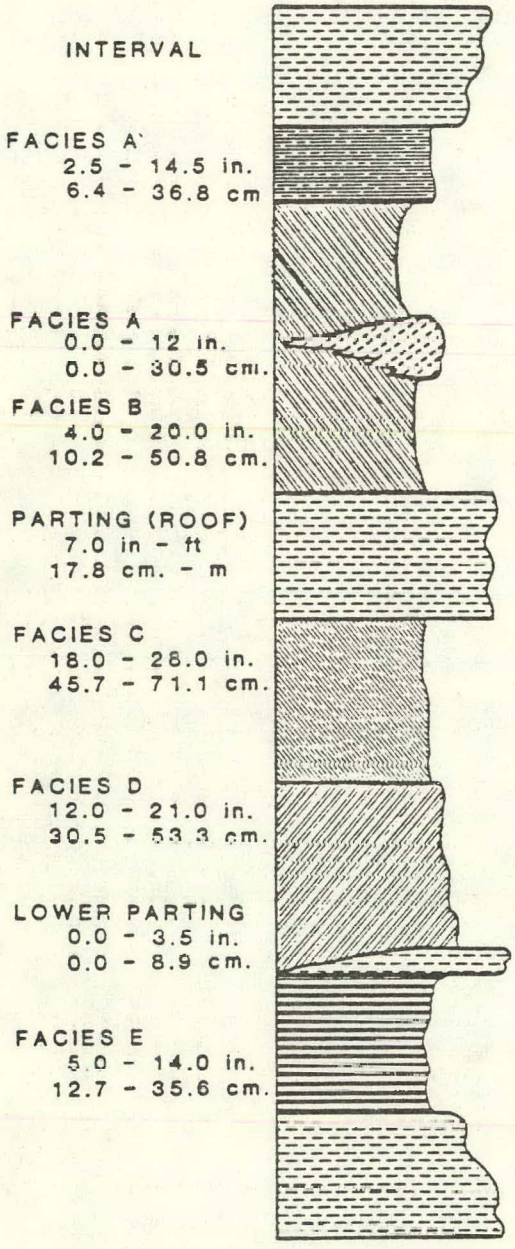


FACIES A - Hard blocky nonbanded impure coal: shaley sometimes displaying fissility: calcite along cleats.

FACIES B - Hard, blocky, barded coal with bright bands 2 to 3 mm thick alternating with attrital (dull) bands 3 to 20 mm thick ; fusain abundant at top of facies: scattered pyrite lenses in basal portion

FACIES A' - Hard, blocky, nonbanded, impure coal: conchoidal fracture: moderately bright, resinous luster: granular texture. Facies absent in someplaces.

PARTING(ROOF) FACIES - Very dark, gray claystone and shale: basal portions commonly dark gray grading upward into medium gray.

FACIES C - Bright, banded coal, columnar fracture: bright bands 3 to 4 mm thick alternating with attrital bands 5mm. thick: distinct fusain layers associated with pyrite: fusain chips at top: calcite and pyrite commonly fill cleats.

FACIES D - Hard, banded coal broken in large blocks; dull luster: bright bands 3 to 15 mm thick, some clear calcite, very little pyrite; some fusain layers and chips.

LOWER PARTING - Dark gray shale to claystone someplaces absent.

FACIES E - Very hard, blocky, banded coal: very dull luster: numerous shale layers; abundant pyrite in lenses and cleats; some calcite in cleats: bright bands 3 to 4 mm thick, dull bands 2 to 3 cm. thick: slickensides parallel stratification in shale layers near base.

Figure 5.14 Generalized Stratigraphy of Upper Freeport Coal Bed/Lucerne No. 6-Homer City No. 1 Mines (from Cecil, Stanton, and Dulong)

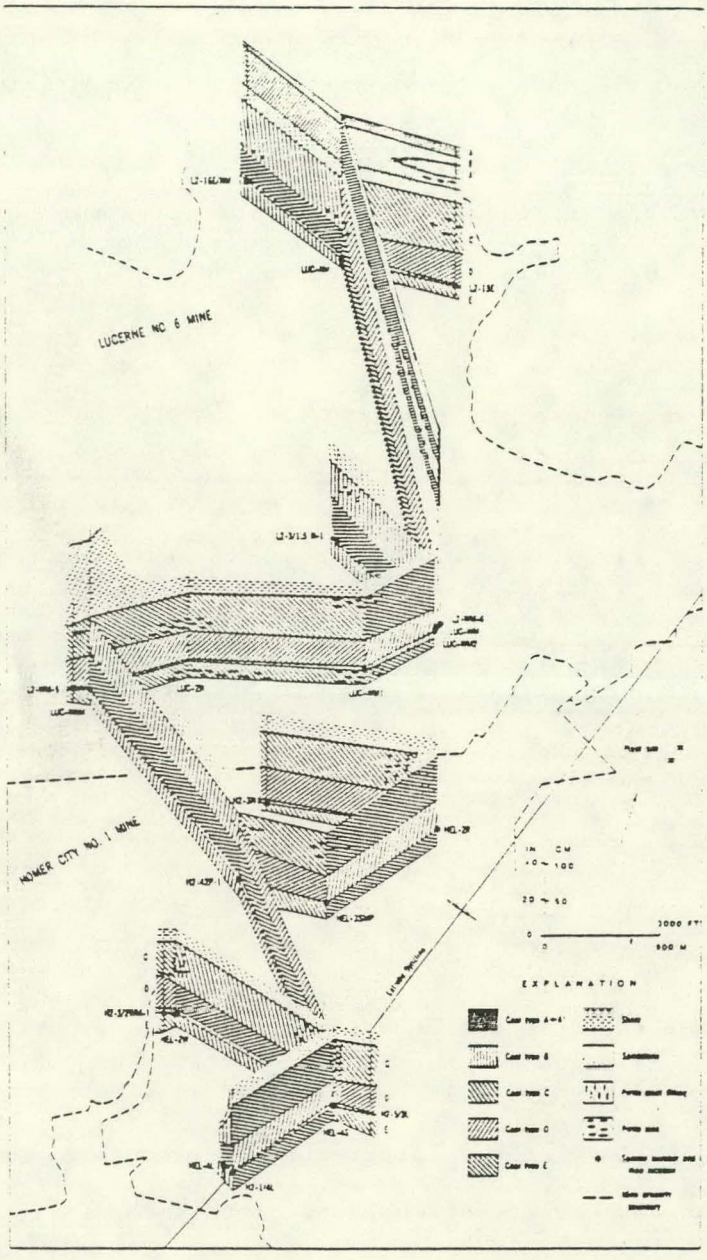


Figure 5.15 Fence Diagram of Upper Freeport Coal Facies/Lucerne No. 6-Homor City No. 1 Mines (from Cecil, Stanton, and Dulong)

contain more massive varieties that should be amenable to removal during coal preparation.

The complete channel and bench channel (i.e., individual face) were removed from the mine at locations described in Figure 5.1c. This diagram also identifies sample numbers, which may be useful for interpreting results. Although not important to this discussion, the nomenclature for the sample number is listed below to avoid confusion.

Sample numbers were chosen to identify each sample logically. For example, decoding of Sample number H2-42P-1.2 is as follows:

Table 5.12 Comparison of Total Iron in 14 x 100 Mesh and 200 Mesh x 0 Unwashed Coal with Pulverized Coal Washed at 14 Mesh x 0

| Gravity Fraction | 14 x 100 Mesh Unwashed | 200 Mesh x 0 Unwashed | Washed 200 Mesh x 0 |
|---|---|---|---|
| +1.30 | 0.283 | 0.26 | 0.16 |
| -1.30/+1.80 | 1.08 | 0.85 | 0.83 |
| -1.80/+2.85 | 0.63 | 0.56 | 0.132 |
| -2.85 | 0.67 | 1.74 | 0.70 |
| Total | 2.66 | 3.31 | 2.01 |

The minerals identified in the Upper Freeport coal, as interpreted from the SEM data, are summarized in Table 5.12. There is strong evidence that the nonpyritic iron is siderite ($FeCO_3$) rather than the hematite, magnetite, or pyrrhotite implied in the earlier discussions of this coal. Iron can also be found in small quantities in the illite. A distinction between the presence of potassium, aluminum, magnesium of iron in the iron was not made, nor was it made in our analysis of mineral matter. Cecil, et al., report the generalized stratigraphic distribution of these minerals in Figure 5.17.

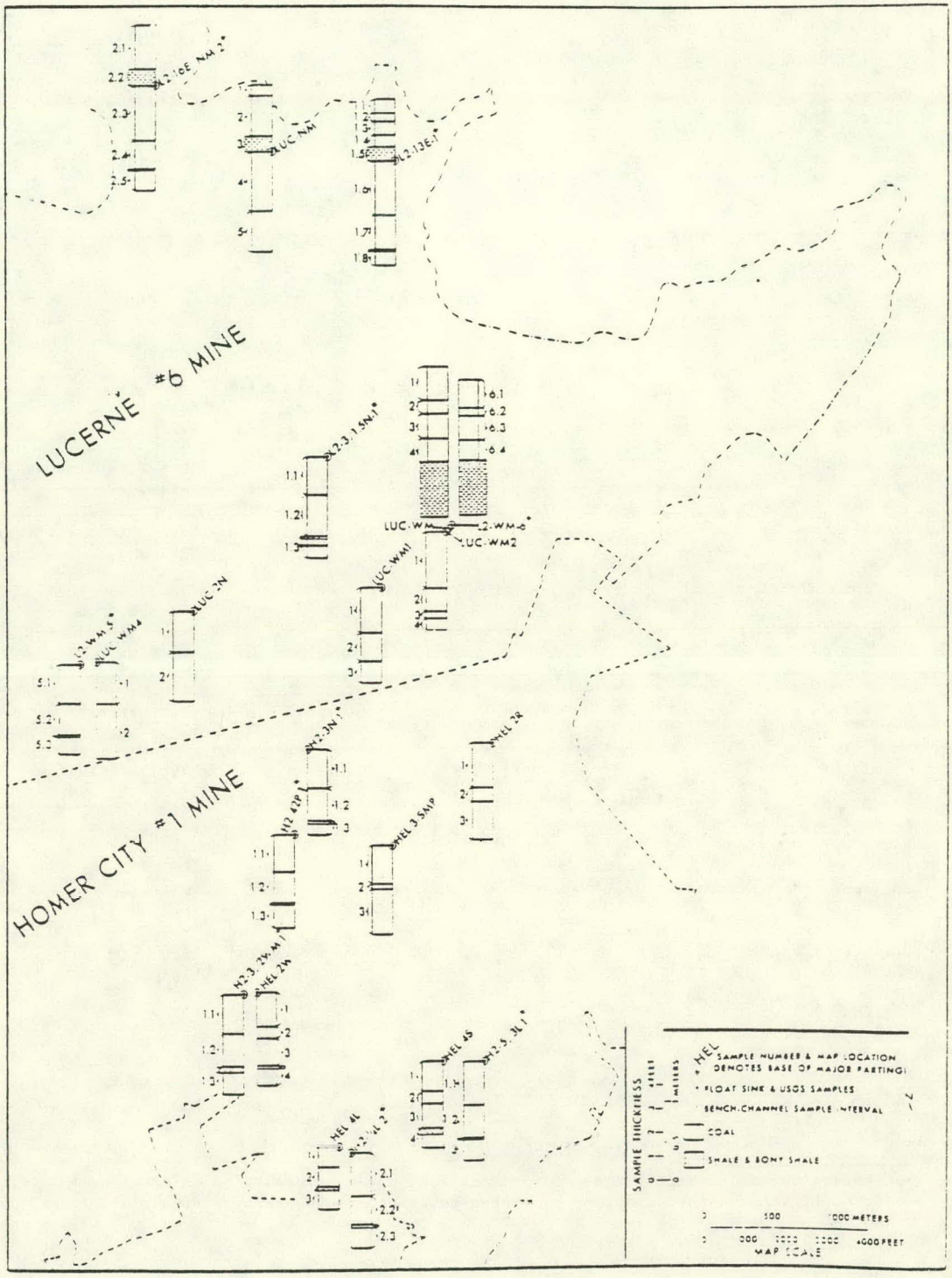


Figure 5.16 Sample Numbers and Map of Complete and Bench-Channel Samples From Lucerne No. 6 and Honer City No. 1 Mines (from Cecil, Stanton, and Dulong)

Table 5.13 Minerals in Upper Freeport Coal as Interpreted from SEM Data

MAJOR MINERALS

Calcite
$CaCO_3$

Kaolinite
$Al_2Si_2O_5(OH_4)$

Illite (and mixed layer clays)
$(K, H_3O)(Al, Mg, Fe)_2(Al, Si)_4O_{10}[OH)_2, H_2O]$

Pyrite-Marcasite
$FeS_2$

Quartz (and opal)
$SiO_2$

Siderite
$FeCO_3$

ACCESSORY MINERALS*

"Ankerite"
$Ca(Fe, Mg, Mn)(CO_3)_2$

Apatite
$Ca_5(PO_4)_3(F, OH, Cl)$

"Argentite"
$Ag_2S$

"Barite"
$BaSO_4$

Calcium Sulphate
$CaSO_4$

Chalcopyrite
$CuFeS_2$

Chlorite
$(Mg, Fe)_5(Al, Si)_4O_{10}(OH)_8$

"Clausthalite"
PbSe

Crandallite
$CaAl_3(PO_4)_2(OH)_5H_2O$

"Diaspore"
AlO(OH)

Feldspar (potash)
$KAi(Al, Si)Si_2O_8$

"Galena"
PbS

Magnetite
$(Fe, Fe_2)O_4$

Halite
NaCl

Iron-Titanium-Oxide
$FeTiO_3$

Manganese Silicate
$MnSiO_3$

"Monazite"
$(Ce, La)PO_4$

"Olivine"
$(Mg, Fe)_2SiO_4$

"Pyrrhotite"
FeS

"Rutile"/"Anatase"
$TiO_2$

Sphalerite
ZnS

"Xenotime"
$YPO_4$

Zircon
$ZrSiO_4$

*Quotation marks indicate mineral identifications based primarily on major-element data. All other identifications have been substantiated by x-ray diffraction.

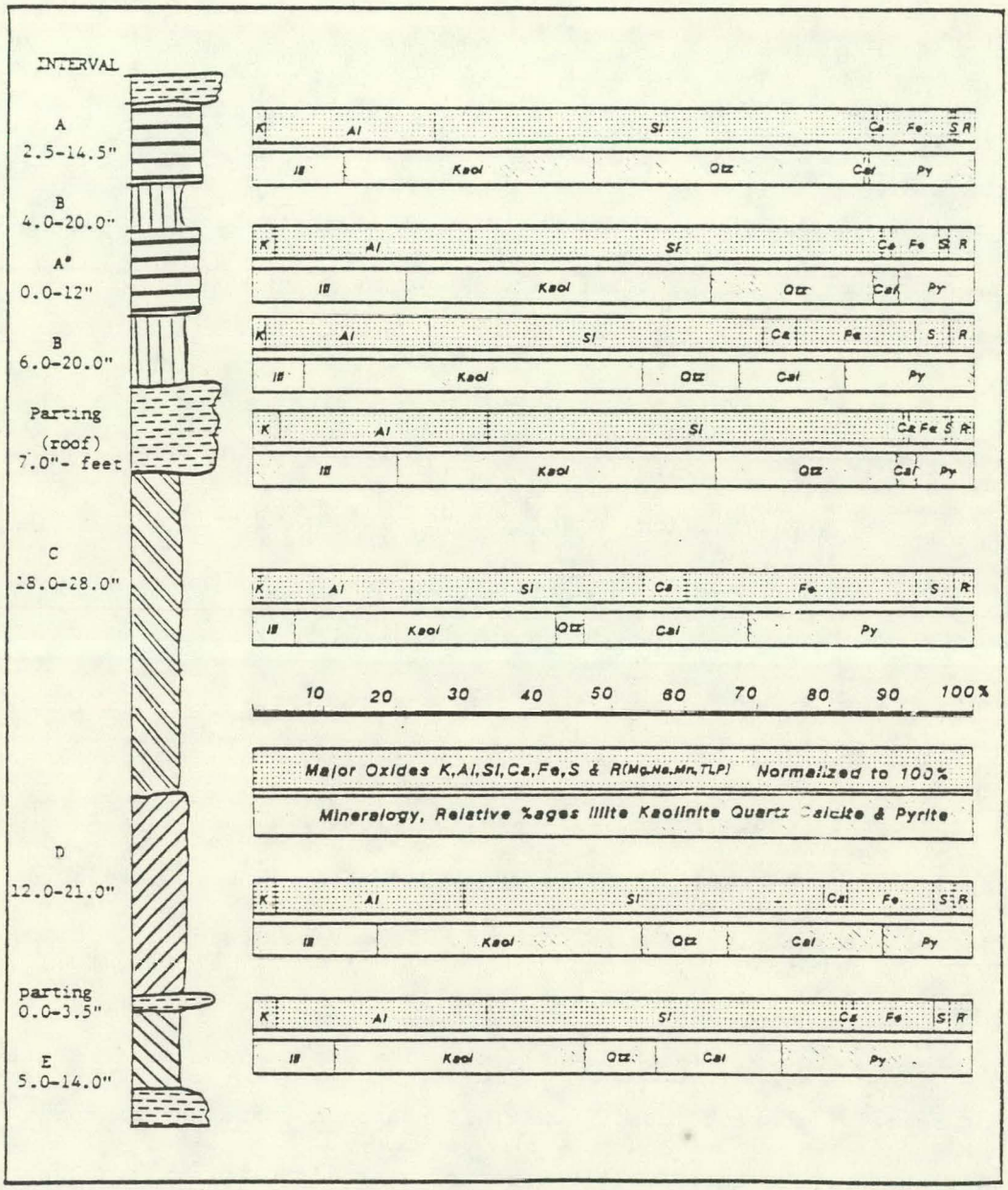


Figure 5.17 Generalized Major Oxide and Corresponding Mineral Data by Coal Facies (from Cecil, Stanton, and Dulong)

Faces C, D, and E are of particular interest; during the mining operation, the coal could be mined indiscrimantely from the individual benches or as a composite mixture. The mining procedure could also change with time. The composition of the mineral matter is decidedly different in each bench, as are the size and morphological structure (i.e., framboids, lenses, or veinlets). This means that the washability of the coal, as well as its fireside slagging and fouling characteristics, is continually changing.

Cecil, et al., have summarized the morphological structure of the pyrite (i.e., cyrstals, framboids, irregular pyrite, and marcasite) the maceral association (i.e., cell filling, maceral replacement, maceral encapsulation, or mineral encapsulation) and size (i.e., 0 to 100 μm) in Figures 5.18 and 5.19 for facies or Benches C, D, and E at three geographic locations. In general, Bench C contains irregular masses of pyrite-->50 μm--associated with macerals and cleats or fractures. This bench should liberate large quantities of pure pyrite and pyrite contaminated with kaolinite, illite, and quartz. This bench should also be more readily beneficiated than either D or E. Bench D contains considerably less pyrite than the others. In several cases it appears to be void of pyrite. Although the form of pyrite varies with each sample, there is a consistent amount of framboids present. The pyrite size is generally small and not readily liberated during washing. Bench E contains framboids and crystals primarily. The particle size is generally very small, which means the pyrite is not readily liberated during beneficiation or pulverizing in preparation for combustion.

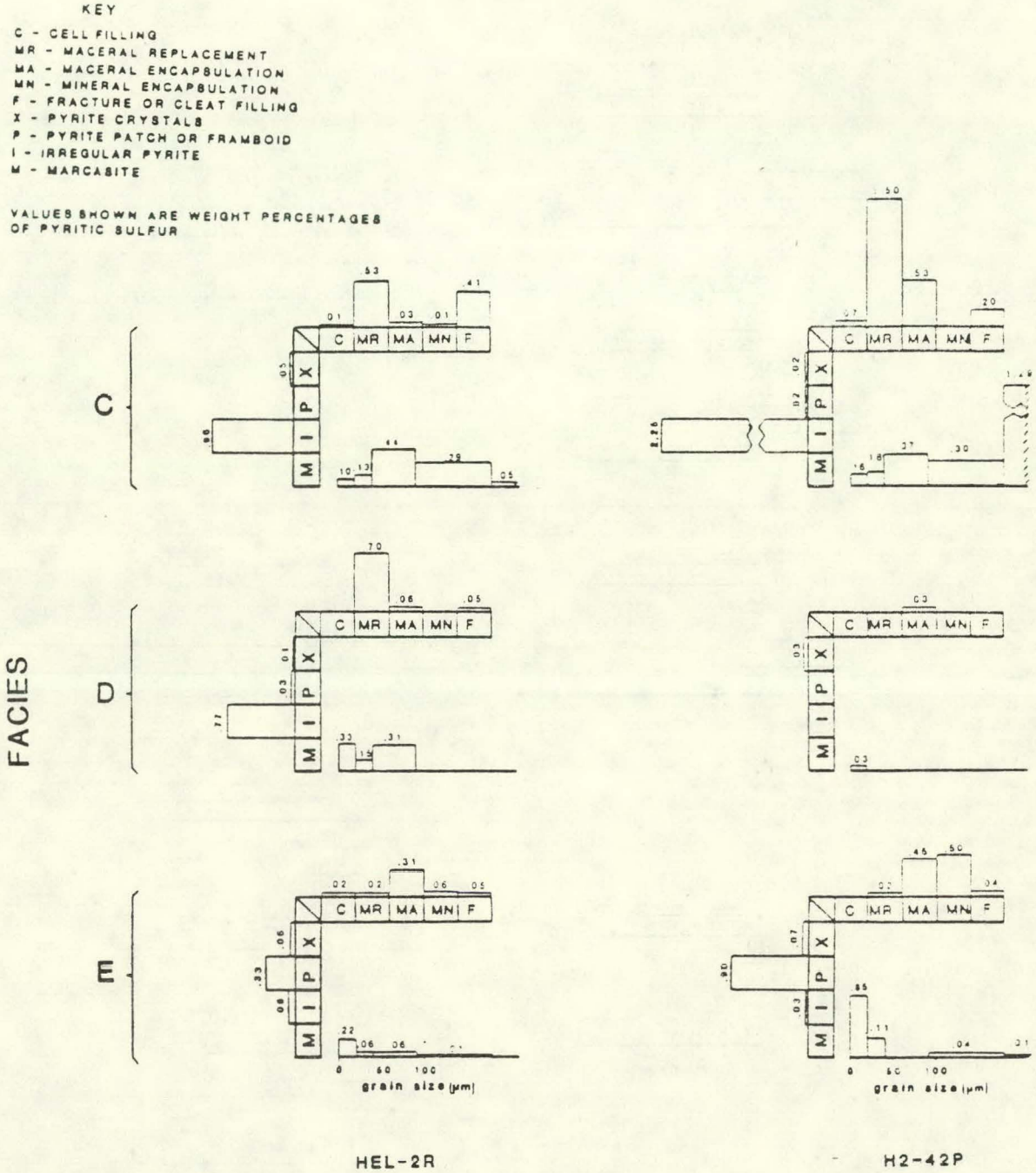


Figure 5.18 Iron Disulfide Forms, Associations, and Grain Sizes in Samples From HEL-2R and H2-42P, Upper Freeport Coal, Homer City, Pennsylvania (from Cecil, Stanton, and Dulong)

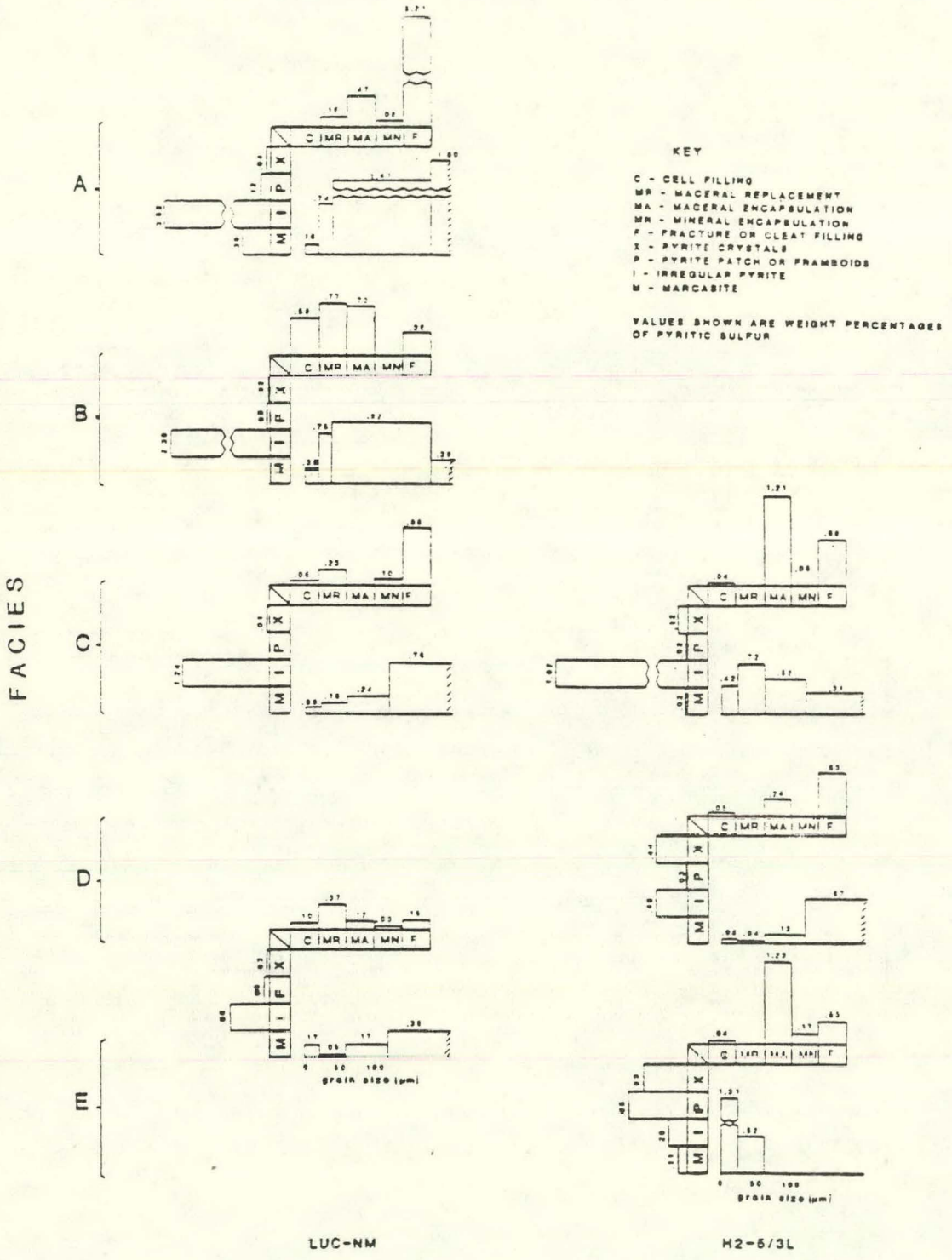


Figure 5.19 Iron Disulfide Forms, Associations, and Grain Sizes in Samples From LUC-NM and H2-5/3L, Upper Freeport Coal, Homer City, Pennsylvania (from Cecil, Stanton, and Dulong)

In Figures 5.20 and 5.21, Cecil, et al., report the geographic variation in iron and sulfur in the three benches--C, D, and E. Qualitatively there appears to be a disparity between the pyritic sulfur reported and the iron reported, particularly in Bench E. Presumably, the difference is caused by the presence of siderite.

Benches C, D, and E were also sink floated at various gravities to determine the washability characteristics of each bench. Unfortunately, the data have not as yet been placed in the open literature. The results clearly show the ability to partition and liberate individual minerals as well as total ash. Bench C is readily beneficiated, whereas E is not.

The variability of the mineral content by geographic location and stratigraphic benches is substantial in the Upper Freeport seam. Because these benches may be mined simultaneously or individually at the discretion of the miner, any coal sampled at the mine mouth and analyzed is representative of that sample only and not the Upper Freeport seam or the coal fed either to the washery or steam generator. Likewise, the results of samples characterized for mineral content or fired in a combustor to evaluate slagging or fouling are representative of that sample only and not the seam. Evaluation of washability or fireside behavior requires establishing the variability of the mineral matter in the coal, its size, and its association with the maceral constituents first. Once the variability of mineral content is established, the impact of mining on consistent production must be determined; otherwise, the coal must be characterized by the least desirable mineral composition and content. To evaluate the impact of mineral constituents on washing or fireside deposition, investigators should

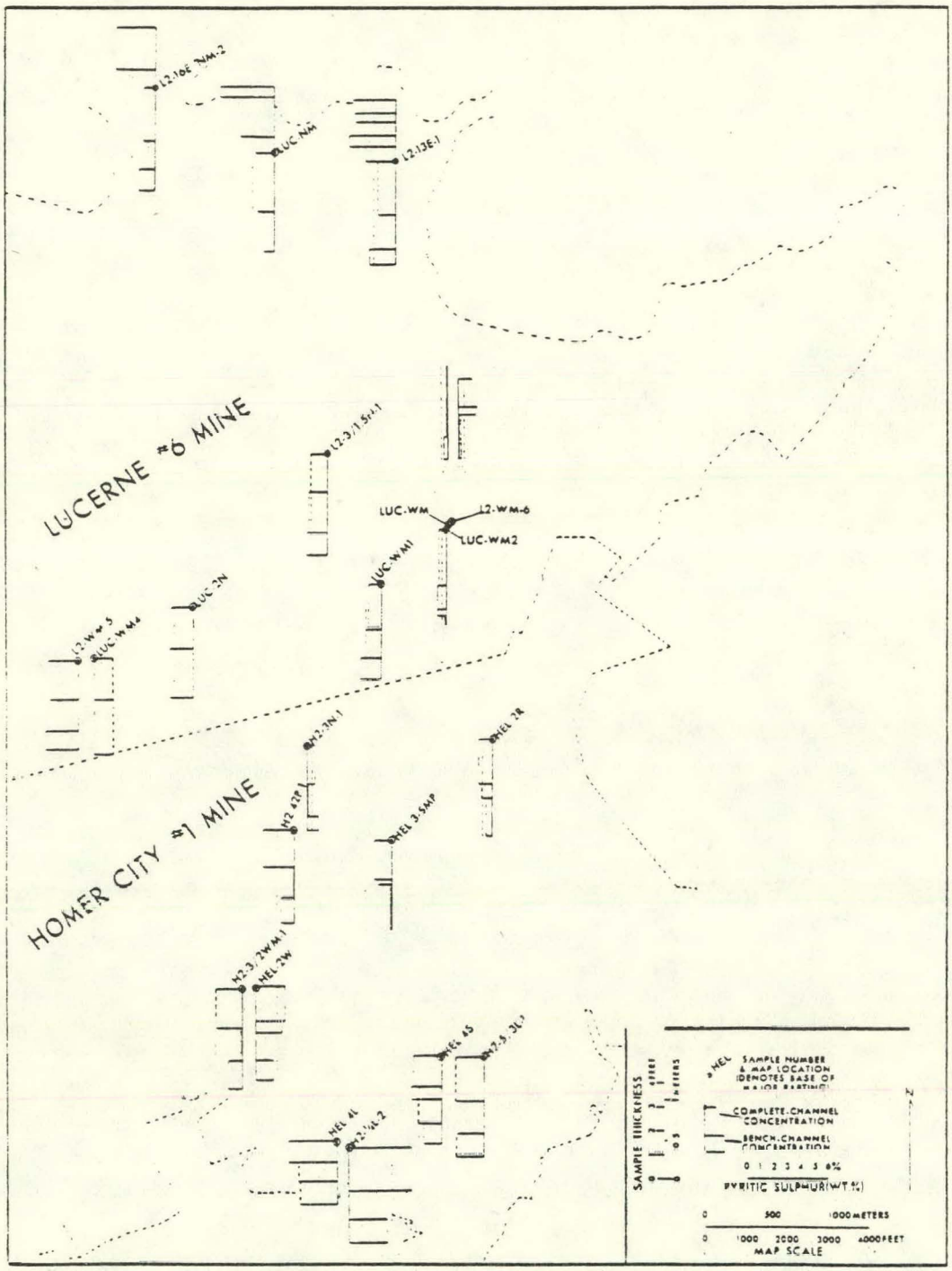


Figure 5.20 Concentration of Pyritic Sulfurs in Complete- and Bench-Channel Samples From Lucerne No. 6 and Homer City No. 1 Mines (from Cecil, Stanton, and Dulong)

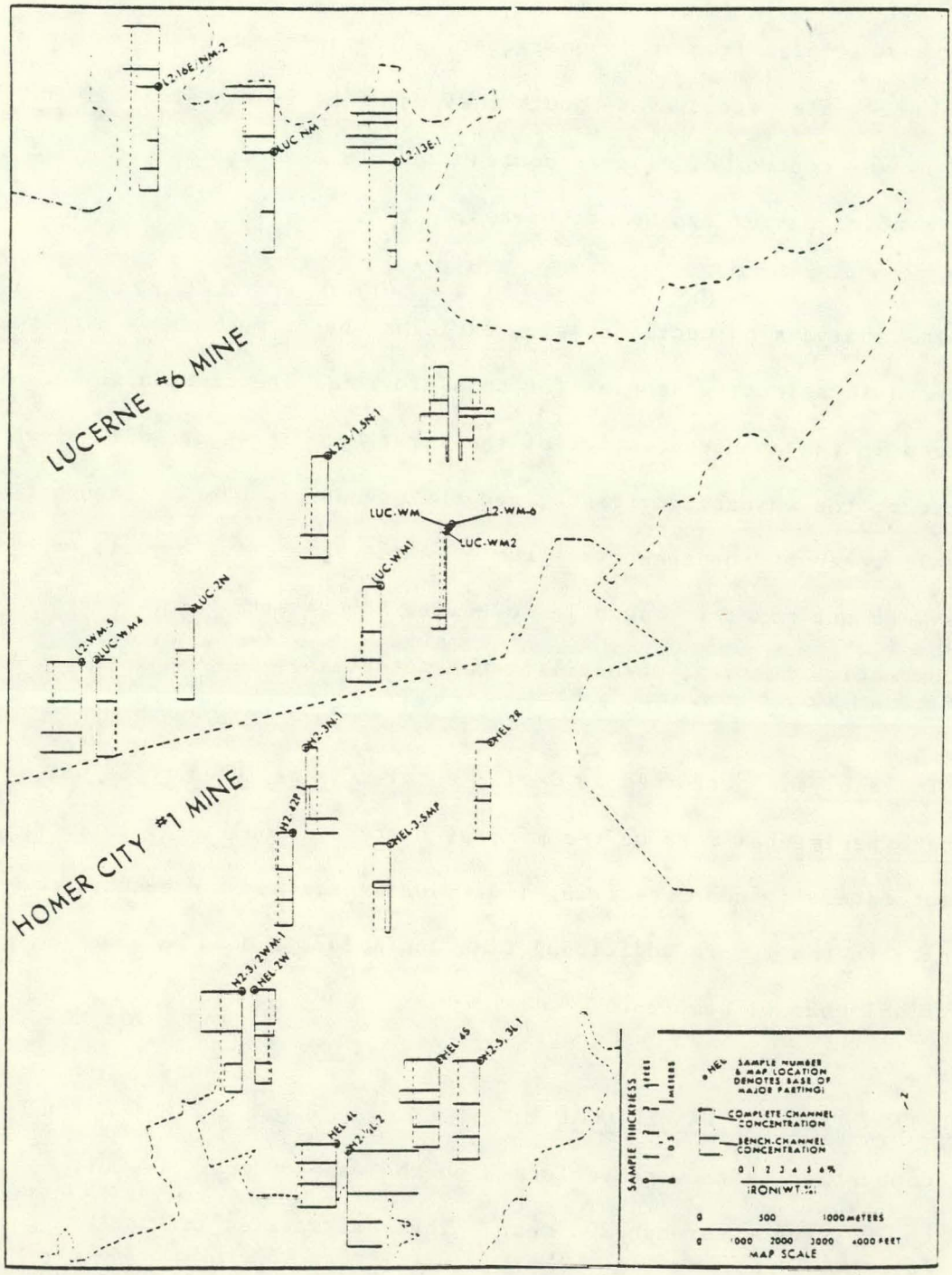


Figure 5.21 Concentration of Iron (Fe) in Complete- and Bench-Channel Samples From Lucerne No. 6 and Homer City No. 1 Mines (from Cecil, Stanton, and Dulong)

select the samples from fully characterized benches rather than from a conveyor belt, stock pile, etc., even though they may come from a single seam. This is the only way control of mineral content and its association with macerals or other mineral matter can be maintained.

The analysis by Cecil, et al., explains why so much difficulty was encountered in selecting samples for this program. The study also explains differences in the characteristics of the first Upper Freeport coal fired in the combustor, the washability tests, and the washed product. Although these coals were all taken at the same time from a sample on a conveyor belt, the individual drums were not mixed in one pile to ensure homogeneity before dividing the pile for combustion testing, washability characterizing, and washing.

The analysis performed by Cecil, et al., is believed to be unique. Their future experimental work on the mineral matter in coal is going to be difficult without carefully characterizing individual seams and the benches constituting a seam. In the future additional time and effort should be spent on acquiring individual channel samples.

## COMBUSTION TESTS OF WASHED COAL

Combustion tests were performed on the washed Upper Freeport coal pulverized to 70 percent through 200 mesh. The coal was fed at 108 lb/h for 10 hours while using 18-percent excess air. The furnace exit was held at 2024°F. The time-averaged operating conditions are summarized in Table 4.1.

By reducing the ash in the coal by 66 percent and the pyritic sulfur by 40 percent, the degree of furnace slagging was substantially reduced. Accumulations on the furnace wall were more fluid than in the previous test with the unwashed coal. The calculated viscosity for the washed and unwashed coal ash and the wall slag produced after firing the washed and unwashed coal appear in Figure 5.22. Figure 5.23 compares the coal ash viscosity of all coals fired to date. The curves illustrate the impact on viscosity of a slight increase in iron concentration. The selective removal of ash over pyrite, resulting from a slight change in mineral characterization within the mine, causes the slag to become more fluid upon beneficiating the oal. The increased fluidity of the ash resulted in the formation of a liquid pond on the furnace floor which ultimately flooded the burner, forcing an outage. In Figures 5.24 and 5.25 a direct comparison is made between the slag formed while firing the washed and unwashed coal on the center and lower slag probes. Figure 5.26 illustrates the upper and lower surfaces of the slag probe immersed in the furnace perpendicular to the direction of flow of the flue gases. As the picture indicates, deposits were just beginning to form, and their bond to the tube surface was extremely light. The fouling probe, illustrated in Figure 5.27, reveals virtually no deposit formation on the leading edge of the first tube. A photograph of the first first tube in the first probe bank of the convection pass after firing the unwashed Upper Freeport coal is included for a direct comparison.

The ash chemistry and ash fusion data for the wall slag and samples of deposit removed from the slagging probes and fouling probes are summarized in Table 5.14. The deposits formed in the furnace, particularly on the slagging

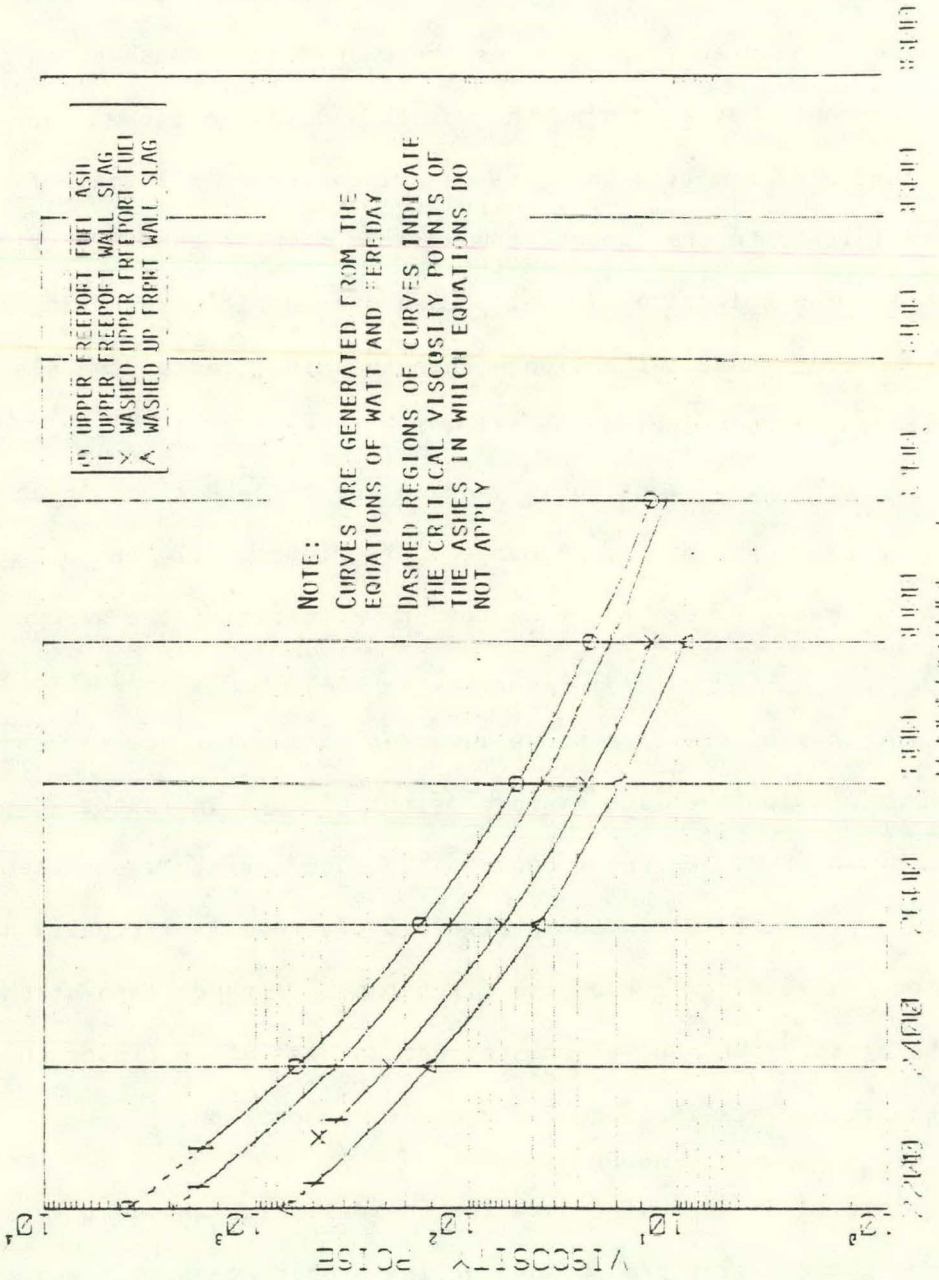


Figure 5.22 Viscosities of Coals and Their Deposits

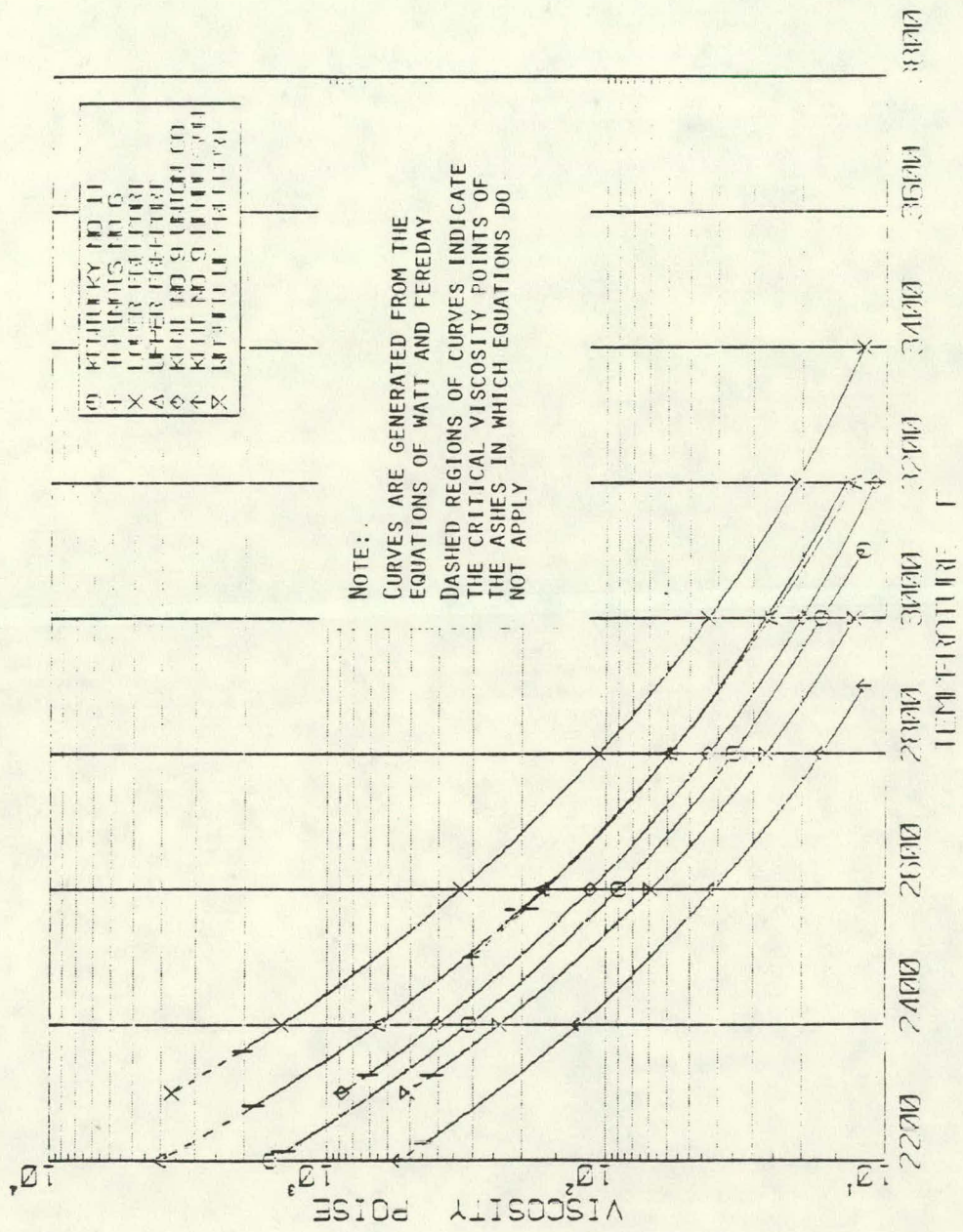


Figure 5.23 Ash Viscosities of Various Coals

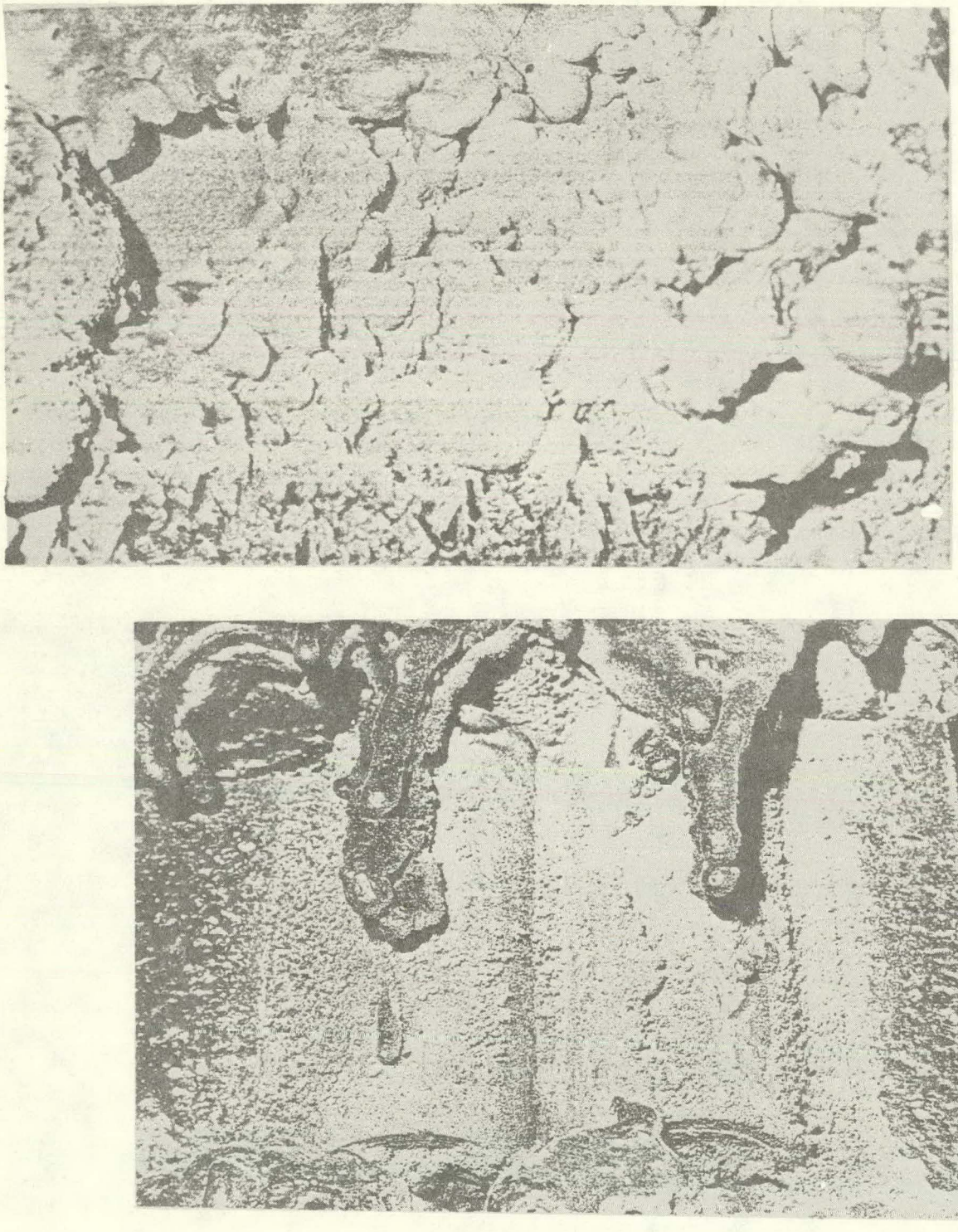

Figure 5.24 Comparison of Lower Slagging Probe After Firing Unwashed (top) and Washed (bottom) Upper Freeport Coal

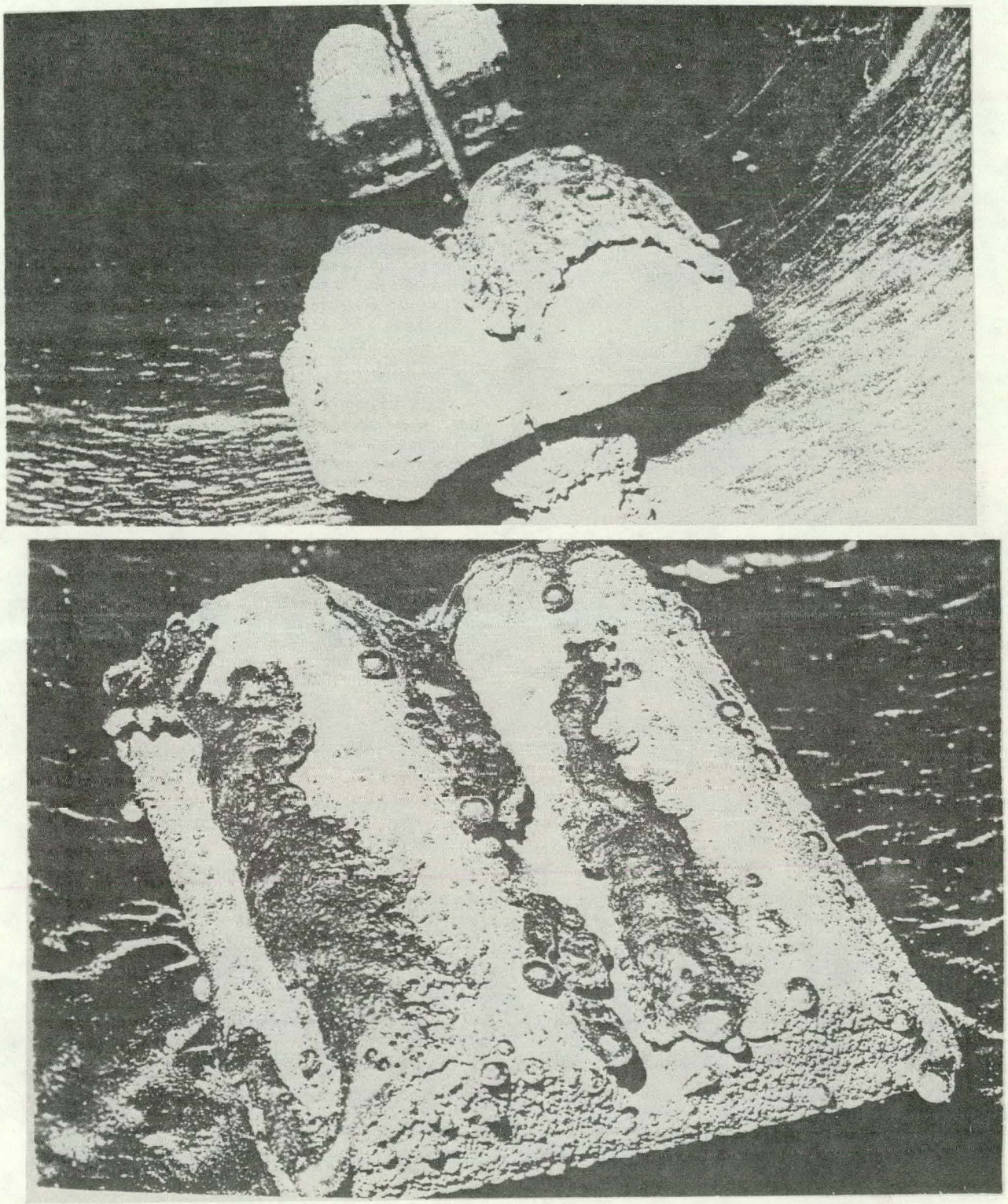

Figure 5.25 Comparison of Center Slagging Probe After Firing Unwashed (top) and Washed (bottom) Upper Freeport Coal

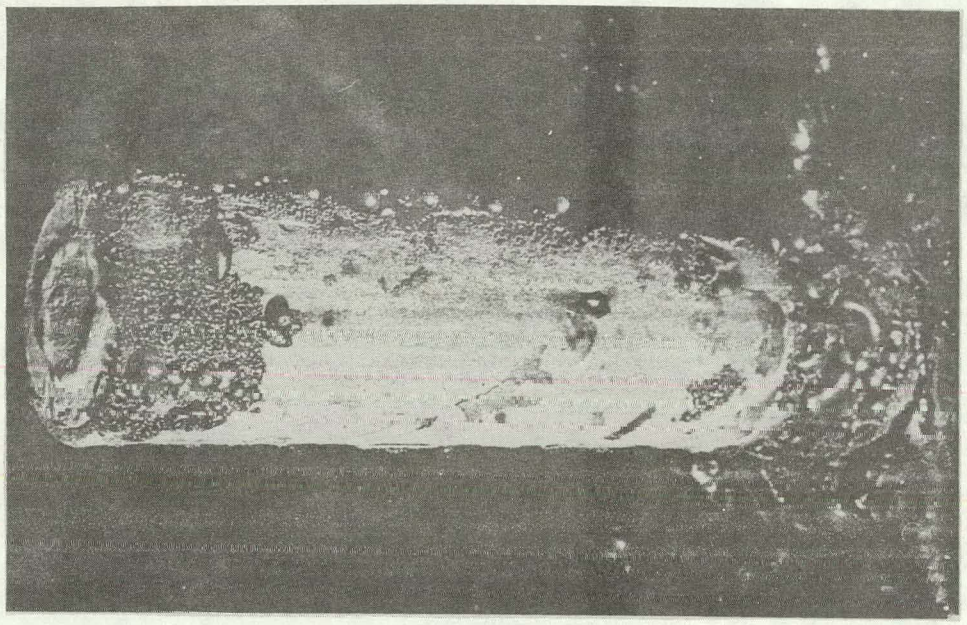

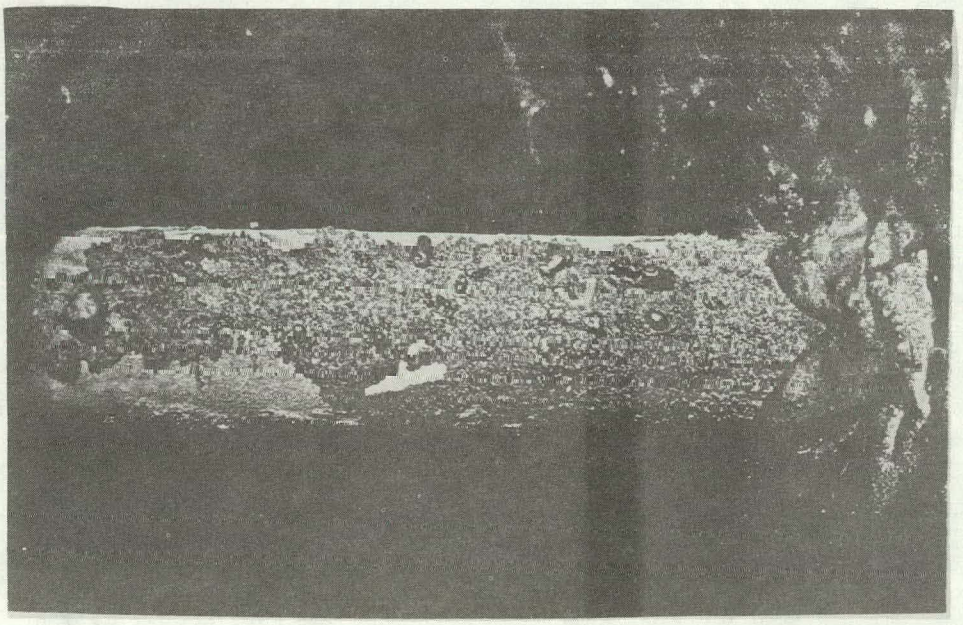

Figure 5.26 Flame (top) and Furnace Exit (bottom) Sides of Probe Immersed Perpendicular to Gas Flow in Furnace--After Firing Washed Coal

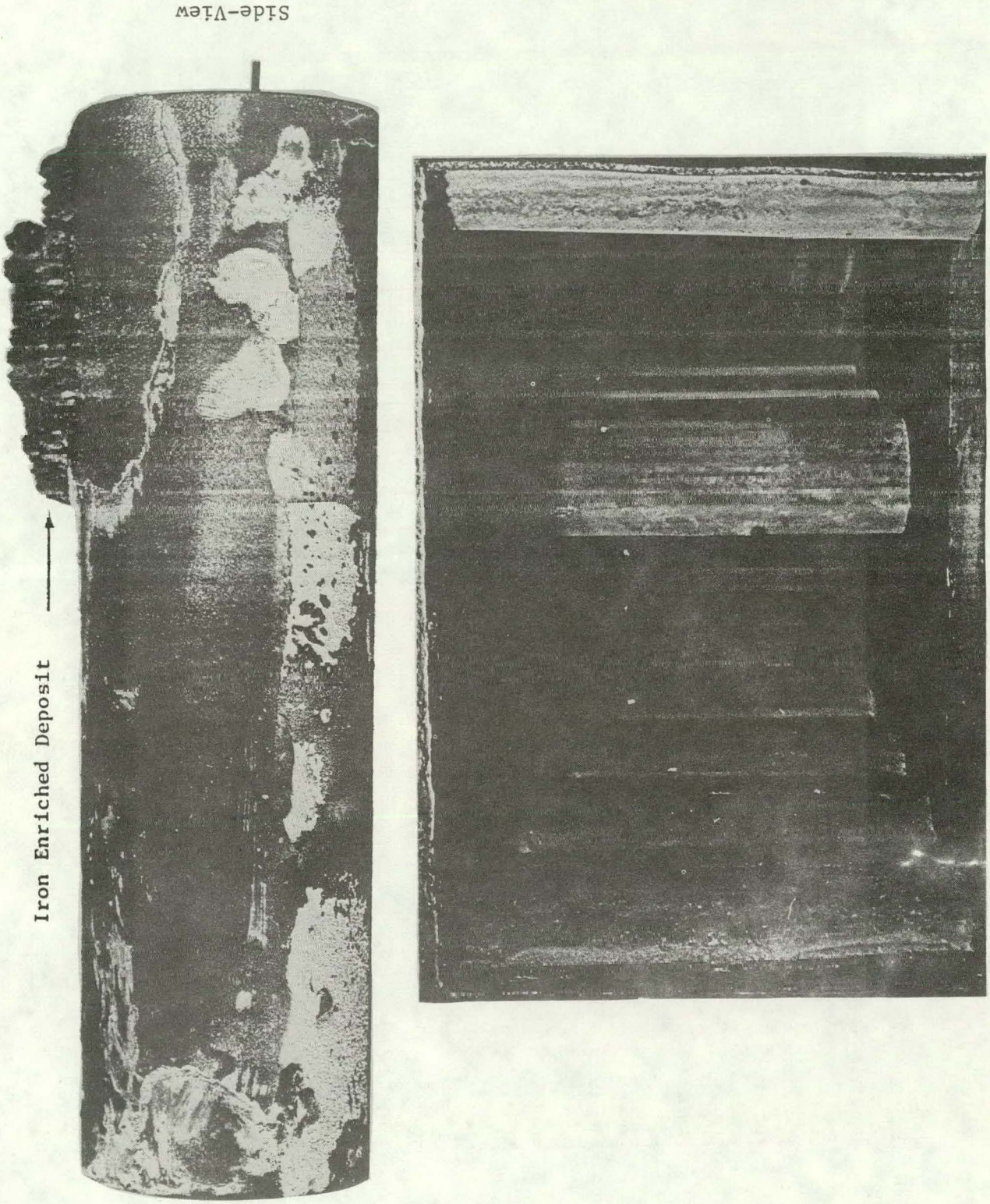


Figure 5.27 Direct Comparison of Fouling Probes After Firing Raw Coal(top) and Coal in Which Liberated Pyrite Was Removed by Washing (bottom)

Table 5.14 Summary of Ash Chemistry and Ash Fusion Data--Combustion Tests of Washed Upper Freeport Coal

| Description | Coal Ash | Wall Slag | | Slagging Probe | | | Fouling Probe | |
|---|---|---|---|---|---|---|---|---|
| | | Lower | Upper | Upper | Center | Lower | 1 | 2 |
| **Ash Chemistry (%)** | | | | | | | | |
| $SiO_2$ | 41.3 | 47.5 | 42.7 | 36.7 | 40.4 | 34.8 | 42.7 | 43.8 |
| $Al_2O_3$ | 25.5 | 24.5 | 24.9 | 22.6 | 24.5 | 20.2 | 23.7 | 24.2 |
| $TiO_2$ | 1.1 | 0.8 | 0.9 | 0.8 | 0.9 | 0.8 | 1.4 | 1.4 |
| $Fe_2O_3$ | 17.1 | 16.7 | 19.9 | 29.5 | 23.4 | 31.7 | 15.0 | 14.4 |
| CaO | 6.4 | 5.4 | 8.0 | 5.7 | 6.6 | 6.3 | 7.1 | 6.5 |
| MgO | 0.4 | 0.8 | 0.8 | 0.7 | 0.7 | 0.8 | 0.7 | 0.8 |
| $Na_2O$ | 0.5 | 1.3 | 0.7 | 0.5 | 0.4 | 0.7 | 1.2 | 1.4 |
| $K_2O$ | 2.5 | 1.9 | 2.1 | 2.0 | 2.4 | 1.8 | 2.6 | 2.5 |
| $SO_3$ | 5.3 | 0.1 | 0.4 | 0.4 | 0.8 | 1.7 | 5.1 | 4.7 |
| $P_2O_5$ | 0.6 | 0.1 | 0.3 | 0.4 | 0.4 | 0.3 | 0.7 | 0.5 |
| **Ash Fusion (°F)** | | | | | | | | |
| Reducing: | | | | | | | | |
| Initial Deformation | 2170 | 1990 | 2070 | 1980 | 2010 | 1900 | --- | 2190 |
| Softening (Sph.) | 2200 | 2050 | 2090 | 2015 | 2040 | 1970 | --- | 2220 |
| Softening (Hem.) | 2240 | 2090 | 2120 | 2030 | 2070 | 2000 | --- | 2250 |
| Fluid | 2270 | 2160 | 2165 | 2105 | 2175 | 2140 | --- | 2370 |
| Oxidizing: | | | | | | | | |
| Initial Deformation | 2440 | 2260 | 2375 | 2380 | 2365 | 2340 | --- | 2330 |
| Softening (Sph.) | 2450 | 2315 | 2410 | 2415 | 2390 | 2380 | --- | 2360 |
| Softening (Hem.) | 2460 | 2350 | 2435 | 2435 | 2425 | 2450 | --- | 2400 |
| Fluid | 2470 | 2400 | 2460 | 2590 | 2460 | 2580 | --- | 2460 |

probes, are enriched with iron by a factor of ≈2. The ash fusion temperatures of the fireside deposits under reducing conditions are below that of the washed coal ash. The small difference between the initial deformation temperature and fluid temperature, in addition to their high iron concentration, accounts for the high fluidity of the ash. The dust removed from the center tube of the fouling probe is slightly depleted of iron and has slightly higher ash fusion temperatures than the washed coal ash does. Table 5.15 makes a direct comparison of the ash chemistry of wall slag deposits, probe slag deposits, and fouling probe deposits for the washed and unwashed coals.

SEM photomicrographs and EDX scans were made of powdery inside surface layers, molten phases, and outside surfaces of slag samples removed from the three furnace probes and the upper and lower furnace wall. The SEM photomicrographs of the powdery layer adjacent to the tube surface and the subsequent layer representing the very beginning of the formation of a molten phase of ash deposited on the lower slagging probe are illustrated in Figure 5.26, along with their corresponding EDX. SEM photomicrographs and EDAX scans of comparable ash deposits on the lower slagging probe while firing unwashed coal are included for a direct comparison between the washed and unwashed cases. There appears to be a greater portion of submicron agglomerates in the washed coal ash (believed to be the residue of slow oxidation of carbon particles at temperatures below flame temperature in the ash from the washed Upper Freeport coal) than in the ash from unwashed Upper Freeport coal. There is an abundance of submicron particles in the ash from the Lower Freeport coal. This was also the case of Kentucky No. 11,

Table 5.15 Comparison of Ash Chemistry of Slag Formed by Washed and Unwashed Coal

| Description | Wal. Slag | | Center Slagging Probe | | Lower Slagging Probe | | 1st Fouling Probe | |
|---|---|---|---|---|---|---|---|---|
| | Washed | Unwashed | Washed | Unwashed | Washed | Unwashed | Washed | Unwashed |
| **Ash Chemistry (%)** | | | | | | | | |
| $SiO_2$ | 47.5 | 47.2 | 40.5 | 47.0 | 34.8 | 51.0 | 42.7 | 11.6 |
| $Al_2O_3$ | 24.5 | 21.2 | 24.5 | 27.8 | 20.2 | 21.7 | 23.7 | 6.7 |
| $TiO_2$ | 0.8 | 1.0 | 0.9 | 1.0 | 0.8 | 1.0 | 1.4 | 0.3 |
| $Fe_2O_3$ | 16.7 | 20.6 | 23.4 | 18.1 | 31.7 | 18.2 | 15.0 | 69.0 |
| CaO | 5.4 | 2.8 | 6.6 | 3.0 | 6.3 | 3.3 | 7.1 | 5.0 |
| MgO | 0.8 | 0.5 | 0.7 | 0.9 | 0.8 | 0.9 | 0.7 | 0.5 |
| $Na_2O$ | 1.3 | 2.5 | 0.4 | 0.4 | 0.7 | 0.4 | 1.2 | 0.1 |
| $K_2O$ | 1.9 | 0.6 | 2.4 | 2.8 | 1.8 | 2.8 | 2.6 | 0.5 |
| $SO_3$ | 0.1 | 0.4 | 0.8 | 1.0 | 1.7 | 0.7 | 5.4 | 3.0 |
| $P_2O_5$ | 0.1 | --- | 0.4 | 0.3 | 0.3 | 0.2 | 0.7 | 0.5 |
| **Ash Fusion (°F)** | | | | | | | | |
| Reducing: | | | | | | | | |
| Initial Deformation | 1990 | 2333 | 2010 | 1955 | 1900 | 2218 | 2190 | 1879 |
| Softening (Sph.) | 2050 | 2361 | 2040 | 2000 | 1970 | 2256 | 2220 | 1900 |
| Softening (Hem.) | 2090 | 2380 | 2070 | 2057 | 2000 | 2339 | 2250 | 1920 |
| Fluid | 2160 | 2419 | 2125 | 2074 | 2140 | 2385 | 2370 | 2000 |
| Oxidizing: | | | | | | | | |
| Initial Deformation | 2260 | 2424 | 2365 | 2319 | 2340 | 2454 | 2330 | 2378 |
| Softening (Sph.) | 2315 | 2460 | 2390 | 2436 | 2380 | 2478 | 2360 | 2600 |
| Softening (Hem.) | 2350 | 2479 | 2425 | 2460 | 2450 | 2519 | 2400 | 2600 |
| Fluid | 2400 | 2570 | 2460 | 2541 | 2580 | 2542 | 2460 | 2600 |

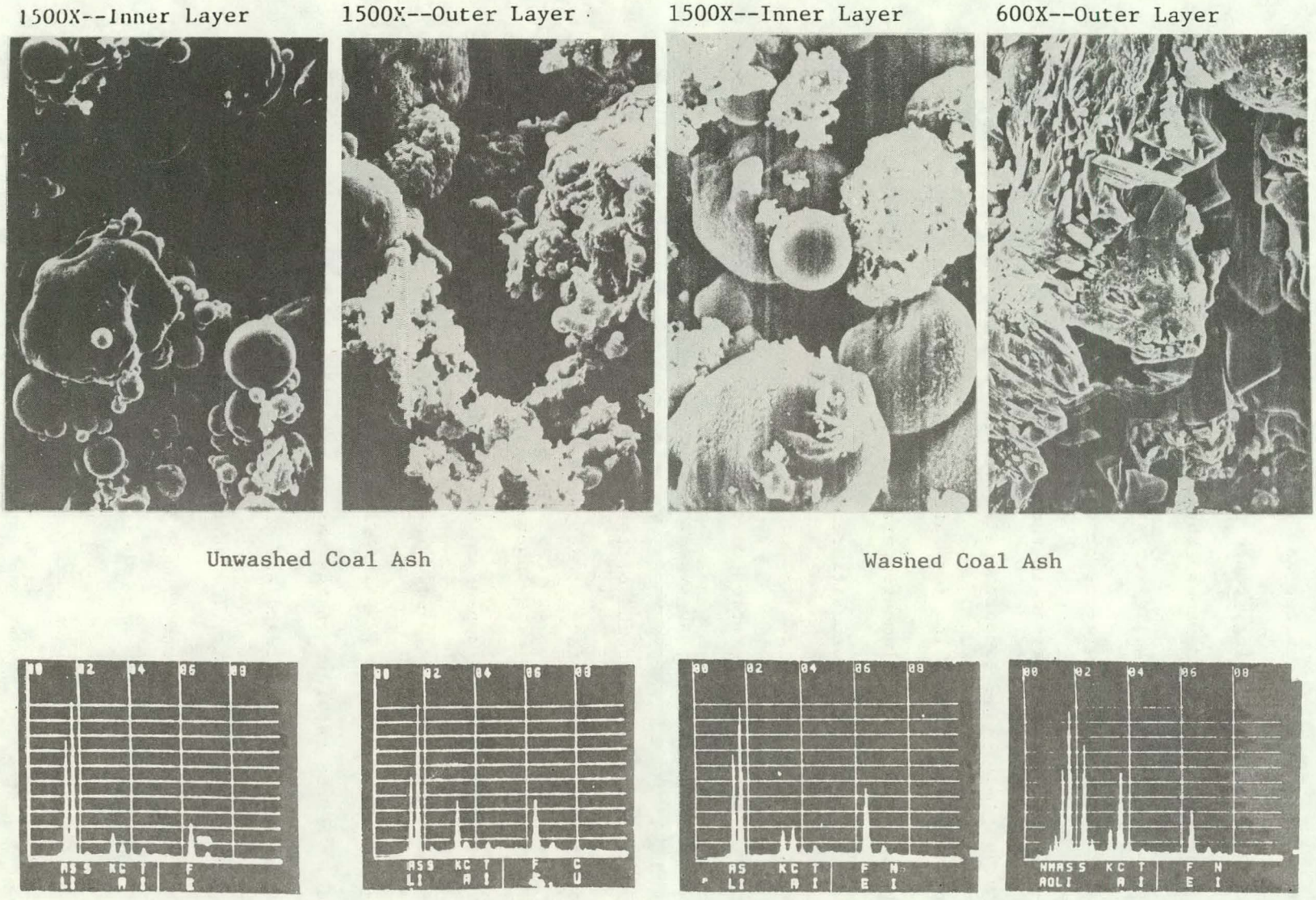


Figure 5.28 Comparison of Inner and Outer Layers of Ash Formed on Lower Slagging Probe While Firing Unwashed and Washed Upper Freeport Coal, Indiana County

where little of the mineral matter was liberated during pulverizing. The slight difference in surface morphology could be due to the source of the ash in the coal (i.e., inherent vs. extraneous liberated ash). The outer layer of ash is highly crystalline in nature. The crystaline substance is believed to be calcium sulfate. There is no evidence of the needle-like crystals rich in FeO, $SiO_2$, and CaO frequently observed in the outermost surface of slag, formed by other iron-rich coal. The temperature within the boundary layer of the lower slagging probe must be quite low for calcium sulfate to form, suggesting the local heat flux, and hence flame temperature, is low. As will be noted in subsequent photomicrographs of deposits removed from the second slag probe located in Segment 3, the local flue gas temperature must be higher as there is evidence of submicron particle agglomeration on the inner layer and completely molten ash on the outer layer. There is no evidence of crystalline calcium sulfate.

SEM photomicrographs and EDX of the innermost powdery layer, fused cross section, and fluid outer surface of deposits formed on the center slagging probe appear in Figure 5.29. The innermost layer is composed of agglomerates of submicron particles which appear to be the burned out remnants of coal particles, possibly as large as 40 μm. The ash is enriched in potassium. The alumina is unusually high in count, implying the source of the ash was predominantly clay. Illite retained in the washed coal is probably the source of this ash. Subsequent layers are fused and show signs of iron and silica enrichment with a depletion in potassium. The outer layer of the deposit contains substantial amounts of calcium and iron. There is evidence of a preponderance of

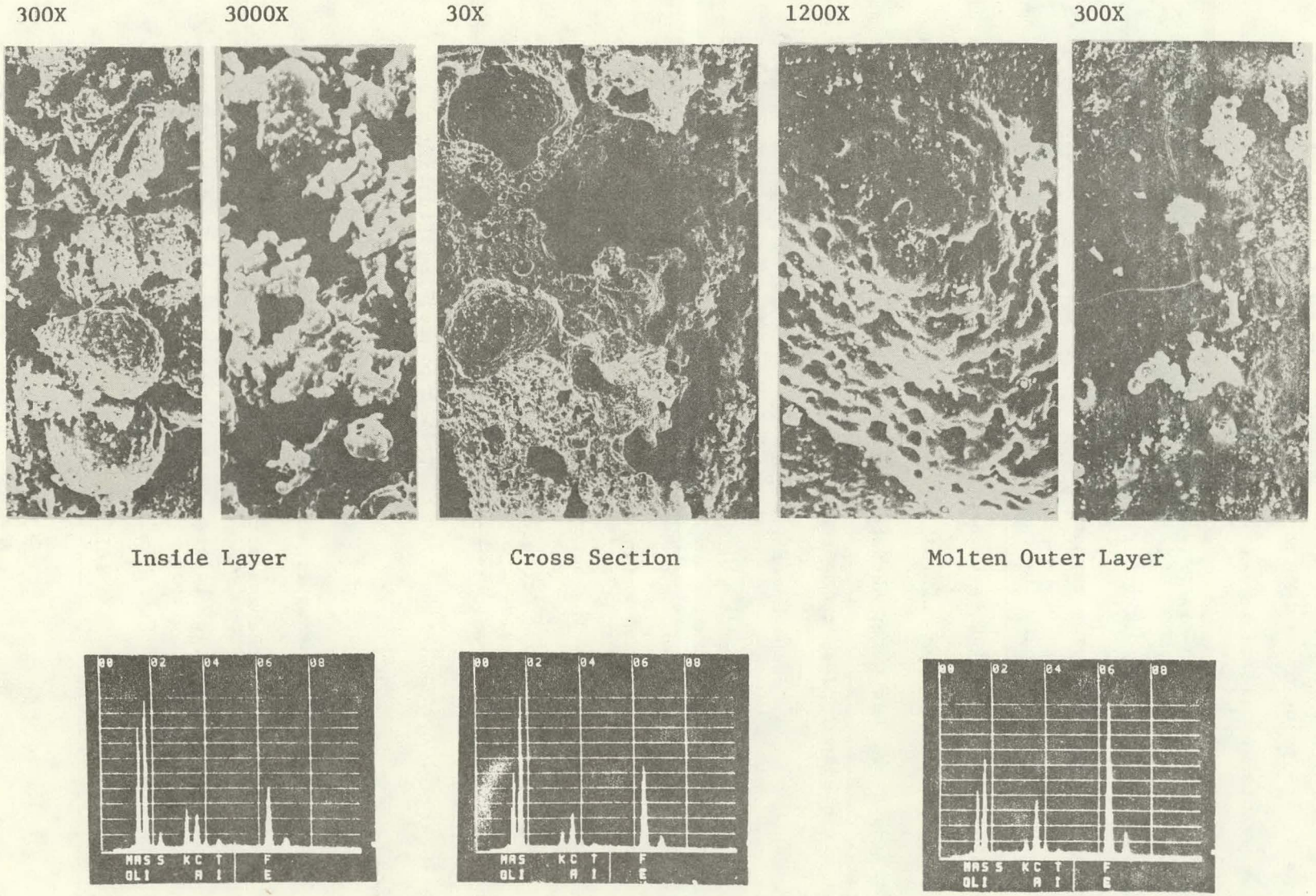


Figure 5.29 SEM Photomicrograph and EDX Scan Comparing Change in Surface Morphology and Elemental Composition of Deposit on Center Slagging Probe

submicron particles going into solution in the outer layer. Occasionally, a 20 μm particle attaches itself to the slag and is dissolved.

If this deposit were allowed to grow thicker by extending the time the probe was exposed to the flue gases or increasing the surface temperature from time zero, as in the case of the furnace wall, we might expect further changes similar to those demonstrated by the wall slag. Figure 5.30 shows the chemistry and morphology of the wall slag cross section and outer surface in the vicinity of the center slag probe. The bulk of the slag appears to be greatly enriched with quartz. However, the outer surface appears to be greatly enriched with iron. This phenomenon appears to be characteristic of slags formed by other coals (i.e., Kentucky No. 9 and Upper Freeport). The Lower Freeport coal slag included calcium as an additional constituent. This same phenomenon has been observed in slag removed from field installations while firing other coals. Figure 5.31 illustrates one such example. As shown in this picture, submicron particles attach themselves to the outer surface and migrate into the molten slag, where they are dissolved. Occasionally, larger particles attach themselves. In some cases small cubic iron-rich crystals attach themselves, indicating that sublimation of volatile iron is taking place, as illustrated in Figure 5.32.

The deposits formed on the upper and lower side of the probe, immersed in the furnace perpendicular to the gas stream and illustrated in Figure 5.26, were examined separately. The initial layers of the deposit formed on the flameside of the probe are composed primarily of unfused ash, remnants of spent char particles enriched with potassium, and sulfur. As illustrated in Figure 5.33, the

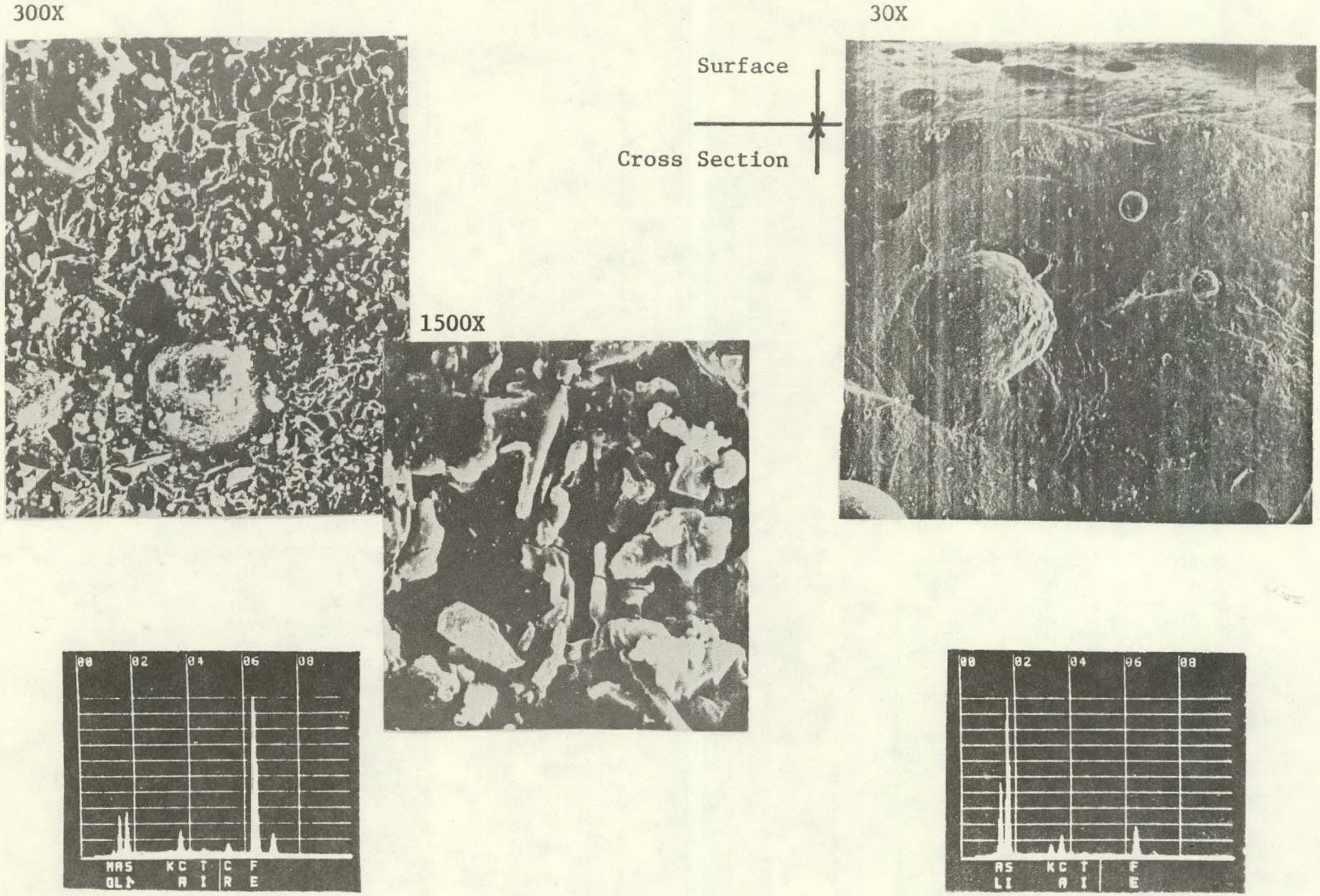


Figure 5.30 SEM Photomicrographs and EDX Scans of Cross Section of Wall Slag, Representing Advanced Stages of Slagging

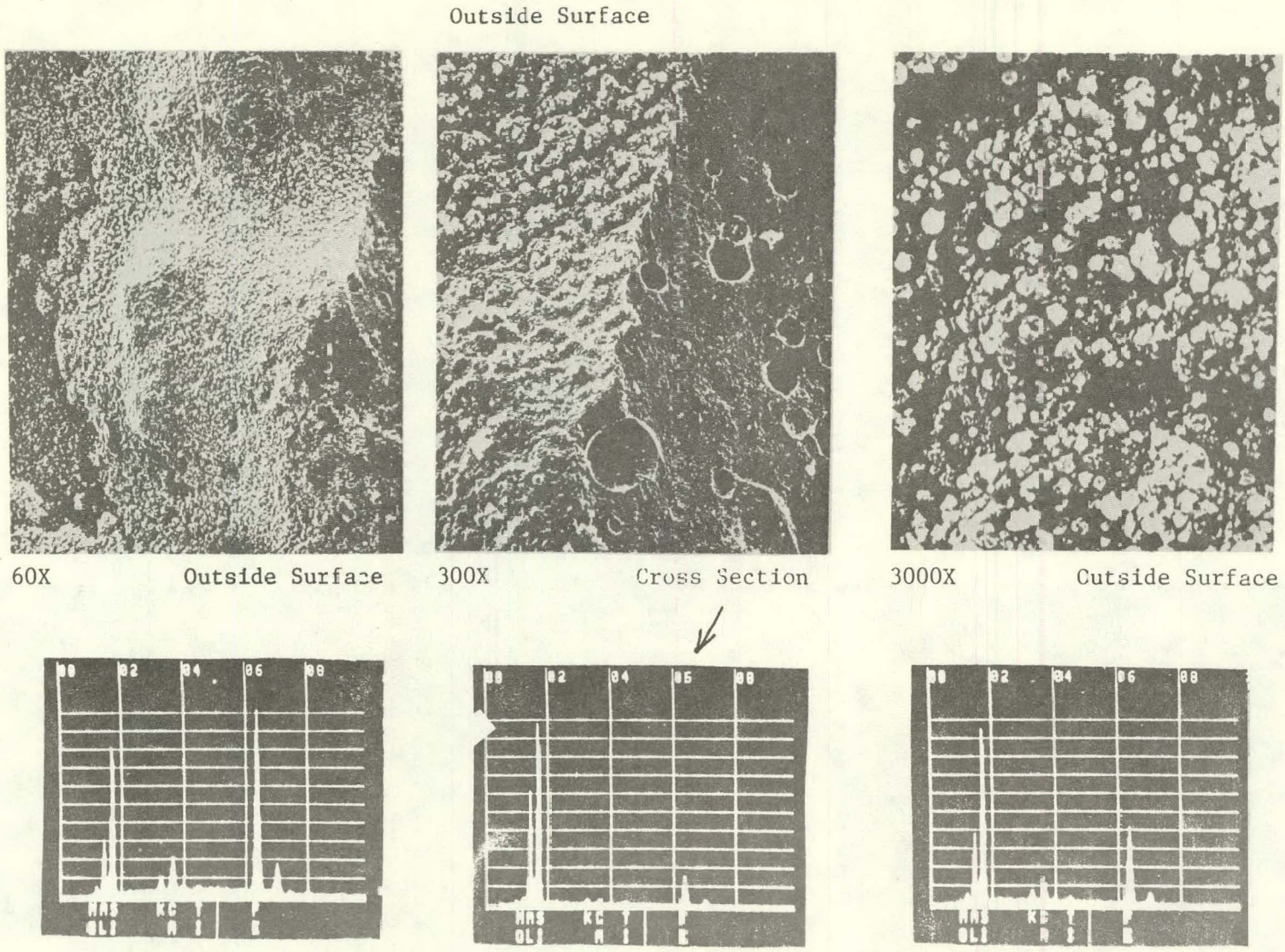


Figure 5.31 SEM Photomicrographs and EDX Analyses of Top Surface and Cross Section of Fused Burner Deposit Formed While Firing Air-Micronized Coal

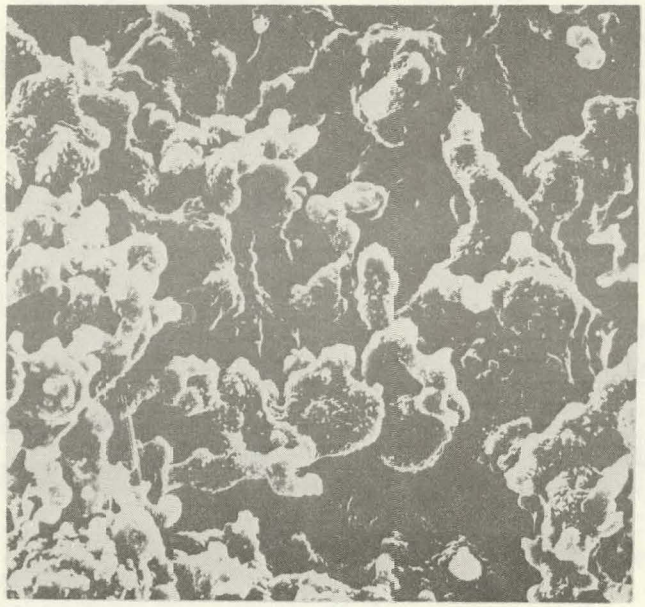

1500X

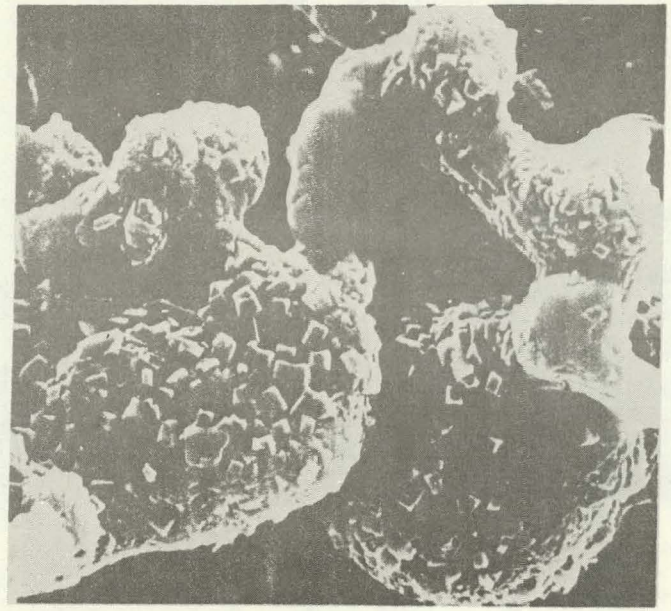

1000X

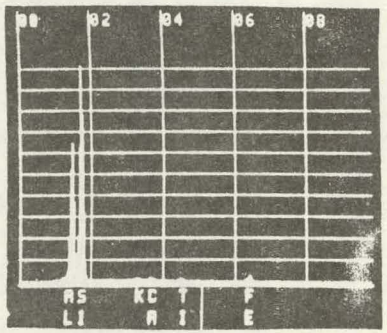


Molten Matrix

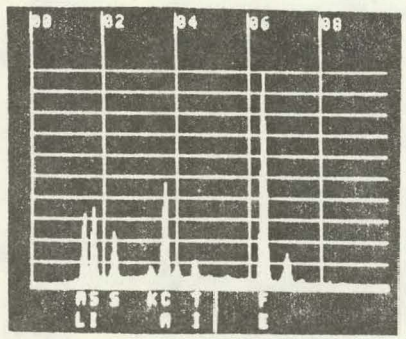


Angular Cubic Crystals

Figure 5.32 SEM Photomicrographs and EDX Analyses of Gas-Side Surface of Fly Ash Deposited on Furnace Boiler Tube Surface While Firing Steam-Micronized Coal

300X--Inside Layer

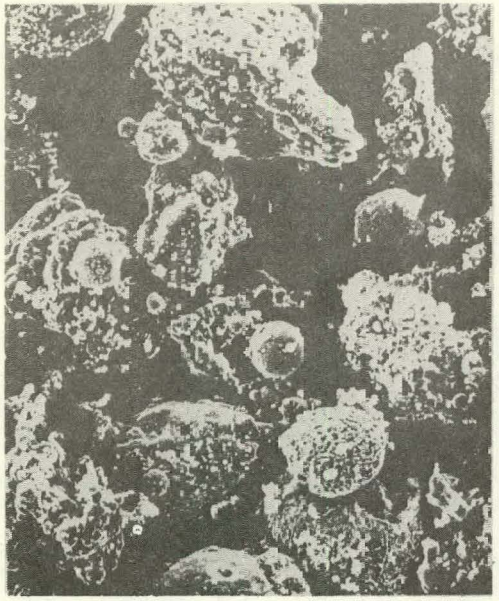

300X--Cross Section

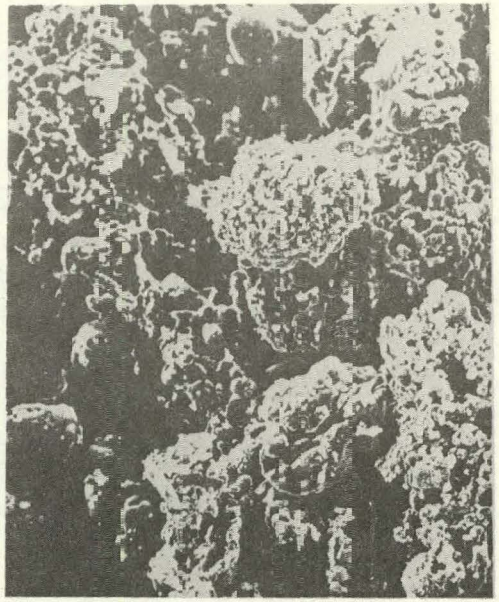

300X--Outer Layer

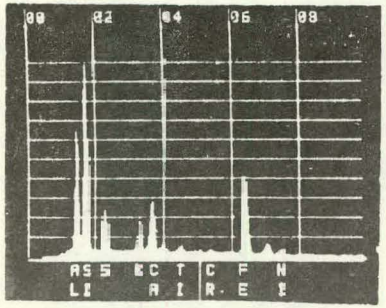


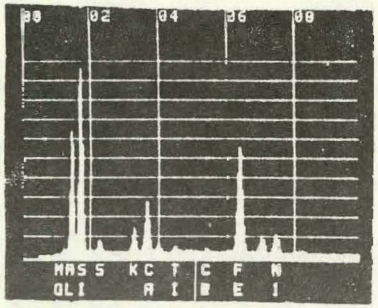


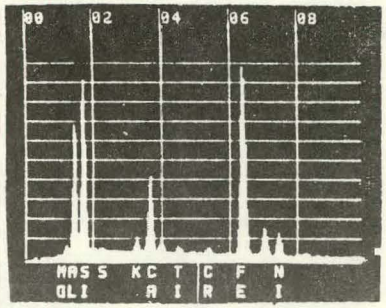


Figure 5.33 SEM Photomicrographs and EDX Scans Showing Surface Morphology of Deposits Accumlated on Frame Side of the Slagging Probe Perpendicular to the Flue Gas Stream

molten material on the outer surface is depleted of sulfur and enriched with iron and calcium to a lesser extent. The particle sizes are 84 μm or less. Since they are not solid spheres, they must be very light. There was no evidence of selective deposition of large, pure pyrite particles. This was not unexpected in this case as the free pyrite was washed from the coal.

The results of the microscopic examination of the upper layers of deposits on the perpendicular probe appear in Figure 5.34. Once again, the inner layers are slightly enriched with potassium, whereas the molten, outer layer is enriched with iron.

The sintered deposits removed from the refractory wall in Segment 6 are illustrated in Figure 5.35. Except for evidence of some melting at the slightly higher flue gas temperatures, the composition and surface morphology closely resemble the dust collected on the fouling probes, which is illustrated in Figure 5.36. Although the sintered deposit morphology resembles deposits formed on the furnace roof while firing unwashed Upper Freeport coal, the chemical composition is quite different. Figure 5.37 compares the surface morphology and composition of the sintered deposit formed by the washed and unwashed coal.

The mechanism for formation of the molten slag is uncertain, as the spheroidized particles contacting the surface are completely solidified. There is evidence in Figure 5.32 that submicron particles, attaching themselves to other particles of dissimilar composition, may form eutectics on the surface with much lower melting temperatures. As material from the large particles

300X--Inside Layer

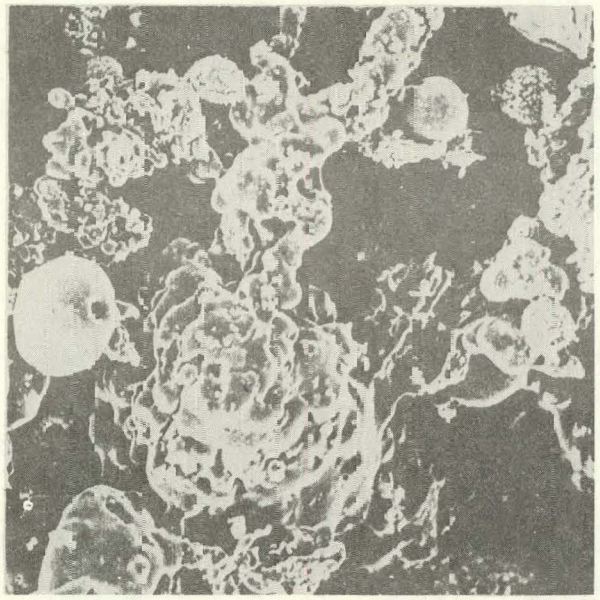

60X--Molten Outside Layer

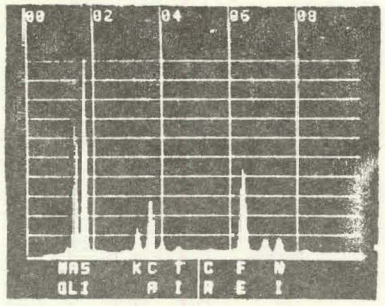


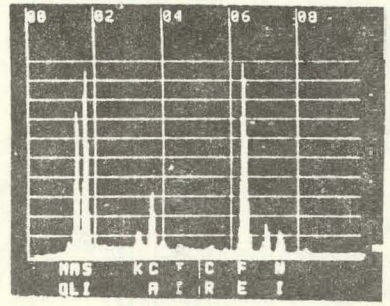


Figure 5.3C SEM Photomicrographs and EDX Scans Showing Surface Morphology and Elemental Composition of Deposit Forming on Top Side of Probe Perpendicular to Flow of Flue Gas in Furnace

MAG. 60X

MAG. 300X

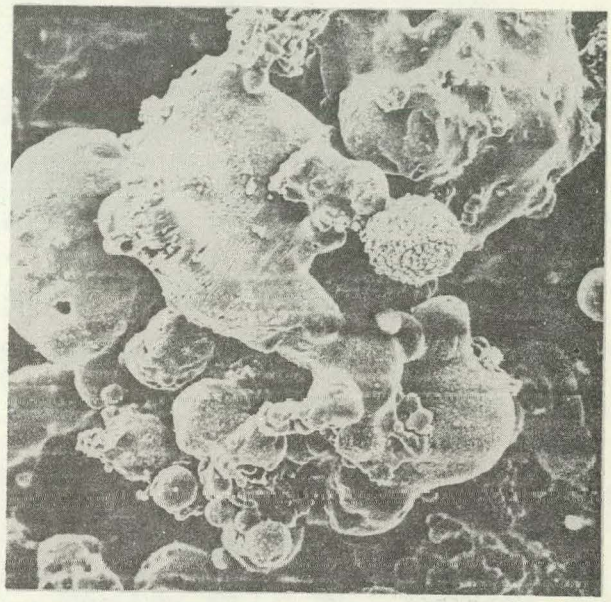

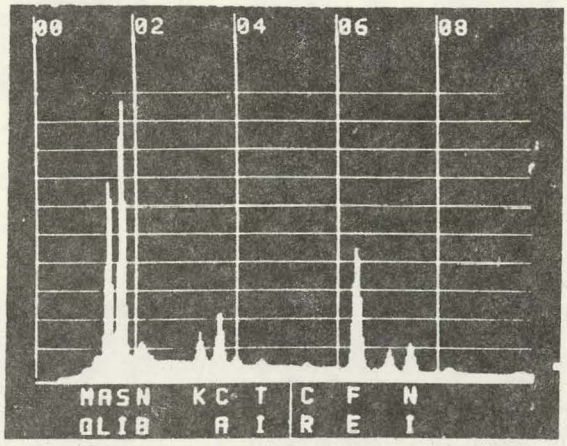


FIGURE 5.35 SEM Photomicrographs and EDAX Scan of Deposit Removed from Refractory in Segment 8 at the Furnace Exit

600X--1st Fouling Probe
Upstream

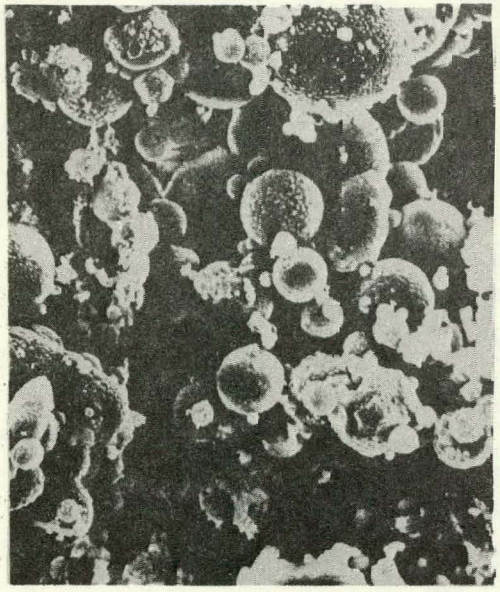

1500X--1st Fouling Probe
Downstream

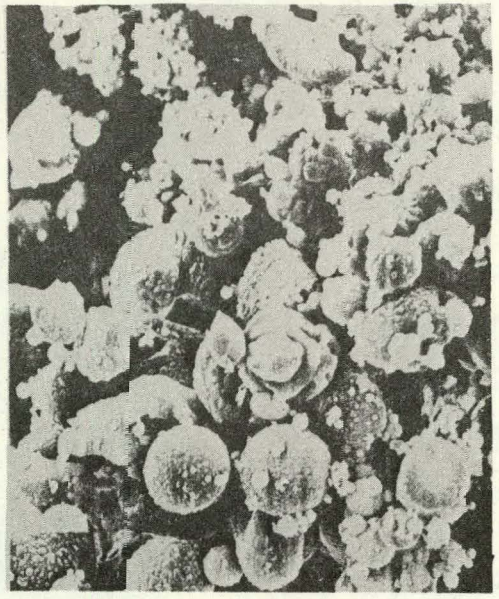

1500X--4th Fouling Probe

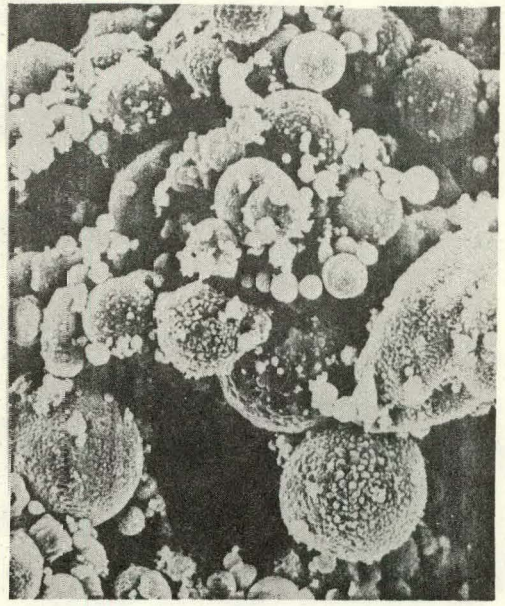

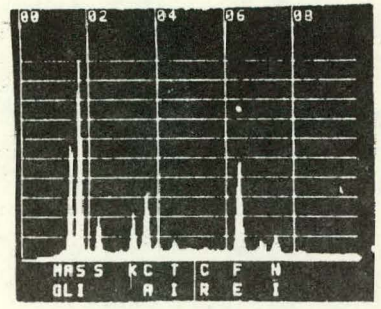


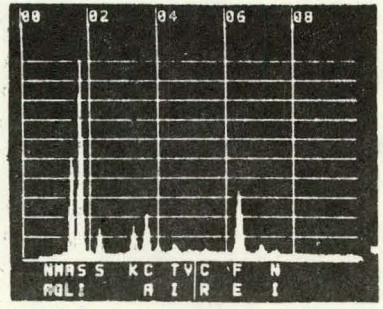


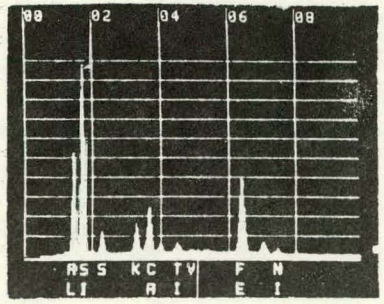


Figure 5.36 Surface Morphology and Elemental Composition of Dust Removed From Fouling Probes After Firing Washed Upper Freeport Coal

300X

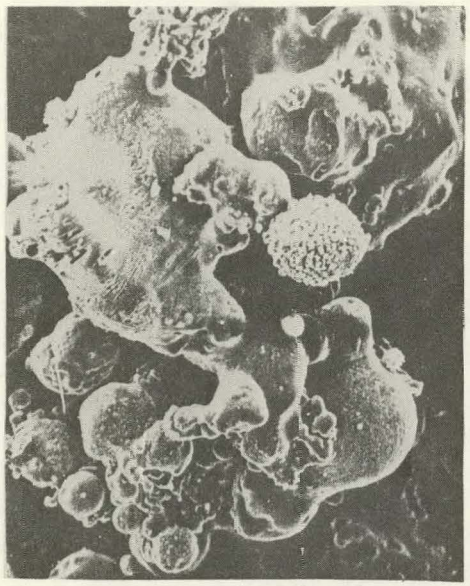

Upper Furnace Wall Deposit

600X

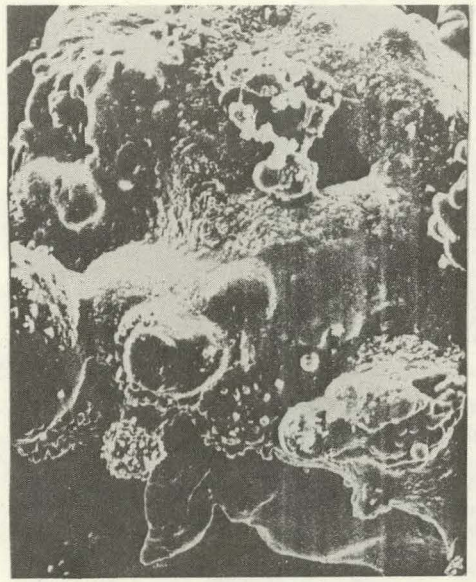

300X

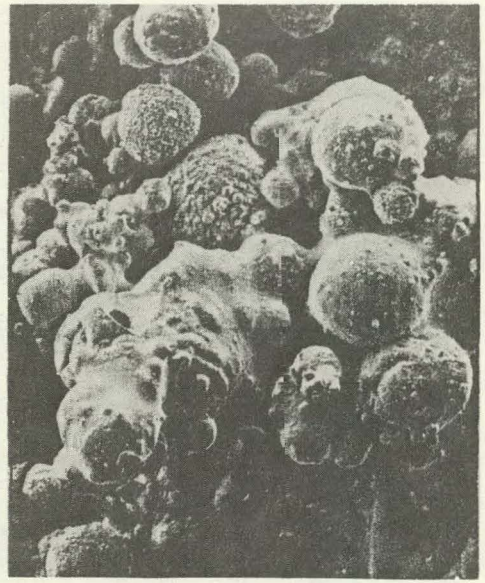

Furnace Roof Deposit

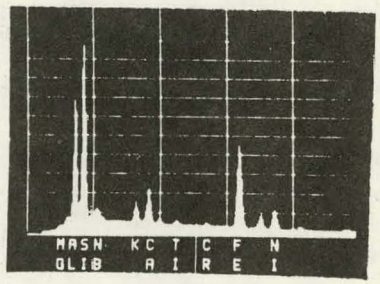


Washed Coal

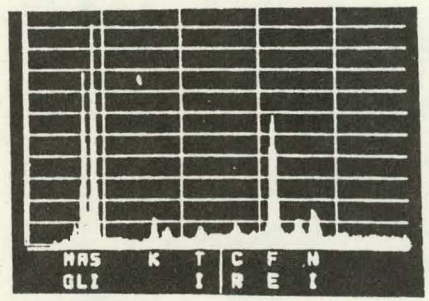


Unwashed Coal

Figure 5.37 Comparison of Surface Morphology and Elemental Composition of Sintered Deposits Removed From Refractory Surface After Firing Washed and Unwashed Upper Freeport Coal

goes into solution, the concentration of the minor constituents approaches that of the larger particle, and the molten phase solidifies. Presumably, the same results could be achieved by condensation of a vapor phase. However, because of the steep temperature gradient within the deposit, there should be some evidence of crystals formed at the dewpoint similar to those found on the first slagging probe.

Coal washing removed large concentrations of illite and liberated pyrite. The extraneous ash was completely removed except for ash liberated in pulverizing from 14 x 100 mesh to 200 mesh x 0. In doing so, the total ash deposited was reduced, despite the apparent low fusion temperatures. As in other investigations, the ash responsible for the initial layers of the deposit was enriched with potassium and believed to be the mineral illite. The molten layers are enriched with iron and calcium. They appear to form because the local ash deposit exceeds the melting temperature of the ash. Iron enrichment occurs in dissimilar composition forming a eutectic at the surface whose melting temperature is decidedly below that of either compound. With subsequent counterdiffusion of components into the existing deposited ash, the two foreign constituents of decidedly different composition are assimilated to form a solid or plastic slag, depending on the local temperatures. The large difference in temperature between the inner and outer layers could explain the difference in deposit composition. The tube surface appears to be at temperatures well below eutectics in the $CaO-FeO-SiO_2$ or $CaO-Fe_2O_3-SiO_2$ system, but not below those of the $K_2O-SiO_2$ system.

There is no evidence of selective deposition by pure, liberated pyrite, as presumably it has been reduced to a minimum by washing.



*U.S. GOVERNMENT PRINTING OFFICE: 1984-746-091/10169